Gaseous Diffusion in Liquids

by

Roger J. Combs, II

Dissertation submitted to the Faculty of the

Virginia Polytechnic Institute and State University

in partial fulfillment of the requirements for the degree of

Doctor of Philosophy

in

Chemistry

APPROVED:

Paul E. Field, Chairman

John G. Mason

George Sanzone

Jimmy W. Viers

James P. Wightman

April 1986

Blacksburg, Virginia

Gaseous Diffusion in Liquids

by

Roger J. Combs

Paul E. Field, Chairman

Chemisty

(ABSTRACT)

Diffusivity of nonreactive gases in liquids provides a means of interpreting structure in the liquid state. Structural models of the liquid state include Hildebrand's condensed gas model and Eyring's pseudo-lattice model. The former model predicts a linear dependence of diffusivity with temperature while the latter model predicts linear dependence of log(D) versus 1/T. The limited temperature dependent diffusivity data to date with a typical precision of $\pm 5\%$ do not permit distinguishing which temperature dependence is more linear. However, the present investigation shows that diffusivities of one gas solute in two nonpolar liquids indirectly supports a linear diffusivity temperature dependence by a Graham's law like relation. At a fixed temperature this relation equates relative diffusivities to the square root of the inverse molecular weights of the respective liquids.

Diffusion of gases into nonpolar liquids have previously been measured by two techniques: (1) a pseudo-steady state technique developed by Hildebrand with diffusion through multiple capillaries and (2) a method by Walkley with diffusion through an open tube. Each of these methods requires prior knowledge of solubility of the gas in the liquid. An apparatus is constructed which combines these methods into a single experiment. Simultaneous solution of the two equations which describe the combined experiment yields both the solubility and diffusion coefficient. Diffusivities and solubilities of nitrogen, argon and oxygen into liquids of carbon tetrachloride and benzene as well as oxygen into water have been studied. The results compare favorably with the literature.

The diffusion cell for this technique consists of a capillary disk, which is flooded with liquid. Gas is admitted into the space over the open solvent. With temperature and pressure constant, volume uptake of the gas in the solvent is monitored. Time-volume uptake data is evaluated by the two diffusion equations. Although the experiment is conceptually easy, a small gas volume change

over a prolonged period of time poses problems in data collection and experiment control. The data collection and control is simplified by dedicating a Microcomputer Interfaced Data Acquisition System (MIDAS) to the experiment.

To my parents,
with gratitude.

Acknowledgements

I express my gratitude and respect to Dr. Paul E. Field for his guidance, assistance and infinite patience in directing this research. Without his close cooperation this work could not have been brought to fruition.

I further acknowledge members of my committee, Dr. John G. Mason, Dr. George Sanzone, Dr. Jimmy W. Viers and Dr. James P. Wightman for their conscientious consideration of the dissertation and helpful suggestions during the course of this work. I also thank for his encouragement and funding during the later part of this investigation.

I am also indebted to those who assisted in constructing and maintaining the experimental apparatus. I thank for his craftsmanship with the glassware as well as and of the electronics shop for helpful suggestions and trouble shooting of various electronic components.

Finally I wish to express my deepest appreciation and gratitude to my family and friends for their unending support and constant encouragement during the course of this research project.

Table of Contents

List of Illustrations

List of Tables

We dance around in a ring and suppose,
But the Secret sits in the middle and knows.

Robert Frost[1]

1.0 INTRODUCTION

There are two structural models of the liquid state, Hildebrand's condensed gas model and Eyring's pseudo-lattice model. The condensed gas model visualizes the gas solute molecule diffusing through the liquid by a random walk process while the pseudo-lattice model indicates the gas molecules move by jumping into vacant sites present in the liquid structure. The temperature dependence of diffusion of gases in liquids should experimentally distinguish which model is more realistic. The condensed gas model predicts a linear variation of diffusivity with temperature, while the pseudo-lattice model predicts linearity of log(D) versus 1/T. Figure 1 shows these two model pictorially. Because of negligible solubility nonreactive gas solutes as diffusing agents function as molecular probes of the liquid structure. Advantages of gas solutes as diffusing agents are variation of size, shape, mass and solute-solvent interaction. Unfortunately various methods for studying gas diffusion in liquids show significant variation in diffusivities.[2] This makes it very difficult to determine from these methods which theoretical treatment is more realistic.

Each method for measurement of gas diffusivity in liquids has a distinct set of boundary conditions. These boundary conditions describe the means by which the concentration gradient is generated. In most cases gas concentrations ranging between saturated solution to degassed solvent are assumed to generate the concentration gradient. Methods often rely only on a previously determined literature value for the gas solubility. It is also common to assume the liquid is completely

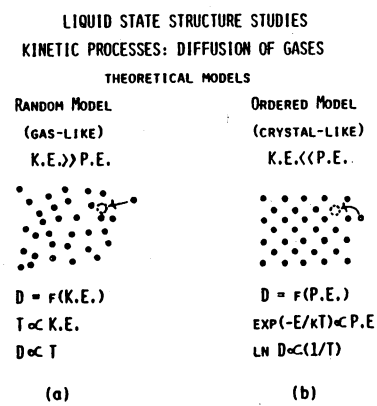

Figure 1. Structural models of the liquid state (a) condensed gas model and (b) pseudo-lattice model.

degassed at the beginning of an experiment. We have developed a new technique which combines two previous methods[3,4] and measures both the diffusivity and solubility of gases into liquids simultaneously. This determination of the solubility eliminates the previous uncertainty in assuming a literature value and also serves to provide an internal consistency check on both solubility and diffusivity.

The diffusivities from the combined technique for several solute/solvent systems are compared to those of other methods. Two studies support the assumptions of the method. One study is computer simulations modeling the combined technique to test the validity of assumed boundary conditions. The second study is an experiment which tests for complete liquid degassing. A criterion based on experiment precision is developed to test when it is possible to determine which diffusivity temperature dependence is more linear. Unfortunately the limited temperature studies in the literature and those of the combined method do not permit determination of the more realistic temperature dependence. However, diffusivities of one gas solute in two nonpolar liquids indirectly support a linear diffusivity temperature dependence by a Graham's Law like relation. At a fixed temperature this relation equates relative diffusivities to the square root of the inverse molecular weights of the respective liquids.

2.0 LITERATURE SURVEY

2.1 Introduction

In the literature on diffusion of gases into liquids two facts are apparent. First, the paucity of diffusion data results from considerable experimental difficulties which attend measurements with slightly soluble gases, with about half of the available data limited to water. Second, diffusion results show large variation over the various techniques. These facts hamper attempts of correlations to explain the temperature dependence of gaseous diffusivity. Ambiguity in gas solubility measurements and correlations parallel those of diffusion. Difficulty in the evaluation of diffusion coefficients is compounded, since a knowledge of these gas solubilities is required. Most diffusion methods rely on independent literature values as a source of solubilities. Few investigators report the method of solvent degassing or a test for extent of degassing. These are points of consideration in this survey.

2.2 *Diffusion methods*

A convenient classification of diffusion methods depends on the dynamics of the solvent and concentration gradient. Figure 2 illustrates the various methods in terms of the solvent dynamics and the concentration gradient. The concentration gradient falls into one of three categories: (1) steady state, (2) pseudo-steady state or (3) non-steady state. A steady state concentration gradient once established is time independent. The pseudo-steady state gradient shows some time variation but closely approximates a steady state. The non-steady state gradient is time dependent. The means of generating these concentration gradients depends on the solvent dynamics. Under liquid motion the methods are either laminar flow or bubble dissolution. For each case a complete understanding of the liquid hydrodynamics is necessary to evaluate the diffusion coefficient from the raw data. Laminar flow methods monitor gas absorption into a liquid jet,[5] a film adhering to a rotating drum,[6] a liquid film flowing down a cylinder or over a sphere/disk.[5, 7, 8] Taylor's method of axial diffusion in a pipe is also an example of laminar flow.[9] Laminar flow methods with the exception of the rotating disk electrode have a non-steady concentration gradient. The rotating disk electrode for diffusivity of oxygen in water depends on a steady state concentration gradient. Each of these methods have the advantage of being fast, on the order of minutes and are relatively insensitive to vibrations as well as fluctuations in temperature and /or concentration gradients. Unfortunately end effects are often very significant which causes uncertainty in the hydrodynamics. This uncertainty in hydrodynamics due to end effects results in deviation from ideal hydrodynamic models. The ideal hydrodynamic models permit calculation of the diffusion coefficient. The end effects in laminar flow techniques such as the liquid jet are deviations from a laminar flow due to turbulence where the liquid jet enters and exits the gas diffusion chamber. For bubble dissolution methods the shrinking bubble size as a function of time is a measure of the gas absorption rate.[10, 11] The bubble dissolution method is assumed to obey steady state boundary conditions. Rapid measurement of diffusivity is again the chief advantage. However these methods are very sensitive to vibration and other sources of convection. Although Johns argues that the convection

terms are small,[12] this is doubtful in view of the consistently higher diffusion values for bubble dissolution with respect to other methods.[13] Walkley reduces convection due to streaming in bubble dissolution by maintaining the gas bubble at a constant size.[14] Maintenance of bubble size by gas displacement from a micropipet monitors gas absorption. Because this method holds the gas liquid interface stationary it is classified as a quiescent liquid method.

Porous disk, capillary and open tube comprise the other categories for quiescent liquid methods. Most of these methods require hours or days and rely on measurement of volumetric gas absorption. Except for the average concentration, inverted tube and open tube techniques, each method simplifies solution of the diffusion equations with steady state boundary conditions.

The porous disk method monitors gas movement across a porous disk separating two compartments. Initially different compartment concentrations maintain the diffusion potential, with saturated solution on one side and pure solvent on the other. The porous disk experiment with solute stripping maintains this state during the duration of the experiment.[15] Since measurements are made after a steady state is reached, this method avoids any effect of initial gas solute adsorption in the porous disk. The method is also relatively rapid with typical run times of two hours. On the other hand the modified Northrop-Anson cell is susceptible to solute adsorption in the disk and requires substantially longer diffusion times.[16] This approach begins with different concentrations in the individual compartments and assumes negligible deviation from these values during the course of the experiment. A disadvantage of both porous disk methods is the requirement of calibration with a known solute/solvent system to determine the cell constant. This constant is a function of solution viscosity and implicitly contains the diffusion path length. Therefore the calibrant viscosity must be close to the solution of interest. For gases in liquids the viscosities are essentially those of the pure liquid. Therefore a calibrant using the same liquid will suffice. Neither the capillary nor the open tube techniques suffer from this calibration problem.

The capillary methods monitor gas transport from or through one or more (parallel) capillaries. In the average concentration method the gas solute migrates from a capillary initially saturated with solute into a large reservoir of unsaturated solvent.[17] The boundary conditions for the capillary method is similar to the porous disk. The capillary approaches a steady state by

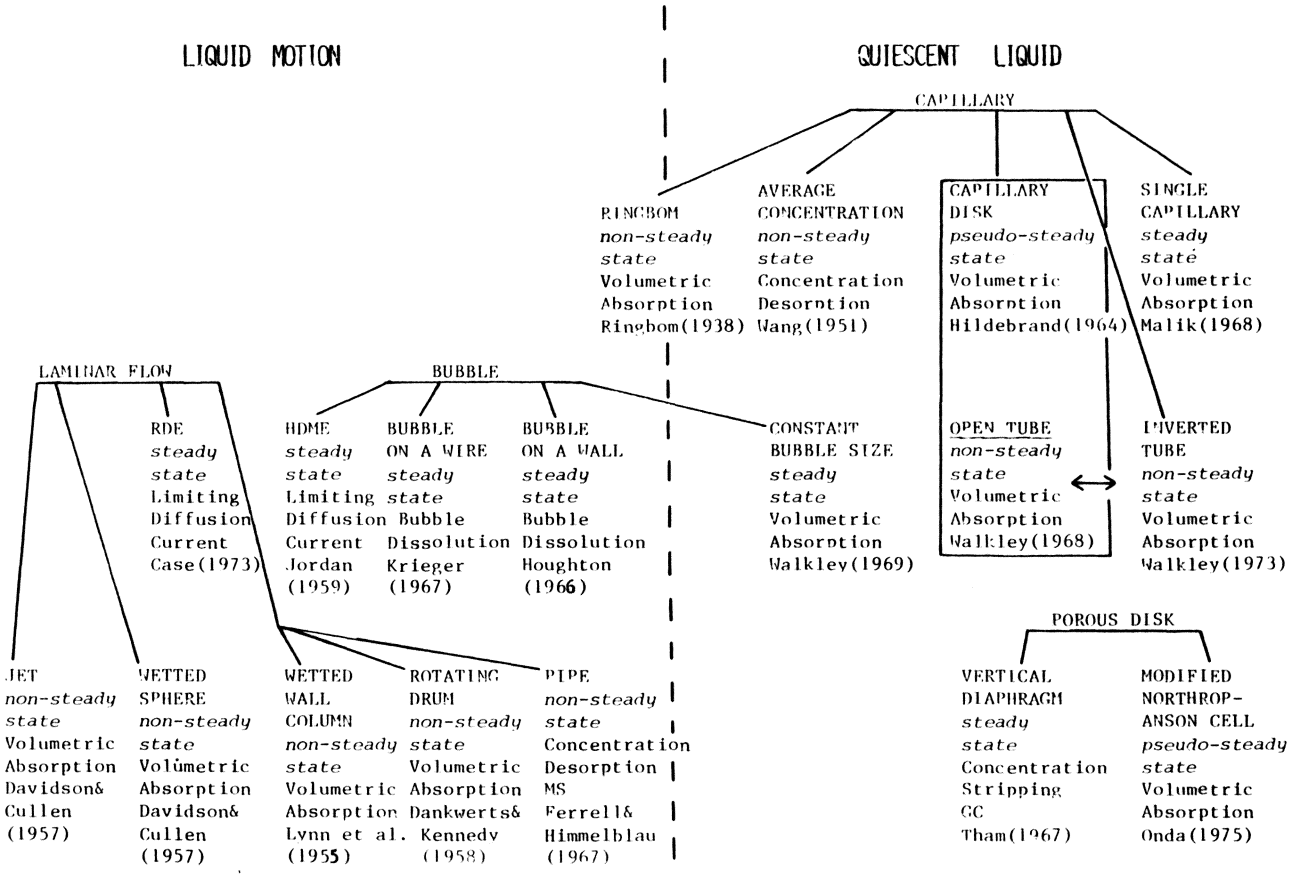

Figure 2. Diffusion methods.

maintaining a saturated solution at the top of the capillary and practically pure solvent at the bottom.[18] For the same boundary conditions the amount of gas solute uptake increases substantially for the capillary disk with the parallel arrangement of many capillaries imbedded in a circular plate.[3] This is a particularly useful modification for gases which are sparingly soluble. A shortcoming of the capillary methods are end effects. End effects are deviations from the steady state boundary conditions at ends of the capillary. These end effects cause uncertainty in the diffusion path length. This can contribute significant error to evaluation of the diffusion coefficient. Minimization of end effects with proper diffusion cell design to less than other sources of experimental error is possible. Fawcett and Canton[19] in an error analysis for the average concentration method conclude that for capillaries as large as 1 mm in diameter experimental precision can not be better than 5 to 10%. They maintain that an improvement in precision to less than 1% with very fine capillaries is possible. On the other hand the use of larger capillaries is commensurate with diffusing sufficient material to satisfy sensitivity requirements in diffusant concentration determinations. This is especially true when diffusants are sparingly soluble gases.

Convection terms can invalidate diffusion results. A possible source of convection is a density gradient. If a gas solute on dissolution into the liquid produces a solution denser than the pure liquid solvent, then convection can result for diffusion methods with gas solute diffusing downward into unsaturated solvent. Walkley's inverted tube method[20] removes this source of convection by diffusing gas upwards through a single capillary. In the open tube method[4] gas diffuses downward into a cylinder of liquid. Walkley's cylinder dimensions are 55 mm in diameter and 250 mm in length. The same nonsteady state diffusion equation describes both the inverted capillary tube and open tube methods. A solution of argon in water is denser than pure water. Walkley's open tube diffusivities for argon in water are consistently several times larger than those from his inverted tube method. The argon in water diffusivities from the constant bubble size method are also consistently larger than the inverted tube values. Walkley ascribes this discrepancy in results to the presence of density driven convection in both the open tube and constant bubble size methods.

The remaining methods in Figure 2 are electrochemical and Ringbom. The diffusion measurements by electrochemical methods rely on conformation of the limiting diffusion current to the

modified Ilkovic equation. This limiting current is totally dependent on the nondisassociated species in solution. Categorizing the Hanging Drop Mercury Electrode[21] under bubble dissolution methods and the Rotating Disk Electrode[8] under laminar flow is consistent with their respective boundary conditions. On the other hand the Ringbom approach is unique, since it encompasses aspects of both quiescent liquid and liquid motion categories.[22] In this technique a pure gas phase separates a gas free water column from a gas saturated column. The gas free column is a dead end column which serves as a gas sink while the gas saturated column is connected to a large reservoir. The rate of liquid displacement of the gas saturated column into the gas space is a measure of the diffusion rate.

This concludes a brief survey which sketches the mechanics of the various diffusion methods. A more critical comparison of the diffusion methods requires consideration of the diffusion results.

2.3 Diffusion Data

About half the literature data of gaseous diffusion in liquids are for gases in water. Due to the interest in biological/ecological mass transport studies and performance of gas electrodes in fuel cell research a large number of diffusion studies for oxygen in water exist. For all of the methods in Figure 2 with the exception of the capillary disk and single capillary the oxygen diffusivity in water is available. Therefore this system serves as a basis of comparison for various experimental techniques.

In 1971 St Dennis and Fell summarized the oxygen in water diffusivity data graphically.[2] This graph is supplemented in Figure 3 with addition of several more recent diffusion values. Also each datum is now designated by experimental method as well as reference number. St Dennis and Fell noted a range of diffusion values at 25°C from 1.87×10^{-5} to 2.60×10^{-5} cm^2/sec. They rejected points 2, 11 and 16 which were outside the 95% confidence interval for a linear least squares fit of the diffusivity and temperature. Since the diffusivity data showed large scatter as a function of

temperature, St Dennis and Fell suggested use of the Stokes-Einstein equation for predicting the diffusivities at various temperatures until more precise values have become available. A range of values at 25°C for the updated graph was from 1.87×10^{-5} to 3.40×10^{-5} cm^2/sec. Two of the new points in the updated graph fell outside the previous confidence interval for the least squares fit of the temperature dependent data. These were point 28 which extended the range at 25°C and point 30. Vivian and King obtained a value of 2.41×10^{-5} cm^2/sec with the porous disk method. Their value, point 7, is cited by St Dennis and Fell as the most reliable value. In contrast, Hung and Dinus's[23] value of 3.40×10^{-5} cm^2/sec, point 28 also used the porous disk method but with a vertical diaphragm and continuously monitoring galvanic cells for oxygen determination. This new value was significantly different from Vivian and King's. Reasons for such variations as well as trends dependent on a specific technique warrants further investigation. Similar scatter is seen in data for other gas liquid systems.[10, 26] Therefore the comparison of methods is limited to diffusivities of oxygen in water.

Wise and Houghton[10] in 1966 used the bubble dissolution method and found that most of the earlier work was 5 to 25% lower than their values. They indicated that the oxygen in water data showed much better agreement to an accuracy of about ± 5%. This paralleled the ± 5% variation of oxygen solubilities from different investigators. They emphasized the advantage of the bubble dissolution method over non-steady state methods. With non-steady state methods the square root of the diffusion coefficient was inversely proportional to the solubility while the former showed an inverse proportionality. Therefore a 10% error in solubility would reflect a 10% error in the diffusion coefficient for bubble dissolution while unsteady state methods would show a 20% error in diffusivity.

The diffusion coefficient for inert gases in liquids is independent of concentration since the solutions are ideally dilute. The knowledge of both the gas solubility and pressure is still necessary to evaluate the diffusion coefficient from experimental data. For initial oxygen concentrations in water ranging from zero to ninety percent of saturation Krieger et al.[11] with the bubble dissolution method demonstrates the concentration independence of the diffusivity coefficient. Their data is reproduced in Table I. It is worth noting that for smaller oxygen concentration ranges (i.e. con-

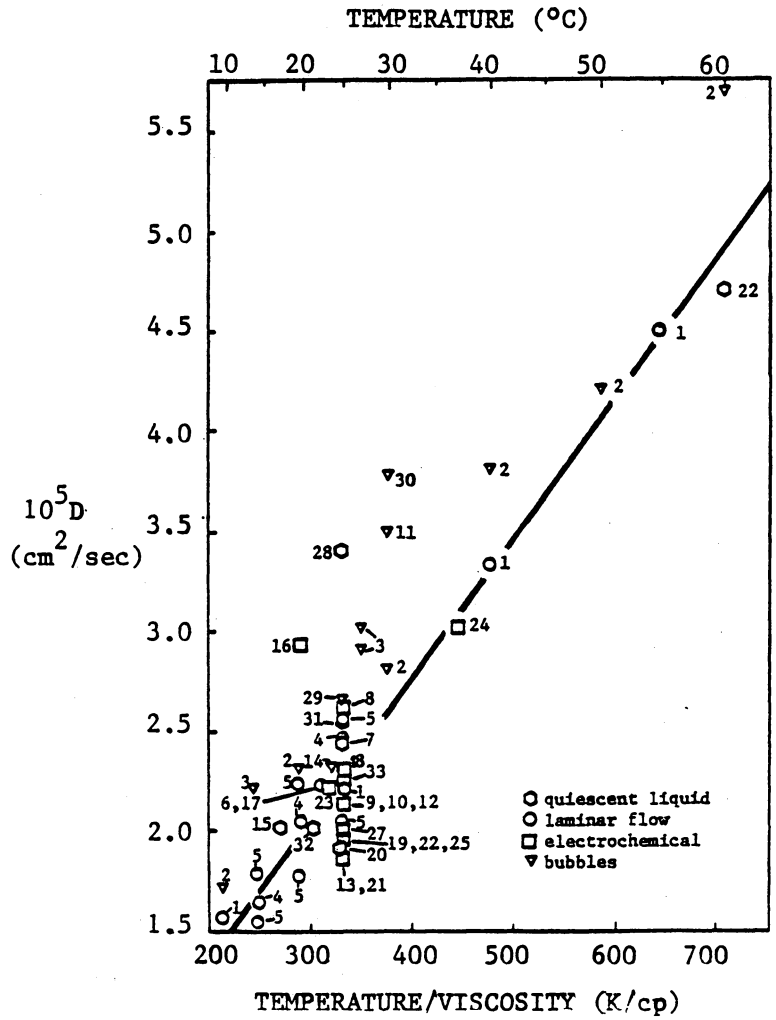

Figure 3. Method comparison with oxygen in water diffusivities. Point (reference): 1-26 (6); 27 (15); 28 (23); 29 (14); 30 (13); 31 (24); 32 (76); and 33 (25).

centration gradient small) the experimental error doubles for diffusivity determinations. The bubble dissolution method is sensitive to vibrations. Therefore an experiment duration of 75 minutes for the smaller 0.03 to 0.05 concentration range versus 10 minutes for the larger 0.98 to 1.00 range might explain the larger error in terms of cell vibrations.

Table I. Concentration dependence of oxygen in water diffusivities with bubble dissolution method. Reproduced from reference 11.

Conc. × 10^6 (moles/cc)	10^5 × D (cm^2/sec)
0.98 to 1.00	3.51 ± 0.17
0.54 to 0.65	3.37 ± 0.20
0.03 to 0.05	3.60 ± 0.32

Duda and Vientas[27] plot oxygen in water diffusivities for various methods as a function of temperature. Contrary to Wise and Houghton, they report larger variation in diffusion results. Two reasons for this disparity in conclusions are the additions and modifications of Duda and Vientas to the previous data of Wise and Houghton. The most important additions are the wetted sphere values of Baird and Davidson[28] which tend to be low. Their modifications are recalculation of diffusivities wherever possible with a common solubility value to make comparisons valid. They note the composite data falls roughly into two groups. The higher group are primarily bubble dissolution results while the lower set includes various laminar flow methods. They advocate that the commonly accepted higher value for the oxygen gas absorption into water may be in error. In support of this position they note the consistently high values of Wise and Houghton which would result from use of too high a calibrant oxygen diffusivity of 2.60 × 10^{-5} cm^2/sec at 25°C. They ascribe Carlson's[29] (1911) high diffusion value of oxygen in water to convection currents. Although the open tube diffusivity for carbon dioxide in water is known to be higher from convection by a density driven gradient,[20] this convection problem with carbon dioxide in water is not sufficient to indite the oxygen in water data as erroneous on the same grounds. Pfeiffer and Krieger[13] cite free

convection as responsible for high bubble dissolution diffusivities. They show experimentally that to obtain acceptable diffusion coefficients by the bubble dissolution methods requires the bubble radius to be less than 0.3 mm and the ratio of DC/η to be less than 4×10^{-8}. C is the gas solubility. The ratio DC/η is the reciprocal of the Schmidt number. According to Byrd et al. this ratio indicates the degree of free convection present. In aqueous solutions of pure gases for measurable bubble sizes the reciprocal of the Schmidt number is too large which makes the bubble dissolution method marginal at best.

Ng and Walkley[14] eliminate the convection experimentally with the constant bubble size technique. A diffusion coefficient of 2.65×10^{-5} cm^2/sec at 25°C is obtained. This value is in close agreement with Vivian and King's value by the porous disk method of 2.41×10^{-5} cm^2/sec as well as Wise and Houghton's calibrant polargraphy value of 2.60×10^{-5} cm^2/sec both at 25°C.

Ward[30] compares the constant bubble size[14] and liquid jet methods.[31] He points out a direct relationship between the reported diffusivities and exposure time of the gas to the liquid. For experimental techniques where the exposure time to the liquid are relatively short (e.g. liquid jet times are on the order of milliseconds) lower diffusivities are reported. On the other hand for experiments with longer exposure times (e.g. constant bubble size times are on the order of minutes) larger diffusivities are reported.

The Einstein function gives the probability of a transition in a system. Ward considers the probability of a gas molecule being condensed or evaporated from or to the surface of the liquid respectively. He incorporates this expression for the probability into the difference expression between the competing rates of gas condensation or evaporation at the liquid surface and derives an equation for the gas absorption rate. For the liquid jet method, assuming instantaneous gas saturation of the liquid, the diffusion coefficient is 1.87×10^{-5} cm^2/sec. The derived rate expression indicates the assumption of instantaneous gas saturation at the gas liquid interface for this experiment is incorrect. The diffusion coefficient from the derived rate expression for the liquid jet method is 2.54×10^{-5} cm^2/sec. This agrees quite well with the constant bubble size diffusivity of 2.65×10^{-5} cm^2/sec. The derived diffusion coefficient for the constant bubble size method is within exper-

imental precision. This emphasizes the importance of the role of boundary conditions in the description of diffusion experiments.

In conclusion various attempts to rationalize the scatter in diffusion data are prevalent in the literature. St Dennis and Fell conclude that the porous disk method gives the most reliable diffusivity of 2.41×10^{-5} cm^2/sec. Scatter in the data may be due to one or more of the following: incorrect solubilities, incomplete solvent degassing, ill defined boundary conditions and convection. This uncertainty in diffusion data hampers attempts not only to predict diffusivity as a function of temperature and to formulate an accurate model for gaseous diffusion in liquids.

2.4 Prediction of Gaseous Diffusion in Liquids

Many correlations for gaseous diffusivities (D) exist in the literature.[10] This may be in a large part due to the scatter in experimental data. There is no one equation which predicts diffusivities for all systems involving a liquid solvent.[32] A reason for this suggests itself in a log-log plot of carbon dioxide diffusivities against viscosities in water and organic liquids.[33] McManamey and Woolen's log-log plot in Figure 4 clearly shows the difference between gas diffusion in organic liquids and in water. Akgerman and Gainer believe that lack of a unifying diffusion equation is due to disregard of the solute-solvent intermolecular forces.[34] To date considerations of solute mass and size as well as solvent viscosity (η) serve as the predominate bases of correlation.

In 1955, Smith and co-workers[22] noted that the diffusivity ratio of nitrogen to argon in water, 1.53 was grossly equal to the inverse ratio of the square roots of the molecular weights, 1.2. More recently Dim and co-workers[35] demonstrated the diffusivity ratio of propane to carbon dioxide each with the same molecular weight, in heptanol and octanol were inversely proportional to the two thirds power of the molar volume ratio of the gas solutes. In fact a value of 0.57 compared quite closely to the diffusivity ratios of propane to carbon dioxide in heptanol and octanol of 0.49 and 0.55 respectively. Given the proportionality between the two thirds power of the volume ratio and

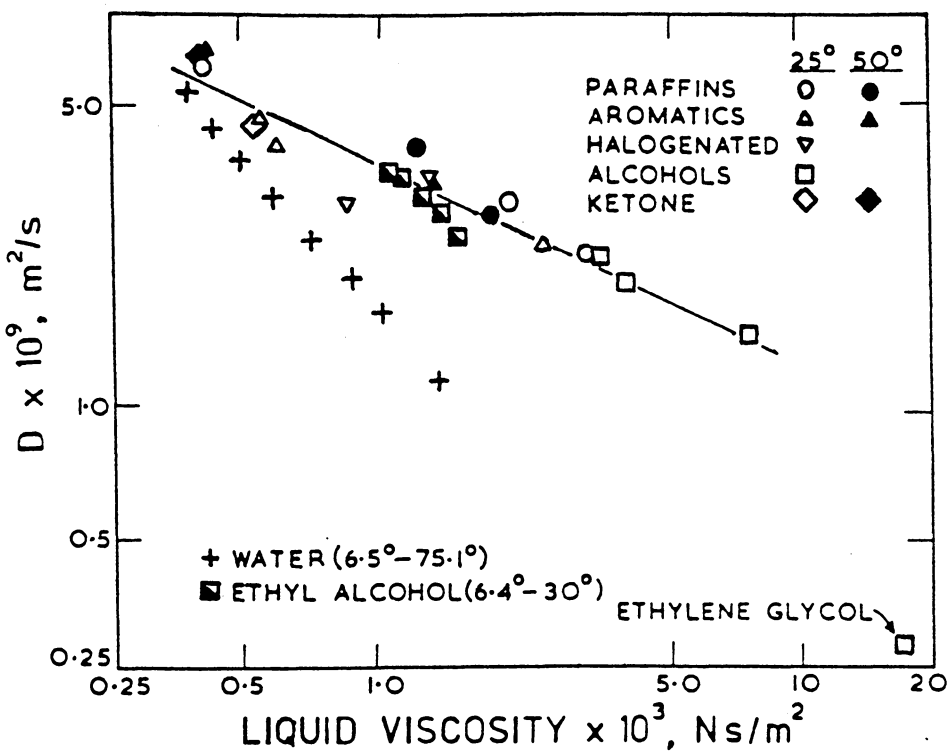

Figure 4. Carbon dioxide diffusion in polar and nonpolar liquids. This plot is Reproduced from reference 33.

cross sectional area, these results are found to be in agreement with Ross and Hildebrand's previously reported observations.[3] They showed a correlation of the product of diffusivities to molecular cross sectional areas for various gas solutes in carbon tetrachloride. A deviation from this constant product for the low molecular weight gases such as hydrogen and helium was subsequently attributed by Hildebrand and co-workers[36] to a quantum mechanical tunneling effect. The diffusion coefficient for a quantum effect increased with the square of the de Boer's quantum parameter i.e. ratio of zero point energy to classical translational energy of the gas liquid system.

Ross and Hildebrand[3] rationalize use of the cross sectional area of the gas solute by appealing to Bearman's treatment of binary diffusion with the liquid radial distribution function. Bearman relates the diffusivity to molecular volumes, v,and frictional coefficients, ζ.

$$D_1^o = v_1 kT/\zeta_{11}$$

$$D_2^\infty = v_1 kT/\zeta_{12}$$

D_1^0 is the liquid self-diffusion and and D_1^∞ the solute diffusivity at infinite dilution. With self-diffusion of carbon tetrachloride and diffusion of argon in carbon tetrachloride, Hildebrand and Ross find that the inverse ratio of the frictional coefficients of 2.57 compares well with 2.80 for the inverse ratio of cross sectional areas. They conclude that the frictional coefficients of different solutes in the same solvent depends mainly on the solute cross sectional area.

Witherspoon and Saraf[37] measured diffusivities with the average concentration method for methane, ethane, propane and n-butane in water and found the product of diffusion coefficient and cross sectional area of the gas solute not as consistent as were that of Ross and Hildebrand. This was ascribed to error in calculating the effective cross sectional areas of a group of hydrocarbons of increasing chain length from gas viscosity data. Subsequently Witherspoon and Bonoli[38] used the same experimental technique to extend this work to cover a larger temperature range as well as additional hydrocarbon solutes. Hildebrand[39, 40] examined this data using the molar volume at the boiling point (V_b) rather than the previous uncertain molecular diameters obtained from either gas viscosity measurements or the difficult to measure critical volume (V_c). The ratio of V_b/V_c is

found to be a constant for various symmetric molecules. Hildebrand found the product of $V_b^{2/3}$ and diffusivity for Witherspoon and Bonoli's data was a constant within the experimental precision. This was expected in part, since the diffusion is correlated to the viscosity and the viscosity of water at 25°C is almost equal to that of carbon tetrachloride.

Many investigators have considered the correlation between viscosity and diffusivity. Houghton and co-workers,[41] in diffusion studies of isobutylene into dinonyl phthalate found that the ratio $D\eta/kT$ (where k is Boltzman's constant) was not constant over the entire temperature range studied. Houghton compared the plots of $\log(1/\eta)$ versus 1/T with log(D) versus 1/T. He concluded that the deviation of $\log(1/\eta)$ from log(D) at lower temperatures indicated a difference between the mechanisms of isobutylene diffusion and dinonyl phthalate self diffusion. Hildebrand[14] related viscosity and diffusion by amplifying the work of Batschinksi (1913). In this formulation, an expression for the fluidity $(1/\eta)$ is derived which is proportional to diffusivity. This relation is expressed in equation 1.

$$D \propto \frac{1}{\eta} = B\frac{(V - V_o)}{V_o} \qquad (1)$$

V_o is the intrinsic molar volume (the volume at which fluidity starts); V, molar volume ; B, proportionality constant (a measure of extent of absorption by liquid molecules of the externally generated momentum of viscous flow).[42] Hildebrand recognized that fluidity depended on the relative liquid expansion, $(V - V_o)/V_o$. The magnitude of expansion proved less than 10% for carbon tetrachloride and benzene at 20°C with low viscosities of 0.97 and 0.65 cp respectively. Self diffusion studies agreed with the fluidity. On extrapolation of carbon tetrachloride diffusion data to zero fluidity, a temperature of -25.0°C resulted which is approximately the melting point of carbon tetrachloride, -23.0°C. Conversely extrapolation to zero fluidity yielded a molar volume of 88.3 cc, very close to the solid carbon tetrachloride molar volume of 87.9 cc. Such a direct comparison for benzene was not possible since carbon tetrachloride is frozen into a solid with rotating molecules while benzene has become a laminar solid at 6.0°C. However the self diffusion slopes

are explained qualitatively by resorting to an equation describing the translational energy, $1/2mv^2 = 3/2(kT)$, where m is the molecular mass and v, the rms speed in free space. Letting b = benzene and c = carbon tetrachloride, the ratio of the energy equations of benzene to carbon tetrachloride resulted in $v_b/v_c = (m_c/m_b)^{1/2} = (154/78)^{1/2} = 1.41$. This compared closely to the ratio of the slopes for the self diffusion temperature plots of 1.63, indicating for nonpolar solvents that mass was the most important factor governing the liquid self diffusion.

Table II. Diffusion Correlations. Variable definitions: 1, solvent index; 2, solute index; η_1, solvent viscosity; R_2 , hard sphere radius of solute; χ_1, association number; M_1, molecular weight of solvent; V_2, molal volume of solute; V_2^*, critical molal solute volume; V_1^*, critical molal volume and N, Avogadro's number.

Stokes-Einstein (1905)	$D_{12} = \frac{kT}{6\eta_1 \pi R_2}$
Wilke-Chang (1955)	$D_{12} = 7.4 \times 10^{-8} \frac{\sqrt{\chi_1 M_1}}{\eta_1 V_2^{2/3}}$
Hildebrand (1971)	$D_{12} = D_{11}\left(\frac{V_1^*}{V_2^*}\right)^{2/3}$
Sridhar-Potter (1972)	$D_{12} = 0.88\frac{V_1^{*4/3}}{N^{2/3}} \frac{RT}{\eta_1 V_o} \frac{1}{V_2^{*2/3}}$

Based on these observations relating to mass, size and viscosity, the various correlations put forth in the literature can be examined. Table II summarizes some correlations along with variable definitions. Many times investigators resort to the Stokes-Einstein correlation (equation 1 of Table II) as in the case of St Dennis and Fell for a rapid estimation of diffusivity. The assumptions in derivation of the Stokes-Einstein equation are that a solute moves through a continuous medium and the solute is represented by a hard sphere. These assumptions may not in general be reasonable for gaseous diffusion in liquids. On the other hand the Wilke-Chang correlation, equation 2 of Table II, is semi-empirical. This equation is based on the qualitative conclusions of Eyring's significant structure theory and the Stokes-Einstein relation.[43] The association number, χ_2 , in part accounts for the variation in the intermolecular potential between solute and solvent for various gas

liquid systems as mentioned by Akgerman and Gainer.[34] Wilke and Chang[43] give values for χ_2 of 2.6 for water and 1.0 for unassociated or nonpolar liquids. Akgerman and Gainer propose the following approximation for the association number (i.e. degree of hydrogen bonding) of various substances when not available.

$$\chi_2 = \left(\frac{\Delta H_{vap}\text{hydrogen bonded substance}}{\Delta H_{vap}\text{homolog}} \right)^{2/3} \tag{2}$$

The homolog is the substitution of a methyl group for a hydroxy group (e.g. the homolog of water is methane). The remaining correlations of Table II of Hildebrand[44] and Sridhar-Potter[45] are also semi-empirical. Hildebrand's correlation relies on the self diffusion of the solvent as well as the previous results of Ross and Hildebrand showing cross sectional area of the gas solute as the major contribution to the gaseous diffusivity. Table III compares equation 3 of Table II to Ross and Hildebrand's data. Hildebrand's correlation is modified by Sridhar and Potter with the substitution of Dullien's[46] equation for self diffusion. Dullien's equation relies on the effective molecular diameters in liquids. Introduction of a correction factor of V_b/V_o accounts for cases where the temperature dependence of the molar volume of expansion is not negligible (e.g. benzene). Sridhar and Potter point out that although the correction factor is simple it lacks theoretical justification. Since Hildebrand[42, 44] purports the relation $V_o = 0.3 * V_b$ to be true for nonassociated liquids, Sridhar and Potter's equation simplifies as follows.

$$D_{12} = 0.28 \frac{V_1^{*\,1/3}}{N^{2/3}} \frac{RT}{\eta_1} \frac{1}{V_2^{*\,2/3}} \tag{3}$$

Table IV is a representative sample of how well this correlation performs. The broader utility of this correlation is the applicability to liquid-liquid systems as well as gas-liquid systems. The omission of correlations in Table II using significant structure theory is noteworthy.

The omission of correlations using significant structure theory is due to the preponderance of experimental evidence inconsistent with such a model of the liquid state.[47] Clearly a model not accounting for any pertinent property of the liquid state is to be disregarded.

Table III. Hildebrand's diffusion correlation results for various gases in carbon tetrachloride at room temperature and one atmosphere.

Gas Solute	CCl_4	CF_4	CH_4	N_2	Ar
V_c(cc/mole)	276	145	98.6	90.0	74.5
$V_c^{2/3}$	42.5	27.5	21.3	20.1	17.7
obs, 10^5D(cm^2/sec)	1.41	2.04	2.78	3.42	3.63
calc, 10^5D(cm^2/sec)	----	2.18	2.87	2.97	3.38

Inconsistencies in Eyring's significant structure model were put forth by Hildebrand. In the past the temperature dependence of both diffusivity and viscosity was represented as the logarithmic value versus reciprocal temperature. This treatment appealed to the analogy of the Arrhenius equation for rate constants. This model is based on the existence of barriers against fluid flow or some kind of quasi-lattice structure with holes into which a solute molecule jumps. Haycock, Alder and Hildebrand[48] considered the rate of diffusion of iodine in carbon tertrachloride as a function of temperature at constant volume where the number of holes would be a constant. Later Watts, Alder and Hildebrand considered the self-diffusion of carbon tertrachloride.[49] In each case, interpretation of the data according to the significant structure theory yielded jump lengths much smaller than molecular diameters. From these studies Hildebrand advocated that the kinetic energy played a predominant role in the temperature dependence of the diffusivity at constant volume rather than the potential energy which is known to be relatively insensitive to temperature. Subsequently equation 1 emphasized the role of the kinetic energy contribution over a wide range of temperatures and pressures for scores of liquids including metals. The fact that the liquid could be so fluid although expanded so little over the intrinsic volume was also evidence against a hole theory with a jumping distance of exactly one molecular diameter according to Hildebrand. Both self-diffusion

of carbon tetrachloride and a freezing point of -23°C for carbon tetracholride with rotating molecules are consistent with equation 1. Since fluidity is proportional to diffusivity, Hildebrand advocates that the temperature dependence of diffusivity should be linear.

Equilibrium solution properties as well as transport properties add support to Hildebrand's condensed gas model of the liquid state. Chapter 3 of reference 50 summarizes the thermodynamic evidence. One especially convincing observation is that partial molal volume of the same gas solute in various nonpolar solvents having very different molar volumes are almost equal.[51, 52] These facts substantiate Hildebrand's view that gas solutes do not jump lengths longer than molecular diameters into holes but rather make their own.

Examination of the diffusion temperature dependence should indicate whether Hildebrand's condensed gas model or Eyring's pseudo-lattice model is better. The diffusion correlations in Table II are informative as to the diffusion process, but as Himmelblau[26] stated in the 1964 review of gaseous diffusion in liquids, the theoretical and semi-theoretical equations of diffusivity do not clearly indicate the temperature dependence because they involve temperature dependent variables such as viscosity or self-diffusion. He also noted that a shortage of reliable data makes it difficult to evaluate the diffusivity temperature dependence. The situation has not improved significantly in the interim. Table V lists the solute solvent systems which have been studied at three or more temperatures to date. These systems are limited in type, temperature range, ΔT, and number of diffusion temperatures, n(T). Comparison of a logarithmic diffusivity as a function of reciprocal temperature to diffusivity as a linear function of temperature requires a limiting experimental precision dependent on the range of diffusivities. A plot of Log(D) versus 1/T for D versus T linear shows deviation from linearity as shown in Figure 5a. The maximum deviation from a straight line connecting the end points of the logarithmic plot, ϵ_{max}, is dependent on the range of diffusivities (i.e. D_{max}/D_{min}). Figure 5b shows that a least squares straight line through the transformed data would require the scatter in diffusivities to be less than $\pm \epsilon_{max}/2$ to determine curvature in Log(D) versus 1/T. For significant curvature, the least squares fit of an additional squared term in the independent variable should show a pronounced reduction in variance.[57] Column 3 of Table V lists an estimate of the largest scatter in diffusivities permissible to test for nonlinear temperature dependence. The

Table IV. Sredhar-Potter diffusion corelation, selected values. For experimental values from reference 34.

Gas/Liquid	T (°C)	obs, 10^5D (cm^2/sec)	calc, 10^5D (cm^2/sec)
O_2/H_2O	20	2.01-2.3	2.1
	25	2.07-2.6	2.4
	40	3.33-3.8	3.44
	60	5.7	5.1
N_2/C_6H_6	25	6.93	5.38
CH_4/CCl_4	25	2.89	3.31

diffusion data in Table V is assumed to have an experimental precision of ± 5% unless the author indicates a larger scatter in the data. At ± 5% precision, the systems of Table V which should be tested for linearity are listed in Table VI. The significant levels are the percent levels at which a linear or quadratic equation cannot be fitted to the data based on the Fisher F test.[57] Only two cases, designated by asterisks, in Table VI indicate a significantly more linear plot. These cases show a better fit for the Log(D) versus 1/T plot. Unfortunately the limited data does not provide a definitive test of the diffusivity temperature dependence. Therefore one would tend to favor the simpler D versus T plot until more precise data become available.

Hildebrand indicates that relative expansion volume $(V - V_o)/V_o$ supports a linear dependence of diffusivity on temperature. Hildebrand[17] notes that the diffusivity ratio of 25°C to 0°C for methane, 1.41; carbon tetrafluroide, 1.41 and nitrogen, 1.48 in carbon tetrachloride are almost identical to the same temperature ratio for $(V - V_o)/V_o$ for carbon tetrachloride, 1.47.

Not only temperature variation of diffusivity but also a range of gas solutes can serve to elucidate the liquid structure. Ross and Hildebrand[3] in 1964 showed that the product of gas solute cross sectional area and diffusion was constant which supported the condensed gas model. Unfortunately cross sectional areas for gases show uncertainty. Therefore in 1971 Hildebrand substitutes

Table V. Literature sources of diffusivity temperature dependent data. Where jet denotes the annular jet method and ws, the wetted sphere method.

Solute/solvent	quoted percent precision	permitted percent precision	n(T)	ΔT	reference
CH_4/H_2O	4	10	56	38	
	4	0.2	4	18	37
	10	8	6	50	10
	2	2	8	35	20
C_2H_6/H_2O	4	10	4	56	1
	4	0.2	4	56	38
	10	6	6	50	10
	--	0.8	3 jet	10	28
	--	0.4	3 ws	10	28
C_3H_8/H_2O	4	13	4	56	38
	4	0.3	4	18	37
	10	7	6	50	10
C_4H_{10}/H_2O	4	13	4	56	38
	4	0.3	4	18	37
	10	14	6	50	10
CH_3Cl/H_2O	2	4	6	25	20
CH_3Br/H_2O	2	4	6	25	20
$CHCl_2F/H_2O$	2	5	6	25	20
CO_2/H_2O	2	4	8	25	20
O_2/H_2O	10	7	6	50	10
	--	0.4 jet	3	10	28
	--	0.6 ws	3	10	28
	--	5	4	45	9
N_2/H_2O	10	8	6	50	10
	--	0.6 jet	3	10	28
	--	0.2 ws	3	10	28
H_2/H_2O	--	4	4	45	9
	--	5	6	50	10
	--	0.3 jet	3	10	28
	--	0.7 ws	3	10	28
Ar/H_2O	2	4	8	35	20
	10	9	6	50	10
	--	2	3	50	54
He/H_2O	10	4	6	50	10
	--	2	4	45	9
	--	0.5	3	50	54
	--	0.6 jet	3	10	28
	--	0.2 ws	3	10	28
Ne/H_2O	2	6	6	50	53
	--	2	3	50	54
Kr/H_2O	2	9	6	50	53
	--	3	3	50	54
Xe/H_2O	2	30	6	50	53
	--	4	3	50	54
CO/H_2O	2	14	6	50	53
NO/H_2O	2	27	6	50	53
Isobutylene/DNP	5	60	5	75	41
CO_2/Toluene	--	1	3	30	55
$H_2/(C_4F_9)_3N$	--	0.1	3	20	56
$Ne/(C_4F_9)_3N$	--	0.9	4	30	56
$Ar/(C_4F_9)_3N$	--	2	4	30	56
$C_2H_6/(C_4F_9)_3N$	--	4	4	25	56
$CF_4/(C_4F_9)_3N$	--	5	4	30	56
$SF_6/(C_4F_9)_3N$	--	0.1	3	10	56

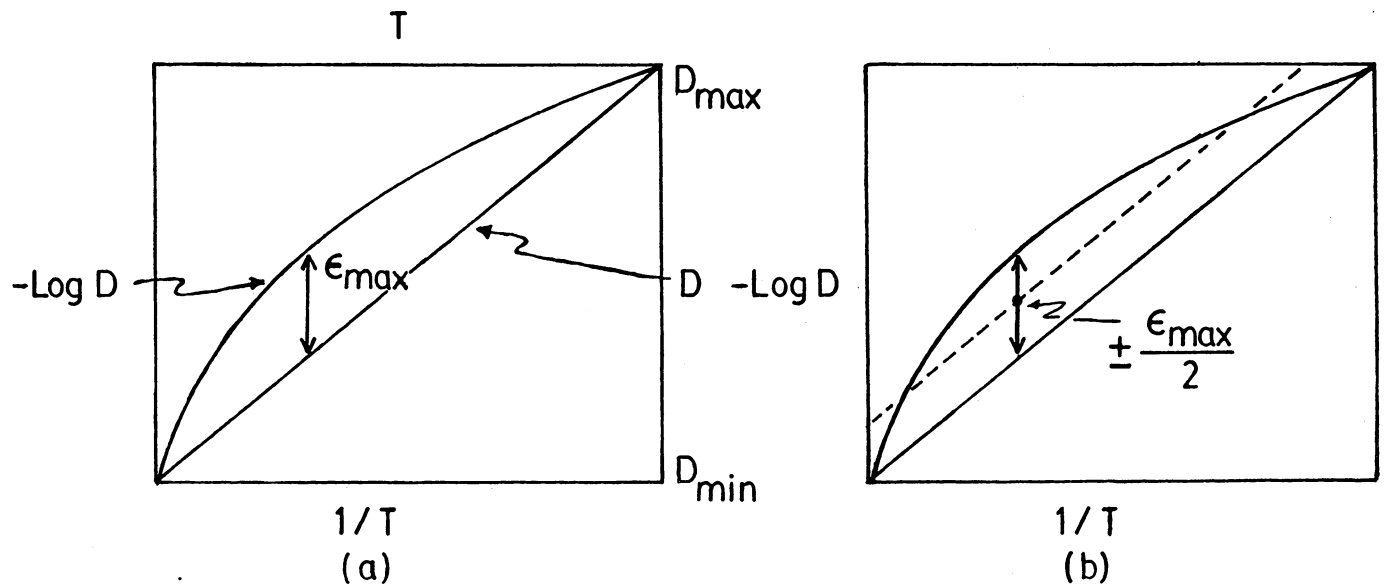

Figure 5. Experimental precision and nonlinearity in diffusivity temperature dependence. (a) Largest deviation of Log D versus 1/T assuming diffusivity varies linearly with temperature (b) Largest permissible scatter in diffusivity data before curvature in Log D versus 1/T plot is no longer detected.

Table VI. Linearity of diffusivity temperature dependence.

Solute/Solvent	D versus T		Log D versus 1/T		reference
	$mT + b$ linear	$a + bT + cT^2$ quadratic	$m(1/T) + b$ linear	$a + b(1/T) + c(1/T)^2$ quadratic	
CH_4/H_2O	0.3	13.8	0.2	24.6	38
C_2H_6/H_2O	0.4	12.1	0.1	25.9	38
C_3H_8/H_2O	0.4	12.1	0.1	19.9	38
C_4H_{10}/H_2O	0.6	1.3	0.1	1.4	38
	0.1	1.4	0.1	13.5	10
Kr/H_2O	0.4	0.2	0.04	0.5	53
Xe/H_2O	0.7	1.6	0.1	12.8	53
CO/H_2O	0.1	27.4	0.1	26.5	53
*NO/H_2O	0.5	0.8	0.1	34.9	53
*Isobutylene/DNP	1.2	1.2	0.01	23.4	41

the more reliable 2/3 power of either boiling point molar volume, V_b, or critical molar volume, V_c, for a measure of the gas solute cross sectional area. Based on fluidity considerations the use of intrinsic molar volume, V_o, is advocated. Hildebrand and Lamoreaux[42] in 1972 noted that the product $DV_o^{2/3}$ failed to be uniform for a larger range of gas solutes than Ross and Hildebrand at 25°C. Since the product $DV_o^{2/3}$ is far from uniform they suggested use of an additional parameter for correlation.

Hildebrand's[42] investigations on the solubility and entropy of solution for nonreactive gases in nonpolar liquids have yielded information pertinent to diffusivity. For example the ratio of the partial molal volumes, V_2, to the molar volumes at boiling points, V_b, for ethylene, methane, and nitrogen in carbon tetrachloride are 33.5, 51.8 and 67% respectively. This expansion is seen to contribute significantly to the diffusivity. A measure of this expansion is the configuration entropy, $\Delta\overline{S}^c$.

The configuration entropy is associated with one of two steps that describes the solution process of nonreactive gases into nonpolar liquids. The first step is the expansion of an ideal gas to a pressure, $P = C_sRT$, equivalent to the gas saturation concentration in the liquid. The second step changes the phase at constant concentration from gas to solution. The entropy of dilution in expanding the gas is $-R\mathrm{Ln}(x_2)$ where x_2 is the mole fraction of gas solute in solution. The configuration entropy is the entropy for a change in the environment of the gas from the gas state to solution state. A reproduction of Hildebrand and Lamoreaux's graph in Figure 6 shows the relationship between the dilution and configuration entropies. The sum of the dilution and configuration entropies is the excess partial molal entropy. To define the excess partial molal entropy it is necessary to consider a hypothetical liquid. This liquid boils at 25°C and 1 atmosphere pressure with a condensation entropy of -21 cal/mole-deg. This entropy of condensation is based on the entropy of 21 nonpolar liquids. The corrected vapor volumes of those liquids (Hildebrand's Rule) give an entropy of vaporization of exactly 21 cal/mole-deg. The entropy in excess of condensing the pure liquid is the excess partial molal entropy by definition.

$$\Delta\overline{S}_2^E = (\overline{S}_2 - \overline{S}_2^g) + \frac{21\ \text{cal}}{\text{mole deg}} \tag{4}$$

Therefore it is the difference of the partial molal entropy of solution and -21 cal/mole-deg as shown in Figure 6. The large to small values of the excess partial entropy represents a progression of gas solutes becoming more and more like the solvent until they coalesce at the intercept into the hypothetical liquid. This progression is interpreted by Hildebrand as the approach of the gas solute's intermolecular potential to that of the liquid.

Hildebrand and Lamoreaux[42] show a correlation between the entropy and the product $DV_o^{1/3}$ in Figure 41a. The conclusion drawn is that the diffusivity is enhanced for gas solutes with low attractive potentials or large configuration entropies. Hildebrand and Lamoreaux's interpretation of this is that the liquid molecules gain added freedom in the vicinity of a gas solute molecule because of attractive forces lower than those of the liquid itself.

In conclusion, Hildebrand's consideration of entropy gives added evidence to the view of gaseous diffusion as a statistical random walk rather than an activated barrier crossing. It also emphasizes the importance of solubilities both in measurement and interpretation of diffusion results. Interpretation of gas diffusivity in nonpolar liquids, to date, has relied on two approaches: (1) diffusivity comparison of various gas solutes into one liquid at a fixed temperature and (2) gas diffusivity temperature dependence of various gases in one liquid. There is little consideration in the literature of one gas solute in various liquids. Indeed this emphasizes a need to consider a wider range of liquids in determining a model for the liquid state with diffusivity data.

2.5 Solubility Considerations

Unlike gaseous diffusion into liquids for which there is only one comprehensive review,[26] gaseous solubility is copiously reviewed. In the most recent review of nitrogen and air solubility in liquids Battino, Rettich and Tominaga[58] in 1984 have cited various literature reviews from Mankhan and Kobe's[59] general review in 1941 to date. Therefore we shall consider aspects of sol-

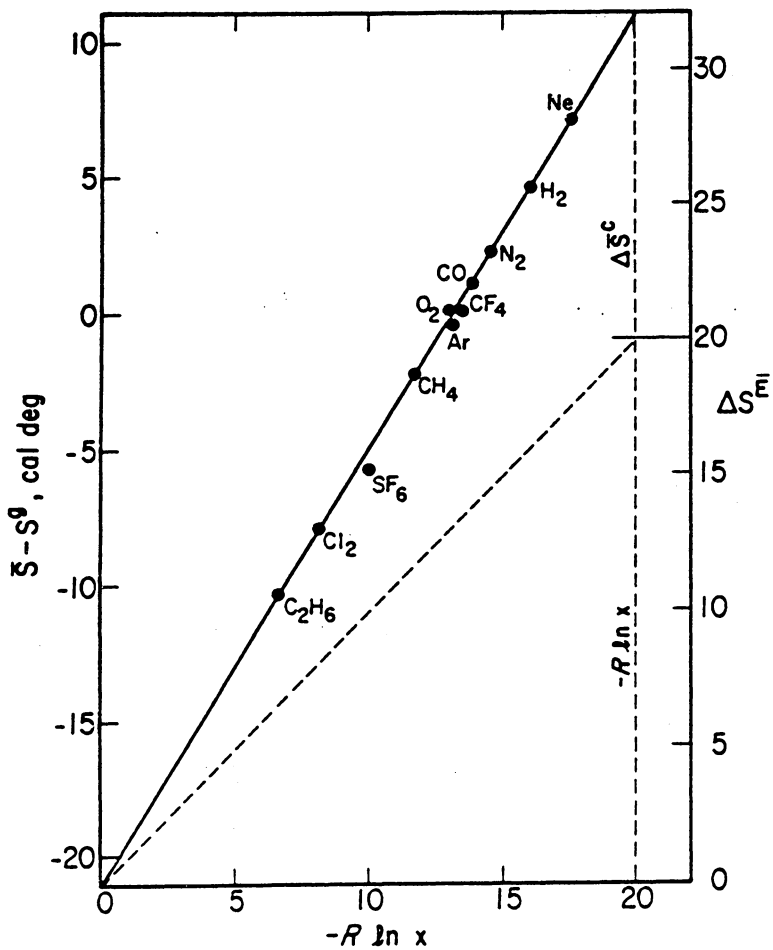

Figure 6. Excess molal entropy for gases in carbon tetrachloride. This is a reproduction of the plot in reference 42.

ubility determination applying to measurement of diffusivity with only a cursory review of solubility models.

Solubility methods rely on either gas absorption or desorption. Absorption begins with degassed solvent and monitors the amount of solute gas required for solution saturation. Conversely desorption starts with a saturated gas solution and strips out all gas. Since only one diffusion method in this survey uses desorption,[24] the focus here will be on absorption.

In most cases the method of solvent degassing for diffusion studies assumes complete degassing. The diffusion literature rarely mentions the degassing procedure. Degassing procedures fall into two categories: (1) evaporation and (2) freeze-melt. Battino and Clever[60] describe each in detail. The evaporation methods usually entail boiling the solvent under partial vacuum for 1 or 2 hours with a loss of 10 to 20% of the solvent. The freeze-melt technique places frozen solvent under vacuum for one hour or more followed by melting the solvent under its own vapor pressure. It is necessary to repeat this procedure at least three times. The advantage of freeze-melt over evaporation is minimization of solvent loss. However, Battino and Clever emphasize that with the freeze-melt method it is more important to check for complete degassing.

Cook and Hanson[61] describe two tests for complete solvent degassing. These tests are liquid compression and base pump pressure. The first test compresses degassed liquid and solvent vapor. If all the solvent does not condense, then the degassing procedure is repeated. Detection of noncondensible gas bubbles smaller than 0.001 cc is possible. We use and describe a comparable method to check for degassing in section 4.5. The second test monitors a vacuum thermocouple gage located between the last solvent trap and the vacuum pump. During evacuation the gage reading should fall from above 1000 microns to base pump pressure. Reaching the base pump pressure indicates only negligible amounts of noncondensible gases are present. Allowing an additional quantity of liquid to evaporate insures complete degassing. The solvent after degassing is then ready for temperature equilibration and subsequent gas absorption measurement.

Horiuti[62] considers gas solubility in various organic solvents. He measures the gas solubility volumetrically. The question of whether the gas buret measuring the gas volume uptake should contain dry gas (dry method) or gas saturated with solvent vapors (wet method) is considered. Little

solvent vapor is found in the gas buret for solvents with a low vapor pressure. However solvent vapor in the gas buret becomes important in consideration of liquids with high vapor pressures. In comparing the dry and wet methods there are two distinct disadvantages of the wet method. First the connection between gas buret and absorption cell is in general at a temperature different from the thermostat. Therefore it is difficult to transfer gas saturated vapor from one vessel to the other without change in composition when the thermostat temperature is greater than that of the connecting line. This is because of solvent condensation in the connecting line. Secondly, for temperature measurements not far below the solvent boiling point the partial pressure of solute is too small for determination of a definite gas saturation end point. In extreme cases equilibrium may appear to exist without any gas transfer to the absorption cell. The first problem certainly applies to the volumetric measurement of gas diffusivities. Hildebrand[42] in the capillary disk experiment maintains that the gas solute in the gas buret is unsaturated with solvent vapor throughout experiment duration due to connection of the diffusion cell and gas buret with a long capillary tube. He contends that the gas flow rate through this capillary tube connection far exceeds the counter diffusion of solvent vapor.

Horiuti's solubility measurements in organic liquids are undoubtedly good in quality; however, the number of independent measurements made on these solute/solvent systems limits their utility as a standard. Battino and Clever[60] suggest oxygen in water is a reliable standard for solubility comparisons. Workers have obtained identical values with different techniques, including both physical and chemical methods, at 25°C and 1 atmosphere pressure. The ready availability of oxygen and water in high purity may in part account for this consistency in reported solubilities. Since literature solubilities are typically used in determination of diffusivities, this is ample reason for selection of this system for comparison of various diffusion methods.

Solubility correlations parallel those of diffusion. Solubility correlations include Uhlig's cavity formation model, Hildebarand's regular solution theory and the statistical mechanical Scaled Particle Theory.

Uhlig's correlation of solubility with surface tension is analogous to the Stokes-Einstein correlation of diffusivity to viscosity. Uhlig[63] derives an expression for solubility on the premise that

the energy of solution is two terms. The first term is the work to form a cavity for the gas solute molecule and is proportional to $4\pi R^2\gamma$, where R is the solute molecule radius and γ, solvent surface tension. The second term is a solvent solute interaction energy (E). The resulting correlation is equation 1 of Table VII relating the Ostwald coefficient (γ') to these energies. γ' is the ratio of gas concentration in the gas phase to gas concentration in the liquid solution.

The Regular Solution Theory employs solubility parameters to predict solubilities and account for small deviations from solution ideality for gases in liquid. This is similar to Hildebrand's correlation of gaseous diffusion to self diffusion. A regular solution has the same entropy and volume of mixing as an ideal solution but the enthalpy of solution may be significantly different from an ideal solution. The solubility parameter is defined by

$$\delta = (\Delta E^{vap}/V_l)^{1/2} \tag{5}$$

where the quantity $\Delta E_{vap}/V_l$, the cohesive energy density, is a measure of the internal pressure of the liquid. ΔE_{vap} is the molal energy of vaporization of the gas and V_l is the molar volume of the liquid. Expression 2 in Table VII[64] provides a semi-empirical equation for the estimation of gas solubility using the solubility parameters of both solute and solvent. It is reliable in the region of one atmosphere pressure for solvents having high internal pressures such as benzene and carbon tetrachloride.

The Scaled Particle Theory (SPT) uses the radial distribution function and requires no input of thermodynamic parameters for determining gas solubility in the liquid.[65] The closest diffusion parallel for SPT is the self diffusion correlations of Dymond for such liquids as carbon tetrachloride and benzene which also use the radial distribution functions as a starting point.[66] SPT builds on statistical mechanical theory of Reiss et al.[67] Pierotti uses the hard sphere approach of SPT for approximation of the radial distribution function for gases in liquids. The only portion of the hard sphere radial distribution function which contributes to chemical interactions is the particle number density in contact with the hard sphere solute particle. The calculation of the reversible work of introducing a spherical particle into a fluid of spherical particles results in the solubility expression 3 of Table VII.

Table VII. Solubility correlations. Variable definition: $Y = \pi a_1 \rho/6$; ρ, n umber density of liquid; γ', Ostwald coefficient; R, solute radius; γ, solvent surface tension; E, solute solvent interaction energy; p_2 , solute gas pressure; V_2, solute molar volume; δ, solubility parameter; K_H, Henry's Law constant; a_1, hard sphere diameter of solvent; a_2, hard sphere diameter of solute; $r = (a_1 + a_2)/2$; V_1, solvent molar volume; R , gas constant and T, temperature.

Uhlig	$\text{Ln}\,\gamma' = \dfrac{(-4\pi R^2\gamma + E)}{kT}$	(1)
Hildebrand	$-\text{Ln}\,x_2 = \text{Ln}\,p_2^o + V_2(\delta_1 - \delta_2)^2/4.5T$	(2)
Scaled	$\text{Ln}\,K_H = [-\text{Ln}(1-Y) + 4.5(Y/(1-Y))^2]$	
Particle	$-(r/a_1)[\sigma Y/(1-Y) + 18(Y/(1-Y))^2]$	
Theory	$+(r/a_1)^2[12Y/(1-Y) + 18(Y/(1-Y))^2]$	
	$-1 + \text{Ln}(RT/V_1)$	(3)

2.6 *Summary*

Diffusion methods have been reviewed with regard to methodology and resultant diffusion data. Because oxygen in water data exists for most methods, this data was considered for method comparison. Battino and Clever[60] have also recommended this system as a convenient standard for solubility measurements.

The basis of various diffusion correlations were considered. In terms of regular solution theory, Hildebrand[42] relates diffusion to the thermodynamic property of configurational entropy. This, among other evidence, lends support to the random walk view of gaseous diffusion rather than an activated barrier crossing hypothesis. Pertinent aspects of solubility measurements to diffusion determinations have been considered and various solubility theories are given analogous to those of diffusivity.

3.0 DIFFUSION CELL CHARACTERIZATION

3.1 Introduction

The open tube method with a non-steady state concentration gradient monitors the rate of gas absorption into a cylinder of degassed liquid which appears infinite in length. The capillary disk method relies on the establishment of a pseudo-steady state concentration gradient across a parallel arrangement of capillaries imbedded in a circular plate. This concentration gradient for the capillary disk method is a gas saturated liquid layer above the disk and approximately zero concentration below it. The gas absorption rate for the capillary disk method is a linear function of time while for the open tube method the gas absorption rate is linear with the square root of time. The methods are combined by flooding the region above the capillary disk with a layer of degassed solvent about 15 mm in depth. Figure 7 shows the diffusion cell, cell dimensions and regions of individual component experiments for the combined technique.

Experiments satisfying either the boundary conditions of the open tube or capillary disk experiments simplify solving the differential equations of Fick's laws for determination of the diffusion

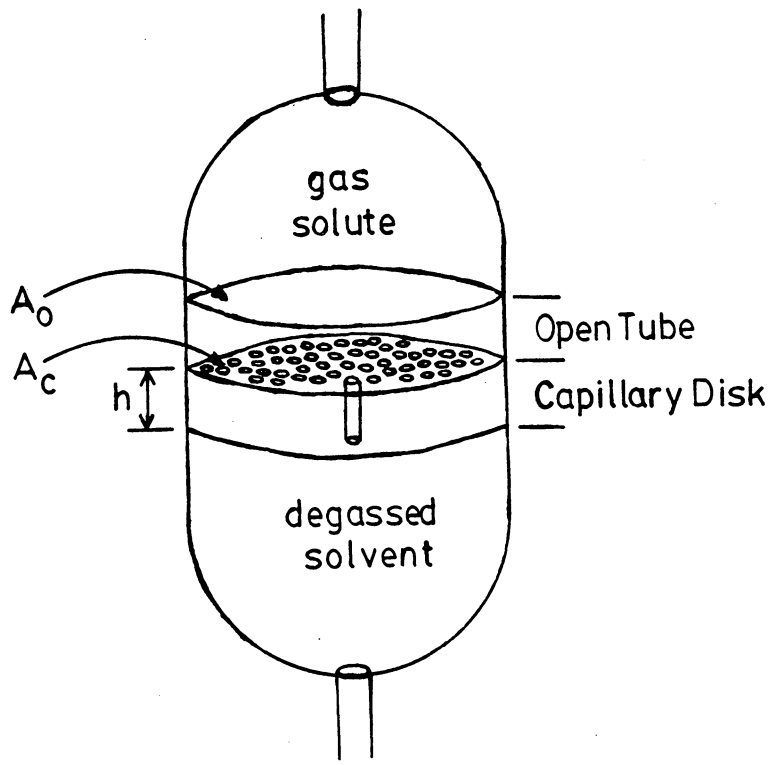

Figure 7. Diffusion cell for combined experiment.

coefficient. Whether the individual boundary conditions for the open tube and capillary disk methods still hold for their counterparts in the combined procedure must be considered. If the boundary conditions were not valid, then calculation of the diffusion coefficient would be erroneous.

Analytical solution of Fick's laws for time dependent boundary conditions may be intractable. Simulation of the diffusion process with finite difference equations can determine the extent of error in calculation of the diffusion coefficient assuming steady state boundary conditions. Potential time dependent variations of the boundary conditions for the capillary disk are (1) liquid above the disk never reaches gas saturation and (2) gas concentration below the disk builds up appreciably over duration of the experiment. These effects are dependent upon the capillary disk cross sectional area, open tube depth above the disk, capillary length and whether the liquid below the disk is stirred or not.

3.2 Fick's Diffusion Laws

In the development of a finite difference simulation of diffusion, the starting point is Fick's laws. Derivation of Fick's second law from his first law emphasizes the role of cross sectional area perpendicular to gas flow. This lays the ground work for cross sectional area considerations in the finite difference simulations. Fick's mathematical description of the process is known as the first and second laws of diffusion. Fick considered the first law as merely a step to obtain the second law.[68, 69]

In Fick's first law a concentration gradient of the solute in solution, dC/dx, is the driving force for a mass flux of solute, J_x, perpendicular to an area, A.

$$J_x = \frac{dN}{dt} = -DA \times \frac{dC}{dx} \tag{6}$$

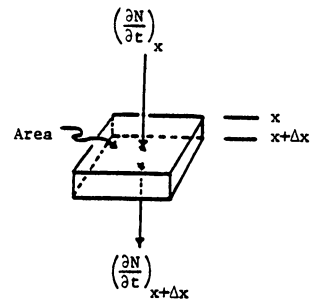

Figure 8. Fick's Second Law.

N is moles of gas solute; t, time (sec); C, concentration (moles/cc); x, distance in the solute mass flow direction (cm). Figure 8 illustrates the terms in the consideration of Fick's second law. It shows a net flux through an enclosed volume. Surfaces of area, A, perpendicular to the direction of flow and separated by a distance Δx is this enclose a volume, $V = A\Delta x$. The net flux through this volume is the difference

$$\text{Accumulation} = \text{Input} - \text{Output}$$

$$A\Delta x(\partial C/\partial t)_V = ((\partial N/\partial t)_x - (\partial N/\partial t)_{x+\Delta x}). \tag{7}$$

Substitution of the First law (equation 6) for fluxes permits rewriting equation 7 in terms of the concentration gradients. Solving this equation for $(\partial C/\partial t)_V$ yields equation 8 which no longer explicitly possesses the area term.

$$(\partial C/\partial t) = D((\partial C/\partial x)_{x+\Delta x} - (\partial C/\partial x)_x) \tag{8}$$

Equation 8 becomes Fick's second law in the limit of Δx going to zero.

$$(\partial C/\partial t)_x = D \underset{\Delta x \to 0}{\text{Limit}} ((\partial C/\partial x)_{x+\Delta x} - (\partial C/\partial x)_x)/\Delta x = D(\partial^2 C/\partial x^2) \quad (9)$$

Fick's diffusion laws are the phenomenological description of gas diffusivity in liquids.

3.3 *Boundary Conditions*

The solute gas absorption rate equations are derived from Fick's laws based on the boundary conditions. The time and distance dependence of concentration for the open tube experiment is found by solving Fick's laws subject to the boundary conditions in equation 10. The distance through which the gas solute has spread after time, t, can be calculated from the root mean square (rms) distance. The rms distance shows that the liquid depth of the open tube experiment appears infinite for the time duration of this experiment. The formation of a saturated liquid layer on introduction of gas solute into the diffusion cell is consistent with a gas piston condensing solvent vapor into a gas saturated liquid layer. The validity of the capillary disk boundary conditions was investigated by Hildebrand and coworkers.[36] They concluded that the boundary conditions were reasonable for the diffusion cell dimensions used.

The open tube boundary conditions are

$$C = 0 \text{ at } t = 0 \text{ for all x,} \quad (10a)$$

$$C = C_s \text{ at } x = 0 \text{ for } t > 0, \text{ and} \quad (10b)$$

$$\underset{x \to \infty}{\text{Limit}} \quad C = 0 \text{ for all } t. \quad (10c)$$

C_s is the gas saturation concentration, i.e. solubility. Solving Fick's laws with these conditions by use of Laplace transforms[70] yields

$$\frac{C}{C_s} = 1 - \sqrt{\pi}\int_0^{\infty} e^{-\beta^2} d\beta \tag{11}$$

where β is $x/2\sqrt{Dt}$. Equation 11 describes the spatial and temporal concentration dependence. To find the concentration dependence on distance, equation 11 is differentiated with respect to distance.

$$(\partial C/\partial x) = \frac{C_s}{\sqrt{\pi Dt}}\exp(-x^2/4Dt) \tag{12}$$

The probability of finding gas solute in a distance between x and $x + dx$ is

$$P(x)dx = [\frac{C_s}{\sqrt{\pi Dt}}\exp(\frac{-x^2}{4Dt})/\int_0^{\infty}\frac{C_s}{\sqrt{\pi Dt}}\exp(\frac{-x^2}{4Dt})dx]dx. \tag{13}$$

The denominator of equation 13 is C_s, since $\int_0^{\infty}\exp(-a^2x^2)dx$ equals (1/2a). The solute spreading distance is calculated from the rms distance as

$$x_{rms} = (<x^2>)^{1/2} = [\int_0^{\infty} x^2 P(x)dx]^{1/2} = [\int_0^{\infty}\frac{x^2}{\sqrt{\pi Dt}}\exp(-x^2/4Dt)dx]^{1/2}. \tag{14}$$

The integral in equation 14 is a standard form, $\int_0^{\infty} x\exp(-a^2x^2)dx$, which equals $(1/4a)\sqrt{\pi/a}$. Therefore equation 14 becomes

$$x_{rms} = \sqrt{2Dt}. \tag{15}$$

Integrating equation 13 between zero and x_{rms} shows that about 68% of the diffusing molecules are encompassed in this distance. Integration of two and three rms distances encloses 95% and 99.7% of the solute respectively. The rms distance indicates that the open tube boundary condition of an infinitely long tube is realistic for the liquid depth and time duration used. For example the diffusion coefficient of nitrogen in carbon tetrachloride is 3.6×10^{-5} cm^2/sec. A diffusion time of thirty minutes with this diffusivity gives a root mean square distance of 0.36 cm. Therefore the open tube portion of the experiment with a liquid depth of 1.5 cm appears of infinite length during the first

30 minutes of the experiment, since three rms distances of about 1 cm contains 99.7% of the diffusing gas solute molecules.

The first portion of the gas volume uptake curve for the open tube experiment exhibits a more shallow slope than later times in Figure 14. Bennett, Ng and Walkley[4] ascribe this time lag to interfacial surface resistance to gas flow. There is a simpler explanation. Prior to gas solute introduction into the diffusion cell, temperature equilibration of the solvent establishes a vapor/liquid equilibrium. Upon introduction of the solute gas into the diffusion cell the expanding gas solute acts as a piston to condense the solvent vapor into a solute saturated liquid layer as shown in Figure 9. This is responsible for the resultant time lag. Therefore boundary condition 10b is deemed reasonable. A more complete discussion of this phenomenon will be deferred until the simulation results are presented in the next section. Condition 10a assumes the liquid is degassed at the beginning of the experiment. Evidence for complete solvent degassing is provided in section 4.5.

Solution of Fick's laws under boundary conditions 10 for the open tube experiment is equation 11. Substitution of equation 11 into Fick's first law equation 6 at $x = 0$, integration with respect to time, and assuming ideal gas behavior of the dissolved gas gives the expression of gas volume uptake as a function of time.

$$\Delta V/\Delta t^{1/2} = C_s D^{1/2}(2A_o/\sqrt{\pi})(RT/P) \tag{16}$$

ΔV is the change in gas volume (cc); P, gas pressure (atmospheres); A_o, open tube cross sectional area (cm^2).

The boundary conditions for a capillary disk experiment are

$$C = C_s \text{ at } x = 0 \text{ for all } t, \tag{17a}$$

$$C = 0 \text{ at } x = h \text{ for all } t, \text{ and} \tag{17b}$$

$$\frac{dC}{dt} = 0 \text{ for all } x \geq 0. \tag{17c}$$

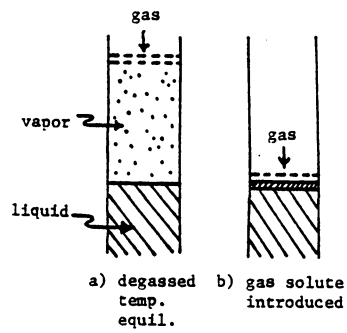

Figure 9. Open Tube Gas Piston.

The capillary length is *h*. Boundary conditions 17a and 17b indicate the establishment of a concentration gradient of saturated solution above the disk and zero concentration below the disk respectively. These are prerequisite for the establishment of a steady state, condition 17c. Hildebrand and co-worker's[36] use a very thin layer of liquid of about 0.5 mm above the capillary disk to insure complete and rapid gas saturation of the solvent over the capillaries. In the combined technique this liquid layer is at least 7.5 mm. Incomplete saturation of this thicker layer would call condition 17a into question. To maintain the steady state, the concentration below the disk must remain at zero for the duration of the experiment. Hildebrand and co-workers contend from experiments varying capillary length, total cross sectional area of capillaries, and solvent volumes below the disk, that significant concentration accumulation under the disk during the experiment is negligible. Evaluating the effect of a thicker liquid layer above the disk or concentration build up below the disk is not straight forward. Designing experiments to test for these effects is time consuming and difficult. One recourse is to simulate the various conditions with the one dimensional diffusion equation and finite difference methods. The next section on finite differences addresses the mechanics and results of this approach. Solution of Fick's laws for the capillary disk experiment under boundary conditions 17 requires consideration of only Fick's first law. Fick's second law is zero

by the steady state boundary condition 17c. Therefore the concentration gradient is a linear function of distance. Boundary conditions 17a and b give the associated slope and intercept.

$$C = -(C_s/h)x + C_s. \tag{18}$$

Substituting equation 18 into Fick's first law, integrating with respect to time, and assuming ideal gas behavior of the dissolved gas yields the gas absorption rate.

$$\Delta V/\Delta t = C_s D(A_c/h)(RT/P) \tag{19}$$

A_c is the capillary disk cross sectional area (cm^2) i.e. total cross sectional area of all the capillaries in the disk.

The open tube and capillary disk methods when combined into a single experiment may be described by both equations 16 and 19. The gas absorption rates are obtained experimentally at constant temperature and pressure. Since the cell dimensions are known simultaneous solution of the diffusion equations 16 and 19 yield both the diffusivity and solubility. The details of the experiment are discussed in section 4.0. Figure 10 illustrates the gas absorption rates obtained from a typical run with the combined experiment. To obtain simultaneously the diffusivity and solubility, the boundary conditions describing the combined experiment are assumed to be those of the individual component experiments. This appears true for the open tube part of the combined experiment. However some question arises for the capillary component assuming gas saturated liquid above the disk and zero or negligible concentration build up under the disk. The method of finite differences offers a way to model the capillary disk experiment and check for substantial concentration buildup under the disk or insufficient gas saturation above the disk. The analytical solutions, equations 16 and 19, for a known diffusivity and solubility provide a reference for the diffusion simulations.

In conclusion the boundary conditions for the combination of the open tube and capillary disk methods into a single experiment warrants further consideration. The method of finite differences offers a means to determine the effect of perturbing the boundary conditions for either the com-

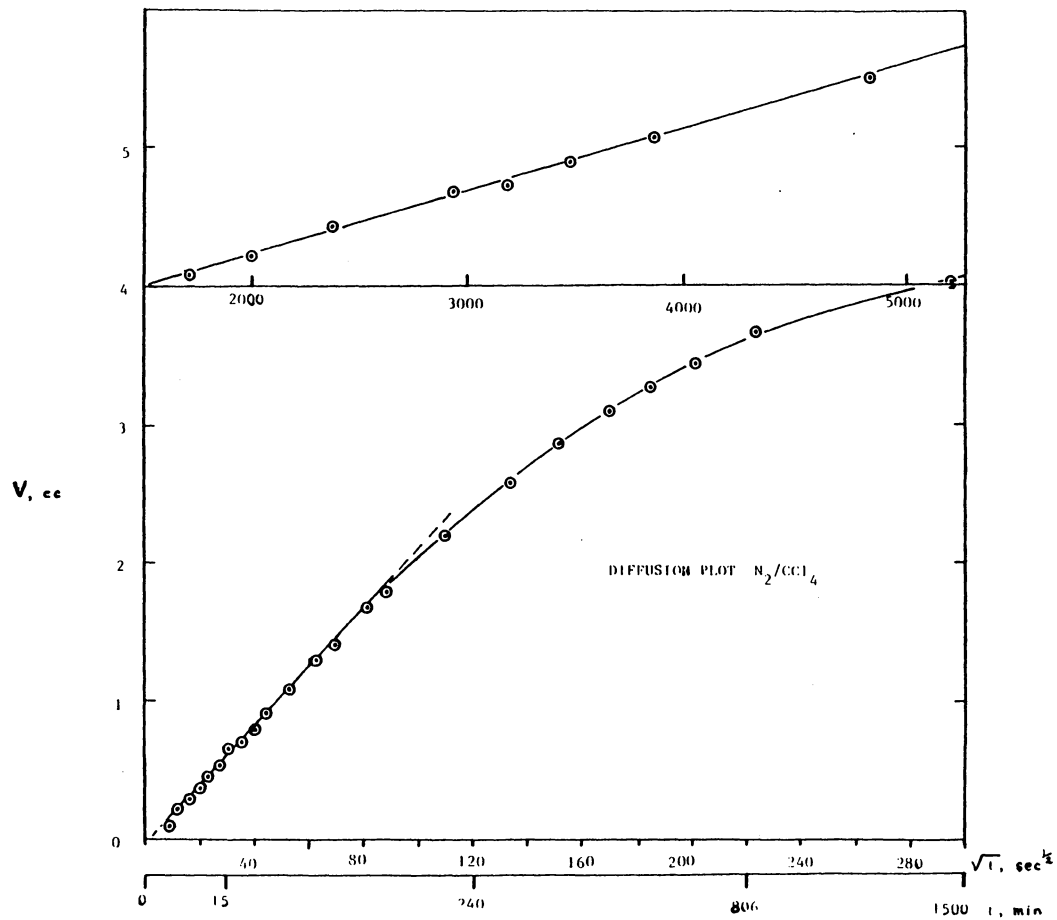

Figure 10. Typical plot of gas volume uptake for the combined experiment with nitrogen in carbon tetrachloride.

bined or individual component experiments. As a point of reference for the simulations the analytical solution of the open tube and capillary disk are given above.

3.4 *Finite Differences*

Regardless of the diffusion method the experimentalist is often limited by the intractability of the differential equations and boundary conditions describing the experiment. Simulation with finite difference methods on a digital computer can circumvent this problem. The finite difference methods are a numerical approach to the solution of the partial differential equations describing a diffusion experiment. The approach is conceptually simple and aids in the understanding of the diffusion process. In this section the finite difference equations for Fick's diffusion laws are first considered along with convergence and stability requirements. Next, implementation of these equations by an algorithm for a computer simulation program is described. Finally, simulation results are presented in terms of the boundary conditions of both the individual and combined methods.

Simulation of gas absorption for a diffusion experiment requires inputs of the gas solubility and diffusion coefficient. Figure 11 shows the (one dimensional) simulation as a grid of spatial, x, and temporal, t, dimensions. The top layer always remains at gas saturation concentration. This condition along with Fick's diffusion laws permits development of an iterative concentration equation in distance and sequential times. The first step is to write Fick's first law as a finite difference for cascading fluxes between volume elements.

$$J(x,t) = \frac{-DA}{\Delta x}\left(C\left(x + \frac{\Delta x}{2},t\right) - C\left(x - \frac{\Delta x}{2},t\right)\right) \qquad (20)$$

The arrows in Figure 11 show this flux development after four time increments. The second step is to express Fick's second law in finite form.

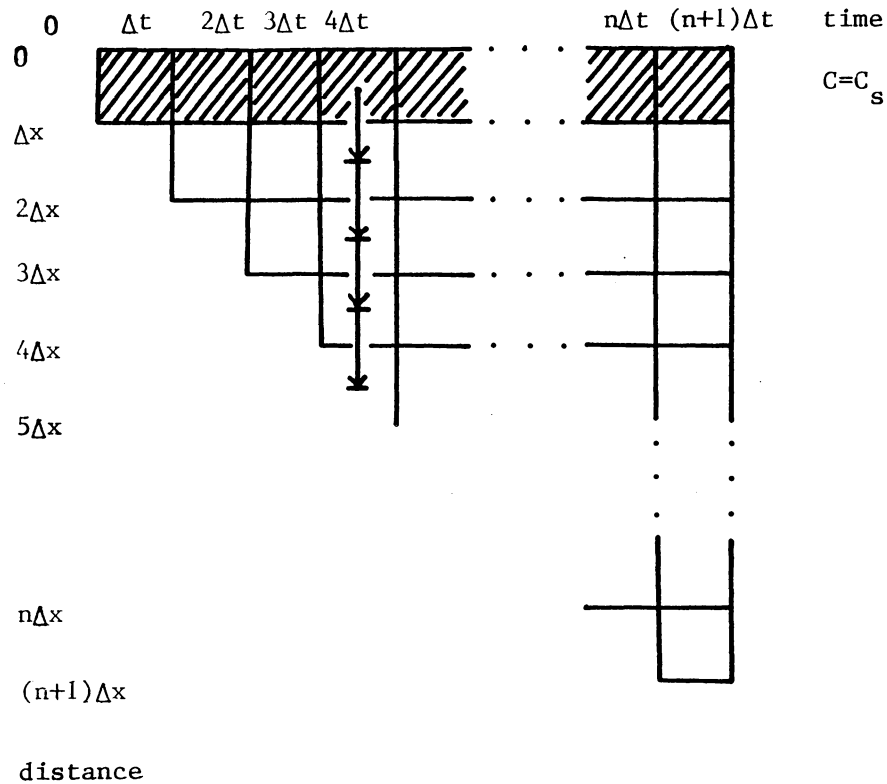

Figure 11. One dimensional diffusion model.

$$\frac{(C(x,t+\Delta t)-C(x,t))}{\Delta t} = \frac{(J(x-\frac{\Delta x}{2},t)-J(x+\frac{\Delta x}{2},t))}{\Delta x} \qquad (21)$$

The final step is to recast the fluxes in equation 21 into concentration gradients according to equation 20 and solve for $C(x,t+\Delta t)$.

$$C(x,t+\Delta t) = C(x,t) + \frac{D\Delta t}{\Delta x^2}(C(x+\Delta x,t) - 2C(x,t) + C(x-\Delta x,t)) \qquad (22)$$

This iteration formula determines the concentration in a volume element at distance x and time $t+\Delta t$ from adjacent elements at time t. The old concentrations at distance x and time t are $o(x)$ while the new concentrations at time $t+\Delta t$ are $n(x)$. Designating the ratio $D\Delta t/(\Delta x)^2$ as s, we rewrite equation 22 as

$$n(x) = s \times (o(x+1) + o(x-1)) + (1 - 2 \times s) \times o(x). \qquad (23)$$

Bard[71] calls the dimensionless ratio s, the model diffusion coefficient. If this ratio exceeds 0.5 the finite difference calculation is not stable. The instability results from round off error in the small differences between concentrations in adjacent boxes used to calculate the new concentrations. This indicates Δx and Δt are not independent. An s larger than 0.5 reflects Δx is too small for a given Δt. The assumption material diffuses only through neighboring boxes no longer holds. The upper cut-off on the amount of material diffusing into a neighboring box is found by writing equation 15 in the form of a model diffusion coefficient. This results in a value of $s = 0.5$. Therefore migration of more than 68% of the gas solute into an adjacent box for one time increment is unrealistic.

Noye[72] and Feldberg[73] discuss details for the solution of the one dimensional diffusion equation by various finite difference equations. They describe equation 21 as the forward time centered space approximation (FTCS). This approximation considers the volume elements above and below the most recent one, for space centering and calculates recent concentrations from previous ones, for forward time. Noye shows by expanding the finite difference equation with a truncated Taylor expansion that the truncation error diminishes most rapidly for $s = 1/6$. The

truncation error for $s = 1/6$ is of the order $\Delta t + \Delta x^2$. Theoretically Δt and Δx may be infinitesimal, but $s \leq 0.5$ limits the number of possible iterations. For instance halving the distance increment requires quartering the time increment to maintain the same s value. Therefore a simulation for the same total time requires eight times as many iterations in time and distance.

The relation between Δx and Δt complicates step size determination. Δt is first chosen by dividing the total diffusion time into some desired number of iterations (e.g. 100, 1000 or 10000). Time required for calculations and amount of storage available govern this choice. Then the stability criterion $s \leq 0.5$ requires selecting s. Finally, s and Δt require Δx be set equal to $(D\Delta t/s)^{1/2}$.

Combination of equation 23 with step sizes obeying stability criterion are the major ingredients of the computer simulation program. Equation 23 suffices for simulating an open tube experiment. Both the capillary disk and combined experiment require consideration of the change in cross sectional areas at the capillary ends from capillary to open tube cross sectional area. The smallest cross section area is a bottleneck and restricts solute flow through the volume elements adjacent to the capillary disk. Figure 12 represents the combined open tube/capillary disk experiment with no stirring below the disk. The right half of this figure lists the interval concentration expressions at various positions in the diffusion cell. Concentration accumulation in the volume increments at both capillary ends is determined by the finite difference equation shown in Figure 12. Because the cross sectional area changes, the appropriate values must be used for the fluxes into and out of these volume elements. The difference of the input and output fluxes scaled by the time increment is the change in the number of moles of solute in the volume increment. Change in concentration is the number of moles divided by the volume. This concentration change added to the old concentration becomes the new concentration. When the cross sectional area terms are equal for fluxes into and out of a given volume element, the equations simplify algebraically to equation 23. This equation requires only one half the number of operations compared to calculation for the volumes at the capillary ends.

Eight cases of diffusion cell boundary conditions are tabulated in Figure 13. Each of these cases consider concentrations above and below the capillary disk. A code for describing these cases are a prefix and suffix to the word CAP. The prefix indicates number of unsaturated liquid layers above

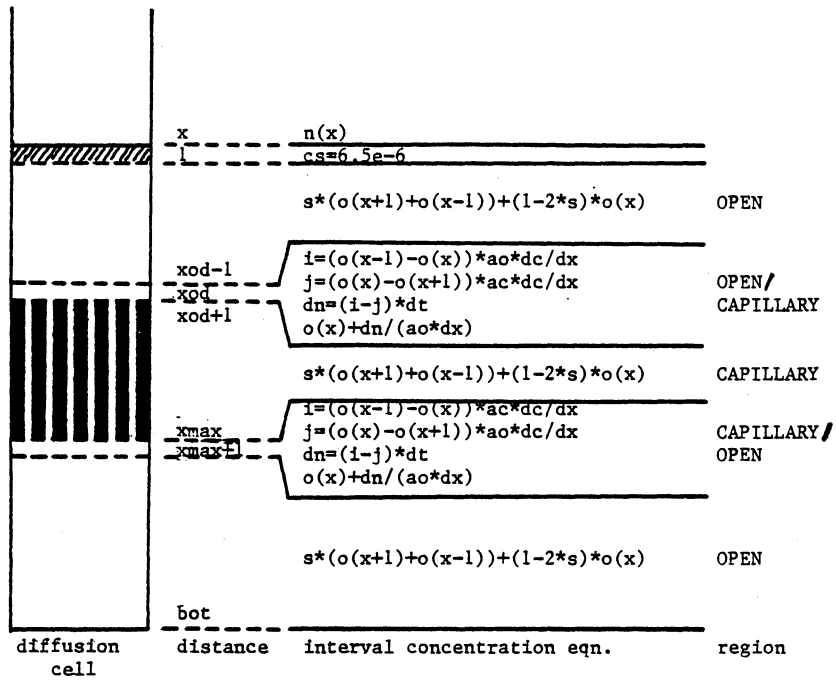

Figure 12. Interval Concentration Equations.

the disk: 0, no unsaturated layers; 1, one unsaturated layer; and N, more than one unsaturated layer. The suffix refers to dispersion of solute under the disk: 0, zero concentration at all times below disk; 1, one very large layer uniformly mixed below disk; N, a finite number of unstirred layers; and ∞, an infinite number of unstirred layers below the disk. These are summarized by

0		0
1	CAP	1
N		N
-		∞

In the following a prefix or suffix of X indicates reference to all conditions, for example XCAP0 includes 0CAP0, 1CAP0 and NCAP0.

Boundary conditions for all but 0CAP0 require changing the modeling equations at the disk ends. At zero concentration below the disk, XCAP0, the old concentration at distance increment $xmax + 1$ is always zero. Therefore equation 23 reduces to $n(xmax + 1) = s \times o(xmax)$. A uniformly stirred concentration below the disk, XCAP1, possesses only an input flux from the last disk layer at $xmax$. V_B is the liquid volume below the disk. B is the total number of gas solute moles to exit from the disk at time t. Therefore concentration below the disk at some time t is B/V_B . An unstirred solution below the capillary disk, XCAPN or XCAP∞, resorts back to equation 23 for determination of gas uptake at distance increments greater than $xmax + 1$. The open tube depth above the capillary disk is treated in accord with the number of increments into which it is divided. The topmost layer is assumed instantaneously gas saturated in accord with boundary condition 10b. The open tube distance increment immediately above the capillary disk is labeled, xod. If the top layer is completely saturated, 0CAPX, then equation 23 is used. For two distance increments above the disk, 1CAPX, the layer immediately above the disk is treated by Fick's first law where the cross sectional area terms appear explicitly. If the open tube depth is three or more volume increments, NCAPX, then the concentrations are found by the equations in the upper portion of Figure 12.

0CAP0 in Figure 13 is the label for the capillary disk simulation program with a saturated layer above the disk and zero concentration below the disk. The basic program 0CAP0 is listed in Appendix A. This program is written for a Timex/Sinclair 2068 microcomputer. The other labels in Figure 13 represent other programs for simulation of the various diffusion cell boundary conditions which are mentioned above. Appendix A also summarizes these programs in terms of changes and

Unsaturated layers above disk	0	1	N=xod-1
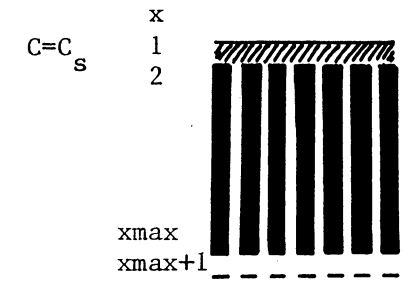 Concentration below disk		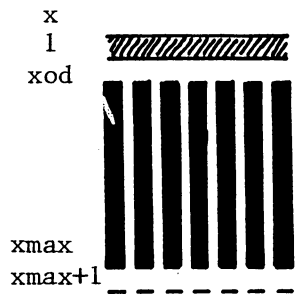	
C=0	0CAP0	1CAP0	NCAP0
Stirred $C=B/V_B$	0CAP1	1CAP1	NCAP1
Open Tube C=interval conc. eqn.			NCAPN NCAP∞

Figure 13. Diffusion simulation programs for various diffusion cell boundary conditions.

modifications necessary to 0CAP0. All these programs have three major functions. These are initialization, iteration and illustration. The initialization portion sets up cell dimensions, inputs diffusion and solubility values as well as determines time and distance increment sizes. The iterative calculations are dependent on which set of conditions in Figure 13 are being simulated. The conditions indicate in what sequence the interval concentration equations are applied at various distance increments along the length of the diffusion cell. Illustration of the relationships between concentration gradients and gas volume uptakes is performed with time dependent plots. In this version of interpreted basic, the program executes faster if seldom used routines are at the listings end.[74] Therefore positions of routines in the listing are first the iterative calculations, second display routines and last initialization.

Two additional experimental factors about the different boundary conditions must be described before considering the simulation results. The first factor concerns interferometric measurements of the open tube boundary condition 10b for a saturated liquid interface. The second factor is the investigation of the effect on diffusion results for various diffusion cell dimensions of the capillary disk experiment by Hildebrand and coworkers.[36]

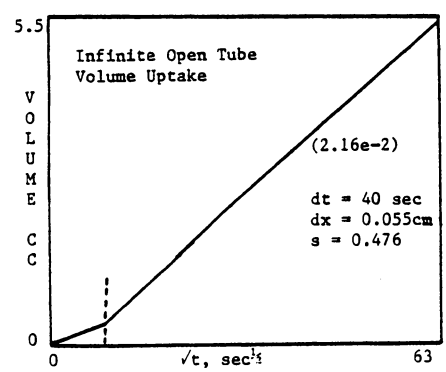

Figure 14. Simulation of open tube experiment.

Instantaneous gas saturation of the top thin layer of liquid is one of the boundary conditions for the infinite open tube experiment. As already noted, Bennett, Ng and Walkley[4] observed a time lag for the establishment of the liquid/vapor equilibrium which they say is not reproducible. They ascribed the displacement of the gas absorption curve as shown in Figure 14, to an interfacial surface resistance to gas flow. Harvey and Smith[75] as well as O'Brien and Hyslop[76] use a technique employing a gas pressure jump into a quiescent liquid for monitoring the gas exchange rate across the gas liquid interface interferometrically. Harvey and Smith use a Mach-Zehnder interferometer while O'Brien and Hyslop employ a Fabry-Perot interferometer. The diffusion technique in each case satisfies conditions of an open tube experiment. Harvey and Smith summarize the initial effect of gas introduction into the diffusion cell in the following.

> At the beginning of absorption, just after gas has been admitted to the cell, a movement of the fringes commences near the surface of the liquid, rises to a maximum value in about 1/2 second and then dies away within 5 seconds, leaving a fringe shift evidently caused by change in concentration of gas in liquid. This preliminary movement of fringes is due to the conduction of heat through the liquid. An alteration of the total pressure in the cell alters the partial pressure of the water vapor above the liquid and brings about condensation or evaporation at the liquid surface with the liberation or absorption of heat.

The concentration effects as they point out are dominant since heat conduction in the liquid is typically an order of magnitude faster than gaseous mass diffusion in the liquid. O'Brien and Hyslop draw the same conclusions monitoring the interface temperature with a thermistor. In both cases a set of baffles were used to disperse gas parallel to liquid surface upon introduction into the diffusion cell. This would tend to lower the gas piston effect and more closely approach the open tube experiment boundary condition 10b of a saturated layer of infinitesimal thickness.

Although the diffusion model we employ is simple by assuming an initial saturation layer of liquid, it accounts for the time lag that Bennet, Ng and Walkley note. The open tube simulation program is listed in Appendix A. Figure 14 illustrates the gas absorption for the open tube simulation. The number in parenthesis is the slope after the initial time lag. The time lag is due to instantaneously saturated top liquid layer and is consistent with experiment. Figure 11 indicates the reason for a time lag that is only one time increment in duration. In the first time increment mass flow is only out of the top layer. Subsequent times have mass fluxes into as well as out of successive volume elements without instantaneous saturation. Since thermal conduction is so rapid in

comparison to mass flow and there is only a small amount of liquid condensation from vapor, we do not consider the temperature effect in the model. Therefore qualitatively the simulation lends support to a gas piston, while the interferometric studies confirm it experimentally.

Ross and Hildebrand[3] in the first publication on the capillary disk technique indicate stirring the liquid below the disk distributes the gas solute uniformly. Subsequently Hildebrand[36] considered the volume below the capillary disk, the capillary length and the cross sectional area as variables in an effort to determine whether concentration build up under the disk is substantial. A substantial concentration build up below the disk would invalidate the boundary conditions 17b and c. Variables of volume below disk, V_B (cc), capillary length, h (cm), and cross sectional area of disk, A_c (cm^2), for the three cells reported are presented in Table VIII. Case A is Ross and Hildebrand's earlier diffusion cell. Cases B and C have volume and cross sectional areas approximately three times larger than case A. The capillary length of case C is about the same as case A, while case B is about five times longer. Hildebrand's results indicate for cases B and C, with volumes below the disk of 206 cc, that the concentration below the disk is initially zero and negligible for the duration of the experiment; for case A with a volume of 77 cc below the disk a small correction is necessary. Malik and Hayduk[77] report on the role of capillary length in obtaining a steady state. Using a 1 mm diameter capillary for ethane in n-hexane and n-heptane they show that a diffusion path length of at least 20 mm eliminates end effects for unstirred solvent below the capillary.

We now compare the assumption of zero concentration below the disk to that of a stirred finite volume below the disk based on computer simulations. Table IX tabulates the program volume uptake slope results of 0CAP0 (C = 0 below disk) and 0CAP1 (stirred finite volume, V_B, below disk). These results are based on Hildebrand's cell dimensions in Table VIII and simulated run times of 72 hours. Table IX also includes the slope according to the steady state solution, equation 19 using Hildebrand's cell dimensions. In cases A and C the slope value of equation 19 is higher than the simulation value of zero concentration below the disk with program 0CAP0 by about 9%. Similarly the simulation of zero concentration below the disk for cases A and C is 10-11% higher than the simulation for Hildebrand's fixed volumes from Table IX. Simulations for case B, boxed

Table VIII. Hildebrand's capillary disk dimensions. h is capillary length; A_c, cross sectional area and V_B, volume below capillary disk.

Diaphragm	A	B	C
h (cm)	0.913	5.04	0.90
A_c (cm^2)	1.994	5.65	5.65
V_B (cc)	77	206	206

in values of Table IX, with the longer capillary length did not converge after 50 time increments which corresponds to 4 hours simulated run time, as for cases A and C or even after 350 time increments corresponding to 30 hours simulated run time. This indicates the difficulty in obtaining a steady state in a very long capillary and raises the question as to the validity of Hildebrand's cell dimensions of case B.

Figure 15 depicts graphically the slopes of Table VII simulations for Hildebrand's cell dimensions of case A, B and C. Figure 15a includes the resultant slopes for each cell dimension with zero concentration below the disk. The upper graph of Figure 15b shows the slopes for stirred finite volumes under the disk for each cell while the lower graph shows variation of concentration gradients across the disk. In view of the concentration gradients it appears that in case B a steady state is never reached while cases A and C show pseudo-steady state behavior.

We next consider simulations based on a cell of comparable cell dimensions to the cell used in this study with capillary length of 1.5 cm and cross sectional areas, A_c = 2.39 and A_o = 20. The diffusivity and solubility used are 3.6×10^{-5} cm^2/sec and 6.5×10^{-6} cc/mole-atm respectively. These same values or cell dimensions, diffusivity and solubility are used for calculation of the slope from the steady state solution, equation 19. Table X is a summary of the conditions for generating the simulation slopes with 0CAP0 and a comparison to the steady state solution of equation 19. The effect of time and distance increment sizes on simulation slopes is shown for approximately a

Table IX. Capillary disk slope comparison of simulations to analytical solution, equation 19. All slopes are scaled by 1×10^6.

Diaphragm	A	B	C
Equation 19	12.50	6.42	32.95
CAP0	11.38	9.26	32.72
C = 0		-7.5hrs-	
below disk		8.27	
		-17.5hrs-	
		7.60	
		-30hrs-	
CAPVB	10.17	9.22	28.90
uniform			
conc. below		8.22	
disk			
		7.54	

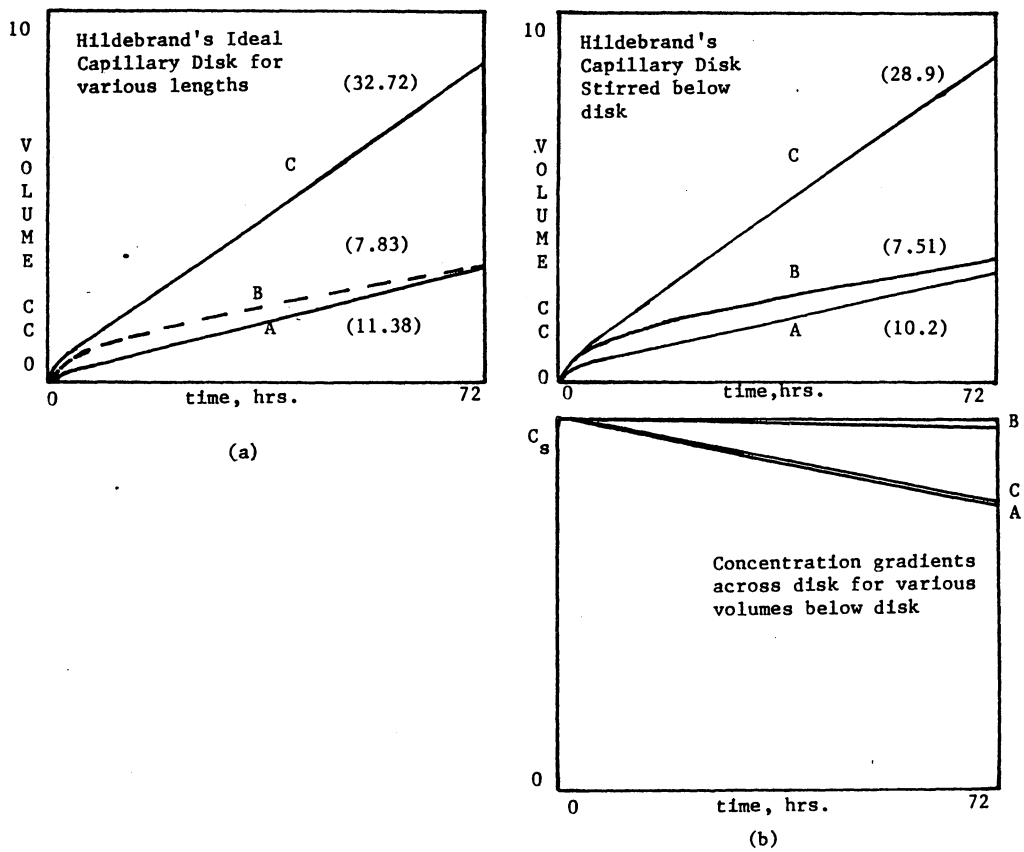

Figure 15. Simulation of Hildebrand's capillary disk experiments: (a) ideal, saturated layer above disk and zero concentration below disk and (b) stirred below disk.

Table X. Parameter effect on simulation convergence to capillary disk slope.

	****							
I	831	851	1040	2500	4114	6480	103680	3710
Δt (sec)	312.5	306	250	104	63	40	2.5	70
Δx (cm)	0.15	0.15	0.15	0.15	0.15	0.055	0.015	0.5
s	0.50	0.49	0.40	0.17	0.10	0.476	0.40	0.01
10^6 Slope	8.28	8.28	8.28	8.28	8.28	8.87	9.02	9.11
% error	9.1	9.1	9.1	9.1	9.1	2.7	1.0	$\cong 0$
	****							

constant over all simulation run time i.e. I $\times$ $\Delta t \cong$ 72hrs. I is the number of time increments. The boxed off values share a common distance increment with decreasing values of the model diffusion coefficient. The case of s = 1/6 $\cong$ 0.17 shows the same % error deviation from equation 19 as the other s values ranging from 0.5 to 0.1. Noye[72] indicated s = 0.17 should minimize the truncation error. The asterisks designate a simulation also run in double precision (i.e. sixteen digit mantissa) on the TRS-80 Model 1 Radio Shack microcomputer. Therefore accumulation of round off error in the mantissa cannot account for the approximately 10% deviation from the analytical solution of equation 19. However, decreasing both step sizes while maintaining the s ratio less than 0.5 for the two columns following the boxed off values results in a gradual convergence to the analytical slope value of 9.11 $\times$ 10^{-6} cc/sec. The number of iterations, execution time and storage requirements become excessive for a value within 1% of the analytical solution. The 103680 iterations on the TS2068 requires about 9 days of computation time with room for storage of only every twentieth calculated gas absorption value. On the other hand the last column in Table X shows convergence and requires fewer iterations. This distance increment is not realistic since in three time increments, 210 sec, gas would emerge from the capillary. The distance increment is also not consistent with the conditions found for the infinite open tube simulation shown in Figure 14 by being 90% greater. Therefore use of this set of parameters is suspect. Since the model is an approxi-

mation and truncation error is the same for various perturbed boundary conditions, the blocked off values of Table X are used. This should still give a basis of comparison between the different boundary conditions.

With time and distance increments of column two of Table X computer simulations are performed for cases of zero or one unsaturated liquid layer above the disk and zero concentration or a uniformly stirred liquid volume below the disk. The results for simulations with 0CAP0, 1CAP0, 0CAP1 and 1CAP1 are shown in Figure 16. A dashed line in Figure 16a is a simulation with 0CAP0 using the time and distance increments from the right most column of Table X. For cases other than 0CAP0 the graphs also incorporate plots of the evolving concentration gradient with concentration scale on the right. The numeric slope values in parenthesis must be scaled by 10^{-6}. The tic marks on the plots indicate the portion of the gas absorption curve over which the slope is calculated. All these values are within 4% of the 0CAP0 simulation slope with the exception of case c of Figure 16, 0CAP1. For 0CAP1 volumes below the capillary disk range from 75 to 4800 cc in case c. A volume of 75 cc is probably too small, recall Ross and Hildebrand's[3] volume of 77 cc. This volume of 75 cc shows an 8% variation in slope. Excluding this value leaves the range of volumes 150 cc to 4800 cc which also lie within 4% of the 0CAP0 case. Therefore for a volume of 150 cc or greater below the disk, the variation of the slope between 0CAP0 and stirred cases, XCAP1, is within $\pm 5\%$.

The addition of an unsaturated layer over the disk does not cause a large change in the slope. Figure 17 show the results of one unsaturated liquid layer above the disk along with variation in the capillary length while maintaining the same cross sectional area. When establishing a concentration gradient across the disk, a capillary length of 6.0 cm is closest to ideal while 1.5 cm is the worst of the three cases. However, there is a trade off in that for a given time period the overall volume uptake for 3.0 cm is about half that of 1.5 cm. Since these runs are over 72 hours in duration, experimentally a capillary length of 1.5 cm with twice the volume uptake is much easier to monitor.

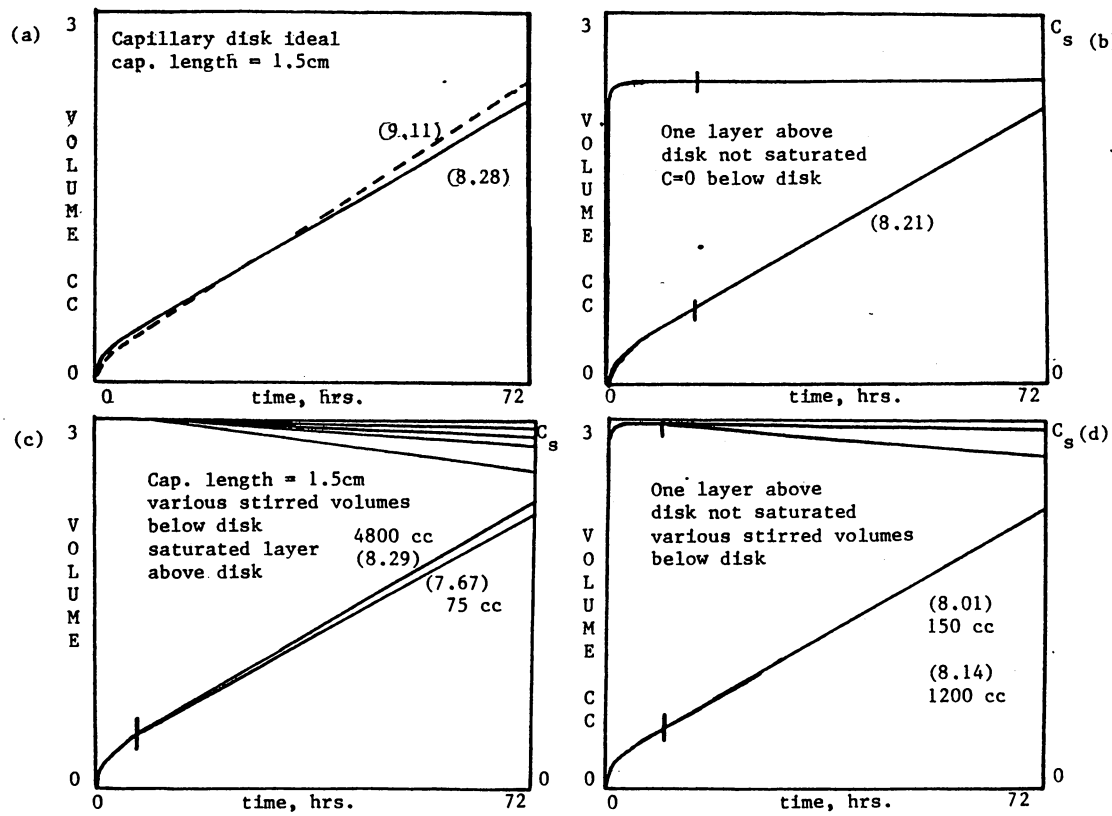

Figure 16. Capillary disk experiment simulations: (a) 0CAP0, zero below disk, (b) 1CAP0, one layer above disk not saturated with zero below disk, (c) 0CAP1, stirred below disk and (d) 1CAP1, one layer above the disk not saturated as well as stirred below the disk.

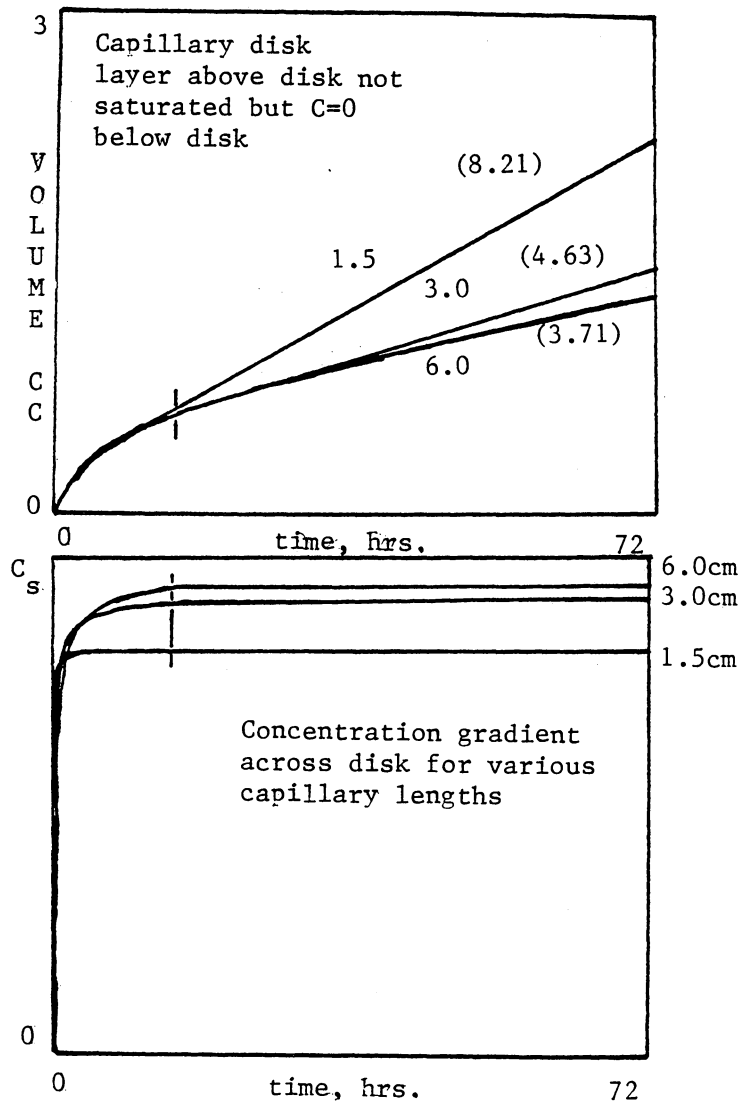

Figure 17. Variation of capillary length, l, in disk experiment with ICAP1. The rate is (r).

Table XI. Influence of liquid depth on open tube slope.

Open Tube Depth (cm)	Volume below disk (cc)	Open Tube Slope × 10^2 ($cc/sec^{1/2}$)
2.25	300	2.25
1.5	150	2.24
1.5	300	2.25
0.75	150	2.25
0.75	300	2.25

If the liquid depth increases to more than one unsaturated layer above the disk then for a short time duration the initial portion of the simulation is the open tube simulation. Table XI tabulates NCAP1 simulation slopes for depths of 0.75, 1.5 and 2.25 cm from the first to fifth time increment (i.e. about 20 minutes). The capillary length is 1.5 cm in all cases. The effect of doubling the volume below the disk is negligible. These open tube slope values are within 4% of the value for the infinite open tube simulation.

Figure 18 delineates the influence of the open tube depth on the capillary disk experiment. Open tube depths are those of Table XI. NCAP0, NCAP1 and NCAP∞ simulate boundary conditions of (a) $C = 0$, (b) uniform concentration and (c) unstirred liquid below the disk respectively. Cases (a) and (b) yield almost identical results for various liquid levels over the disk. However case (c) in general shows a slope value about 10% less. This is a worse case value since lateral diffusion is instantaneous for this simulation immediately below the disk. This is unrealistic and a more reasonable model would be equality of the lateral to vertical diffusion. The concentration gradients for case (c) show a slow variation with time accounting for the lower slope value.

Confining the open tube below the disk to a finite number of steps corresponding to fixed volumes of 150, 300 and 600 cc yields the same slopes as for the infinite open tube below the disk. Figure 19 shows these results from simulation with NCAPN. Varying the capillary length from

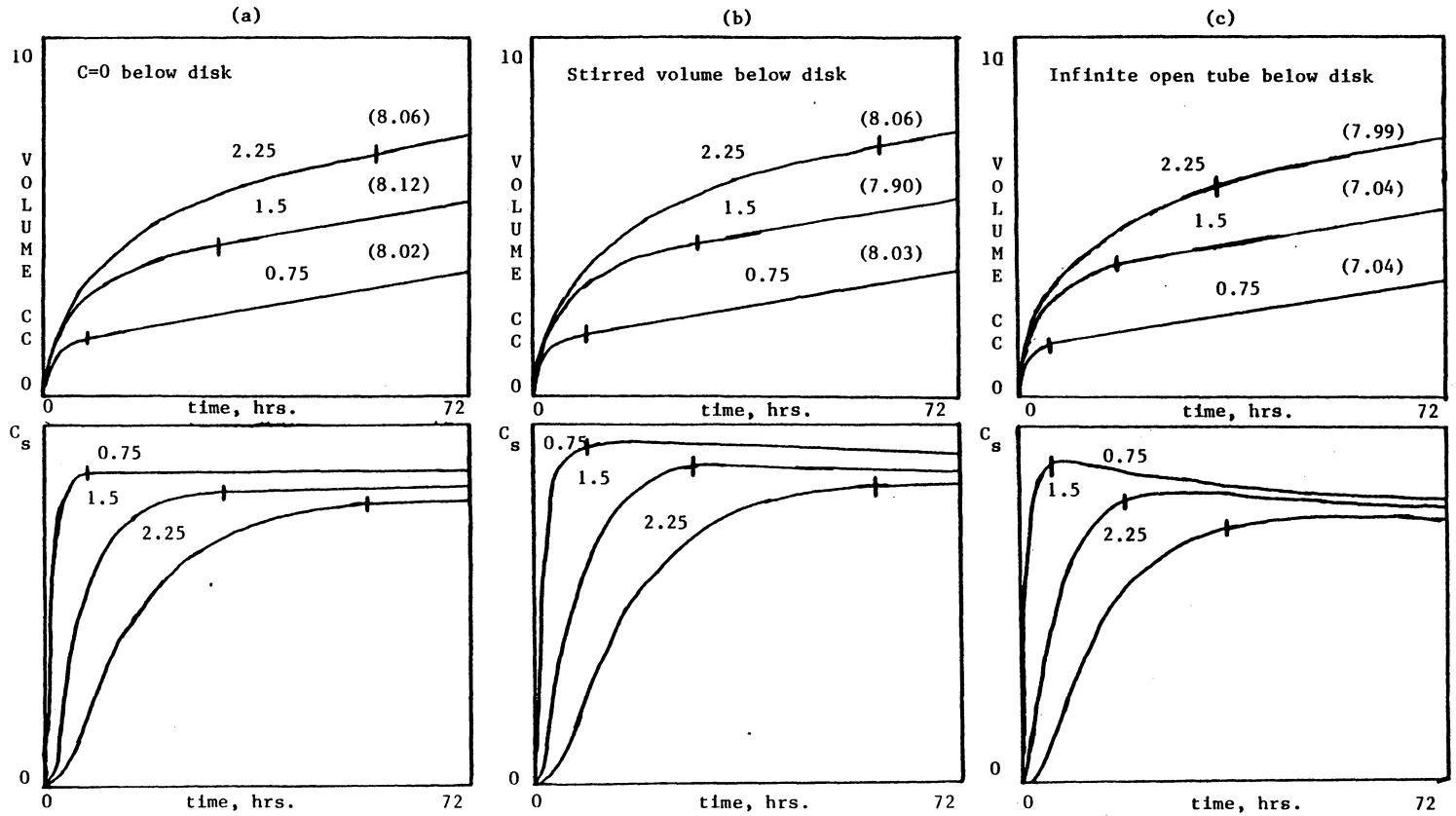

Figure 18. Simulation of combined experiment: (a) NCAP0, zero concentration below disk, (b) NCAP1, stirred below disk and (c) NCAP∞, unstirred below disk.

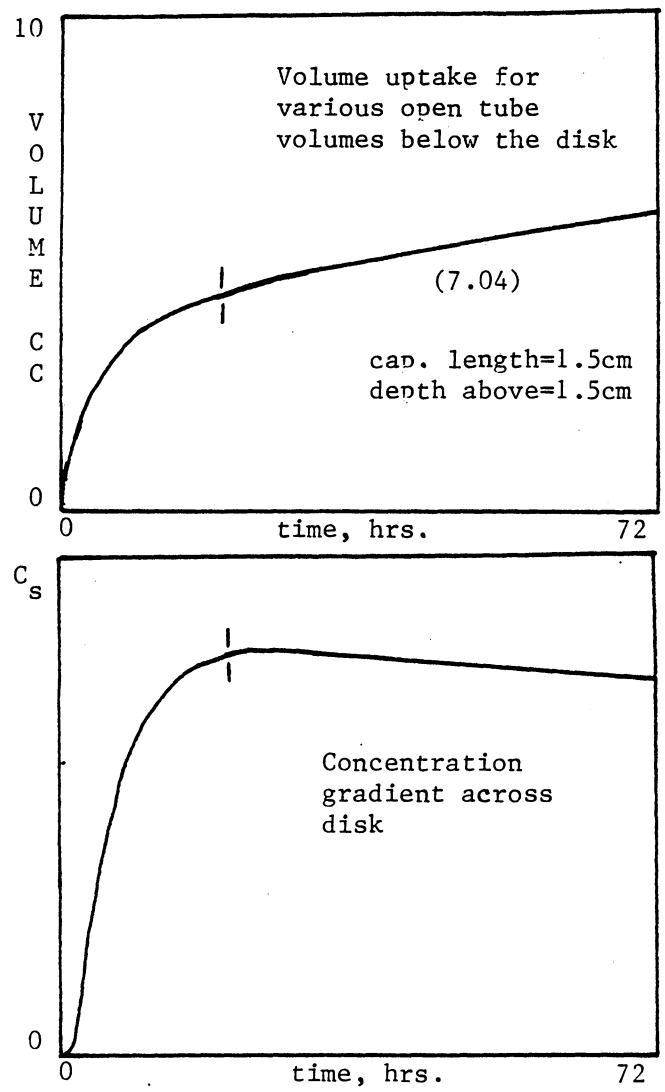

Figure 19. Simulation of unstirred volume below capillary disk. Capillary length is 15 mm; open tube depth, d; rate, (r).

3.0 to 6.0 cm in Figures 20 and 21 respectively for zero or uniform concentration under the disk give results similar to those of 1.5 cm in Figure 18. This similarity is in the trend of capillary slopes with the open tube depth above the capillary disk. The total gas absorption is smaller as well as corresponding slopes for the longer capillaries. Although the concentration gradients more closely approach those of 0CAP0 with the longer capillaries the time to establish a steady state across the disk becomes prohibitively long for open tube liquid depths of 1.5 and 2.25 cm above the disk.

In summary the uniform concentration below the disk gives the same results either with or without an open tube liquid layer over the disk. These values are within 4% of the 0CAP0 simulation with $C=0$ below the disk and a saturated layer immediately above the disk. However, employing the open tube below the disk results in about 10% deviation below that of the 0CAP0 case. This is in part due to the assumption of instantaneous lateral diffusion below the capillaries. Malik and Hayduk[77] in a single capillary experiment do not employ stirring below the capillary. They argue a capillary of approximately 1 mm diameter is small enough to eliminate any convection in the capillary but that enough convection is present to disperse uniformly the solute as it emerges from the bottom of the capillary. The lower end of the capillary is conically ground to aid in dissipating the solute exiting the capillary. A draw back of this single capillary experiment is determination of the diffusion path length. A meniscus at the top of the capillary complicates the calculation, since the depth of the upper most saturated layer is not known. As to dispersion of gas in the open tube over the disk, Houghton et al.[41] detect convection by the onset of a rapid change in the later portion of the slope of the volume versus square root of time curve. Perhaps this fact could help in estimating the amount of convection in the nonstirred open tube below the disk. The open tube simulations show agreement between both an infinite and a finite liquid depth over the capillary disk.

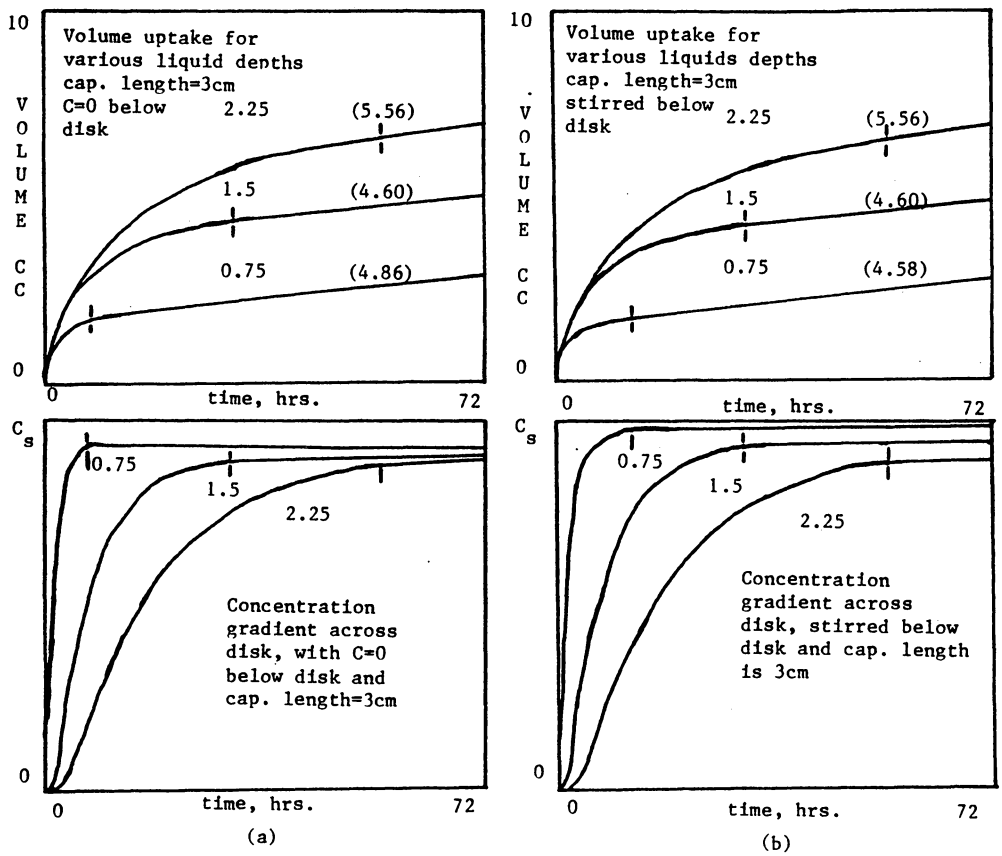

Figure 20. Combined experiment simulation capillary length 3 cm: (a) NCAP0, zero concentration below disk and (b) NCAP1, stirred below the disk.

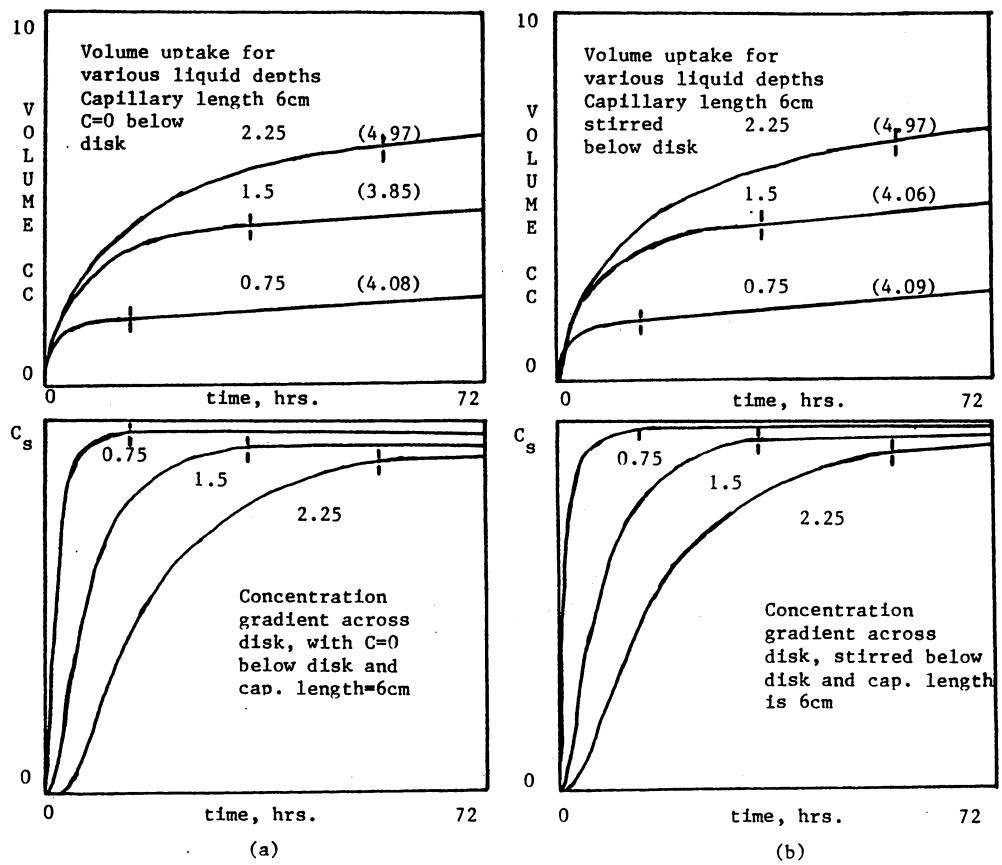

Figure 21. Combined experiment simulation capillary length 6 cm: (a) NCAP0, zero concentration below disk and (b) NCAP1, stirred below the disk.

3.5 *Summary*

Investigation of deviations from ideal boundary conditions of the open tube and capillary disk experiments given by boundary conditions of equations 10a,b,c and 17a,b,c were computer simulated using finite difference methods. The results indicated a worse case deviation of 10% below the 0CAP0 capillary disk case for the capillary disk in series with the open tube experiment. Since this worse case assumes an unrealistic instantaneous lateral diffusion below the disk, it provides an upper limit of 10% error for concentration build up beneath the disk. This error was still within the $\pm$ 10% error typically reported for many diffusion measurements.

The finite open tube over the capillary disk for various liquid depths and finite times was found to agree with the infinite open tube for finite times. This was in keeping with the distance values that were indicated by the root mean squared solute spreading distance given by equation 15. The interferometric experiments of Harvey and Smith, and O'Brien and Hyslop, supported the supposition that a gas piston caused the initial time lag in the open tube experiment, by condensation of solvent vapor into a gas saturated liquid layer. This also was corroborated by the open tube simulation since the first time increment showed the same time lag behavior. These various considerations of individual and combined experiments supported the use of the steady state boundary conditions and provided assurance of the reliability of the combined technique.

4.0 EXPERIMENTAL PROCEDURE

4.1 Introduction

The combined technique is a composite of the open tube and capillary disk experiments. Both the combined technique and individual component experiments maintain pressure and temperature of the diffusion cell constant while monitoring the gas volume uptake. The previous chapter shows that equations 16 and 19 describe the combined technique under a set of specific boundary conditions. Each boundary condition with the exception of completely degassed solvent has been shown valid. A test is described which shows the liquids are degassed by refluxing. Rewriting equations 16 and 19 below facilitates the simultaneous calculation of both gas solubility and diffusivity into the liquid from the combined technique data.

$$K_o = C_s D^{1/2} = (\pi^{1/2}/2A_o)(P/RT)(\Delta V/\Delta t^{1/2}) \tag{24}$$

$$K_c = C_s D = (h/A_c)(P/RT)(\Delta V/\Delta t) \tag{25}$$

The experiment fixes all terms on the right most side of each equation above with the exception of the gas absorption rate. The gas absorption rate is determined experimentally. Simultaneous

solution of equations 24 and 25 for the unknowns of solubility and diffusivity results in the equations below.

$$C_s = K_o^2/K_c \tag{26}$$

$$D = (K_c/K_o)^2 \tag{27}$$

A typical experiment takes up to seventy two hours. Total gas volume uptake for such a system is approximately 4 cc of gas. Although the experiment is conceptually easy, this small volume change over a prolonged period of time poses problems in data collection and experiment control. Manual and automated apparatuses have been employed. Both rely on maintenance of constant pressure and temperature while measuring the gas volume decrease. Both diffusion cells are almost identical. The diffusion cell consists of an alumina disk sandwiched with Viton O-rings between two bell housings made from 50 mm pyrex O-ring unions. The disk is 80 mm in diameter and 15 cm thick. It contains 304 symmetrically spaced holes having 1 mm diameters. Volumes of the bell housings are 150 cc each for the automated apparatus while 75 cc for the upper and 300 cc for the lower in the manual apparatus. The manual apparatus relies on maintaining a constant pressure with a mercury leveling bulb attached to a gas buret. A microcomputer monitors the pressure by sensing the levels in a differential manometer and driving a gas tight syringe with a stepper motor. The times are logged at successive equal volume decrements from a real time clock. This approach eliminates the tedious process of manual data collection and requires operator assistance only at the beginning and end of each experiment. Each apparatus requires an accurate knowledge of the cross sectional areas of the diffusion cell. Calibration runs were made using literature diffusivity and solubility values of various gas/liquid systems, observed gas volume uptake slopes, and equations 24 and 25 to calculate A_o and A_c. Accurate determination of the gas absorption rate requires volume calibration of the gas buret or gas-tight syringe for the manual and automated apparatuses respectively. Weights of aliquots of displaced mercury were used for volume calibration in each apparatus.

4.2 *Manual Apparatus Description*

The major components of the manual apparatus are the diffusion cell, differential manometer and gas buret. A description of the diffusion cell is given above. Figure 22 shows the manual apparatus. Temperature of the diffusion cell is maintained by immersion in a constant temperature water bath. Degassed solvent is introduced through the bottom of the cell. Gas pressure in the cell is monitored and controlled with a differential oil manometer and gas buret respectively. One arm of the differential manometer is connected to the system while the other is attached to a thermostated ballast bulb of 250 cc. This ballast volume is approximately equal to the system gas space. Gas is displaced in the gas buret with mercury by means of a leveling bulb. The gas buret is thermostated by circulating water through a water jacket connected to the diffusion cell water bath. With the exception of the glass line connecting the manifold and diffusion cell of 1 mm capillary tubing, the connection lines between the parts of the apparatus and manifold are 2 mm diameter tubing. The manifold is made from 5 mm diameter glass tubing. During system evacuation residual solvent is removed with a dry ice trap. Initial gas pressure is set with an open mercury manometer.

4.3 *Manual Operation*

Operation of the manual apparatus consists of the following sequence of steps: solvent degassing; system evacuation; solvent transfer to diffusion cell followed by temperature equilibration; initial gas pressure set with open manometer; gas solute introduction into diffusion cell; and manual volume adjustment of gas buret to maintain the pressure.

Solvent is degassed by refluxing for a period of approximately eight hours. Degassed solvent is isolated from the atmosphere and cooled to room temperature before transferring to an evacuated

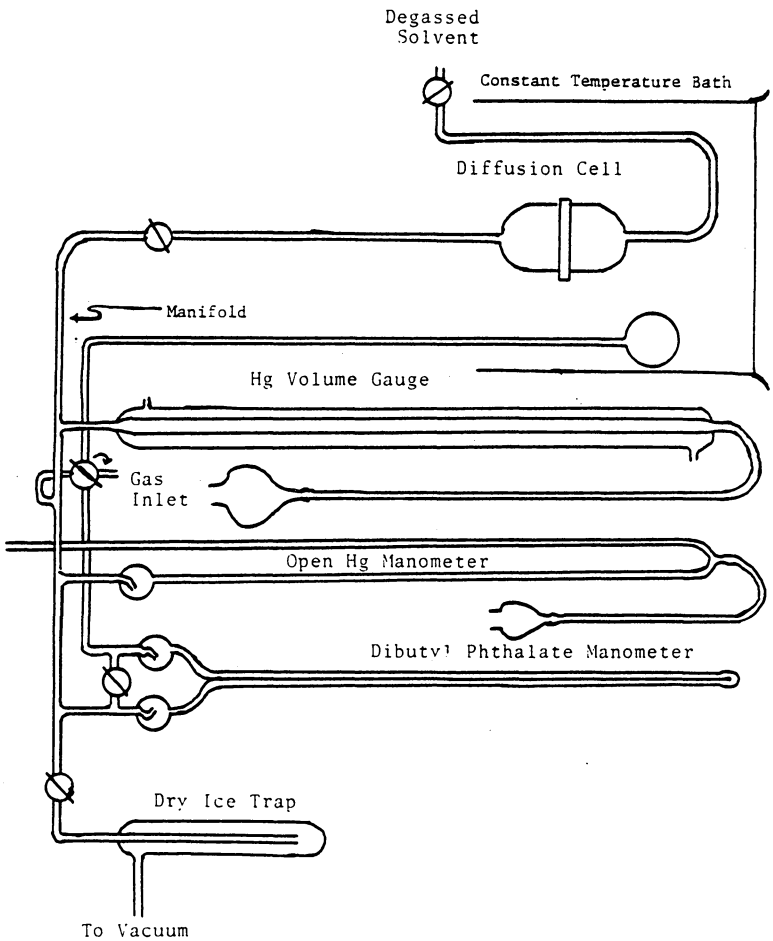

Figure 22. Manual Diffusion/Solubility Apparatus.

diffusion cell. An isopropanol dry ice trap is used to catch residual solvent during diffusion cell evacuation. Degassed solvent is siphoned under its own vapor pressure from the reflux flask into the evacuated diffusion cell by isolating the cell and opening the solvent inlet valve. The liquid is gently introduced into the evacuated cell and disk is flooded to a depth of about 15 mm before closing the solvent inlet.

The diffusion cell is isolated from the manifold. The gas pressure is initially set by opening the gas inlet valve connected to the gas solute cylinder. Initial pressure is read from the open mercury manometer. The gas inlet valve is closed upon setting the initial pressure. The system is then allowed to thermally equilibrate at least two hours.

The experiment is initiated by opening the diffusion cell valve. Gas is introduced into the diffusion cell and the timer is started. After the manometer levels stop oscillating, the differential manometer and open manometer valves are closed. The reference pressure is set and the open manometer is isolated from the manifold. The gas buret level is read with a cathetometer and the height recorded for a zero time reading. Adjustment of the system gas volume is made with the gas buret leveling bulb to maintain a constant pressure by balancing the differential manometer levels. The new height and time reading are recorded. The measurements are repeated every three to four minutes for the first hour, ten to fifteen minutes for the next six hours and four hour intervals for the following two to three days.

This method differs from Ross and Hildebrand's[3] capillary disk method by having a liquid depth of about 15 mm over the disk rather than the 0.5 mm they employed. This flooded area is an open tube experiment as described by Bennett, Ng and Walkley,[4] but differs by having a depth of 15 mm rather than their 250 mm. Ross and Hildebrand degas by the freeze-melt method rather than solvent refluxing. Bennett, Ng and Walkley emphasize temperature equilibration of 24 hours prior to an experiment but do not indicate method of solvent degassing. The two hour temperature equilibration period is the time required for a constant reading from a platinum resistance thermometer embedded in the capillary disk.

4.4 *Manual Apparatus Calibrations*

Diffusion measurements require two calibrations. The first calibration is of the gas buret. This permits an accurate measure of the volume of gas displaced on changing the mercury level in the gas buret. The second calibration is of the diffusion cell cross sectional areas of A_c and A_o. Each of these calibrations are critical for the simultaneous determination of diffusivity and solubility.

Calibration of the gas buret requires weighing the amount of mercury displaced for a level difference. Dividing this weight by the mercury density yields the volume associated with the level difference. Table XII tabulates these measurements. The average volume to height ratio is $9.21 \pm 0.14 \times 10^{-2}$ cc/mm. This volume to height ratio indicates a tubing internal diameter of 10.8 mm which compares quite well with 10.6 mm measured with calipers for 13 mm glass tubing.

Diffusion cell cross sectional area calibration uses literature diffusion coefficient values for both the open tube and capillary disk. These literature diffusivities are summarized in Table XIII. These diffusivities, the literature solubility values of Table XIV and the gas absorption rates in Appendix C permit calculation of diffusion cell areas using equations 24 and 25. Figure 23 lists the calculated areas from the various gas/liquid systems studied. The scatter in the data for the open tube plot Figure 23a indicates that 50 mm tubing area (19.63 cm^2) is a good choice. For gas solutes in carbon tetrachloride, only Hildebrand's revised values show a large discrepancy from 19.63 cm^2. The derived areas from the gas diffusivity in benzene are too low for argon and too high for oxygen while those of nitrogen are more in line with the values of gas solutes in carbon tetrachloride. The literature diffusivity of argon in benzene is cited as being anomalously high by Walkley et al. Therefore the calculated area is somewhat low. On the other hand the bubble dissolution determination of oxygen diffusivity in benzene must be too small to result in such a large value for the calibrant area. In contrast, all the calibrant areas in Figure 23b for the 304, 1 mm diameter capillaries show disagreement with the calculated cross sectional area 2.387 cm^2. This disagreement is attributed to covering the capillaries around the outer perimeter of the disk with the sealing O-ring. A reduction of the capillary disk area to 2.058 cm^2 for covering the forty two peripheral capillaries shows much

Table XII. Gas Buret Volume Calibration.

Height (mm)	Mercury Weight (grams)	Volume displaced (cc)	Volume height × 10^2 (cc/mm)
8.2	10.4690	0.773	9.43
8.6	10.8771	0.804	9.34
8.9	11.3672	0.840	9.43
9.0	11.2609	0.832	9.24
9.0	11.2438	0.831	9.23
9.5	11.6454	0.860	9.06
9.8	12.1274	0.895	9.14
9.9	12.6613	0.935	9.45
10.0	12.3511	0.912	9.12
10.5	13.1621	0.972	9.26
10.8	13.3857	0.989	9.16
11.5	14.2873	1.059	9.18
17.4	21.3919	1.580	9.08
19.2	23.8780	1.764	9.19
19.2	24.0173	1.774	9.24
19.5	24.6041	1.818	9.32
21.4	25.2070	1.915	8.95
22.4	27.4342	2.027	9.05
22.6	28.1651	2.081	9.21
23.4	30.3905	2.245	9.59
24.0	29.6638	2.191	9.13
25.3	31.6367	2.399	9.16
26.3	32.4144	2.394	9.10
27.0	33.8257	2.499	9.25
29.8	36.8308	2.721	9.13
31.9	39.4758	2.916	9.14
32.4	39.7328	2.935	9.06
38.1	46.8050	3.458	9.07
Average			9.21
BESD			±0.14

Table XIII. Literature diffusion coefficients at one atmosphere and room temperature. Superscripts are literature references.

Gas/Liquid	10^5D (cm^2/sec) Capillary (rev) Disk	Open tube	Other
Ar/CCl_4	3.63[3] (4.85)[42]	3.71[4]	
N_2/CCl_4	3.42[3] (4.76)[42]	3.63[4]	
O_2/CCl_4	3.82[36]		3.71[82] at 25.4°C
Ar/C_6H_6	11.2[4]	NR[4]	
N_2/C_6H_6	6.93[4]	7.20[4]	
O_2/C_6H_6			2.89[11] at 29.6°C

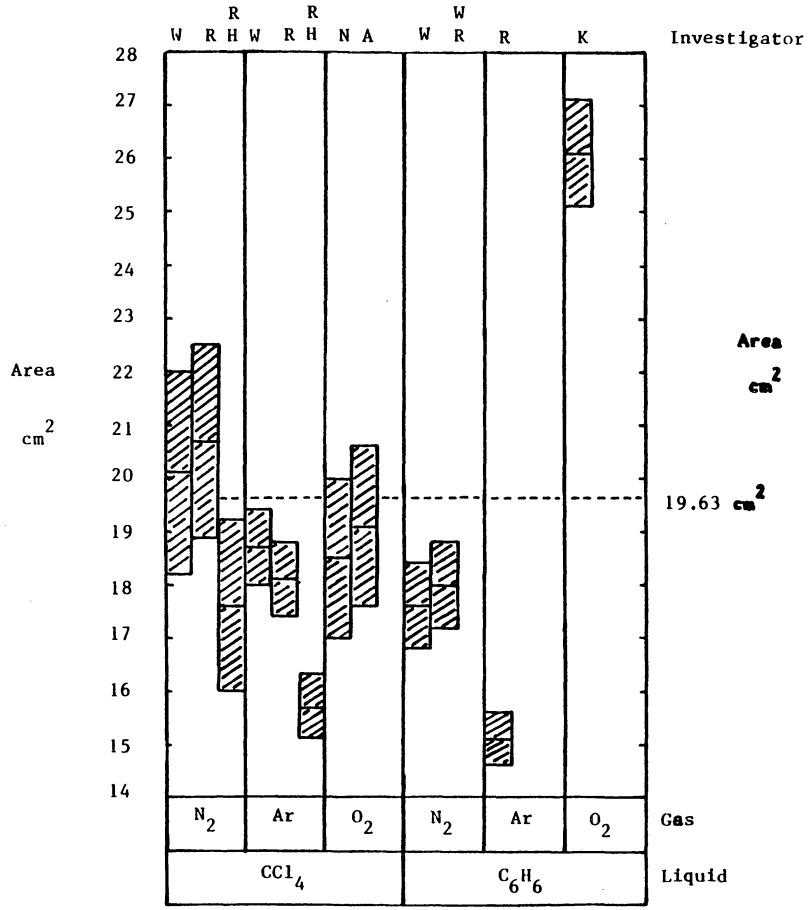

(a) Open Tube Area Calibration

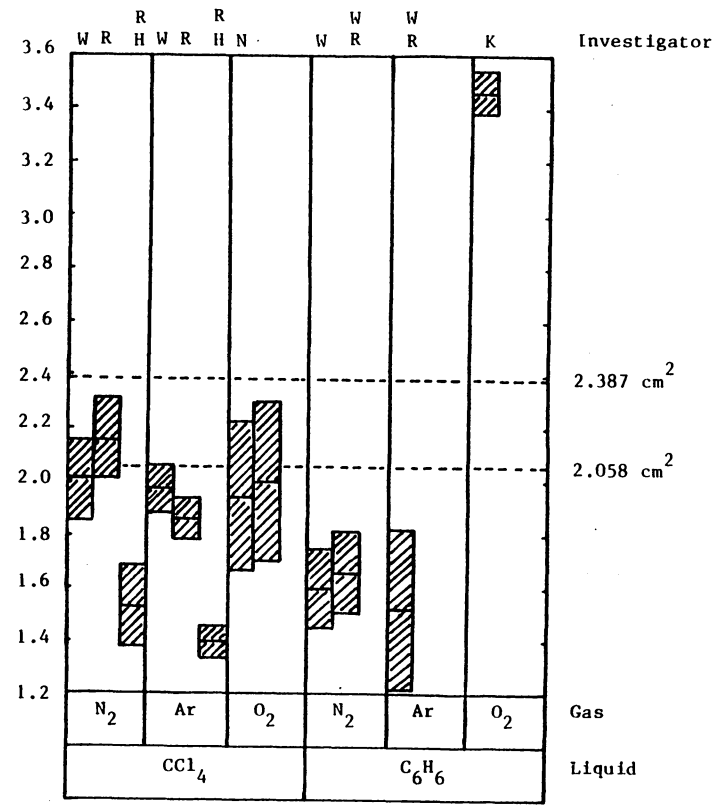

(b) Capillary Disk Area Calibration

(reference)
W: open tube, Walkley (4)
R: capillary disk, Ross (3)
RH: revised capillary disk, Hildebrand (42)
N: capillary disk, Nakanishi (36)
A: porous disk, Akgerman (82)
WR: capillary disk, Walkley (4)
K: bubble dissolution, Krieger (11)

Figure 23. Calibration of diffusion cell cross sectional areas: (a) open tube area and (b) capillary disk area.

better agreement with the derived areas in Figure 23b. Again the same trend in discrepancies in areas as for the open tube is found.

Table XIV. Gas solubilities in mole fractions at one atmosphere and room temperature from reference 50.

	CCl_4	C_6H_6
N_2	6.39[64]	4.42
Ar	13.44	8.77
O_2	12.0	8.15

4.5 Solvent Degassing Procedure

Data used to calibrate the cross sectional areas of the diffusion cell relies on adherence to the ideal open tube and capillary disk boundary conditions. Boundary conditions of zero concentration initially for all distances along the open tube experiment and zero concentration below the capillary for the duration of the capillary disk experiment emphasizes the need for complete solvent degassing. The formation of an instantaneously saturated top liquid layer for the open tube experiment and a saturated layer above the capillary disk to maintain a steady state for the duration of the capillary disk experiment are assumed boundary conditions. Determination of the gas solubility permits a check on the validity of the gas saturation conditions. The previous agreement of the cross sectional areas for different gas liquid systems indicates that diffusion coefficients agree with the literature and are internally consistent with the solubilities.

Battino and Clever[60] point out that although a necessary criterion for complete degassing is reproducibility of solubility measurements, this is not sufficient because of possible repetition of systematic error. They suggest two tests for determining complete solvent degassing. Descriptions of these tests and methods of degassing were previously described in section 2.5.

To address the question of complete solvent degassing, the freeze melt method was used for comparison to solvent refluxing. The test for complete degassing with the freeze-melt method, was a variation on the previously described compression method. The apparatus for solvent degassing and complete degassing test is illustrated in Figure 24. A McLeod gage was attached to the vacuum manifold used for pumping on the frozen solvent. The vacuum pump used gave a vacuum better than 100 microns as indicated by a previously calibrated thermocouple gage. During the interim between freeze cycles the solvent vapor is allowed to equilibrate at room temperature in the vacuum manifold and McLeod gage. Subsequently raising the mercury level in the McLeod gage to position A in Figure 24, compression of the vapor was observed with the liquid at position C. These compressions obtained during various freeze-melt cycles are tabulated in Table XV. Since solvent vapor was present in both the enclosed volume of the McLeod gage and the manifold, the solvent vapor pressure effects cancels. Use of the ideal gas law for compression $P_{initial} \times V_{initial} = P_{final} \times V_{final}$ with $V_{initial} =$ 250 cc permitted calculation of $P_{initial}$, since V_{final} and P_{final} are measured. The Henry's Law constant is defined $K_p = C_s/P$, where C_s was the dissolved gas concentration and P the gas solute saturating pressure. K_p at one atmosphere pressure is C_s by definition. This value is 6.66×10^{-6} moles/cc for nitrogen in carbon tetrachloride. Scaling the pressure obtained in cycle 6 of Table XV by this Henry's Law constant indicated a gas concentration of 3.0×10^{-10} moles/cc, which is essentially degassed as compared to a value approximately ten thousand times greater for gas saturation at one atmosphere pressure.

The degassed solvent is siphoned into the flask previously used for solvent refluxing through a transfer line. Liquid transfer relies on the vapor pressure of the degassed solvent in the freeze-melt flask to push the solvent into the collection flask. The degassed solvent is then siphoned into the diffusion cell. The diffusion experiment with liquid degassed by the freeze-melt method gives gas absorption rates indicated by the asterisks in Table XIX. These rates are plotted in Figure 40 and

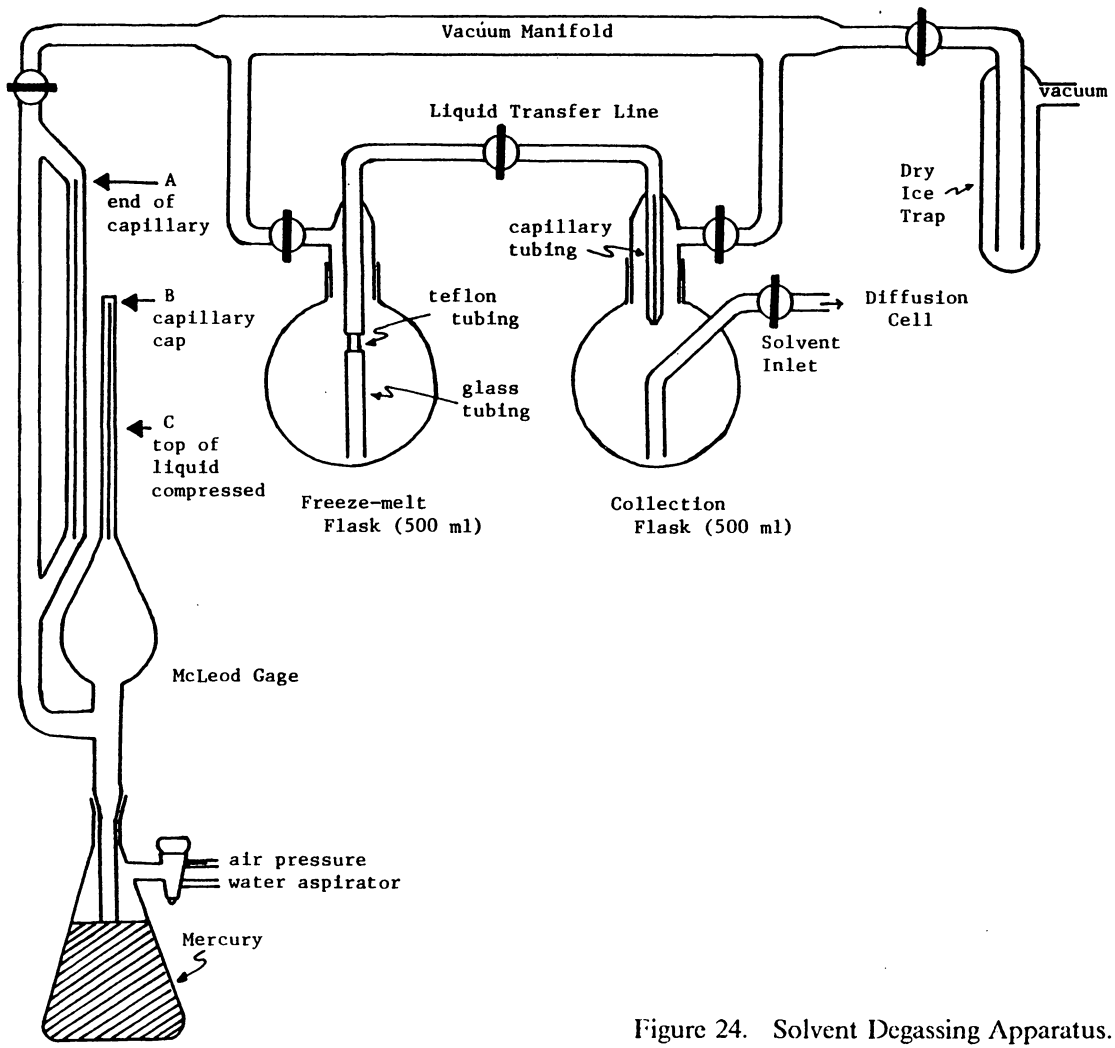

Figure 24. Solvent Degassing Apparatus.

Table XV. McLeod gage measurement to determine extent of solvent degassing.

Pumping Cycle	P_{final} (mm) A-C	Gas Space in Capillary (mm) B-C	Capillary Volume (cc)	$10^4\frac{V_f}{V_i}$	$10^2P_{initial}$ (torr)
3	178.2	58.7	0.046	1.8	3.2
5	174.0	54.5	0.043	1.7	3.0
6	180.0	60.5	0.048	1.9	3.4

designated with filled in points. Since no significant deviation is observed from the slopes obtained from degassing by refluxing, it is concluded that the solvent was completely degassed for all runs.

4.6 Automated Apparatus Description

The automated apparatus differs from the manual one both in the method of data acquisition and in the monitoring and control of pressure and temperature. The diffusion cell is the same except for a volume approximately 150 cc rather than the previous 300 cc under the capillary disk. Figure 25 is a diagrammatic view of the automated apparatus.

Data acquisition is performed with an Intel 8085 microprocessor based microcomputer. The computer and its operation are described in reference 78. Memory expansion of the Processor and Memory (PAM) board is documented in Appendix B. Results from the automated apparatus are comparable to the manual apparatus. Control in the automated apparatus is improved by continuously monitoring system pressure (P_x) and readjusting for fluctuation from the reference pressure (P_{ref}).

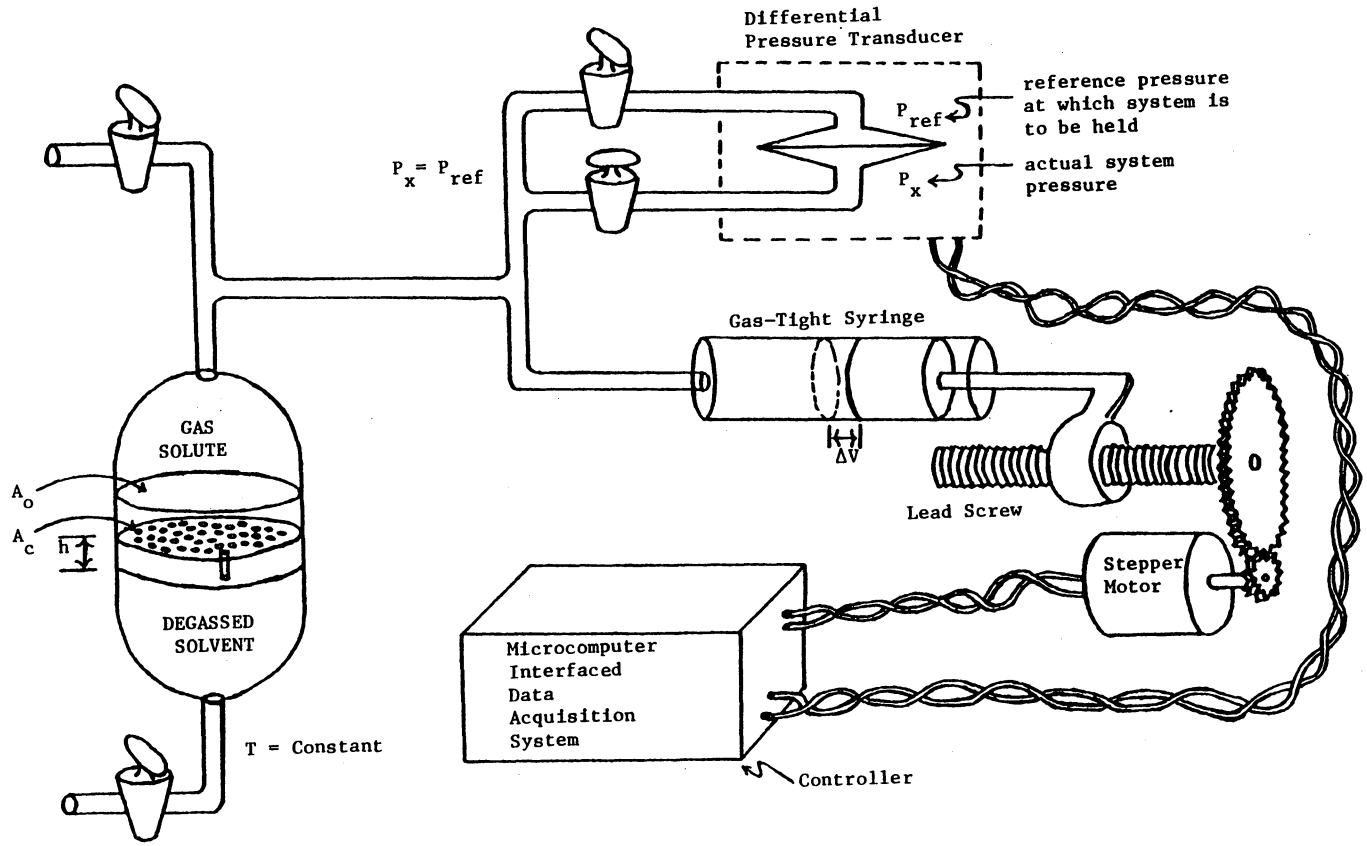

Figure 25. Automated Diffusion/Solubility Apparatus.

The automated apparatus is constructed in a housing and oven of a Beckman GC-5 Gas Chromatograph. The diffusion cell is thermostated in the oven with dimensions of approximately a cubic foot. The syringe and differential pressure transducer are placed in a compartment adjacent to the oven. A separate temperature control maintains the syringe compartment at a higher temperature than the oven during a run. The apparatus for solvent degassing, liquid transfer lines and gas inlet values are external to the GC housing but in an air stirred and thermostated hood. The microcomputer and interface electronics are located outside the hood.

The pressure sensor is a differential oil manometer. Chlorophyll B dissolved in dibutyl phthalate allows the oil levels to be detected with a pair of phototransistor detectors. Light emitting diode lamps serve as the light sources for the detectors. Painted plexiglass blocks hold the detectors and lamps. Figure 26 shows attachment of these blocks to the glass tubing of the manometer. The detectors in the blocks are initially positioned slightly above the oil levels. Subsequent pressure differentials between the reference ballast bulb and diffusion cell causes an oil level to fall below one or the other of the detectors. When the oil level in an arm of the differential manometer falls below a detector, light from the lamp is no longer blocked by the oil and switches on the phototransistor. The upper portion of Figure 27 is the circuit schematic for monitoring the phototransistors. Each phototransistor collector is biased to + 5V with a 10 Kohm resistor and is connected to a voltage comparator. The comparator output is open collector. Adding a 1 Kohm pull-up resistor to the comparator output makes the output TTL compatible. The comparator output signal of logic 1 (+ 5V) or 0 (GND) indicates status of the detectors. Buffers gate this status onto the microcomputer data bus. An input from these buffers results in one of three states for data bits D3 and D2. Table XVI shows the correspondence between these bit combinations and the differential pressure status. For example, with the system pressure lower than the set reference pressure, data bits D3 and D2 are logic states 0 and 1 respectively. This indicates an absence of the reference level (logic 0) and presence of the system level (logic 1). Constant monitoring of the indicators permits detection of a deviation from the reference pressure.

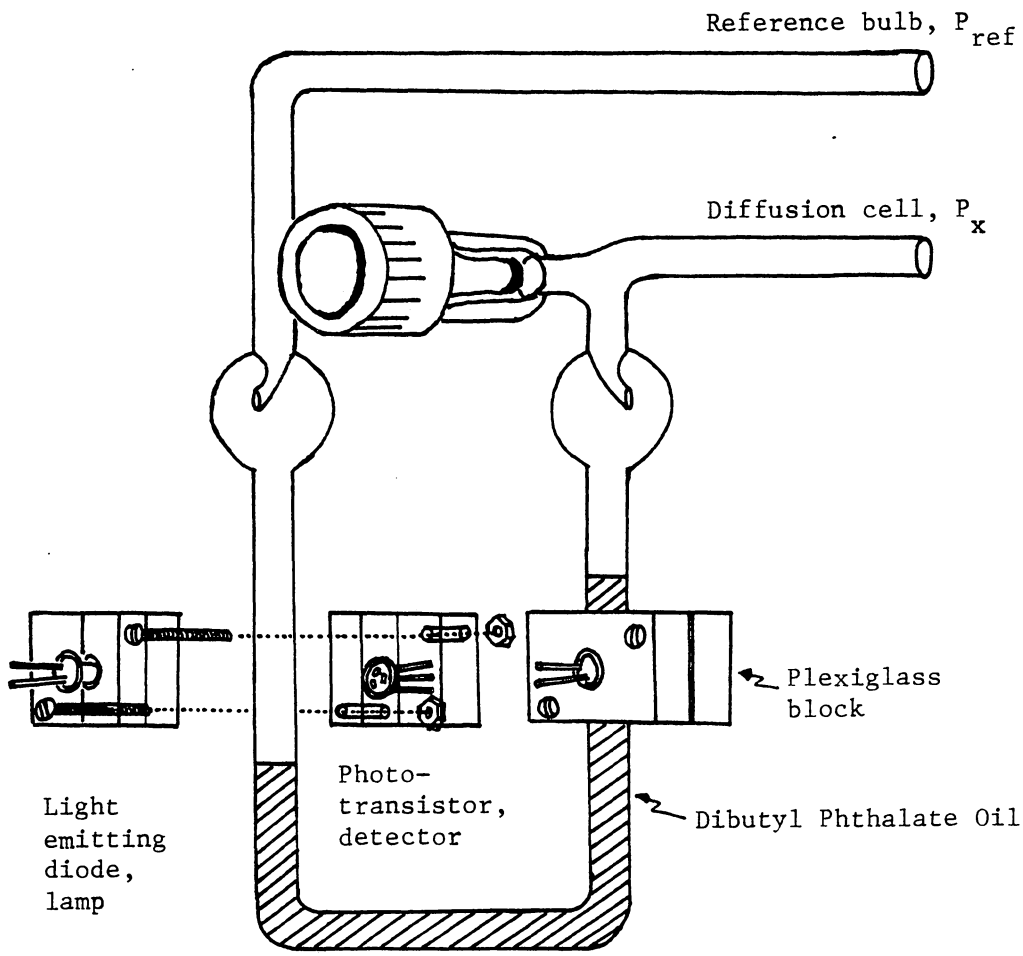

Figure 26. Differential Manometer Assembly.

Table XVI. Detector status in pressure monitoring.

Device 72 Hex Data Bits (ref) (x)		Differential Pressure	
D3	D2	Deviation	Condition
1	1	none	$P_{ref} = P_x$
0	1	negative	$P_{ref} > P_x$
1	0	positive	$P_{ref} < P_x$

Moving a gas-tight syringe allows the pressure adjustment to the reference pressure. The gas-tight syringe is composed of a precision bore Hamilton 1010LT housing and a teflon plunger holding two Buna-N O-rings 0.8 cm apart for the gas-tight seal to the housing. A lead screw moves the syringe. If the volume is out of the syringe range, a pair of limit switches (Figure 27) prompt the processor to terminate the run. Figure 28 illustrates the interface circuit for the Phillips Haydon stepper motor which drives the lead screw. Reference 79 describes most of the details of interfacing this stepper motor. The interface circuit of reference 79 differs from the circuit here. The difference is in transmission of data to the latch which controls the driver transistors of the stepper motor. The signals are transmitted at RS-232 signal levels (± 12V). Conversion of the TTL level signals (0 to + 5V) to RS-232 levels is made with the MC1488 and MC1489, quad driver and quad receiver. Data at RS-232 signal levels are more immune to noise and permit data transmission upto 50 ft without signal loss. This longer distance permits the location of the interface circuit to be a distance of 10 ft from the stepper motor. Extursion of mercury from the syringe was used for volume calibration. Given the mercury density at room temperature subsequent weighings yield the volume to step ratio. The calibration results are given in Table XVII. The volume to step ratio was about 3240 steps/cc.

The number of steps to maintain constant pressure is proportional to the gas volume uptake. After a gas volume uptake decrement of about 0.06 cc (200 steps) the time is logged. By logging points at equal volume decrements rather than volumes at fixed time increments, more data points

Table XVII. Gas tight syringe volume calibration.

Number of Steps	Mercury Weight (grams)	Volume Displaced (cc)	Steps Volume (steps/cc)
1000	4.1961	0.3094	3232
1000	4.2001	0.3097	3228
1000	4.1934	0.3092	3233
1000	4.2159	0.3109	3216
2000	8.3480	0.6156	3249
2000	8.3848	0.6183	3234
2000	8.4133	0.6204	3223
2000	8.3158	0.6132	3261
2000	8.3154	0.6132	3261
4000	16.7305	1.2338	3242
4000	16.7249	1.2333	3243
4000	16.6648	1.2290	3255
4000	16.5623	1.2214	3275
8000	33.2271	2.4504	3265
Average			3244
BESD			± 17

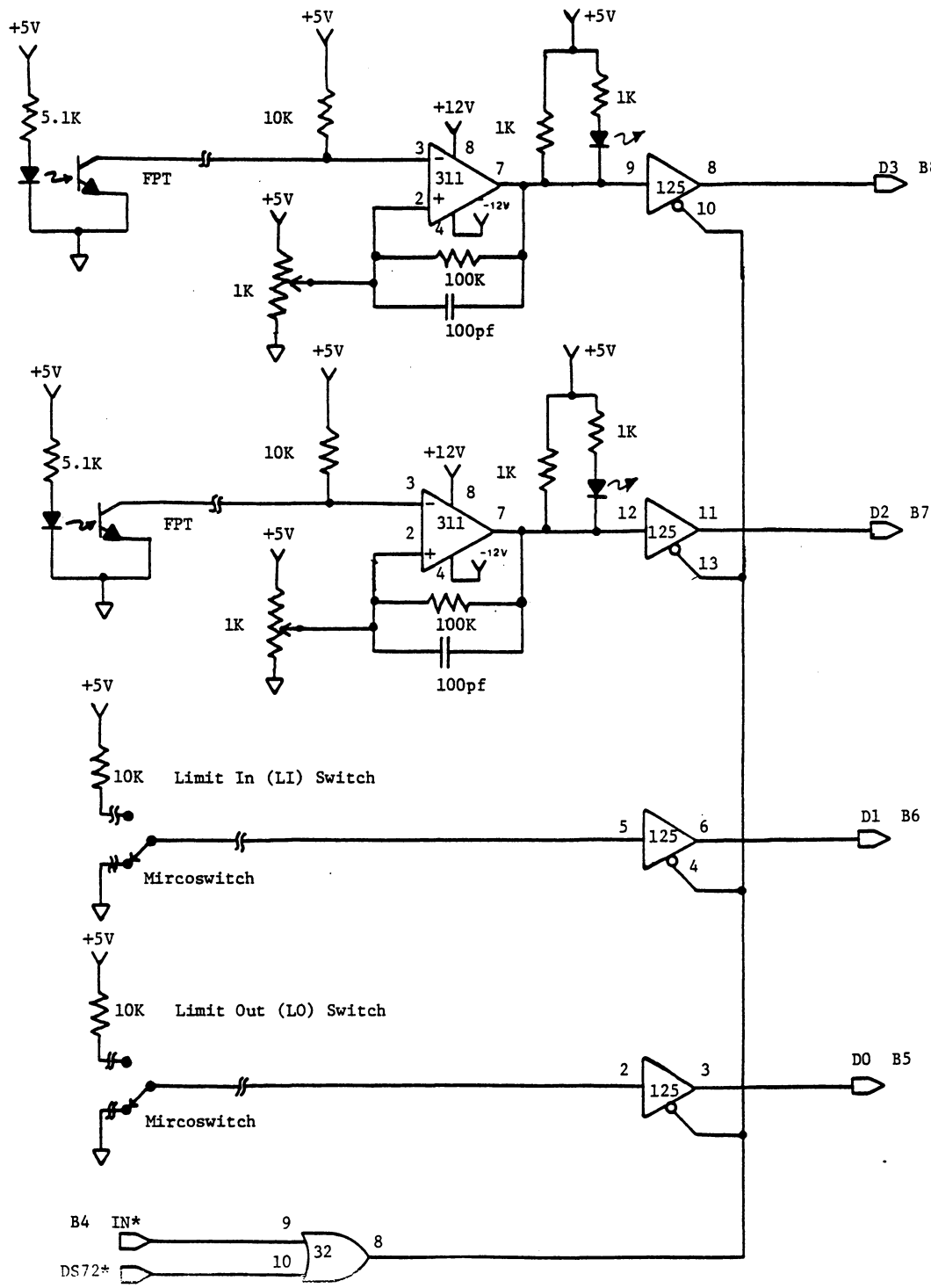

Figure 27. Manometer oil level detection and syringe limit switches.

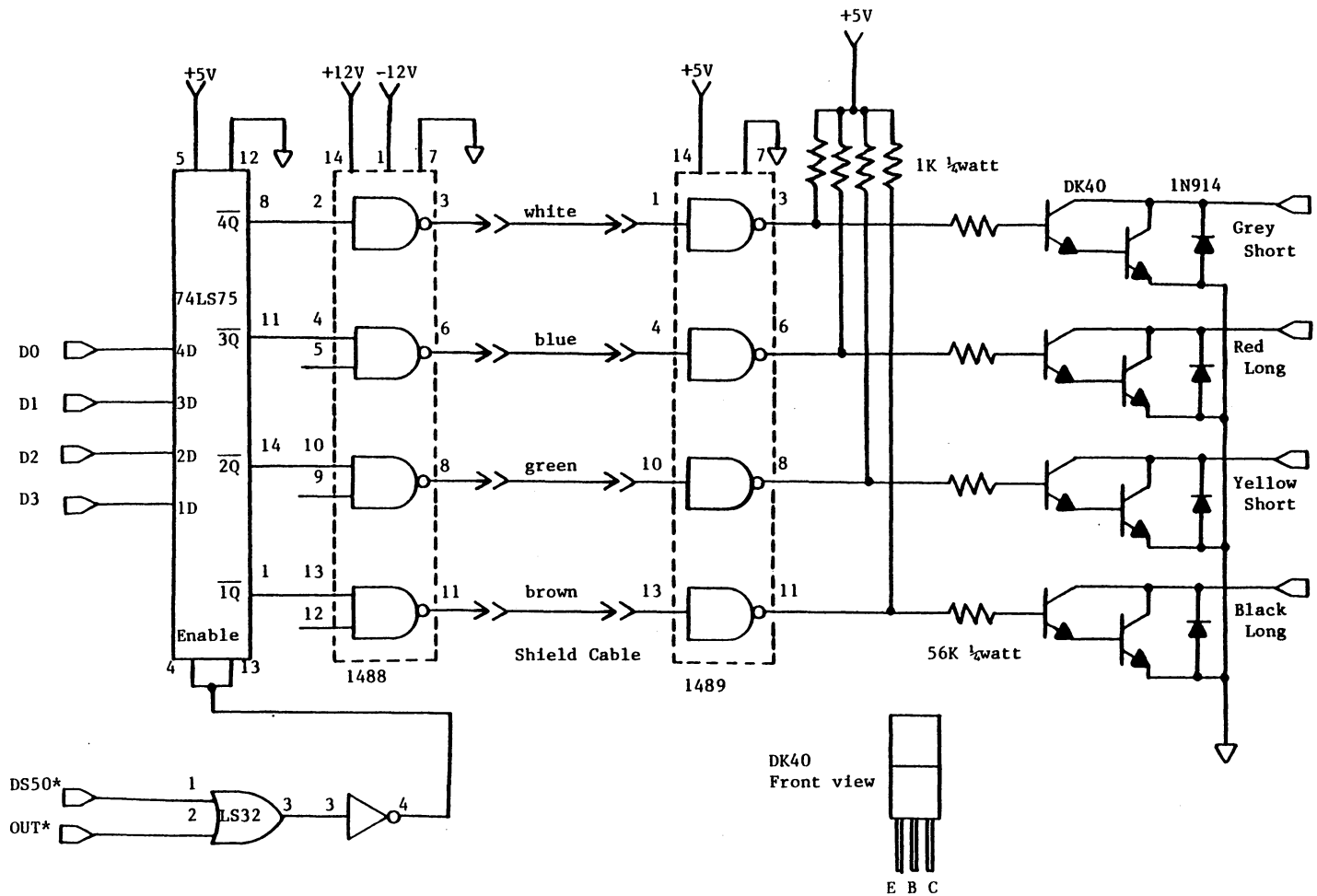

Figure 28. Stepper Motor Interface Circuit.

are logged over the rapid open tube portion of the experiment where needed. Over the much slower gas volume uptake of the capillary disk portion fewer points are required and logged. This is illustrated in Figure 29 with equal volume decrements. Volume uptake at a particular time is determined from position in the data list. Time is recorded explicitly along with a direction byte to indicate direction of syringe movement. A hexadecimal value FF indicates that syringe movement is out while 00 indicates in or syringe compression. Temperature at various positions in the apparatus are also recorded. The temperature record indicated effects of temperature fluctuations on the gas absorption rate. Figure 30 is the circuit schematic of the real time clock which records decrement volume times and permits temperature monitoring and control every fifteen seconds. Details on the clock circuit and operation are described by Field.[80]

Three portions of the diffusion apparatus require temperature monitoring and control. The most critical portion is the oven containing the diffusion cell. Second is the syringe compartment. Least important is the area surrounding the apparatus. In temperature control of the diffusion cell a Quad Diode Thermometer (QDT) sensor is used. The QDT developed by Field[80] is shown in Figure 31. This thermometer is composed of four 1N914 signal diodes. There is an inverse relation between resistance and temperature for a diode. Four diodes are necessary to magnify the temperature response by four when incorporating the diodes into an RC portion of a monostable circuit. This circuit used for digital temperature monitoring is shown in Figure 32. A control signal enables the monostable and a logic one output pulse results. The output pulse duration depends on the QDT temperature. With this in mind considerations of QDT construction, operation and calibration are summarized from reference 80.

Figure 31 shows diode positioning in the QDT assembly. This allows good thermal contact between all four diodes. After soldering diode interconnections a coat of epoxy resin provides electrical insulation. A twisted wire pair minimizes inductive pickup and connects the QDT into the monostable RC network.

Equation 28 describes the charging across the capacitor in the RC network when the monostable shown in Figure 32 receives an enabling pulse.

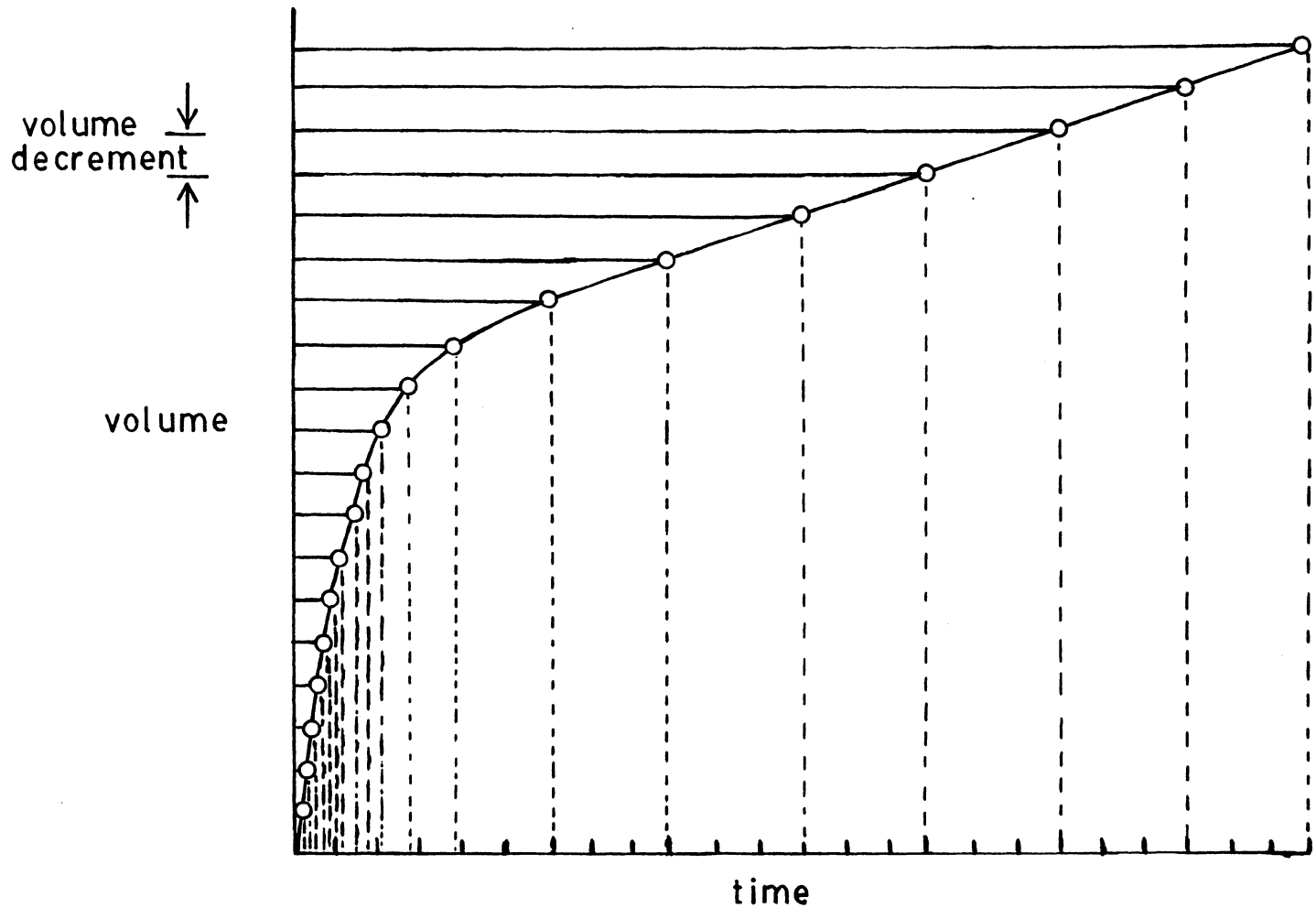

Figure 29. Data collection with equal volume decrements.

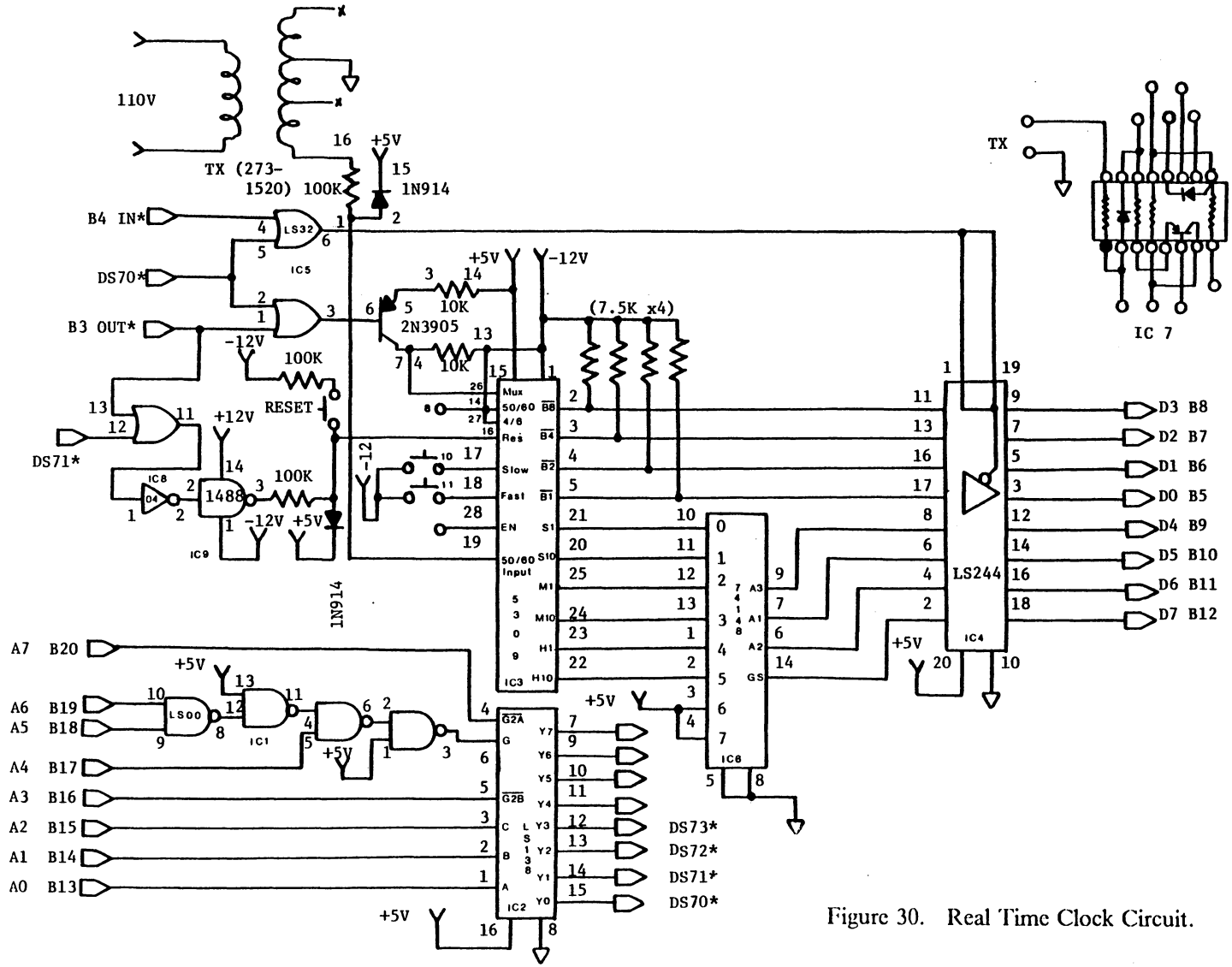

Figure 30. Real Time Clock Circuit.

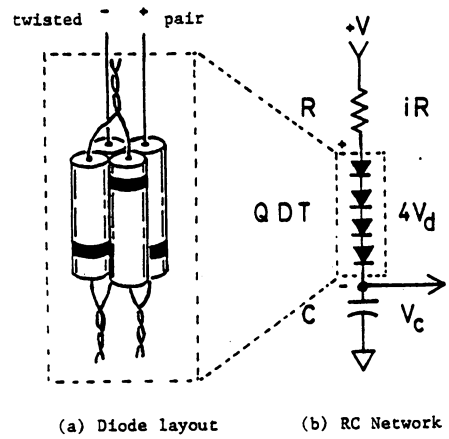

Figure 31. QDT layout and incorporation in RC network.

$$V_c = V(1 - \exp(t/RC)) \tag{28}$$

The monostable output switches to logic 1 and remains there until the capacitor charges to two thirds the supply voltage, V. At this time, the monostable shorts the capacitor to ground. Solving equation 28 for this time, t, gives a monostable pulse of $t = 1.10 \times RC$, where resistance and capacitance are in units of ohms and farads respectively. A 10 Kohm resistor in series with a QDT nominally 50 Kohm at room temperature and a 1.0 μF tantalum capacitor provide the resistance and capacitance respectively for the RC network. The resultant time constant is about 66 msec at room temperature. Gating the monostable output pulse onto the data bus with a buffer provides a digital temperature input. The microcomputer increments a sixteen bit counter with a 15 μsec delay between counts for determination of monostable pulse duration. A pulse duration of 66 msec translates to 4400 counts. This agrees quite well with the calibration values at 25 °C in Figure 33.

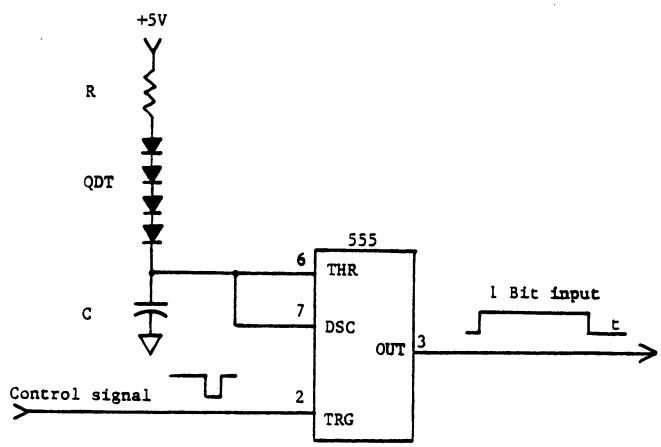

Figure 32. Temperature measurement with monostable circuit.

It also gives a rationale for selection of resistor and capacitor values, since these values yield a range of sufficient precision for the temperature range of 0 to 60 °C.

In temperature calibration, readings from the QDT and a mercury thermometer calibrated at 0°C were taken over a 0 to 60°C temperature range. To avoid systematic error in calibration, measurements were made first at room temperature, next from the lowest temperature upto room temperature and finally from the highest temperature down to room temperature. As apparent from the resultant calibration curves of Figure 33 the temperature data converged at room temperature which indicated no systematic errors in readings obtained by either heating or cooling. A difference of about 100 counts accounts for a 1°C temperature change. A variation in count of about 5 for a fixed temperature reflected a precision of ± 0.05°C in temperature measurement with the QDT. The temperature calibrations of the QDTs gave a best least squares fit to an equation of the form

$$\mathrm{Ln}(QDT\ counts) = \frac{A}{T^4} + \frac{B}{T^2} + C. \tag{29}$$

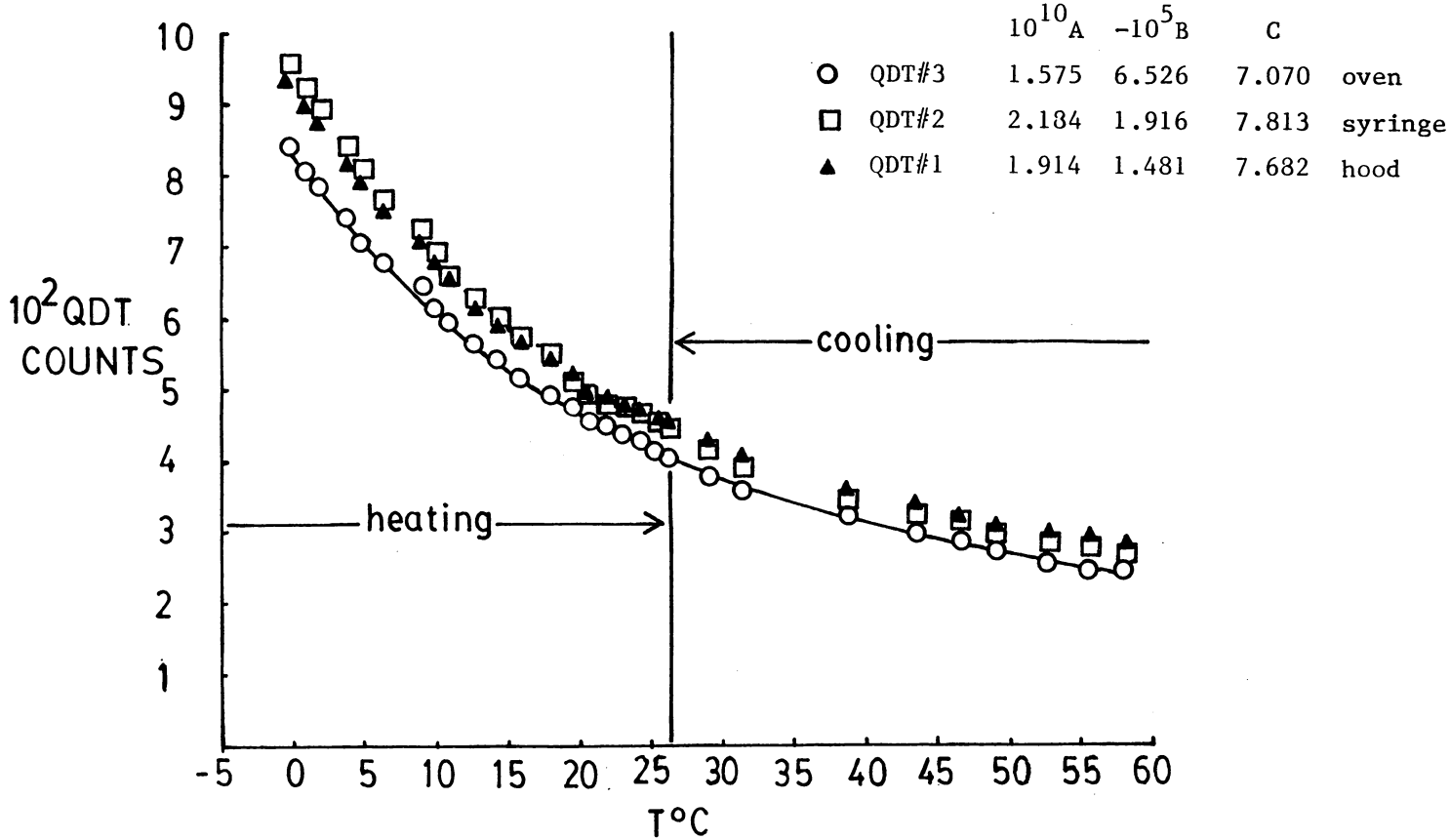

Figure 33. QDT temperature calibration.

The least square constants for the three QDTs are listed in Figure 33. For QDT number 3, the least squares fit of the data is shown in Figure 33. The program in Listing 5.4 of reference 80 performed this least square fit on a Model-1 Radio Shack Microcomputer. In practice as many as eight QDTs are easily monitored with four dual monostables configured as an eight bit thermometer port. Figure 34 is the schematic of the eight bit port used.

The QDTs were sampled every fifteen seconds. The oven heater was activated contingent on the oven QDT count. For an oven count higher than a setpoint count, the oven temperature was too low. Subsequently the oven heater was turned on for a time duration dependent on the deviation from the setpoint count. If the oven count was lower than the setpoint count, then the heater was not activated because the oven temperature was too high. Cooling coils placed inside the oven minimized overshooting by acting as controlled heat sinks. This permitted better over all oven temperature control and was essential for temperature control below room temperature.

The oven heater control circuit is illustrated in Figure 35. The heater is turned on by a pair of Silicon Controlled Rectifiers (SCRs). These SCRs control the voltage applied to the oven heater and are fired by an unijunction transistor. The emitter of the unijunction transistor is biased with a bipolar PNP transistor. The base of the bipolar transistor is turned on or off with an optically isolated 7474 data latch. The oven heater is activated with output of a logic 0 to the data latch and is deactivated with a logic 1. The heater on-time is determined by the magnitude of excursion the oven count took from the setpoint count.

Temperature regulation in the syringe compartment uses the on/off thermostat circuit shown in Figure 36. The sensor is the AD590 two terminal IC temperature transducer. A current proportional to the sensor temperature results. Resistors R1 and R2 convert this current into a voltage. A comparator compares a setpoint temperature voltage with the temperature dependent voltage. The comparator output switches on when the temperature dependent voltage falls below the reference voltage. Otherwise the comparator output is zero volts and the heater relay remains open. This on/off control using the AD590 provides control to ± 1°C. The air surrounding the apparatus in the hood is also thermostated with an on/off regulator. The sensor is a mercury switch and temperature control is to ± 2 °C.

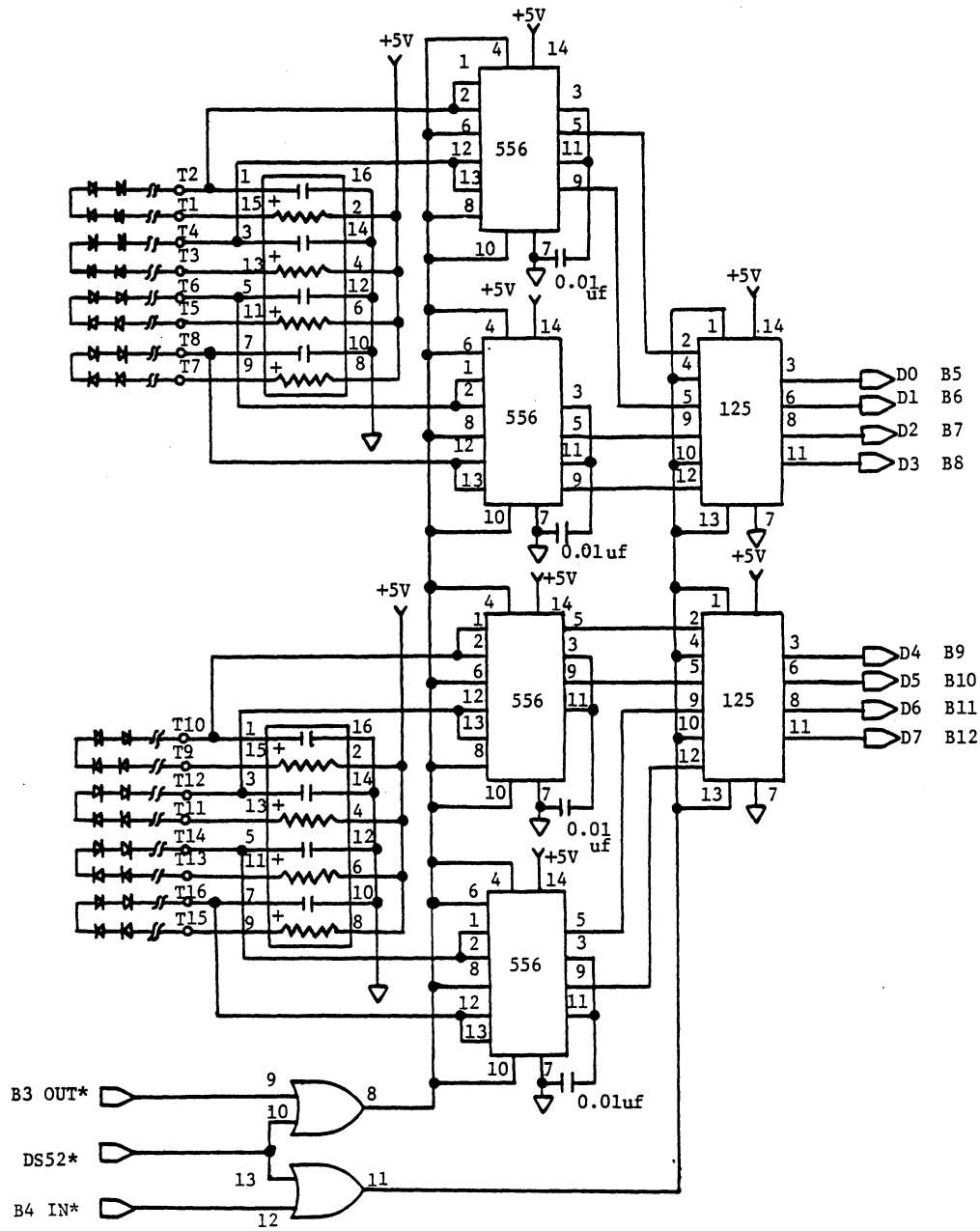

Figure 34. Eight bit thermometer port.

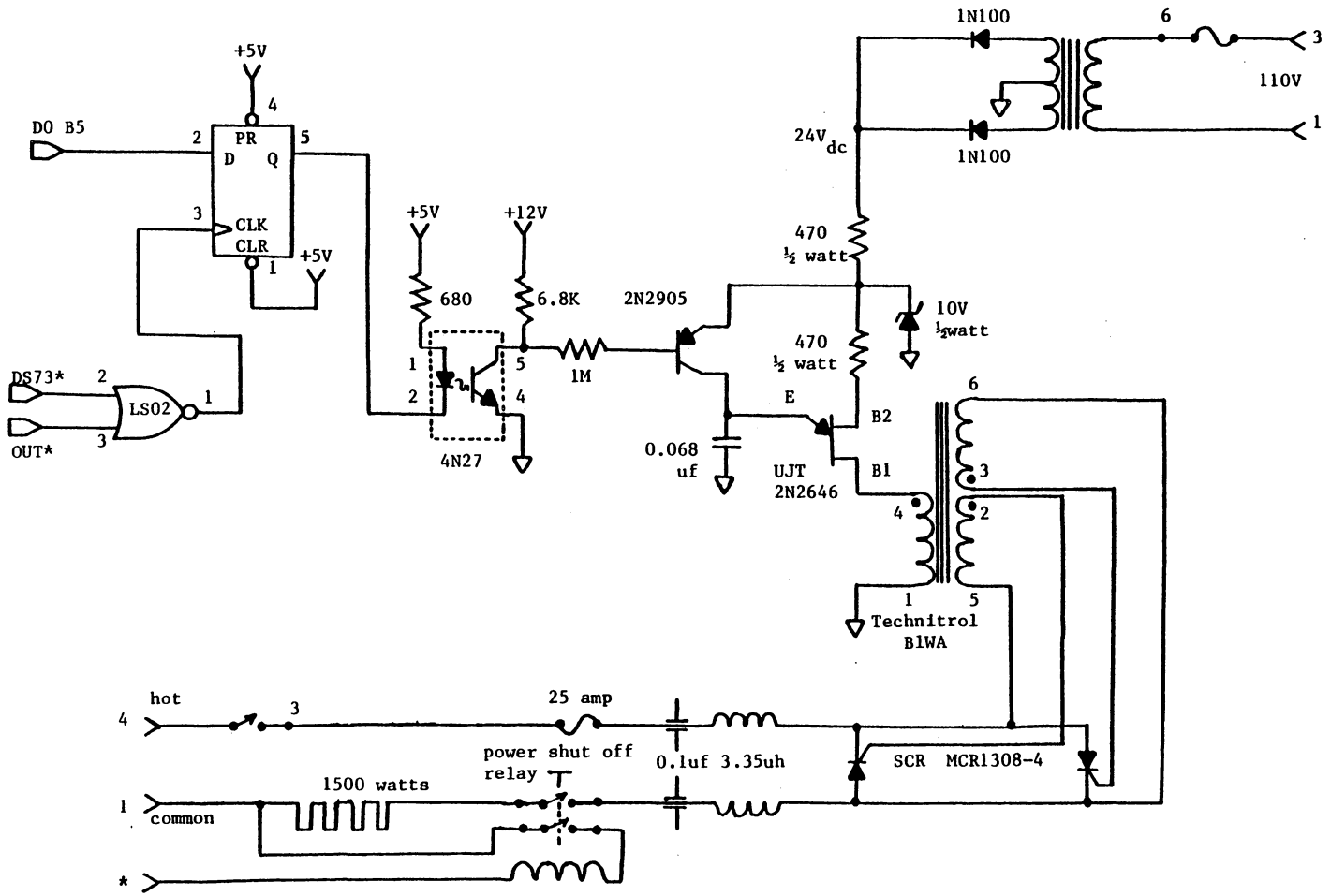

Figure 35. Oven heater control.

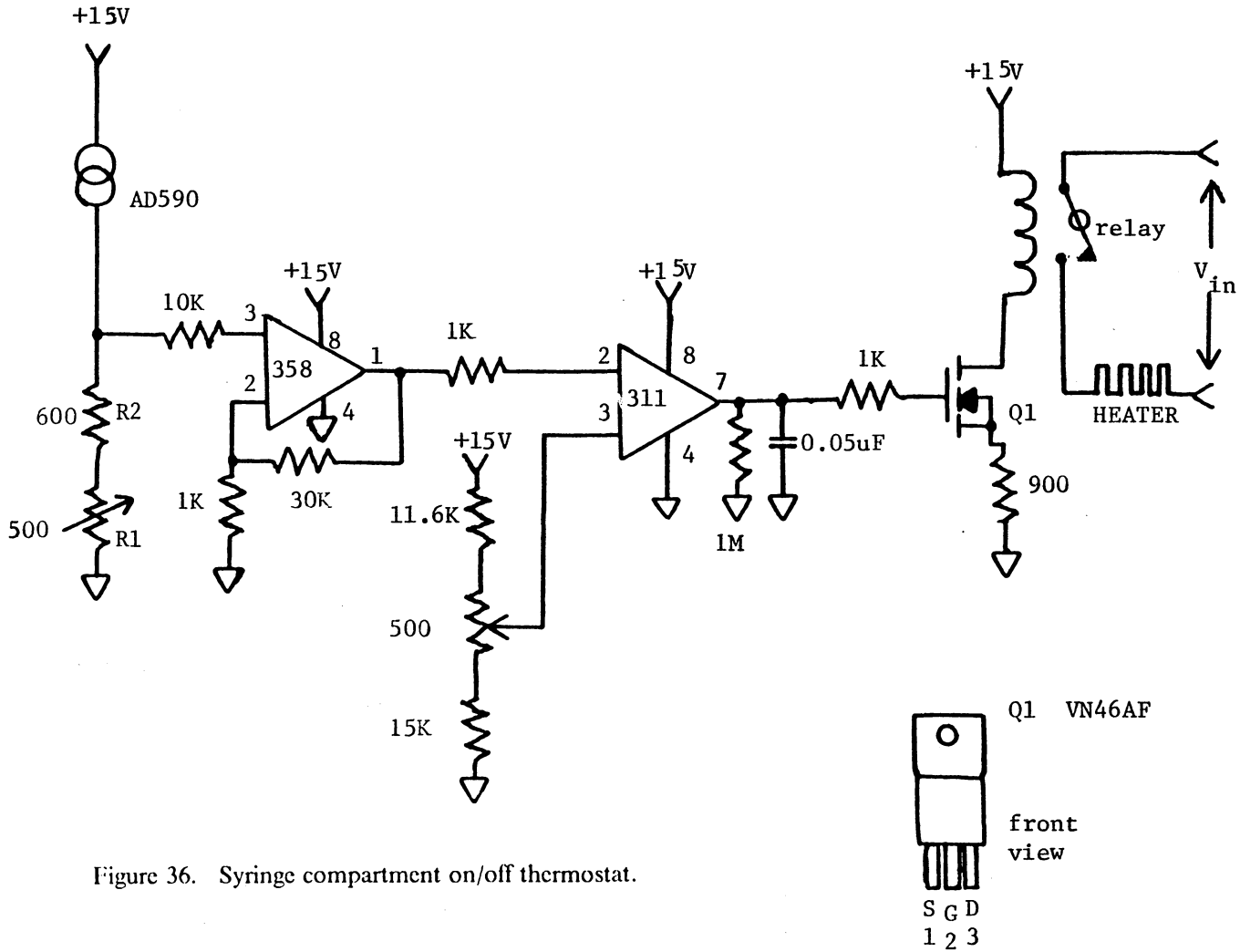

Figure 36. Syringe compartment on/off thermostat.

4.7 *Software*

The program TRACK coordinates the hardware activities of temperature and pressure control and data acquisition. Before execution of this program, the operator must perform several initialization tasks. These tasks include degassing solvent and transfer into evacuated diffusion cell, running the temperature control program (CONTEP) to allow diffusion cell temperature equilibration for at least two hours, pressurization of the apparatus except for the diffusion cell with gas, introduction of the solute gas into the diffusion cell, and closing the differential manometer valve.

After the initialization, TRACK is executed by pressing a momentary debounced switch which generates an enabling pulse on the Restart 5.5 line of the 8085 microprocessor. A maskable interrupt results and sets the program counter to hexadecimal address 002C. This location contains an absolute jump instruction to TRACK's starting address.

A listing of TRACK and CONTEP is contained in Appendix B. Various routines at addresses from hexadecimal addresses 1346 to 143A are used to check for pressure leaks, to monitor precision in oven temperature control and to calibrate the gas-tight syringe volume. Further documentation of the programs CONTEP and TRACK are contained in the flowcharts of Figures 37 and 38 respectively.

In Figure 37, CONTEP requests input parameters of temperature setpoint and delay count. The delay count determines heater on time for each oven count above the setpoint count. Next the real time clock is read. A flowchart of CLOCK in Appendix B outlines the steps in reading the clock and storing the time. Adding an offset time of fifteen seconds to the current time determines the time of the next QDT query and possible temperature correction. Disabling interrupts during a temperature correction avoids the possibility of additional oven heater on time due to interrupt servicing. The temperature imbalance subroutine (TEPIMB) in Appendix B determines whether to activate the oven heater, and for what time duration, dependent on a difference count. The positive difference count between the oven and setpoint counts turns on the heater for a period proportional to this count. The proportionality constant is the delay count. This is the time delay

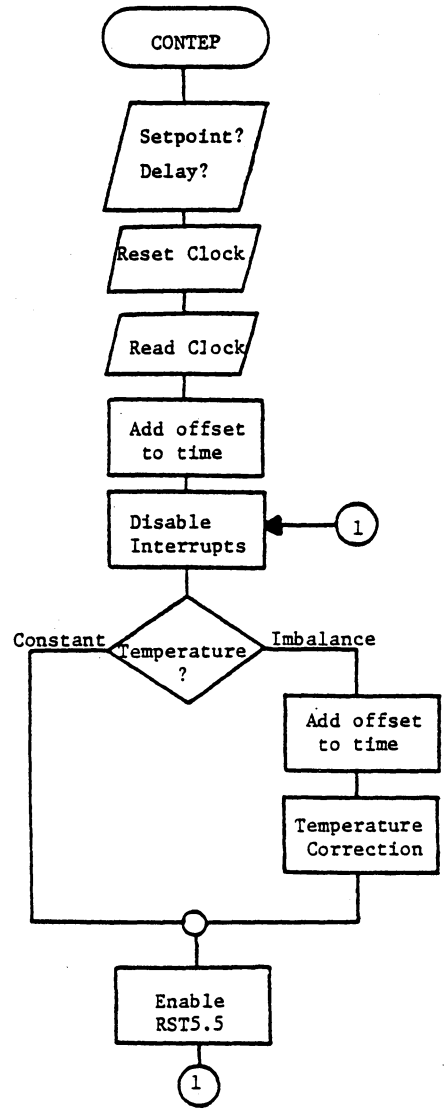

Figure 37. Control Temperature Program (CONTEP) Flowchart.

per difference count. The subroutine TEMPA in Appendix B reads and stores the QDT counts in a memory buffer. The subroutine FIND retrieves the current oven count from the buffer which is subsequently used by TEPIMB.

After diffusion cell equilibration TRACK execution not only performs the previous temperature control function of CONTEP, but also controls pressure and records gas volume changes as shown in Figure 38. Previous CONTEP subroutines permit diffusion cell temperature control. The program TRACK monitors the differential manometer levels. If TRACK detects an out-of-balance manometer signal, then the program initiates syringe movement. The syringe movement continues until the pressure difference is nulled out by balancing the manometer oil levels. A pressure drop caused by gas absorption into the diffusion cell requires syringe compression to level the manometer oil levels. After every 200 steps (0.06 cc) the time is recorded in memory by the program RECORD. The total gas volume change is determined from the position of the datum in the data list. RECORD updates the data pointer and saves a delimiter byte to indicate syringe direction (hexadecimal FF = In and 00 = Out), time (format: secs.mins.hrs.) as well as three QDT counts (oven.syringe.hood). This data format as well as memory buffer maps are summarized in Appendix B.

4.8 Summary

A combined technique of the open tube and capillary disk methods into a single experiment was described. Two apparatuses for the combined technique have been described. There were three important considerations which insured validity of results from these experiments: gas buret or gas-tight syringe volume calibration, cross sectional area determination of the diffusion cell and a test for complete solvent degassing.

A comparison of the advantages and disadvantages of the apparatuses must include considerations of experimental limiting error. Temperature and pressure are held constant in the

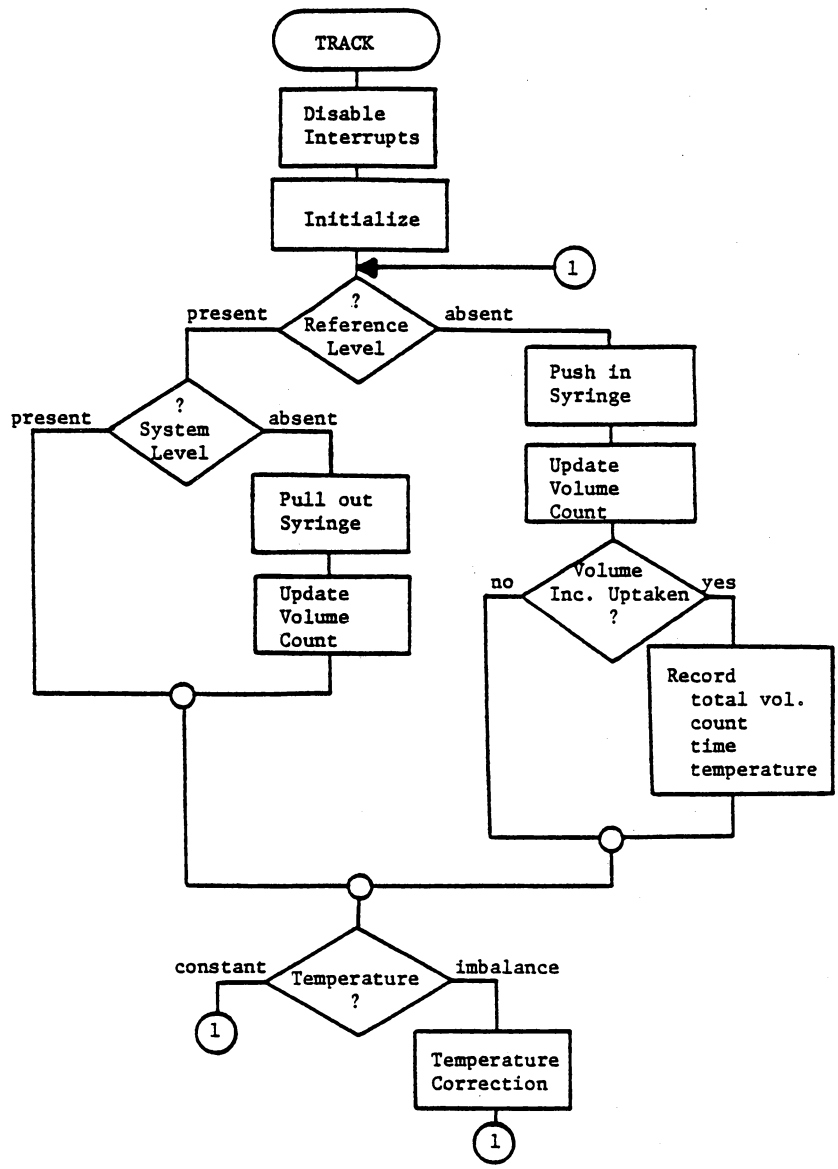

Figure 38. TRACK Program Flowchart.

diffusion/solubility experiments to a precision of ± 0.1°C and ± 0.04 torr respectively. The precision of volume change measurement for gas absorption is found by calibration to be ± 1.5% for the manual and ± 0.5% for the automated apparatus. The measurement of volume change and continual pressure monitoring by the automated apparatus is a significant advantage over the manual apparatus. However, no significant improvement for diffusivity and solubility results is found for the automated approach. This is probably due to a small but finite leak rate of the gas tight syringe compared to the perfect seal of the gas buret. One way to eliminate this leak is replacement of the syringe with a bellows. A bellows would provide a pressure seal comparable to the mercury glass seal of the gas buret. Advantage of the manual apparatus is it's inherent simplicity. It's disadvantage is the acquisition and reduction of the data by hand. The O_2/H_2O diffusion experiment with the manual apparatus is considered in section 5.2. Because of the slight solubility of this system, results from this experiment verify that temperature control is the limiting error of apparatuses.

5.0 RESULTS AND DISCUSSION

5.1 Introduction

Gas diffusivities and solubilities from the combined technique compare well with literature values. With the exception of argon in benzene, literature diffusivities, for argon and nitrogen into carbon tetrachloride and benzene, from the open tube and capillary disk methods are within the experimental precision of the combined technique. Oxygen diffusivities in carbon tetrachloride and benzene provide a comparison of the combined technique to the porous disk and bubble dissolution methods respectively. Various solubility measurements for oxygen in water have been made to a precision of better than 1%.[81] Therefore oxygen in water is a standard for technique comparison of both gas solubility and diffusivity in liquids. The oxygen in water diffusivity from the combined technique falls within the range of reported values from other methods at room temperature.

The results from the combined technique agree with Hildebrand's various correlations of gas diffusivity in liquids to gas solute cross sectional area[3], liquid self diffusion, liquid fluidity[44] and solution configuration entropy.[42] Gas diffusivities of the same gas solute in carbon tetrachloride and benzene from the combined technique are found to give a simple relation between relative diffusivities and solvent molecular weights.

5.2 *Diffusivity Data*

The diffusion experiments performed with the combined technique fall into one of three categories: (1) diffusivity of one gas solute at various pressures and room temperature, (2) various gas solute diffusivities at one atmosphere pressure and room temperature and (3) diffusivity of one gas solute at various temperatures and one atmosphere pressure. Variation of the gas solute pressure for nitrogen in carbon tetrachloride at constant temperature indicates that the resultant gas solubilities obey Henry's Law and gas absorption rates show no pressure dependence. These two observations confirm that the diffusion coefficient is concentration independent. Gas diffusivities and solubilities for seven gas/liquid systems at room temperature and one atmosphere pressure agree well with the literature.[3, 4, 82] The gas diffusivities for nitrogen in carbon tetrachloride at constant pressure vary linearly with temperature in agreement with Ross and Hildebrand's results.

The diffusion and solubility results as a function of pressure from the combined experiment for nitrogen in carbon tetrachloride are summarized in Table XVIII. The ampersand (@) denotes an experiment which shows disagreement in results between the combined and individual methods. Also the calculated solubility is no longer consistent with the Henry's Law value. These discrepancies are indicative of such systematic errors as pressure leaks and temperature fluctuations in the diffusion cell. The solubilities as a function of pressure are plotted in Figure 39. The concentrations extend from about 3×10^{-6} to 9×10^{-6} moles/cc. The Henry's Law constant is just the solubility at one atmosphere pressure. This constant from the combined technique is 6.75×10^{-6} moles/cc-atm, which is very close to Horiuti's[62] value of 6.63×10^{-6} moles/cc-atm. This is illustrated graphically by the random distribution of solubilities about the Henry's Law line in Figure 39. The gas volume uptake slopes for these experiments show pressure independence. These slopes are tabulated in Table XVIX and are plotted in Figure 40. This pressure independence of the gas volume uptake slopes and conformance of the solubilities to Henry's Law confirms the concentration independence of the diffusion coefficient. To prove the concentration independence of the diffusivity, the diffusion equations 16 and 19 are solved for the diffusion coefficient.

Table XVIII. Pressure dependence of nitrogen in carbon tetrachloride diffusivities. @ denotes a questionable data point.

Date mon: day: yr	Pressure (torr)	Temperature (°C)	$10^5 D_{open}$ (cm^2/sec)	$10^5 D_{cap}$ (cm^2/sec)	$10^5 D_{comb}$ (cm^2/sec)	$10^6 C_{comb}$ (moles/cc)	$10^6 C_{lit}$ (moles/cc)
05: 02: 84	370.0	25.0	3.04	3.00	2.96	3.28	3.24
05: 09: 84@	441.0	25.0	3.86	3.16	2.60	4.71	3.86
04: 24: 84@	517.7	25.0	4.50	3.42	2.60	5.97	4.53
09: 26: 84@	687.7	26.1	2.54	3.33	4.36	4.60	6.04
10: 28: 84@	727.6	25.9	2.90	3.56	4.38	5.19	6.38
01: 25: 84	760.8	25.0	3.69	3.69	3.71	6.64	6.66
03: 09: 84	761.8	25.0	3.45	3.65	3.87	6.30	6.67
03: 03: 84	772.5	25.0	3.83	3.69	3.56	7.01	6.76
04: 04: 84	961.4	25.0	4.03	3.69	3.29	9.31	8.42
03: 27: 84	1021.9	25.0	3.45	3.45	3.44	8.96	8.35
04: 17: 84	1033.4	25.0	3.49	3.43	3.38	9.19	9.05
03: 20: 84	1047.1	24.9	3.49	4.02	4.64	7.95	9.17
Average			3.64	3.59	3.56	6.75	
BESD			±0.36	±0.28	±0.49	±0.56	

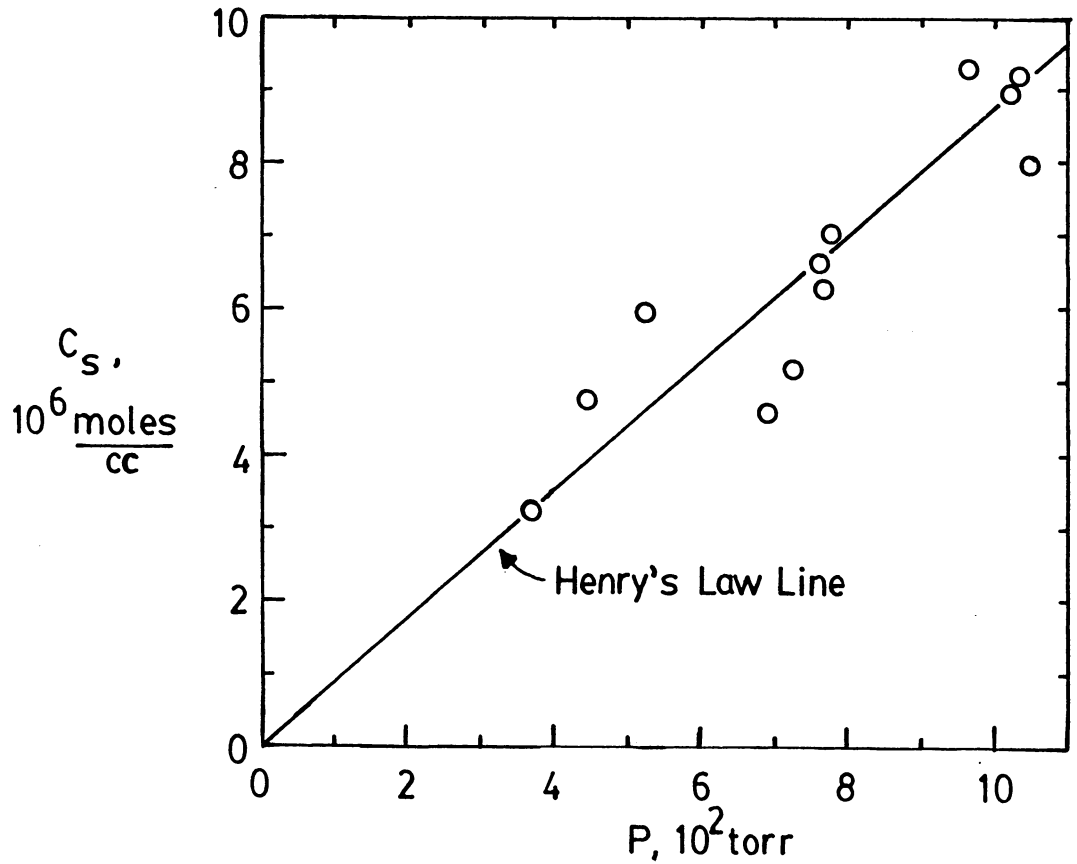

Figure 39. Solubility pressure dependence of nitrogen in carbon tetrachloride.

Table XIX. Pressure dependence of gas uptake slopes for nitrogen in carbon tetrachloride. * indicates solvent degassing by freeze-melt method.

Gas Pressure (torr)	10^2Open Tube Slope (cc/sec)	10^6Capillary Disk Slope (cc/sec)
370.0	1.99	6.71
441.0	2.24	7.07
517.7	2.42	7.64
687.7	1.83	7.49
727.6*	1.95*	7.99*
760.8	2.19	8.26
761.8	2.12	8.17
772.5	2.23	8.24
961.4	2.29	8.14
1021.9	2.12	7.71
1033.4	2.13	7.67
1047.1	2.13	8.99
Average	2.14	7.84
BESD	± 0.16	± 0.60

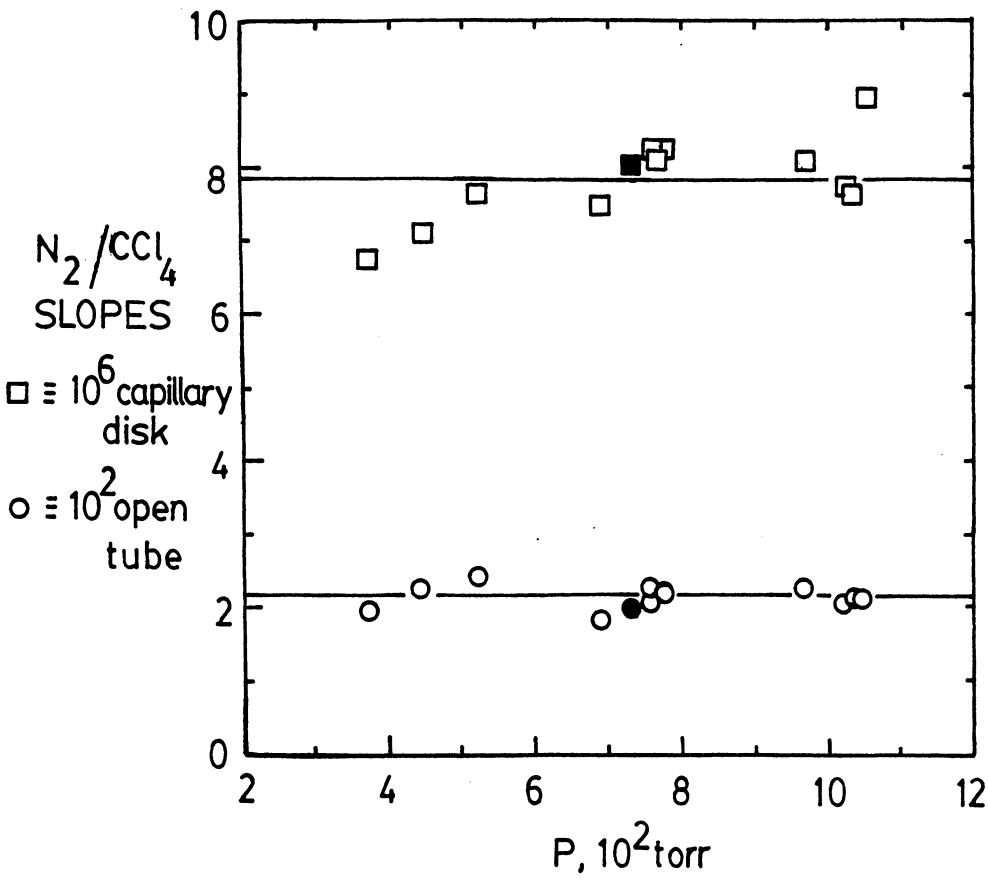

Figure 40. Pressure independence of gas volume uptake slopes for nitrogen in carbon tetrachloride. Filled in points indicate solvent degassing by freeze-melt method.

$$D^{1/2} = \frac{\pi^{1/2}}{2A_o}\frac{1}{RT}\frac{P}{C_s}\frac{\Delta V}{\Delta t^{1/2}} \tag{30}$$

$$D = \frac{h}{A_c}\frac{1}{RT}\frac{P}{C_s}\frac{\Delta V}{\Delta t} \tag{31}$$

Given the slopes are pressure independent and P/C_s is the reciprocal of the Henry's Law constant, it follows from the above equations that the diffusivity is concentration independent.

Diffusivities and solubilities of gases in nonpolar solvents from the combined technique are summarized in Table XX. The first and second columns are the diffusion coefficients from the open tube and capillary disk portions of the experiment. These values are calculated from the gas absorption rate data (i.e. slopes in Appendix C), literature solubilities in column six, and equations 30 and 31. Columns three and four are simultaneous solubilities and diffusivities from equations 24 and 25 using only gas volume uptake data. The remaining columns columns five and six are literature values for diffusivity and solubility from various literature sources. Gas volume absorption rates used in these calculations are derived from the data listed in Appendix C. This data is listed along with the plotted curves.

Comparison of the open tube and capillary disk methods to the combined technique is provided by the diffusivities of nitrogen and argon in carbon tetrachloride and benzene. Walkley's[4] open tube results provides a comparison to Ross and Hildebrand's[3] capillary disk method. With the exception of argon in benzene, values from the different methods agree well. Walkley reports that the capillary disk method yields an anomalously high diffusion coefficient for argon in benzene almost twice that of nitrogen in benzene. He speculates that the inability to obtain consistent results for argon in benzene with the open tube method is due to the generation of a steady state at the gas liquid interface. A constant flux at the interface is incompatible with the open tube boundary conditions.

With the exception of argon in benzene the combined technique yields solubilities where the experimental precision around the 68% confidence level, encompasses the literature values. These solubilities are internally consistent with the diffusivities from each portion of the experiment. The

Table XX. Solubility and diffusivity results from the combined technique with nonpolar liquids.

Liquid	$10^5 D_{open}$	$10^5 D_{cap}$	$10^5 D_{comb}$	$10^6 C_{comb}$	$10^5 D_{lit}$	$10^6 C_{lit}$	Gas Solute
CCl_4	3.64 ± 0.36	3.59 ± 0.28	3.56 ± 0.49	6.75 ± 0.56	3.63[4] 3.42[3] 4.76[42]	6.65[64]	N_2
	3.11 ± 0.25	3.27 ± 0.13	3.46 ± 0.29	13.14 ± 0.93	3.71[4] 3.63[3] 4.85[42]	13.90[50]	Ar
	3.40 ± 0.56	3.59 ± 0.52	3.79 ± 0.47	12.06 ± 0.45	3.82[36] 3.71[82]	12.38[50]	O_2
C_6H_6	5.83 ± 0.54	5.58 ± 0.53	5.35 ± 0.60	5.17 ± 0.22	7.20[4] 6.93[4]	4.99[50]	N_2
	6.65 ± 0.42	7.55 ± 0.51	8.70 ± 0.93	8.55 ± 0.39	11.2[4]	9.87[50]	Ar
	5.11 ± 0.39	4.86 ± 0.12	4.65 ± 0.27	9.56 ± 0.61	2.89[11] ± 0.31 @ 29.6°C	9.13[50]	O_2

combined technique diffusion results for argon in benzene although higher than nitrogen in benzene are substantially lower than Walkley's value with the capillary disk method. The argon in benzene diffusion coefficients from this work become progressively larger in the order of open tube, capillary disk, and combined experiment in Table XX. These large diffusivities of argon are attributable to convection in the diffusion cell. Houghton et al.[41] measured the diffusion of isobutylene into dinonyl phthalate and noted that a more rapid absorption rate in the later portion of the absorption curve as indication of convection. Figure 41 shows a gas volume uptake slope of argon in benzene for the open tube portion of the combined technique. The later portion of this gas absorption slope clearly indicates the presence of convection. Therefore the slope before the onset of convection is used in calculation of the diffusion coefficient.

An explanation of the higher diffusivities lies in the source of the convection. If the gas solution density were larger than that of pure liquid, then convection would have resulted by mixing of a heavier solution layer over a less dense pure liquid. This is consistent with the trend of diffusivities reported in Table XX for argon in benzene. For the open tube experiment of short time duration the density driven convection would appear only at later times in the volume uptake curve. The capillary disk with liquid volumes about one tenth that of the open tube volume and long times to establish a steady state might be subject to streaming through the disk, substantially increasing the apparent diffusivity. A capillary disk experiment with only a shallow liquid layer of about 1 mm in depth above the disk permitted a test for streaming through the disk due to the open tube convection above the capillary disk portion of the combined experiment. The capillary disk with no open tube flooding above the disk gave nearly an identical diffusion coefficient to that of the capillary disk portion of the combined technique. This discounts streaming due only to the open tube portion of the experiment. Since K_o is smaller than K_c in equation 27, the calculated diffusivity for the combined experiment would appear even larger than the capillary disk result. Elimination of a density driven convection is possible with either Walkley's inverted tube method[20] or Tse and Sandall's gas desorption approach.[24] The diffusivity determination of the argon in benzene by either the inverted tube or desorption method would determine if the convection source is density driven.

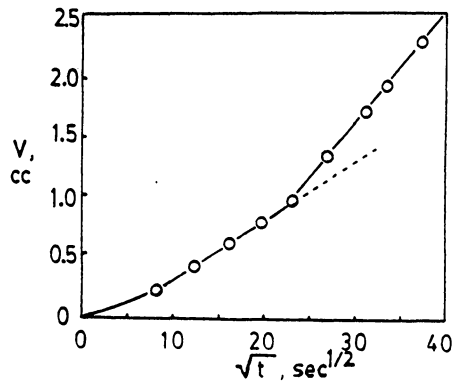

Figure 41. Convection in open tube experiment for argon in benzene. Increased absorption rate at later times indicate convection.

Comparison of the combined technique to various other methods is made with the gas solute oxygen in carbon tetrachloride. For the capillary disk, combined and porous disk methods diffusivities in Table XX are virtually identical. The diffusivity of oxygen into benzene for the combined technique is about twice that of Krieger's bubble dissolution value.[11] The bubble dissolution value appears too low especially in view of the higher temperature of 29.6 °C . The combined technique diffusivity appears more reasonable since it is about the same as nitrogen in benzene.

The diffusivity of oxygen in water provides a comparison of the combined technique to a wide variety of methods which are listed in Figure 2. The solubility of oxygen in water (1.274×10^{-6} moles/cc-atm)[81] is about ten times less than oxygen in carbon tetrachloride or benzene. This requires a gas buret significantly more sensitive for measurement of the smaller gas absorption. A gas buret radius of 2.17 mm is used. This new radius is about one half the previous one of 5.14 mm which is was used for the previous solvents. The ratio of the cross sectional areas is about one sixth. Using a solubility of 1.274×10^{-6} moles/cc-atm and gas volume uptake slopes from Appendix C the calculated diffusion coefficients are 3.02×10^{-5} cm^2/sec and 1.92×10^{-5} cm^2/sec for the open tube and capillary disk portions of the combined method respectively. These values bracket the "best" value from Vivian and King[4] of 2.41×10^{-5} cm^2/sec. Unfortunately the small gas volume uptake of about 0.3 cc in 48 hours for the capillary disk is sensitive to small temperature fluctuations about the diffusion cell temperature for the lines connecting the

diffusion cell and gas buret. Figure 42 illustrates the effect of temperature fluctuations in the connecting lines on the gas absorption rate for the capillary disk portion of the combined experiment. The least squares line is drawn through the gas absorption data giving a slope of $0.82 \pm 0.24 \times 10^{-6}$ cc/sec. The temperature difference between the diffusion cell and air surrounding the connection lines are plotted for all but the first few data points. The variation of the first few points during the course of the experiment indicated another variable responsible for the erratic gas absorption behavior. Subsequent plotting of the temperature difference between cell and lines for the remaining data confirmed the temperature dependence of the gas absorption rate in Figure 42. The large error in the slope for the capillary disk absorption indicates the need for improved temperature control for a more accurate oxygen in water diffusivity assignment. However the oxygen in water diffusivities from this work are certainly consistent with the other literature values shown in Figure 3.

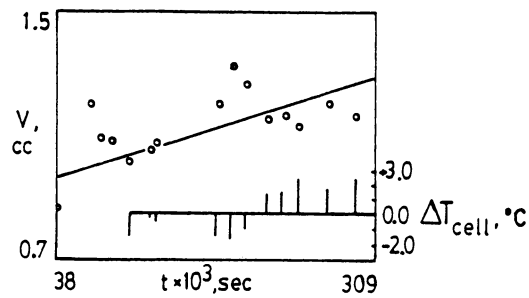

Figure 42. Effect of temperature variation on capillary disk experiment for oxygen in water.

Hildebrand proposes a simple linear relationship between diffusivity and temperature for inert gases in nonpolar liquids.[42] Results from this work for nitrogen in carbon tetrachloride at temperatures of 0, 10 and 25°C do not reject this premise and are plotted in Figure 43b. The results of Ross and Hildebrand[3] for temperatures of 0 and 25°C fall within the experimental precision at the

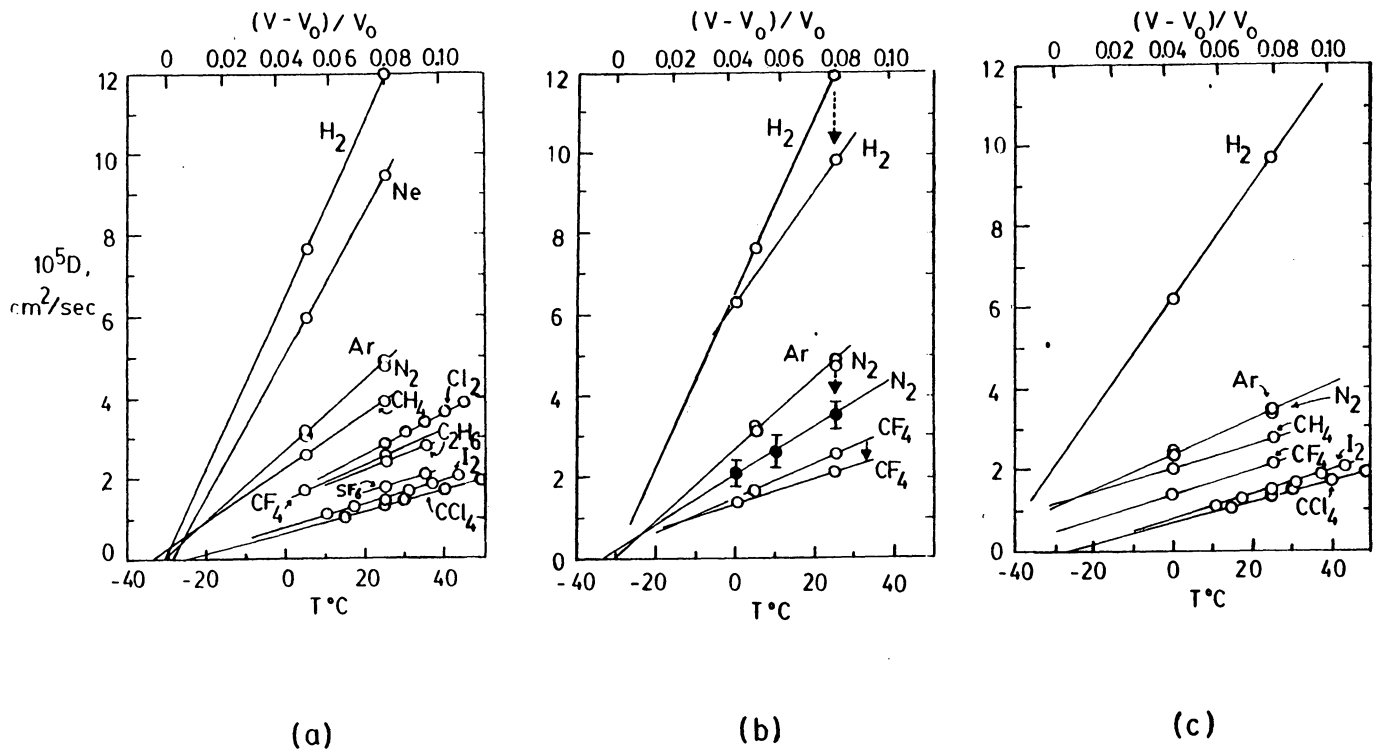

Figure 43. Comparison of gas diffusivities in carbon tetrachloride: (a) Lamoreaux's revised values, (b) comparison of selected values from Lamoreaux and Ross as well as results from the combined method and (c) Ross's values. The filled in points are combined method results Plot (a) is a reproduction of Lamoreaux's graph from reference 42.

68% confidence level for the combined method. Hildebrand and Lamoreaux[42] later indicate that uncertainties in the earlier work of Ross and Hildebrand gave diffusivities which are too small. These uncertainties are ascribed to neglect of the vapor pressure of the solvent which lowers the partial pressure of the gas over the liquid and to presence of solvent vapor in the gas buret. The revised values for argon and nitrogen in carbon tetrachloride are about 25% larger than those of Ross and Hildebrand. Results from both Walkley's open tube experiment and the present method call these revised values into question. The present method accounts for the vapor pressure lowering and eliminates solvent vapor in the gas buret. Horiuti[62] advocates elimination of gas vapor from the gas buret for accurate solubility measurements. The solubility measurements with the present method for all but argon in benzene agree with the Henry's Law value in Table XX. This gives added confidence in the present method's diffusion values. Figure 43 shows (a) Hildebrand and Lamoreaux's revised values, (b) the arrows emphasize the difference between selected diffusivities of Lamoreaux compared to those of Ross, and (c) Ross and Hildebrand's previous values. Lamoreaux's revised values fall outside the experimental precision at the 68% confidence level for the present method as shown by the filled circles in Figure 43b, however Ross's previous values are included as well as Walkley's open tube values.

The diffusivity results from the combined technique can be summarized as follows. First, the pressure dependence for the diffusivity of nitrogen in carbon tetrachloride shows that the diffusivity is independent of concentration. Second, the diffusivities at room temperature and one atmosphere pressure permit comparison to various other techniques and show overall good agreement with the literature. Finally, the temperature dependence of the diffusivity for nitrogen into carbon tetrachloride is linear and calls Lamoreaux's revised values into question.

5.3 *Analysis of Diffusion Results*

Systematic investigation of gas diffusivity in nonpolar solvents is amenable to two approaches: (1) diffusion of various gas solutes in one solvent or (2) diffusion of one gas solute in various solvents. Hildebrand uses the former approach and proposes various diffusion correlations. These correlations relate gas diffusivity in liquids to various contributions of solute molecular cross sectional area, liquid self diffusion, solution configuration entropy and solvent viscosity. The results from the present study do not discount any of these various interpretations. The second approach of studying one gas in various solvents has been given little consideration in the literature. We have found a simple relationship for relative gas diffusivities of one solute in carbon tetrachloride and benzene to the solvent molecular weights. This permits the prediction of the diffusivity of oxygen in cyclohexane. The predicted value agrees well with Krieger's bubble dissolution diffusivity value,[11] which is the only one available. The only other literature source for a solute in various nonpolar solvents is Stokes's values for iodine.[83] These diffusivities of iodine in carbon tetrachloride and methylated benzenes also follow the observed solvent molecular weight relation.

Hildebrand and Ross show with the exception of the gas solutes of hydrogen and deuterium, that the product of the gas solute cross sectional area and gas diffusivity in carbon tetrachloride is constant. In a later paper,[42] Hildebrand and Lamoreaux note that because the reported molecular diameters for an individual gas solute disagree, it is better to use the two thirds power of the intrinsic, boiling point or critical molar volume as a measure of gas solute cross sectional area. The volume at zero fluidity is defined as the intrinsic volume, V_o. Table XXI lists the measures of cross sectional areas for the gas solutes studied where volumes are molar quantities. Table XXII tabulates the product of the diffusivity and the various measures of gas solute cross sectional area for nitrogen, argon and oxygen in carbon tetrachloride and benzene. These products in carbon tetrachloride are much the same for results from both the capillary and combined methods. For benzene only the combined technique diffusivities are available. The open tube value is used for argon in benzene because of convection in the diffusion cell with this system. The product of gas solute cross sec-

Table XXI. Measures of cross sectional areas of gas solutes.

Gas Solute	σ(Å)	V_o(cc)	V_b(cc)	V_c(cc)
N_2	3.70	30.0	35.4	90.0
Ar	3.42	24.8	28.6	74.5
O_2	3.43	24.6	27.9	78.0

tional area and diffusivity in benzene indicate a somewhat lower value for oxygen than for argon or nitrogen. Overall these results support Ross and Hildebrand's premise of invariance in the product of diffusivity and gas solute cross sectional area.

Hildebrand[44] predicts gas diffusivity by scaling the self diffusion of the liquid by the ratio of the cross sectional areas of the liquid to the gas solute. In view of the difficulty of making precise determinations of diffusivity Hildebrand says that the agreement between calculated and observed values is good. Table XXIII provides a comparison of both the capillary disk and combined methods to Hildebrand's calculated value for the gas solutes investigated. The results from the present method show reasonable agreement with Hildebrand's equation in Table II.

Individual gas solute molecules take random walks in movement through the liquid; the driving force for diffusion is statistical that is the effect of entropy increase approaches a maximum randomness in distribution of the gas solute in the liquid. Therefore the entropy of solution should yield information applicable to diffusivity. Hildebrand and Lamoreaux show that the product of diffusivity and gas solute cross sectional area for a wider range of gas solutes than considered by Ross and Hildebrand is far from uniform. They suggest that configuration entropy is a source of additional information and use it as an additional parameter to explain the trend in the gas diffusivity-cross sectional area product. The configuration entropy has been defined in section 2.4.

Hildebrand and Lamoreaux indicate that the configuration entropy results from the solvent molecules surrounding a solute molecule of small attractive potential being held less tightly and gaining thermal freedom of motion. This added freedom of expansion for the configuration entropy in Table XXIV indicates that about half the configuration entropy is attributable to this expansion. Therefore the configuration entropy involves more than just an expansion.

Table XXII. Invariance of diffusivity and cross sectional area product. C are combined technique results; R, Ross and Hildebrand's capillary disk results. For argon in benzene open tube diffusivities are used.

Liquid	$10^{21}D\sigma^2$		$10^5 DV_o^{2/3}$		$10^5 DV_b^{2/3}$		$10^5 DV_c^{2/3}$		Gas Solute
	C	R	C	R	C	R	C	R	
	49	47	34	33	38	37	71	69	N_2
CCl_4	40	42	29	31	32	34	61	64	Ar
	44	45	32	32	35	35	69	70	O_2
	73	--	52	--	58	--	107	--	N_2
C_6H_6	78	--	56	--	62	--	118	--	Ar
	55	--	39	--	43	--	85	--	O_2

Hildebrand and Lamoreaux plot $DV_o^{2/3}$ against $\Delta\bar{S}^c$ in Figure 44a. This plot indicates an enhancement of diffusivity for solutes with low attractive potentials or large configuration entropies. Diffusivities from the combined method call the revised values into question. Figure 44b is the same type of plot with Ross and Hildebrand's data. This plot includes the diffusivities from the combined experiment shown as filled in points. The correlation with configuration entropy is not under question but rather the extent of the correlation is subject to question. The ratio of the least square slopes of the revised to the previous values is approximately two. In each case the best estimate of

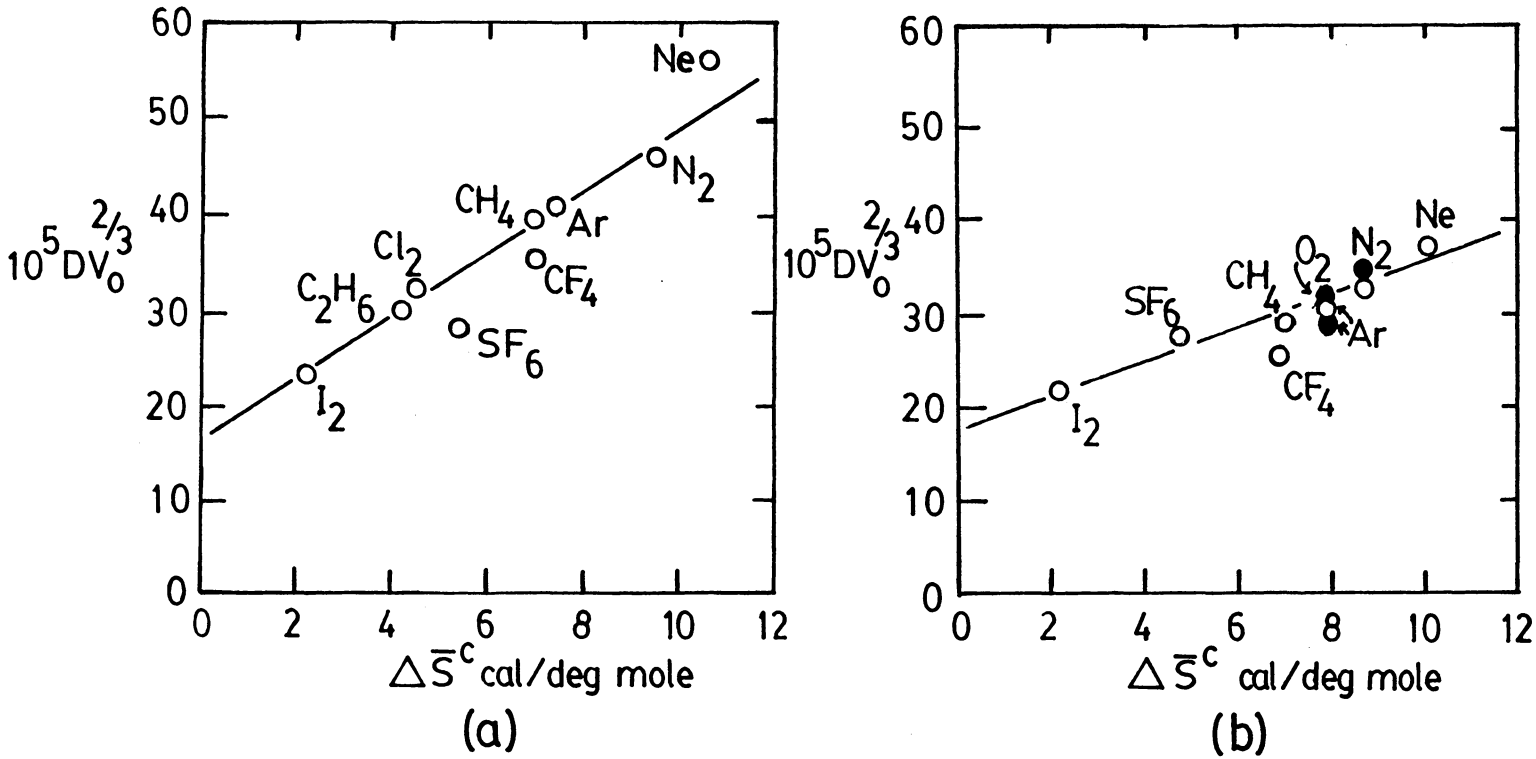

Figure 44. Relation of diffusivity to gas solute cross sectional area and configuration entropy. Filled in points are combined method results. Plot (a) is from reference 42.

the standard error is about ten percent. With only limited data for benzene and gas solute cross sectional areas almost identical for this study such a plot is not informative for benzene.

The correlation with configuration entropy supports a diffusion model where the gas solute molecules take random walks with mean free paths between collisions short compared to molecular diameters. Eyring et al. contend that gaseous diffusion in liquids occurs by jumps into nearby vacancies which have dimensions of molecular diameters. These jumps require the gas solute to surmount an energy barrier. In the former model the emphasis is placed on the kinetic energy in the liquid while the later indicates the potential energy plays a predominant role. The temperature is a measure of the kinetic energy in the liquid. Therefore the diffusivity temperature dependence should serve to indicate which model is more realistic. Figure 43 shows that the diffusivity of various gas solutes into carbon tetrachloride are linear with temperature. The results from the present method do not reject the hypothesis of a simple linear temperature dependence. Erying's model of liquid diffusion predicts an Arrhenius type relation between diffusivity and temperature (i.e. Ln(D) versus 1/T is linear). For various gas solutes in carbon tetrachloride, Hildebrand's condensed gas model of the liquid state describes the diffusion process more simply. Scatter in the diffusivity data does not permit determination of which plot gives the better linear fit. Hildebrand calculates a jumping distance for iodine in carbon tetrachloride of 31.5 Å. This distance is far too large for an intermolecular distance and lends support to Hildebrand's model.[49]

The gas diffusivity in carbon tetrachloride begins at zero fluidity according to Hildebrand. He writes the fluidity in terms of the relative volume expansion $(V - V_o)/V_o$, in equation 1. In Figure 43a extrapolation of the temperature dependent diffusivities to zero diffusivity show that all diffusion lines converge to about -31°C. This temperature is where both the diffusivity and fluidity become zero for carbon tetracholride with a molar volume of 90 cc. The ratios of Ross and Hildebrand's diffusivities in carbon tetrachloride at 25 to 0°C are 1.41 for methane and carbon tetrafluroide, and 1.48 for nitrogen. These ratios are virtually identical to the ratio of the relative volume expansion, 1.47 for carbon tetrachloride at 25 and 0°C . The ratio of 1.68 for the diffusivities of nitrogen in carbon tetrachloride from the combined method agrees with Ross and Hildebrand's results. The later results of Hildebrand and Lamoreaux plotted in Figure 43 show a

Table XXIII. Comparison of observed and calculated diffusivities. The asterisk indicates the open tube diffusivity.

	N_2	Ar	O_2	
CCl_4	3.56	3.46	3.79	10^5D_{comb}
	3.42	3.63	3.82	10^5D_{cap}
	2.97	3.38	3.38	10^5D_{calc}
C_6H_6	5.35	6.65*	4.65	10^5D_{comb}
	4.40	4.98	5.01	10^5D_{calc}

much greater dependence. Neither the experimental precision of the present work nor that of Hildebrand permits a test of the validity of a linear temperature dependence as compared to that of Log D versus 1/T.

The preceding has focused on the diffusion of various gases into one liquid. We now turn to a second approach for investigating gas diffusivities and consider one gas solute in various liquids. Such data in the literature is sparse. Hildebrand considers the relative self diffusivities of carbon tetrachloride and benzene.[44] These relative diffusivities are related through the equation $1/2mv^2 = 3/2(kT)$ where m is molecular mass; v, the rms speed in free space; k, Boltzmann constant; T, temperature. For the same temperature $v_b/v_c = (m_c/m_b)^{1/2}$, where b denotes benzene and c, carbon tetrachloride. If the diffusivities are proportional to the rms speed in free space, then D_b/D_c equals v_b/v_c. The ratio of the self diffusivities. 1.56 at room temperature is approximately the square root of the inverse molecular weight ratio 1.41 = $(158/78)^{1/2}$. The relative gas diffusivities in benzene and carbon tetrachloride from this work also obey the relation at room temperature. Table XXV summarizes the ratios of solute diffusivities in benzene to those in carbon tetrachloride for each gas solute and each part of the combined experiment. The gas solutes of nitrogen and oxygen agree well with the square root of the inverse molecular weight ratio of 1.41. The larger diffusivities of argon in benzene has already been attributed to convection in the diffusion cell. This

Table XXIV. Contribution of the entropy of expansion to the configuration entropy.

Liquid	$-R\ \mathrm{Ln}x_2$	$\Delta\bar{S}^c$	$\Delta\bar{S}^{exp} = (\bar{V}_2 - V_b)\delta_1/T$	Gas Solute
	14.5	8.7	4.2	N_2
CCl_4	13.2	7.9	3.8	Ar
	13.0	7.8	4.3	O_2
	15.3	8.6	5.0	N_2
C_6H_6	13.9	8.0	4.1	Ar
	14.1	7.9	5.1	O_2
H_2O	21.2	16.5	4.8	O_2

leads to ratios substantially larger. A search of the literature for diffusivities of gas solutes investigated here in other nonpolar liquids yielded only Krieger's value of 5.31×10^{-5} cm^2/sec for oxygen in cyclohexane at 29.6°C. In view of the higher temperature, this diffusivity is consistent with the average value of 4.7×10^{-5} cm^2/sec at 25°C predicted by the above relation between solute diffusivity and solvent molecular weight as given in Table XXVI.

Table XXV. Ratio of solute diffusivities in benzene to carbon tetrachloride at room temperature and one atmosphere.

Gas Solute	Open Tube	Capillary Disk	Combined Experiment
N_2	1.60	1.55	1.50
Ar	2.13	2.37	2.51
O_2	1.50	1.35	1.23

A search of the literature for additional confirmation of the diffusivity molecular weight relation with other inert gas solutes in a series of nonpolar liquids is almost nonexistent. To date only Stokes's work with iodine is available.[83] Figure 45 shows Stokes's iodine data in the relationship between relative diffusivities and the square root of the inverse molecular weight ratios normalized to carbon tetrachloride. Clearly the correlation holds for carbon tetrachloride and various methylated benzenes which are spherical or pseudo-spherical respectively. The alkanes and dioxane show large deviations. The deviation of dioxane is probably due to a charge transfer complex.[50] The larger diffusivities of the alkanes may be due to their chain like structure. Orientations of these chains might permit channels in which the iodine can diffuse more rapidly. To verify this hypothesis investigations for longer chains and branched alkanes are necessary.

Table XXVI. Predicted diffusivity, D_c, of oxygen in cyclohexane, based on solvent mass and oxygen diffusivity, D_s, in CCl_4 or C_6H_6. D_c is equal to $D_s \times \sqrt{M_s/M_c}$. All values are scaled by 10^6.

Solvent, s	Open Tube	Capillary Disk	Combined Experiment
CCl_4	4.60	4.86	5.13
C_6H_6	4.73	4.50	4.30

5.4 Summary

The experimental results overall agree with the literature. A pressure study for nitrogen in carbon tetrachloride shows the solutions are ideally dilute with the diffusion coefficient concentration independent. The diffusivities and solubilities at room temperature and one atmosphere pressure with the exception of argon in benzene are internally consistent and in harmony with values from other methods. The larger diffusivity for argon in benzene is attributed to convection in the diffusion cell. A linear temperature dependence of the diffusivity for nitrogen in carbon tetrachloride is consistent for the results from the present method.

Interpretation of the diffusivities is in accord with Hildebrand's various correlations. These correlations focus on many gas solutes in one liquid. An alternate approach of one gas solute in many liquids indicates a simple Graham's Law type relationship between relative diffusivities and liquid molecular weights. Unfortunately such data in the literature is sparse and more work is necessary to determine the limitations of this Graham's Law type relation. This is indicated by Stokes's work with iodine in various solvents.

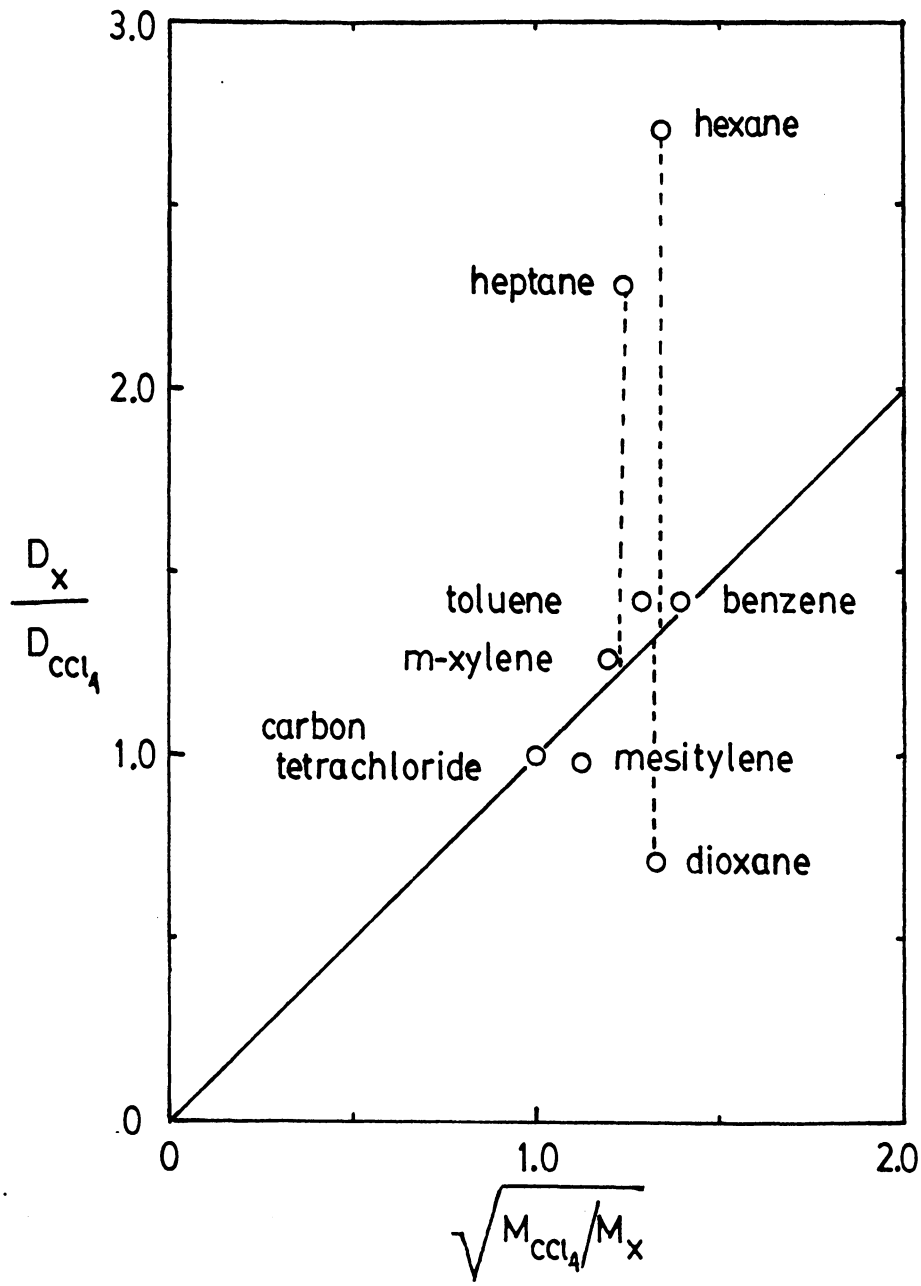

Figure 45. Relation of relative iodine diffusivities and liquid molecular weights. Data for plot is from Stokes.[83]

6.0 SUMMARY

The combination of the open tube and capillary disk methods into a single experiment is shown to be valid. The determination of the solubility in addition to the gas diffusivity into the liquid provides an internal check on the diffusion results. Diffusivities of nitrogen, argon and oxygen into carbon tetrachloride and benzene by this combined technique agree well with the literature. A Graham's Law type relationship between the ratio of diffusivities of the same gas solute in different solvents and the square root of the inverse molecular weight ratio of the solvents is found. This relation permits a prediction of the diffusivity of oxygen in cyclohexane which is consistent with Krieger's bubble dissolution value. A pressure study with nitrogen in carbon tetrachloride showed that the solubilities obey Henry's Law and the gas absorption rates are pressure independent. These facts prove the concentration independence of the diffusion coefficient. The diffusivity temperatue dependence for nitrogen in carbon tetrachloride from the combined method is consistent with Ross and Hildebrand's results. A Graham's Law like relation for the relative diffusivities indirectly supports a linear temperature dependence. Therefore Hildebrand's condensed gas model of the liquid state is more realistic than Eyring's pseudo-lattice model.

There are two immediately obvious avenues for extending this study. First is the refinement of the apparatus temperature control to allow accurate temperature data for oxygen in water to be obtained. Figure 3 illustrates the scatter in the oxygen in water diffusivity data for various methods.

This scatter surely warrants a more critical evaluation of this data and the associated methods. The second extension is the determination of gas diffusivities in liquid alkanes such as hexane, octane, decane, dodecane and isohexane to determine the possible limitations of the Graham's Law like diffusion relation. Diffusivities of iodine in various nonpolar solvents by Stokes indicate anomalously higher diffusivities for hexane and heptane than those in carbon tetrachloride and benzene. Stokes's work emphasizes the need for these additional measurements.

Bibliography

1. R. Frost, "The Poems of Robert Frost", Modern Library Ed., Random House, NY, 1946, p.422.
2. C.E. StDennis and C.J.D. Fell, *Can. J. Chem. Eng.*, **49**, 885 (1971).
3. M. Ross and J.H. Hildebrand, *J. Chem. Phys.*, **40**, 2397 (1964).
4. L. Bennett, W.Y. Ng and J. Walkley, *J. Phys. Chem.*, **72** 4699 (1968).
5. E.J. Cullen and J.F. Davidson, *Trans. Faraday Soc.*, **53**, 113 (1957).
6. P.V. Danckwerts and A.M. Kennedy, *Chem. Eng. Sci.*, **8**, 201 (1958).
7. S. Lynn, J.R. Staatemeier and H. Kramers, *Chem. Eng. Sci.*, **4**, 58 (1955).
8. B. Case, *Electrochimica Acta*, **18**, 293 (1973).
9. R.T. Ferrell and D.M. Himmelblau, *AIChEJournal*, **13**, 702 (1967).
10. D.L. Wise and G.H. Houghton, *Chem. Eng. Sci.*, **21**, 999 (1966).
11. I.M. Krieger, G.W. Mulholland and C.S. Dickey, *J. Phys. Chem.*, **71**, 1123 (1967).
12. L.E. Johns, Jr., *J. Phys. Chem.*, **71**, 4566 (1967).
13. W.F. Pfeiffer and I. Krieger, *J. Phys. Chem.*, **78**, 2516 (1974).
14. W.Y. Ng and J. Walkley, *Can. J. Chem.*, **47**, 1075 (1969).
15. M.J. Tham, K.K. Bhatia and K.E. Gubbins, *Chem. Eng. Sci.*, **22**, 309 (1967).
16. H. Takeuchi, M. Fujine, T. Sato and K. Onda, *J. Chem. Eng. Japan*, **8**, 252 (1975).
17. J.H. Wang, *J. Amer. Chem. Soc.*, **72**, 4181 (1951).

18. V.K. Malik and W. Hayduk, *Can. J. Chem. Eng.*, **46**, 462 (1968).

19. N.C. Fawcett and R.D. Canton, Jr., *Anal. Chem.*, **48**, 228 (1976).

20. D.M. Maharajh and J. Walkley, *Can. J. Chem.*, **51**, 944 (1973).

21. J. Jordan and W.E. Bauer, *J. Amer. Chem. Soc.*, **81** 3915 (1959).

22. R.E. Smith, E.T. Friess and M.R. Morales, *J. Phys. Chem.*, **59**, 382 (1955).

23. G.W. Hung and R.H. Dinus, *J. Chem. Eng. Data*, **17**, 449 (1972).

24. F.C. Tse and O.C. Sandall, *Chem. Eng. Commun.*, **3**, 147 (1979).

25. Yatskovski and Fedotov, *Soviet Electrochem.*, **5**, 99 (1969).

26. D.M. Himmelblau, *Chem. Rev.*, **64**, 527 (1964).

27. J.L. Duda and J.S. Vientas, *AIChEJournal*, **14**, 286 (1968).

28. M.H.J. Baird and J.F. Davidson, *Chem. Eng. Sci.*, **17**, 473 (1962).

29. T. Carlson, *J. Amer. Chem. Soc.*, **33**, 1027 (1911).

30. C.A. Ward, *J. Chem. Phys.*, **67**, 229 (1977).

31. S.H. Chaing and H.L. Toor, *AIChEJournal*, **5**, 165 (1959).

32. A. Akgerman and J.L. Gainer, *J. Chem. Eng. Data*, **17**, 372 (1972).

33. W.J. McManamey and J.M.Woolen, *AIChEJournal*, **19**, 667 (1973).

34. A. Akgerman and J.L. Gainer, *Ind. Eng. Chem. Fundam.*, **11**, 373 (1972).

35. A. Dim, G.R. Gardner, A.B. Ponter and T. Wood, *J. Chem. Eng. Jap.*, **4**, 92 (1971).

36. K. Nakaniahi, E.M. Voigt and J.H. Hildebrand, *J. Chem. Phys.*, **42**, 1860 (1965).

37. P.A. Witherspoon and D.N. Saraf, *J. Phys. Chem.* **69**, 3752 (1965).

38. P.A. Witherspoon and L. Bonoli, *Ind. Eng. Chem. Fundam.*, **8**, 589 (1969).

39. J.H. Hildebrand, *Proc. Nat. Acad. Sci. USA*, **64**, 1329 (1969).

40. J.H. Hildebrand, *Proc. Nat. Acad. Sci. USA*, **64**, 1531 (1969).

41. G.H. Houghton, A.S. Kesten, J.E. Funk and J. Coull, *J. Phys. Chem.*, **65**, 649 (1961).

42. J.H. Hildebrand and R.H. Lamoreaux, *Proc. Nat. Acad. Sci. USA*, **69** 3428 (1972).

43. C.R. Wilke and P. Chang, *AIChJournal*, **1**, 264 (1955).

44. J.H. Hildebrand, *Science*, **174**, 490 (1971).

45. T. Sridhar and O.E. Potter, *AIChEJournal*, **23**, 590 (1977).

46. F.A.L. Dullien, *AIChEJournal*, **28**, 62 (1972).

47. B.J. Alder and J.H. Hildebrand, *Ind. Eng. Chem. Fundam.*, **12**, 387 (1973).

48. E.W. Haycock, B.J. Alder and J.H. Hildebrand, *J. Chem. Phys.*, **21**, 1601 (1953).

49. H.B. Watts, B.J. Alder and J.H. Hildebrand, *J. Chem. Phys.*, **23**, 659 (1955).

50. J.H. Hildebrand, J.M. Prausnitz and R.L. Scott, "Regular and Related Solutions", Van Nostrand Reinhold Co., NY, 1970.

51. W.R. Grimes, N.V. Smith and B.M. Watson, *J. Phys. Chem.*, **62**, 862 (1968).

52. E.B. Smith and J. Walkley, *J. Phys. Chem.*, **66**, 597 (1962).

53. D.L. Wise and G. Houghton, *Chem. Eng. Sci.*, **23**, 1211 (1968).

54. A.J.H. Boerboom and G. Keyln, *J. Phys. Chem.*, **50**, 1086 (1969).

55. Sovova' and Prochazka, *Chem. Eng. Sci.*, **31**, 1091 (1976).

56. J.H. Hildebrand and R.H. Lamoreaux, *Proc. Nat. Acad. Sci. USA*, **71**, 3321 (1974).

57. P.E. Field, "Physical Methods in Chemistry", Experiment 2.3, VPI&SU, 1979.

58. R. Battino, T.R. Rettich and T. Tominaga, *J. Phys. Chem. Ref. Data*, **13**, 563 (1984).

59. A.E. Markam and K.A. Kobe, *Chem. Rev.*, **28**, 519 (1941).

60. R. Battino and H.L. Clever, *Chem. Rev.*, **66**, 395 (1966).

61. M.W. Cook and D.N. Hanson, *Rev. Sci. Instrum.*, **28**, 370 (1957).

62. J. Horiuti, *Sci. Papers Inst. Phys. & Chem. Res.*, **17**, 126 (1931).

63. H.H. Uhlig, *J. Phys. Chem.*, **41**, 1215 (1937).

64. J.H. Hildebrand and R. Scott, "The Solubility of Nonelectrolytes", 3rd ed., Dover, NY, 1964.

65. R.A. Pierotti, *J. Phys. Chem.*, **67**, 1840 (1963).

66. J.H. Dymond, *Chem. Soc. Lon. Faraday Soc.*, **68**, 1789 (1972).

67. H. Reiss, H.L. Frisc and J.L. Lebowitz, *J. Chem. Phys.*, **31**, 369 (1959).

68. R.D. Pomeroy, W.N. Lacey, N.F. Schudder and F.P. Stapp, *Ind. Eng. Chem.*, **25**, 1014 (1933).

69. W. Jost, "Diffusion in Solids, Liquids, Gases", 3rd ed., Academic Press, NY, 1960.

70. H.S. Carlaw and J.C. Jaeger, "Conduction of Heat in Solids", Oxford Clarendon Press, 1947, p.33.

71. A.J. Bard and L.R. Faulker, "Electrochemical Methods", John Wiley & Sons, NY, 1980, pp.675-698.

72. B.J. Noye in "Numerical Simulation of Fluid Motion", B. J. Noye, ed., North Holland, Amsterdam, 1978, pp.1-112.

73. S.W. Feldberg in "Electroanalytical Chemistry", Vol 3, A.J. Bard, ed., Marcel Dekker, NY, 1969, pp.199-296.

74. C.F. Durang, "Timex/Sinclair 2068 Personal Color Computer User Manual", Timex Corp., 1983, pp.139-140.

75. E.A. Harvey and W. Smith, *Chem. Eng. Sci.*, **10**, 274 (1959).

76. R.N. O'Brien and W.F. Hyslop, *Can. J. Chem.*, **55**, 1415 (1977).

77. V.K. Malik and W. Hayduk, *Can. J. Chem. Eng.*, **46**, 462 (1968).

78. P.E. Field and R.J. Combs, *Amer. Lab.*, **12**(10), 75 (1980).

79. R.J. Combs and P.E. Field, *Amer. Lab.*, **15**(11), 100 (1983).

80. P.E. Field, "Computer Assisted Home Energy Management", Howard Sams Pub. Co., Indianapolis, Indiana, 1982.

81. H.L. Clever and R. Battino, "The Solubilities of Gases in Liquids: in Techniques of Chemistry", Vol. 8, Part 1, ed. M.R.J. Dack, John Wiley & Sons, NY, 1975, p.385.

82. A. Akgerman, "Predicting Gas-Liquid Diffusion Coefficient" PhD Diss. UVA (1971).

83. R.H. Stokes, P.J. Danlop and J.R. Hall, *Trans. Faraday Soc.*, **49** 886 (1953).

Appendix A. SIMULATION PROGRAM DOCUMENTATION

I. Open tube simulation listing.

II. Capillary disk simulation, 0CAP0.

- A. Iteration.
- B. Initialization.
- C. Illustration.

III. Variable definition list.

IV. Overlays to 0CAP0 for simulating other diffusion cell boundary conditions.

```
 900 REM OCAPO;Initialization an
d iteration.
1000 GO SUB 3000
1010 FOR t=2 TO size
1020 FOR x=top TO xmax
1030 LET n(x)=s*(o(x-1)+o(x+1))+
(1-2*s)*o(x)
1040 LET n=n+n(x)*ac*dx
1070 NEXT x
1075 LET n(xmax+1)=s*o(xmax): LE
T b=b+n(xmax+1)*ac*dx: LET n=n+
b
1080 LET v(t)=298.2*82.05*n: LET
 n=0
1090 FOR x=2 TO xmax: LET o(x)=n
(x): NEXT x: LET c(t)=n(xod)-n(
xmax+1)
1100 NEXT t



1105 REM Indicate simulation ove
r.
1110 BEEP .1,0: PAUSE 6: IF INKE
Y$="" THEN  GO TO 1110
1120 STOP



2990 REM Initialization.
3000 INPUT "Size = ";size
3010 INPUT "Cap length (cm) ";h:
 DIM v(size): DIM c(size)
3015  INPUT "Open tube depth (cm
)  ";od
3020  CLS : LET co=6.5e-6
3030 LET n=0: LET dc=3.6e-5
3035 INPUT "Open tube area (cm2)
 ";ao
3040 INPUT "dt (sec) ";dt: INPUT
 "dx (cm) ";dx: INPUT "Capillar
y disk area (cm2) ";ac
3045 LET xod=INT (od/dx): LET xm
ax=INT (h/dx)+xod
3046 DIM o(xmax+1): DIM n(xmax+1
)
3047 LET o(xmax+1)=0: LET n(xmax
+1)=0
3050 FOR k=1 TO size: LET v(k)=0
: LET c(k)=0: NEXT k
3055 FOR k=2 TO xmax+1: LET n(k)
=0: LET o(k)=0: NEXT k
3060 LET b=0: LET o(1)=co: LET n
(1)=co: LET b=0
3070 LET s=dc*dt/(dx*dx): LET to
p=xod+1
3080 FLASH 1: PRINT AT 10,10;"Si
mulating": FLASH 0
3085 RETURN
```

```
 900 REM Open tube simulation.
1000 GO SUB 3000
1010 FOR t=2 TO size
1020 FOR x=2 TO t
1030 LET n(x)=s*(o(x-1)+o(x+1))+
(1-2*s)*o(x)
1040 LET n=n+n(x)*ao*dx
1060 PRINT AT 6,0;x;" ";n(x);"
 ";
1070 NEXT x
1080 LET v(t)=298.2*82.05*n: LET
 n=0
1090 FOR x=2 TO t: LET o(x)=n(x)
: NEXT x: PRINT AT 0,0;t;"  ";
1100 NEXT t
1110 BEEP .1,0: PAUSE 6: IF INKE
Y$="" THEN  GO TO 1110
1130 CLS : FOR t=2 TO size STEP
20: PAUSE 0: PRINT AT 15,0;" v(
";t;") = ";v(t): PRINT AT 16,0;
"dV/dt^(1/2) = ";(v(t)-v(t-20))
/(SQR (t*dt)-SQR ((t-20)*dt)):
NEXT t
1150 PAUSE 0
1152 CLS : PLOT 0,0: DRAW 0,175:
 DRAW 255,0: DRAW 0,-175: DRAW
-255,0
1155 LET tmax=SQR (size*dt)
1160 LET xo=0: LET yo=0: PLOT 0,
0: FOR t=2 TO (size-1): LET xp=
INT (SQR (t*dt)*255/tmax): LET
yp=INT (v(t)*175/v(size-1)): DR
AW xp-xo,yp-yo: LET xo=xp: LET
yo=yp: PRINT AT 1,1;xp;"  ";yp;
"  ": PRINT AT 2,1;t: NEXT t
1170 STOP
3000 INPUT "Size = ";size
3010 DIM v(size): DIM o(size): D
IM n(size)
3020 CLS : LET co=6.5e-6
3030 LET n=0: LET dc=3.6e-5
3040 INPUT "dt (sec) = ";dt: INP
UT " dx (cm) = ";dx: INPUT "Ope
n tube area (cm2) = ";ao
3050 FOR k=1 TO size: LET o(k)=0
: LET n(k)=0: LET v(k)=0: NEXT
k
3060 LET o(1)=co: LET n(1)=co: L
ET s=dc*dt/(dx*dx): RETURN
```

```
2000 REM Illustration.
2005 CLS : PRINT AT 5,5;"Options
": PRINT AT 6,6;"#1 Capillary d
isk": PRINT AT 7,6;"#2 Slope V
vs. t": PRINT AT 8,6;"#3 Final
conc. gradient": PRINT AT 9,6;"
#4 Open tube": PRINT AT 10,6;"#
5 Slope V vs. sqrt t"
2010 INPUT "Enter option no.";on

2015 LET on=2030+on*10: GO SUB o
n
2021 OVER 1: PLOT xp,0: DRAW 0,1
75
2022 IF INKEY$="1" THEN  OVER 0:
 PRINT AT 19,25;t: PAUSE 0: RET
URN
2023 DRAW 0,-175: OVER 0: RETURN

2025  BEEP .1,0: PAUSE 6: IF INK
EY$="" THEN  GO TO 2025
2026 RETURN
2030 CLS : PLOT 0,0: DRAW 0,175:
 DRAW 255,0: DRAW 0,-175: DRAW
-255,0: RETURN
2040 GO SUB 2030
2041 INPUT "Scale volume max ";v
max
2042 LET xo=0: LET yo=0: PLOT 0,
0: FOR t=2 TO size: LET xp=INT
(t*255/size): LET yp=INT (v(t)*
175/vmax): DRAW xp-xo,yp-yo: LE
T xo=xp: LET yo=yp: PRINT AT 20
,20;t
2043 IF INKEY$="s" THEN  PRINT A
T 20,8;v(t);" ";: PAUSE 0
2044 NEXT t: GO SUB 2025
2045 PAUSE 0
2046 LET xo=0: LET yo=0
2047 FOR t=2 TO size: PLOT xo,yo
: LET xp=INT (t*255/size): LET
yp=INT (c(t)*175/co): DRAW xp-x
o,yp-yo: GO SUB 2021
2048 IF INKEY$="s" THEN  PRINT A
T 19,8;t;" ";: PRINT AT 20,8;c(
t);" ";: PAUSE 0
2049 PRINT AT 19,20;t;" ";: PRIN
T AT 20,15;c(t);" ";: LET xo=xp
: LET yo=yp: NEXT t: PAUSE 0: R
ETURN
2050 CLS : INPUT "time t1 ";t1:
INPUT "time t2 ";t2: LET slope=
(v(t2)-v(t1))/((t2-t1)*dt): PRI
NT "Slope (cc/sec) = ";slope: P
AUSE 0: RETURN
2060 CLS : PRINT "Final disk con
c grad ": FOR x=xod TO xmax+1:
PRINT x;" ";n(x): NEXT x: PAUSE
 0: RETURN
2070 GO SUB 2030
2071 INPUT "Max time increment o
pen? ";tinc: INPUT "Max vol sca
le (cc) ";vmax: LET xp=INT (SQR
 (t)*255/SQR (tinc)): LET yp=IN
T (v(t)*175/vmax): DRAW xp-xo,y
p-yo: LET xo=xp: LET yo=yp: PRI
NT AT 1,1;xp;" ";yp;" ": PRINT
AT 2,1;t
2073  IF INKEY$="s" THEN  PRINT
AT 16,15;SQR (t*dt);" ": PRINT
AT 17,15;" v = ";v(t): PAUSE 0
2074 OVER 1: PLOT xp,0: DRAW 0,1
75: OVER 0: PAUSE 0: NEXT t: PA
USE 0: RETURN
2080 CLS : INPUT "time t1 ";t1:
INPUT "time t2 ";t2: LET slope=
(v(t2)-v(t1))/(SQR (t2*dt)-SQR
(t1*dt)): PRINT "V vs sqrt t (c
c/sec1/2) = ";slope: PAUSE 0: R
ETURN
```

Variable definitions

ac	:total capillary disk cross sectional area (cm2)
ao	:open tube cross sectional area (cm2)
b	:moles of gas passing through disk
bot	:number of steps for finite open tube below disk
c(t)	:concentration gradient across disk at time t (moles/cc)
co	:gas saturation concentration (moles/cc)
dc	:gas diffusion coefficient (cm2/sec)
dt	:time increment (sec)
dx	:distance increment (cm)
h	:capillary length (cm)
i	:flux into a volume element
j	:flux out of a volume element
n	:total moles uptake
n(x)	:new volume element concentration at distance x*dx (moles/cc)
od	:open tube liquid depth (cm)
o(x)	:old volume element concentration at distance x*dx (cm)
size	:number of iterations
t	:time increment counter
top	:number of space increments to first disk layer
vb	:liquid volume below disk (cc)
x	:distance increment counter
xmax	:number of space increments to bottom volume element of disk
xod	:distance to volume element of disk

```
 900 REM 0CAP1
1075 LET i=(o(xmax)-o(xmax+1))*a
c*dc/dx: LET dn=i*dt: LET b=b+d
n: LET n(xmax+1)=b/vb: LET n=n+
dn
1080 LET v(t)=298.2*82.05*(n+b)
3005 INPUT "Vol below disk (cc)
";vb
```

```
 900 REM 1CAP0
1015 LET x=2: LET i=(o(x-1)-o(x)
)*ao*dc/dx: LET j=(o(x)-o(x+1))
*ac*dc/dx: LET dn=(i-j)*dt: LET
 n(x)=o(x)+dn/(ao*dx)
```

```
 900 REM 1CAP1
1015 LET x=2: LET i=(o(x-1)-o(x)
)*ao*dc/dx: LET j=(o(x)-o(x+1))
*ac*dc/dx: LET dn=(i-j)*dt: LET
 n(x)=o(x)+dn/(ao*dx)
1075 LET i=(o(xmax)-o(xmax+1))*a
c*dc/dx: LET dn=i*dt: LET b=b+d
n: LET n(xmax+1)=b/vb: LET n=n+
dn
1080 LET v(t)=298.2*82.05*(n+b)
3005 INPUT "Vol below disk (cc)
";vb
```

```
 900 REM NCAPN
1012 FOR x=2 TO xod-1: LET n(x)=
s*(o(x-1)+o(x+1))+(1-2*s)*o(x):
 LET n=n+n(x)*ao*dx: NEXT x
1015 LET i=(o(x-1)-o(x))*ao*dc/d
x: LET j=(o(x)-o(x+1))*ac*dc/dx
: LET dn=(i-j)*dt: LET n(x)=o(x
)+dn/(ao*dx): LET n=n+dn
1071 LET i=(o(x-1)-o(x))*ac*dc/d
x: LET j=(o(x)-o(x+1))*ao*dc/dx
: LET dn=(i-j)*dt: LET n(x)=o(x
)+dn/(ao*dx): LET n=n+dn
1072 FOR x=xmax+2 TO xmax+2+bot:
 LET n(x)=s*(o(x+1)+o(x-1))+(1-
2*s)*o(x): LET n=n+n(x)*ao*dx:
NEXT x
1075: REM
1090 FOR x=2 TO xmax+3+bot: LET
o(x)=n(x): NEXT x: LET c(t)=n(x
od)-n(xmax+1)
3046 DIM o(size): DIM n(size)
3047 INPUT "No. of steps below d
isk ";bot
3055 FOR k=2 TO size: LET n(k)=0
: LET o(k)=0: NEXT k
```

```
 900 REM NCAP0
1012 FOR x=2 TO xod-1: LET n(x)=
s*(o(x-1)+o(x+1))+(1-2*s)*o(x):
 LET n=n+n(x)*ao*dx: NEXT x
1015 LET i=(o(x-1)-o(x))*ao*dc/d
x: LET j=(o(x)-o(x+1))*ac*dc/dx
: LET dn=(i-j)*dt: LET n(x)=o(x
)+dn/(ao*dx): LET n=n+dn
```

```
 900 REM NCAP1
1012 FOR x=2 TO xod-1: LET n(x)=
s*(o(x-1)+o(x+1))+(1-2*s)*o(x):
 LET n=n+n(x)*ao*dx: NEXT x
1015 LET i=(o(x-1)-o(x))*ao*dc/d
x: LET j=(o(x)-o(x+1))*ac*dc/dx
: LET dn=(i-j)*dt: LET n(x)=o(x
)+dn/(ao*dx): LET n=n+dn
1075 LET i=(o(xmax)-o(xmax+1))*a
c*dc/dx: LET dn=i*dt: LET b=b+d
n: LET n(xmax+1)=b/vb: LET n=n+
dn
1080 LET v(t)=298.2*82.05*(n+b)
3005 INPUT "Vol below disk (cc)
";vb
```

```
 900 REM NCAP∞
1012 FOR x=2 TO xod-1: LET n(x)=
s*(o(x-1)+o(x+1))+(1-2*s)*o(x):
 LET n=n+n(x)*ao*dx: NEXT x
1015 LET i=(o(x-1)-o(x))*ao*dc/d
x: LET j=(o(x)-o(x+1))*ac*dc/dx
: LET dn=(i-j)*dt: LET n(x)=o(x
)+dn/(ao*dx): LET n=n+dn
1071 LET i=(o(x-1)-o(x))*ac*dc/d
x: LET j=(o(x)-o(x+1))*ao*dc/dx
: LET dn=(i-j)*dt: LET n(x)=o(x
)+dn/(ao*dx): LET n=n+dn
1072 FOR x=xmax+2 TO t: LET n(x)
=s*(o(x+1)+o(x-1))+(1-2*s)*o(x)
: LET n=n+n(x)*ao*dx: NEXT x
1075: REM
1090 FOR x=2 TO t: LET o(x)=n(x)
: NEXT x: LET c(t)=n(xod)-n(xma
x+1)
3046 DIM o(size): DIM n(size)
3047: REM
3055 FOR k=2 TO size: LET n(k)=0
: LET o(k)=0: NEXT k
```

Appendix B. AUTOMATED APPARATUS DOCUMENTATION

I. Modification of processor board for 2Kbytes read and write memory.

II. Data acquisition and experiment control program documentation.

A. Machine language listings.

B. Flowcharts.

C. Memory map and format of various buffers, acquired data and machine stack.

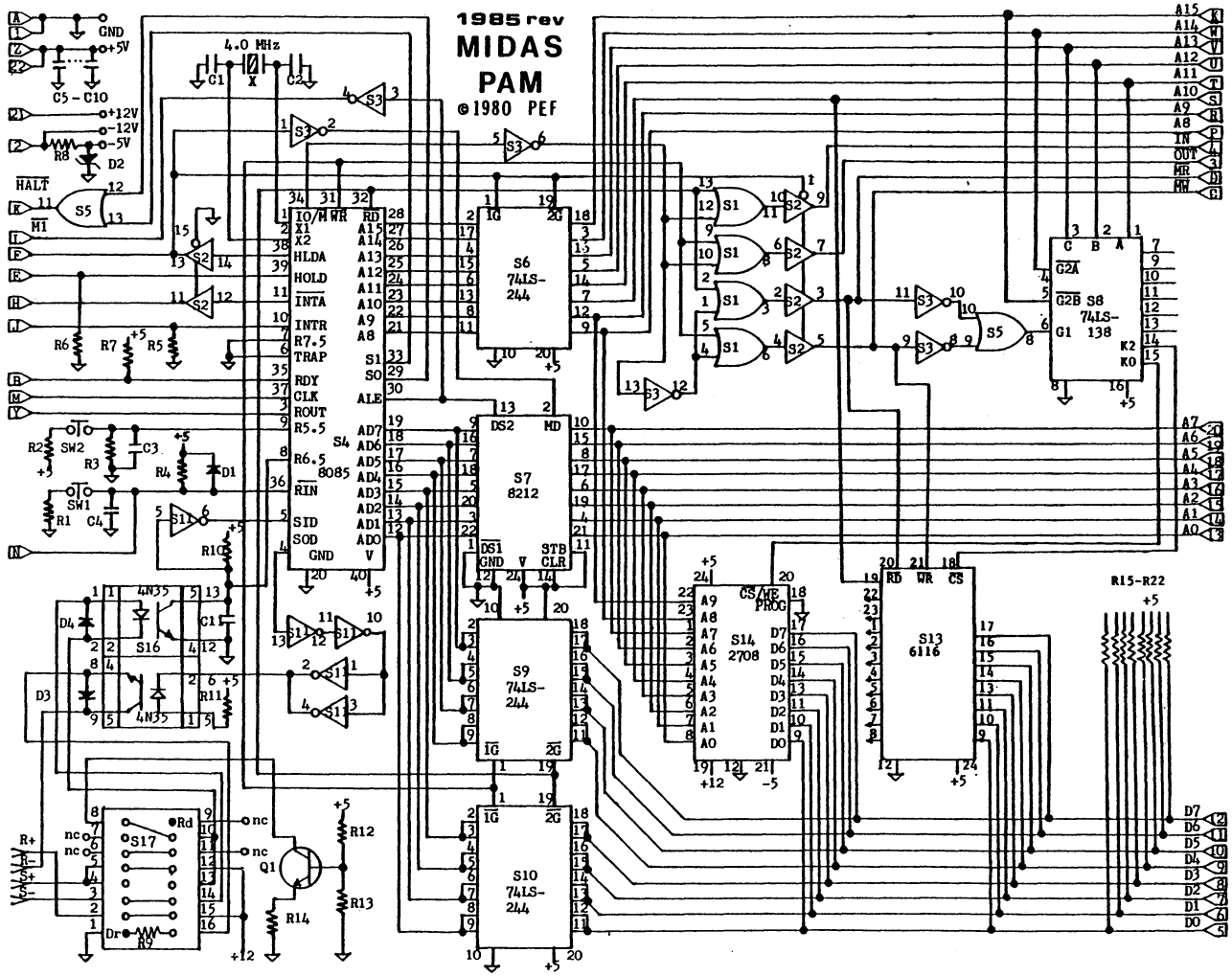
1985 rev
MIDAS
PAM
©1980 PEF
4.0 MHz
GND
+5V
C5 - C10
+12V
-12V
-5V
R8
D2
HALT
MI
S5
S1
S2
S3
R6
R7
R5
R2
SW2
R3
C3
R4
D1
SW1
R1
C4
R10
4N35
D4
S16
C11
D3
R11
S17
Rd
Dr
R9
nc
Q1
R12
R13
R14
+12
IO/M WR RD
X1
X2
HLDA
HOLD
INTA
INTR
R7.5
TRAP
RDY
CLK
ROUT
R5.5
R6.5
RIN
SID
SOD
GND
S4
8085
AD7
AD6
AD5
AD4
AD3
AD2
AD1
AD0
A15
A14
A13
A12
A11
A10
A9
A8
S1
S0
ALE
V
S6
74LS-
244
S7
8212
DS2
MD
DS1
STB
CLR
S9
74LS-
244
S10
74LS-
244
S14
2708
CS WE
PROG
S13
6116
RD WR CS
R15-R22
G2A
G2B S8
74LS-
G1 138
K2
K0
A15
A14
A13
A12
A11
A10
A9
A8
IN
OUT
MR
MW
A7
A6
A5
A4
A3
A2
A1
A0
D7
D6
D5
D4
D3
D2
D1
D0

```
                00100 ; TRACK:  MAINTAINS A CONSTANT PRESSURE AND
                00110 ;         TEMPERATURE ON THE D/S CELL WHILE
                00120 ;         MONITORING VOLUME UPTAKE AS A
                00130 ;         FUNCTION OF TIME.
                00140 ;
                00150 ;       TEMPERATURE- SENSOR, QDTS
                00160 ;                    ACTUATOR, ON/OFF HEATER
                00170 ;       PRESSURE- SENSOR, DIF DBP MANOMETER
                00180 ;                 ACTUATOR, STEPPER MOTOR &
                00190 ;                           GAS TIGHT SYRINGE
                00200 ;       VOLUME- SENSOR, # OF STEPPER STEPS
                00210 ;       TIME- SENSOR, MM5309 DIGITAL CLOCK
                00220 ;
                00230 ;
C8C8            01000 COUNT   EQU 51400
0196            01010 CLEAR   EQU 0196H
00DB            01020 KEY     EQU 00DBH
00D3            01030 DSPLY   EQU 00D3H
0073            01040 HTR     EQU 73H
0072            01050 STATUS  EQU 72H
0033            01060 SWORD   EQU 33H
0071            01070 RESET   EQU 71H
1000            01080         ORG 1000H
1000 54         01090 LABELS  DEFB 54H        ;'T'
1001 50         01100         DEFB 50H        ;'P'
1002 54         01110         DEFB 54H        ;'T'
1003 45         01120         DEFB 45H        ;'E'
1004 53         01130 LABSTP  DEFB 53H        ;'S'
1005 59         01140         DEFB 59H        ;'Y'
1006 41         01150         DEFB 41H        ;'A'
1007 4C         01160         DEFB 4CH        ;'L'
1008 45         01170         DEFB 45H        ;'E'
1009 44         01180 LABDLY  DEFB 44H        ;'D'
100A CD9601     01190 INIT    CALL CLEAR      ;EXPERIMENTAL PARAMETERS
100D 210410     01200         LD HL,LABSTP
1010 CDC312     01210         CALL LABEL
1013 CDAE12     01220         CALL NUMBER     ;SETPT FOR OVEN
1016 212508     01230         LD HL,0825H
1019 CDED12     01240         CALL PACKIT
101C CD9601     01250         CALL CLEAR
101F 210910     01260         LD HL,LABDLY
1022 CDC312     01270         CALL LABEL
1025 CDAE12     01280         CALL NUMBER     ;DELAY COUNT
1028 212308     01290         LD HL,0823H
102B CDED12     01300         CALL PACKIT
102E CD9601     01310 CONTEP  CALL CLEAR      ;CONTROL OVEN TEMP
1031 D371       01320         OUT (RESET),A   ;RESET CLOCK
1033 CD9D11     01330         CALL CLOCK
1036 CD2B11     01340         CALL PACSEC
1039 212108     01350         LD HL,0821H
```

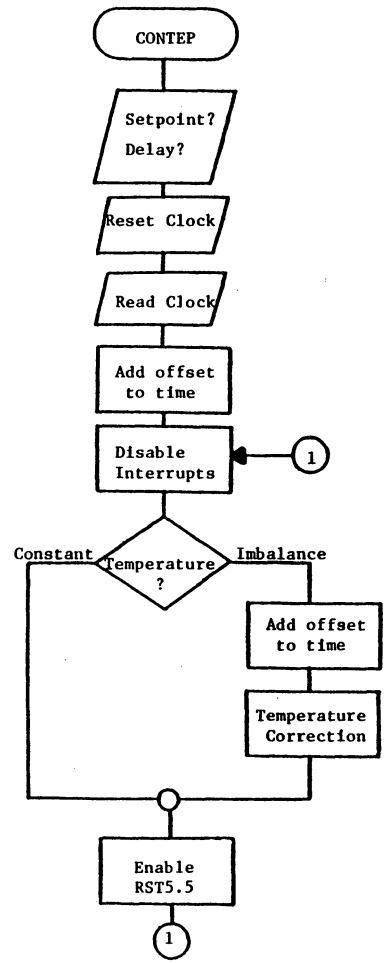

```
103C CD1E11   01360          CALL ADOFST     ;INIT 15SEC OFFSET
103F F3       01370 HTRCOL   DI              ;DISABLE INTERRUPTS
1040 CD0C11   01380          CALL ISITIM     ;HTR CONTROL
1043 C24C10   01390          JP NZ,EXPYET
1046 CD1E11   01400          CALL ADOFST
1049 CDD210   01410          CALL TEPIMB
104C FB       01420 EXPYET   EI              ;ENABLE RST5.5
104D 3E0E     01430          LD A,0EH        ;INTERRUPT TO
104F 30       01440          DEFB 30H        ;START EXPT: SIM INSTR
1050 C33F10   01450          JP HTRCOL
1053 F3       01460 TRACK    DI              ;START EXPT!!!!
1054 211E08   01470          LD HL,081EH     ;INIT DATA PTR
1057 3E26     01480          LD A,26H
1059 77       01490          LD (HL),A
105A 3E08     01500          LD A,08H
105C 23       01510          INC HL
105D 77       01520          LD (HL),A
105E 23       01530          INC HL
105F 3E00     01540          LD A,0          ;INIT VOL INC CNTR
1061 77       01550          LD (HL),A
1062 CD9601   01560          CALL CLEAR      ;CLEAR DSPLY BUF
1065 D371     01570          OUT (RESET),A   ;RESET CLOCK
1067 CD9D11   01580          CALL CLOCK
106A CD2B11   01590          CALL PACSEC
106D 212108   01600          LD HL,0821H
1070 CD1E11   01610          CALL ADOFST
1073 01C8C8   01620          LD BC,COUNT     ;NUM OF INC STEPS
1076 3E33     01630          LD A,SWORD
1078 F5       01640          PUSH AF         ;SAVE SWORD
1079 DB72     01650 LEVELR   IN A,(STATUS)   ;IS REF LEVEL
107B E608     01660          AND 8           ;PRESENT?
107D C29310   01670          JP NZ,LEVELS
1080 DB72     01680          IN A,(STATUS)   ;LEVEL ABSENT
1082 E601     01690          AND 1
1084 C2C110   01700          JP NZ,FINIS     ;FINISHED?
1087 F1       01710          POP AF          ;RESTORE SWORD
1088 CD8311   01720          CALL CWSTEP     ;PUSH IN SYRINGE
108B F5       01721          PUSH AF         ;SAVE CUR SWORD
108C 0D       01730          DEC C           ;RECORD IT IN COUNT
108D CC4B11   01740          CALL Z,VOLIN    ;INC VOL CHANGE?
1090 C3AA10   01760          JP MONTEP
1093 DB72     01770 LEVELS   IN A,(STATUS)   ;IS SYS LEVEL
1095 E604     01780          AND 4           ;PRESENT?
1097 C2AA10   01790          JP NZ,MONTEP    ;IF YES CK REF LEVEL
109A DB72     01800          IN A,(STATUS)   ;LEVEL ABSENT
109C E602     01810          AND 2
109E C2C110   01820          JP NZ,FINIS     ;FINISHED?
10A1 F1       01830          POP AF          ;GET SWORD
10A2 CD7A11   01840          CALL CCSTEP     ;PULL SYRINGE OUT
10A5 F5       01841          PUSH AF         ;SAVE CUR SWORD
```

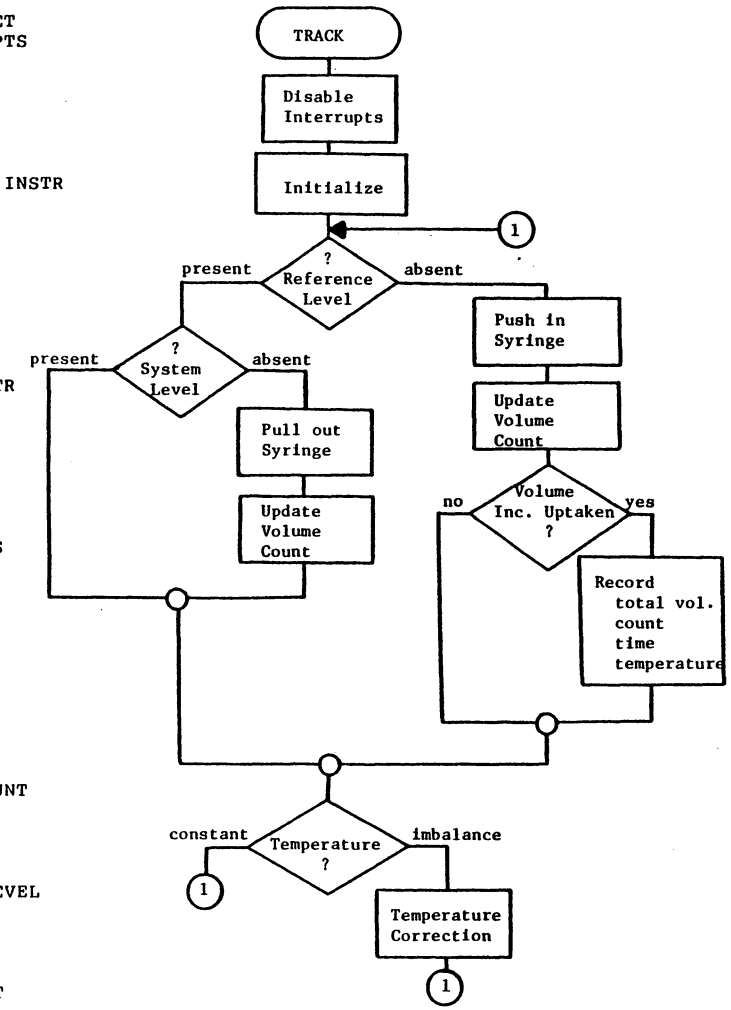

```
10A6 05       01850          DEC B
10A7 CC3611   01860          CALL Z,VOLOUT    ;INC VOL CHANGE?
10AA F5       01880 MONTEP   PUSH AF          ;SAVE REGS
10AB C5       01890          PUSH BC
10AC D5       01900          PUSH DE
10AD E5       01910          PUSH HL
10AE CD0C11   01920          CALL ISITIM      ;TIME TO CORRECT?
10B1 C2BA10   01930          JP NZ,NOTIM      ;NO SO RESTORE REGS
10B4 CD1E11   01940          CALL ADOFST      ;GET TIME OFFSET
10B7 CDD210   01950          CALL TEPIMB      ;CORRECT TEMP
10BA E1       01960 NOTIM    POP HL           ;RESTORE REGS
10BB D1       01970          POP DE
10BC C1       01980          POP BC
10BD F1       01990          POP AF
10BE C37910   02000          JP LEVELR
10C1 C7       02010 FINIS    RST 0            ;RET TO MONITOR
10C2 1604     02020 FIND     LD D,04H         ;FIND OVEN QDT
10C4 010608   02030          LD BC,BUFFER
10C7 0A       02040 TESTIT   LD A,(BC)
10C8 03       02050          INC BC
10C9 03       02060          INC BC
10CA 03       02070          INC BC           ;NEXT QDT
10CB A2       02080          AND D
10CC CAC710   02090          JP Z,TESTIT      ;FIND IT?
10CF 0B       02100          DEC BC           ;YES
10D0 0B       02110          DEC BC           ;GET PTR TO CNT
10D1 C9       02120          RET
10D2 CDBF11   02130 TEPIMB   CALL TEMPA       ;READ QDT'S
10D5 CDC210   02140          CALL FIND        ;GET OVEN COUNT
10D8 0A       02150          LD A,(BC)
10D9 6F       02160          LD L,A
10DA 03       02170          INC BC
10DB 0A       02180          LD A,(BC)
10DC 67       02190          LD H,A
10DD 012508   02200          LD BC,0825H
10E0 CD3213   02210          CALL GETNUM      ;SETPOINT TEMP ---> DE
10E3 BA       02220          CP D
10E4 C2EA10   02230          JP NZ,DIFFER
10E7 7D       02240          LD A,L
10E8 BB       02250          CP E
10E9 C8       02260          RET Z            ;TEMP A CONSTANT
10EA CD0411   02270 DIFFER   CALL COMPLT      ;NEGATE HL
10ED 19       02280          ADD HL,DE
10EE D8       02290          RET C            ;NEG? DON'T CORRECT
10EF CD0411   02300          CALL COMPLT      ;NEGATE DIFF COUNTS SO>0
10F2 3E00     02310          LD A,00H
10F4 D373     02320          OUT (HTR),A      ;TURN HTR ON
10F6 2B       02330 HTRDLY   DEC HL           ;WAIT*CNTS
10F7 CD8C11   02340          CALL WAIT
10FA 7D       02350          LD A,L
```

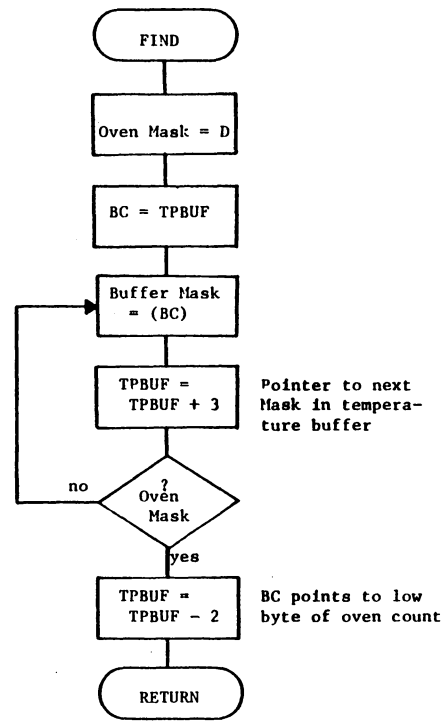

```
10FB B4       02360          OR H
10FC C2F610   02370          JP NZ,HTRDLY
10FF 3E01     02380          LD A,01H
1101 D373     02390          OUT (HTR),A      ;TURN HTR OFF
1103 C9       02400          RET
1104 7D       02410 COMPLT   LD A,L           ;2'S CMPLT OF HL
1105 2F       02420          CPL
1106 6F       02430          LD L,A
1107 7C       02440          LD A,H
1108 2F       02450          CPL
1109 67       02460          LD H,A
110A 23       02470          INC HL
110B C9       02480          RET
110C CD9D11   02490 ISITIM   CALL CLOCK       ;IS IT TIME YET?
110F CD1C12   02500          CALL WATCH
1112 CDD300   02510          CALL DSPLY
1115 CD2B11   02520          CALL PACSEC
1118 212108   02530          LD HL,0821H      ;PREVIOUS CLK&OFFSET
111B 46       02540          LD B,(HL)
111C B8       02550          CP B
111D C9       02560          RET
111E C615     02570 ADOFST   ADD A,15H        ;ADD OFFSET TIME
1120 27       02580          DAA
1121 FE60     02590          CP 60H
1123 DA2911   02600          JP C,OFFSET
1126 C640     02610          ADD A,40H
1128 27       02620          DAA
1129 77       02630 OFFSET   LD (HL),A
112A C9       02640          RET
112B 210108   02650 PACSEC   LD HL,0801H      ;PACK SECONDS IN CLK BUF
112E 7E       02660          LD A,(HL)
112F 07       02670          RLCA
1130 07       02680          RLCA
1131 07       02690          RLCA
1132 07       02700          RLCA
1133 2B       02710          DEC HL
1134 B6       02720          OR (HL)
1135 C9       02730          RET
00C8          02740 NOUT     EQU 200          ;# INC STEPS OUT
00C8          02750 NIN      EQU 200          ;# INC STEPS IN
1136 CD9D11   02760 VOLOUT   CALL CLOCK
1139 CD6011   02770          CALL GETPTR
113C 36FF     02780          LD (HL),0FFH     ;ID FOR OUT
113E 23       02790          INC HL
113F CD6D11   02800          CALL SAVPTR
1142 CDE911   02810          CALL VOLCNT
1145 CD4C12   02820          CALL RECORD
1148 06C8     02830          LD B,NOUT        ;INC STEPS OUT
114A C9       02840          RET
114B CD9D11   02850 VOLIN    CALL CLOCK
```

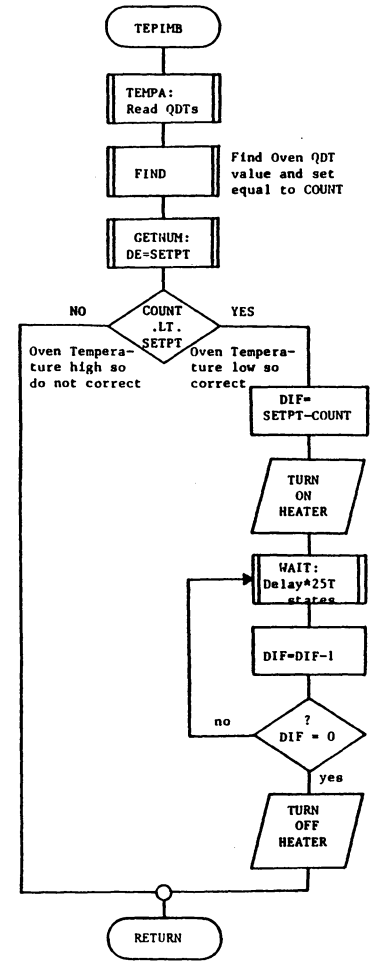

```
114E CD6011   02860          CALL GETPTR
1151 3600     02870          LD (HL),0       ;ID FOR VOL UPTAKE
1153 23       02880          INC HL
1154 CD6D11   02890          CALL SAVPTR
1157 CDE911   02900          CALL VOLCNT
115A CD4C12   02910          CALL RECORD
115D 0EC8     02920          LD C,NIN        ;INC STEPS IN
115F C9       02930          RET
1160 D5       02940 GETPTR   PUSH DE
1161 F5       02950          PUSH AF
1162 111F08   02960          LD DE,081FH     ;GET CUR. DATA PTR.
1165 1A       02970          LD A,(DE)
1166 67       02980          LD H,A
1167 1B       02990          DEC DE
1168 1A       03000          LD A,(DE)
1169 6F       03010          LD L,A
116A F1       03020          POP AF
116B D1       03030          POP DE
116C C9       03040          RET
116D D5       03050 SAVPTR   PUSH DE
116E F5       03060          PUSH AF
116F 111F08   03070          LD DE,081FH     ;SAVE CUR. DATA PTR.
1172 7C       03080          LD A,H
1173 12       03090          LD (DE),A
1174 1B       03100          DEC DE
1175 7D       03110          LD A,L
1176 12       03120          LD (DE),A
1177 F1       03130          POP AF
1178 D1       03140          POP DE          ;RESTORE DE
1179 C9       03150          RET
0050          03160 STP      EQU 50H         ;STEPPER MOTOR
117A 0F       03170 CCSTEP   RRCA            ;UPDATE SWORD
117B D350     03180          OUT (STP),A     ;TAKE A STEP
117D F5       03190          PUSH AF         ;WAIT FOR STP RESPONSE
117E CD3A13   03200          CALL DELAY
1181 F1       03210          POP AF
1182 C9       03220          RET
1183 07       03230 CWSTEP   RLCA            ;UPDATE SWORD
1184 D350     03240          OUT (STP),A     ;TAKE A STEP
1186 F5       03250          PUSH AF         ;WAIT FOR STP RESPONSE
1187 CD3A13   03260          CALL DELAY
118A F1       03270          POP AF
118B C9       03280          RET
118C F5       03290 WAIT     PUSH AF         ;(11)
118D D5       03300          PUSH DE         ;(11)
118E 012308   03310          LD BC,0823H     ;(10)
1191 CD3213   03320          CALL GETNUM     ;(10)   :59 T STATES
1194 1B       03330 PAUSE    DEC DE          ;(5)    :N*25+22 T STATES
1195 7A       03340          LD A,D          ;(5)    :
1196 B3       03350          OR E            ;(5)    :
```

```
1197 C29411   03360          JP NZ,PAUSE      ;(7/10) :
119A D1       03370          POP DE           ;(10)
119B F1       03380          POP AF           ;(10)
119C C9       03390          RET              ;(10)
0070          03400 CLK      EQU 70H          ;CLOCK CODE
0800          03410 TIME     EQU 0800H        ;BUFFER FOR CUR TIME
119D E5       03420 CLOCK    PUSH HL          ;READ CLOCK
119E C5       03430          PUSH BC
119F F5       03440          PUSH AF          ;SAVE CLOCK BYTE IN A
11A0 210008   03450          LD HL,TIME       ;BUFFER CALLED TIME
11A3 D370     03460          OUT (CLK),A      ;MULTIPLEX
11A5 DB70     03470          IN A,(CLK)
11A7 2F       03480          CPL
11A8 4F       03490          LD C,A
11A9 E670     03500          AND 70H
11AB 07       03510          RLCA
11AC 07       03520          RLCA
11AD 07       03530          RLCA
11AE 07       03540          RLCA
11AF 85       03550          ADD A,L          ;CALC PTR
11B0 6F       03560          LD L,A
11B1 79       03570          LD A,C
11B2 E60F     03580          AND 15
11B4 77       03590          LD (HL),A        ;GET A DIGIT
11B5 7D       03600          LD A,L
11B6 FE00     03610          CP 0
11B8 C2A011   03620          JP NZ,CLOCK+3    ;FINISHED?
11BB F1       03630          POP AF
11BC C1       03640          POP BC
11BD E1       03650          POP HL
11BE C9       03660          RET
0806          03670 BUFFER   EQU 0806H        ;CUR TEMP BUFFER
0052          03680 TIMER    EQU 82           ;QDT
11BF E5       03700 TEMPA    PUSH HL          ;TEMPERATURE MONITOR
11C0 D5       03710          PUSH DE          ;READ ALL QDTS
11C1 C5       03720          PUSH BC
11C2 F5       03730          PUSH AF
11C3 210608   03740          LD HL,BUFFER
11C6 110000   03750          LD DE,0
11C9 D352     03760          OUT (TIMER),A    ;RESET MONOSTABLE
11CB 0EFF     03770          LD C,0FFH
11CD 13       03780 DURA     INC DE
11CE DB52     03790          IN A,(TIMER)     ;WAIT FOR A TIMER
11D0 A9       03800          XOR C            ;TO CHANGE STATE
11D1 CACD11   03810          JP Z,DURA
11D4 77       03820          LD (HL),A        ;SAVE MASK
11D5 23       03830          INC HL
11D6 A9       03870          XOR C
11D7 4F       03890          LD C,A           ;UPDATE MASK
11D8 73       03900          LD (HL),E        ;SAVE DURATION
```

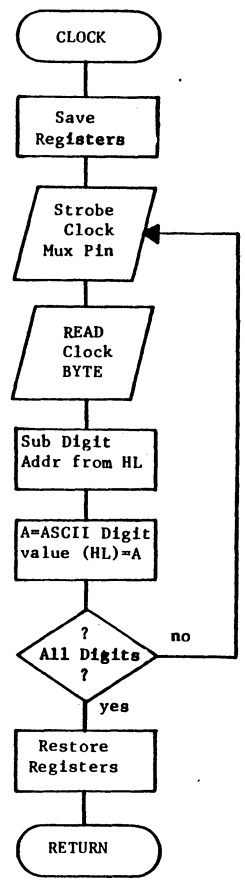

CLOCK BYTE

D7	D6	D5	D4	D3	D2	D1	D0
DIGIT ADDR.				CLOCK DIGIT			

S1 S10 M1 M10 H1 H10
routine reads S1 last

```
11D9 23       03910          INC HL          ;COUNT IN BUFFER
11DA 72       03920          LD (HL),D
11DB 23       03930          INC HL
11DC 97       03940          SUB A
11DD 81       03950          ADD A,C         ;HAVE ALL TIMERS
11DE 13       03960          INC DE          ;COUNTED OUT?
11DF 13       03970          INC DE
11E0 13       03980          INC DE
11E1 C2CD11   03990          JP NZ,DURA
11E4 F1       04000          POP AF
11E5 C1       04010          POP BC
11E6 D1       04020          POP DE
11E7 E1       04030          POP HL
11E8 C9       04040          RET
11E9 D5       04050 VOLCNT   PUSH DE         ;UPDATE VOL. COUNT
11EA E5       04060          PUSH HL
11EB 11F70F   04070          LD DE,0FF7H
11EE 212008   04080          LD HL,0820H
11F1 78       04090          LD A,B
11F2 B7       04100          OR A
11F3 C2FF11   04110          JP NZ,INCNT     ;VOL. INC. IN OR OUT?
11F6 7E       04120          LD A,(HL)       ;VOL. INC. OUT!!!
11F7 3D       04130          DEC A
11F8 77       04140          LD (HL),A
11F9 CD0812   04150          CALL UNPACK     ;DSPLY VOL. COUNT
11FC E1       04160          POP HL
11FD D1       04170          POP DE
11FE C9       04180          RET
11FF 7E       04190 INCNT    LD A,(HL)       ;VOL. INC. IN
1200 3C       04200          INC A
1201 77       04210          LD (HL),A
1202 CD0812   04220          CALL UNPACK     ;DSPLY VOL. COUNT
1205 E1       04230          POP HL
1206 D1       04240          POP DE
1207 C9       04250          RET
1208 6F       04260 UNPACK   LD L,A          ;HEX BYTE
1209 E60F     04270          AND 0FH         ;INTO HEX DIGITS
120B CD4412   04280          CALL ASCII
120E 12       04290          LD (DE),A
120F 7D       04300          LD A,L
1210 E6F0     04310          AND 0F0H
1212 1F       04320          RRA
1213 1F       04330          RRA
1214 1F       04340          RRA
1215 1F       04350          RRA
1216 CD4412   04360          CALL ASCII      ;CONVERT HEX DIG INTO
1219 13       04370          INC DE          ;ASCII CHARACTER
121A 12       04380          LD (DE),A
121B C9       04390          RET
121C E5       04400 WATCH    PUSH HL         ;DSPLY VALUE IN
121D D5       04410          PUSH DE         ;CLOCK BUFFER ON
```

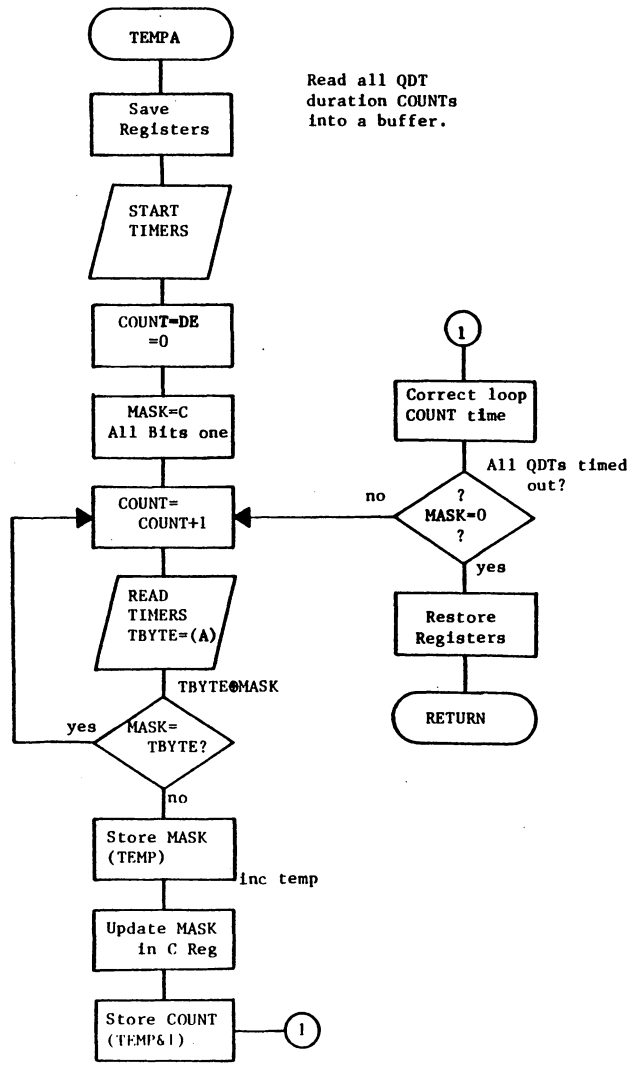

```
121E 210008   04420          LD HL,TIME      ;9 DIGIT DSPLY
1221 11FA0F   04430          LD DE,0FFAH
1224 7E       04440 OVER     LD A,(HL)
1225 CD4412   04450          CALL ASCII
1228 12       04460          LD (DE),A
1229 7D       04470          LD A,L          ;PUT ASCII VAL IN
122A FE02     04480          CP 2            ;DSPLY BUFFER
122C CC3E12   04490          CALL Z,POINT
122F FE04     04500          CP 4
1231 CC3E12   04510          CALL Z,POINT
1234 23       04520          INC HL
1235 13       04530          INC DE
1236 FE06     04540          CP 6
1238 C22412   04550          JP NZ,OVER
123B D1       04560          POP DE
123C E1       04570          POP HL
123D C9       04580          RET
123E 1A       04590 POINT    LD A,(DE)       ;TURN ON DEC. PT.
123F F680     04600          OR 80H
1241 12       04610          LD (DE),A
1242 7D       04620          LD A,L
1243 C9       04630          RET
1244 C630     04640 ASCII    ADD A,30H       ;CONVERT TO ASCII
1246 FE3A     04650          CP 3AH
1248 D8       04660          RET C
1249 C607     04670          ADD A,7
124B C9       04680          RET
124C E5       04690 RECORD   PUSH HL         ;LOG DATA PT.
124D D5       04700          PUSH DE         ;FORMAT:
124E C5       04710          PUSH BC         ;  FRAME0:DELIMITER
124F F5       04720          PUSH AF         ;         00H VOLIN
1250 CD6011   04730          CALL GETPTR     ;        0FFH VOLOUT
1253 7C       04740          LD A,H          ;  FRAME1:SECONDS
1254 FE0F     04750          CP 0FH          ;  FRAME2:MINUTES
1256 C25F12   04760          JP NZ,CONT      ;  FRAME3:HOURS
1259 7D       04770          LD A,L          ;  FRAME4:LC QDT1
125A FE3C     04780          CP 3CH          ;  FRAME5:HC QDT1
125C D2C110   04790          JP NC,FINIS     ;  FRAME6:LC QDT2
125F 010108   04800 CONT     LD BC,TIME+1    ;  FRAME7:HC QDT2
1262 0A       04810 SAVE     LD A,(BC)       ;  FRAME8:LC QDT3
1263 07       04820          RLCA            ;  FRAME9:HC QDT3
1264 07       04830          RLCA
1265 07       04840          RLCA
1266 07       04850          RLCA
1267 5F       04860          LD E,A
1268 0B       04870          DEC BC
1269 0A       04880          LD A,(BC)
126A B3       04890          OR E
126B 77       04900          LD (HL),A
126C 23       04910          INC HL
```

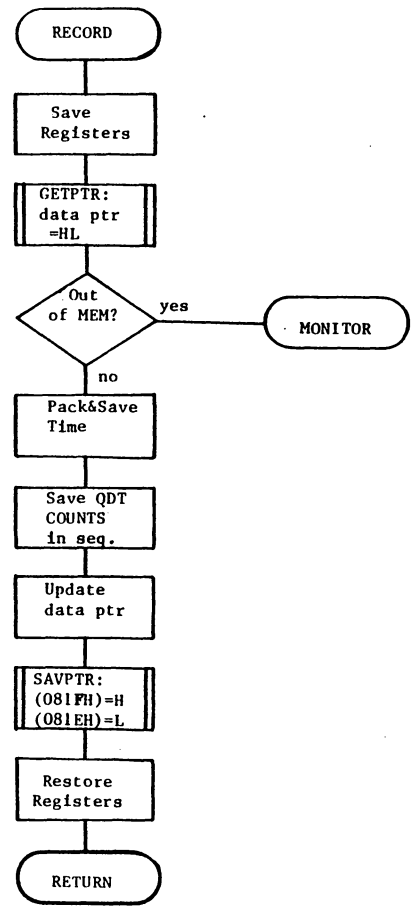

```
126D 03       04920          INC BC
126E 03       04930          INC BC
126F 03       04940          INC BC
1270 79       04950          LD A,C
1271 FE07     04960          CP 7
1273 C26212   04970          JP NZ,SAVE
1276 1604     04980          LD D,4
1278 010608   04990 DEVNO    LD BC,BUFFER
127B 0A       05000 TEST     LD A,(BC)       ;GET A MASK
127C 03       05010          INC BC          ;SEARCH FOR
127D 03       05020          INC BC          ;CORRECT DEV #
127E 03       05030          INC BC
127F A2       05040          AND D
1280 CA7B12   05050          JP Z,TEST
1283 0B       05060          DEC BC
1284 0B       05070          DEC BC
1285 1EFF     05080          LD E,0FFH
1287 1C       05090 BITEST   INC E
1288 1F       05100          RRA
1289 D28712   05110          JP NC,BITEST    ;QDT TIMED OUT?
128C 7B       05120          LD A,E
128D 07       05130          RLCA            ;MULTIPLY BY 2
128E 5F       05140          LD E,A          ;ADJ DATA PTR
128F E5       05150          PUSH HL
1290 D5       05160          PUSH DE
1291 1600     05170          LD D,0
1293 19       05180          ADD HL,DE
1294 0A       05190          LD A,(BC)       ;GET LBYTE FROM BUFFER
1295 77       05200          LD (HL),A       ;PUT IT IN DATA FILE
1296 03       05210          INC BC
1297 23       05220          INC HL
1298 0A       05230          LD A,(BC)
1299 77       05240          LD (HL),A
129A D1       05250          POP DE
129B E1       05260          POP HL
129C 7A       05270          LD A,D
129D 1F       05280          RRA
129E 57       05290          LD D,A
129F D27812   05300          JP NC,DEVNO     ;FINISHED?
12A2 110600   05310          LD DE,06H
12A5 19       05320          ADD HL,DE       ;ADJ DATA PTR
12A6 CD6D11   05330          CALL SAVPTR
12A9 F1       05340          POP AF
12AA C1       05350          POP BC
12AB D1       05360          POP DE
12AC E1       05370          POP HL
12AD C9       05380          RET
12AE 1E00     05390 NUMBER   LD E,0          ;E=DIGIT POSITION
12B0 CDDB00   05400 ATEST    CALL KEY
12B3 FE2C     05410          CP 2CH
```

```
12B5 CAC212   05420          JP Z,TAF        ;INC.? NEXT COMMAND?
12B8 CD1913   05430          CALL SHIFT      ;NO, SO ENTER NUMBER
12BB 57       05440          LD D,A
12BC CDD512   05450          CALL BUFDSP
12BF C3B012   05460          JP ATEST
12C2 C9       05470 TAF      RET             ;# QUERY FINISHED
12C3 F5       05480 LABEL    PUSH AF
12C4 C5       05490          PUSH BC
12C5 01FF0F   05500          LD BC,0FFFH     ;BC=DSPLY BUFFER
12C8 7E       05510 TAG      LD A,(HL)       ;HL=LABEL PTR.
12C9 02       05520          LD (BC),A
12CA 2B       05530          DEC HL
12CB 0B       05540          DEC BC
12CC 79       05550          LD A,C
12CD FEFA     05560          CP 0FAH
12CF C2C812   05570          JP NZ,TAG       ;LOAD LABEL IN DSPLY BUF
12D2 C1       05580          POP BC
12D3 F1       05590          POP AF
12D4 C9       05600          RET
12D5 F5       05610 BUFDSP   PUSH AF         ;DSPLY NUMBERS
12D6 C5       05620          PUSH BC         ;ENTERED FOR
12D7 01F70F   05630          LD BC,0FF7H     ;SETPT & DSPLY
12DA 79       05640          LD A,C
12DB 83       05650          ADD A,E         ;E DIGIT POSITION
12DC 4F       05660          LD C,A
12DD 7A       05670          LD A,D          ;D # FOR DSPLY
12DE E60F     05680          AND 0FH
12E0 C630     05690          ADD A,30H
12E2 FE3A     05700          CP 3AH
12E4 FAE912   05710          JP M,LTN        ;# .LT. NINE?
12E7 C607     05720          ADD A,7
12E9 02       05730 LTN      LD (BC),A
12EA C1       05740          POP BC
12EB F1       05750          POP AF
12EC C9       05760          RET
12ED F5       05770 PACKIT   PUSH AF         ;CONVERTS 2 ASCII CHAR
12EE C5       05780          PUSH BC         ;INTO HEX BYTE
12EF 01FA0F   05790          LD BC,0FFAH
12F2 0A       05800 OTHER    LD A,(BC)
12F3 FE3A     05810          CP 3AH
12F5 FAFA12   05820          JP M,NTA        ;LESS THAN TEN?
12F8 C609     05830          ADD A,9         ;NO, SO ADJUST IT
12FA E60F     05840 NTA      AND 0FH
12FC 07       05850          RLCA
12FD 07       05860          RLCA
12FE 07       05870          RLCA
12FF 07       05880          RLCA
1300 0B       05890          DEC BC          ;GET MDIGIT
1301 5F       05900          LD E,A
1302 0A       05910          LD A,(BC)
```

```
1303 FE3A     05920          CP 3AH
1305 FA0A13   05930          JP M,ISIT        ;IS IT TEN?
1308 C609     05940          ADD A,9
130A E60F     05950 ISIT     AND 0FH          ;GET LDIGIT
130C 83       05960          ADD A,E          ;PACKIT
130D 77       05970          LD (HL),A
130E 2B       05980          DEC HL
130F 0B       05990          DEC BC
1310 79       06000          LD A,C
1311 FEF6     06010          CP 0F6H
1313 C2F212   06020          JP NZ,OTHER      ;ANY OTHER DIGITS?
1316 C1       06030          POP BC
1317 F1       06040          POP AF
1318 C9       06050          RET
1319 F5       06060 SHIFT    PUSH AF          ;SHIFT #'S LEFT ON
131A C5       06070          PUSH BC          ;DSPLY BY UPDATING
131B D5       06080          PUSH DE          ;DSPLY BUFFER
131C E5       06090          PUSH HL
131D 01FA0F   06100          LD BC,0FFAH
1320 21F90F   06110          LD HL,0FF9H
1323 7E       06120 LEFT     LD A,(HL)
1324 02       06130          LD (BC),A
1325 0B       06140          DEC BC
1326 2B       06150          DEC HL
1327 79       06160          LD A,C
1328 FEF7     06170          CP 0F7H
132A C22313   06180          JP NZ,LEFT       ;ALL DIGITS SHIFTED?
132D E1       06190          POP HL
132E D1       06200          POP DE
132F C1       06210          POP BC
1330 F1       06220          POP AF
1331 C9       06230          RET
1332 F5       06240 GETNUM   PUSH AF          ;(11)  :59 T STATES
1333 0A       06250          LD A,(BC)        ;(7)
1334 57       06260          LD D,A           ;(4)
1335 0B       06270          DEC BC           ;(6)
1336 0A       06280          LD A,(BC)        ;(7)
1337 5F       06290          LD E,A           ;(4)
1338 F1       06300          POP AF           ;(10)
1339 C9       06310          RET              ;(10)
133A D5       06320 DELAY    PUSH DE          ;DELAY FOR MOTOR
133B 110009   06330          LD DE,0900H      ;TO RESPOND
133E 1B       06340 MCNT     DEC DE
133F 7A       06350          LD A,D
1340 B3       06360          OR E
1341 C23E13   06370          JP NZ,MCNT
1344 D1       06380          POP DE
1345 C9       06390          RET
              06391 ;
              06392 ; SYSLKT ALLOWS A RAPID LEAK CHECK TO BE MADE
```

```
                06393 ; BY NOTING TIME IN CLOCK BUFFER ON RETURN TO
                06394 ; THE MONITOR PROGRAM
                06395 ;
1346 D371       06400 SYSLKT  OUT (RESET),A   ;RAPID SYSTEM PRESSURE
1348 CD9601     06410         CALL CLEAR      ;CHECK
134B DB72       06420         IN A,(STATUS)   ;READ DBP MANO
134D 6F         06430         LD L,A
134E CD9D11     06440 CHIT    CALL CLOCK      ;READ THE TIME
1351 CD1C12     06450         CALL WATCH      ;SET UP DSPLY
1354 CDD300     06460         CALL DSPLY      ;SHOW IT
1357 DB72       06470         IN A,(STATUS)   ;HAS STAT CHANGED?
1359 F5         06480         PUSH AF
135A 11F70F     06490         LD DE,0FF7H     ;DE=BUFPTR
135D D5         06500         PUSH DE
135E E5         06510         PUSH HL
135F CD0812     06520         CALL UNPACK
1362 E1         06530         POP HL
1363 D1         06540         POP DE
1364 F1         06550         POP AF
1365 BD         06560         CP L            ;CK WITH INIT STAT
1366 CA4E13     06570         JP Z,CHIT
1369 C7         06580         RST 0           ;RETURN TO MONITOR
                06581 ;
                06582 ; HTRCK ALLOWS THE HEATER CONTROL CIRCUIT TO BE
                06583 ; CHECKED BY NOTING OVEN QDT COUNT ON KAD DISPLAY
                06584 ;
136A CD9601     06590 HTRCK   CALL CLEAR      ;CHECK HTR CONTROL
136D 210410     06600         LD HL,LABSTP
1370 CDC312     06610         CALL LABEL
1373 CDAE12     06620         CALL NUMBER
1376 212508     06630         LD HL,0825H     ;SAVE SETPT
1379 CDED12     06640         CALL PACKIT
137C CD9601     06650         CALL CLEAR
137F 210910     06660         LD HL,LABDLY
1382 CDC312     06670         CALL LABEL
1385 CDAE12     06680         CALL NUMBER
1388 212308     06690         LD HL,0823H     ;SAVE DELAY
138B CDED12     06700         CALL PACKIT
138E CD9601     06710 TEPCON  CALL CLEAR
1391 D371       06720         OUT (RESET),A   ;RESET CLOCK
1393 CD9D11     06730         CALL CLOCK
1396 CD2B11     06740         CALL PACSEC
1399 212108     06750         LD HL,0821H     ;OFFSET TIME
139C CD1E11     06760         CALL ADOFST
139F CDBD13     06770 COLHTR  CALL QDTCNT
13A2 CDB113     06780         CALL TIMYET
13A5 C29F13     06790         JP NZ,COLHTR
13A8 CD1E11     06800         CALL ADOFST
13AB CDD210     06810         CALL TEPIMB
13AE C39F13     06820         JP COLHTR
```

```
13B1 CD9D11   06830 TIMYET  CALL CLOCK
13B4 CD2B11   06840         CALL PACSEC
13B7 212108   06850         LD HL,0821H     ;OFFSET TIME
13BA 46       06860         LD B,(HL)
13BB B8       06870         CP B
13BC C9       06880         RET
13BD F5       06890 QDTCNT  PUSH AF         ;GET OVEN QDT CNT
13BE C5       06900         PUSH BC
13BF D5       06910         PUSH DE
13C0 E5       06920         PUSH HL
13C1 CDC210   06930         CALL FIND
13C4 0A       06940         LD A,(BC)
13C5 11FD0F   06950         LD DE,0FFDH     ;DSPLY BUF POS.
13C8 CDDB13   06960         CALL UNPKIT
13CB 03       06970         INC BC
13CC 0A       06980         LD A,(BC)
13CD 11FF0F   06990         LD DE,0FFFH     ;DSPLY BUF POS.
13D0 CDDB13   07000         CALL UNPKIT
13D3 CDD300   07010         CALL DSPLY
13D6 E1       07030         POP HL
13D7 D1       07040         POP DE
13D8 C1       07050         POP BC
13D9 F1       07060         POP AF
13DA C9       07070         RET
13DB C5       07080 UNPKIT  PUSH BC         ;UNPACK CNT
13DC D5       07090         PUSH DE         ;PUT IT IN DSPLY BUF
13DD 4F       07100         LD C,A
13DE 00       07110         NOP
13DF 00       07120         NOP
13E0 00       07130         NOP
13E1 E6F0     07140         AND 0F0H
13E3 1F       07150         RRA
13E4 1F       07160         RRA
13E5 1F       07170         RRA
13E6 1F       07180         RRA
13E7 CDF613   07190         CALL CONASC
13EA 12       07200         LD (DE),A
13EB 1B       07210         DEC DE
13EC 79       07220         LD A,C
13ED E60F     07230         AND 0FH
13EF CDF613   07240         CALL CONASC
13F2 12       07250         LD (DE),A
13F3 D1       07260         POP DE
13F4 C1       07270         POP BC
13F5 C9       07280         RET
13F6 C630     07290 CONASC  ADD A,48D
13F8 FE3A     07300         CP 3AH
13FA D8       07310         RET C
13FB C607     07320         ADD A,7D
13FD C9       07330         RET
```

```
                07331 ;
                07332 ; LEVIND PERMITS LEVEL INDICATOR CIRCUITRY AND
                07333 ; INDICATORS TO BE ADJUSTED BEFORE A RUN
                07334 ;
13FE CD9601     07340 LEVIND  CALL CLEAR
1401 DB72       07350 LOOK    IN A,(STATUS)
1403 11F80F     07360         LD DE,0FF8H      ;DE=BUFPTR
1406 CDDB13     07370         CALL UNPKIT
1409 CDD300     07380         CALL DSPLY
140C C30114     07390         JP LOOK
                07391 ; INSTP AND OUTSTP ARE FOR STEPPING THE STEPPER
                07392 ; MOTOR A NUMBER OF STEPS DEPENDING ON THE VALUE
                07393 ; PLACED A 0823H, DIRECTIONS ARE IN AND OUT
                07394 ; RESPECTIVELY
                07395 ;
140F 3E33       07400 INSTP   LD A,33H         ;INIT SWORD
1411 012308     07410         LD BC,0823H      ;BC PTR TO NSTEPS
1414 CD3213     07420         CALL GETNUM      ;GET NUM IN DE
1417 F5         07430         PUSH AF
1418 F1         07440 ISTEP   POP AF
1419 CD8311     07450         CALL CWSTEP
141C F5         07460         PUSH AF
141D 1B         07470         DEC DE
141E 7A         07480         LD A,D
141F B3         07490         OR E
1420 C21814     07500         JP NZ,ISTEP
1423 F1         07510         POP AF
1424 C7         07520         RST 0            ;RETURN TO MONITOR
1425 3E33       07530 OUTSTP  LD A,33H         ;INIT SWORD
1427 012308     07540         LD BC,0823H
142A CD3213     07550         CALL GETNUM
142D F5         07560         PUSH AF
142E F1         07570 OSTEP   POP AF
142F CD7A11     07580         CALL CCSTEP
1432 F5         07590         PUSH AF
1433 1B         07600         DEC DE
1434 7A         07610         LD A,D
1435 B3         07620         OR E
1436 C22E14     07630         JP NZ,OSTEP
1439 F1         07640         POP AF
143A C7         07650         RST 0            ;RETURN TO MONITOR
0000            07660         END
00000 TOTAL ERRORS
```

SYMBOL TABLE

ADOFST	111E	INCNT	11FF	PAUSE	1194
ASCII	1244	INIT	100A	POINT	123E
ATEST	12B0	INSTP	140F	QDTCNT	13BD
BITEST	1287	ISIT	130A	RECORD	124C
BUFFER	0806	ISITIM	110C	RESET	0071
CCSTEP	117A	ISTEP	1418	SAVE	1262
CHIT	134E	KEY	00DB	SAVPTR	116D
CLEAR	0196	LABDLY	1009	SHIFT	1319
CLK	0070	LABEL	12C3	STATUS	0072
CLOCK	119D	LABELS	1000	STP	0050
COLHTR	139F	LABSTP	1004	SWORD	0033
COMPLT	1104	LEFT	1323	SYSLKT	1346
CONASC	13F6	LEVELR	1079	TAF	12C2
CONT	125F	LEVELS	1093	TAG	12C8
CONTEP	102E	LEVIND	13FE	TEMPA	11BF
CWSTEP	1183	LOOK	1401	TEPCON	138E
DELAY	133A	LTN	12E9	TEPIMB	10D2
DEVNO	1278	MCNT	133E	TEST	127B
DIFFER	10EA	MONTEP	10AA	TESTIT	10C7
DSPLY	00D3	NIN	00C8	TIME	0800
DURA	11CD	NOTIM	10BA	TIMER	0052
EXPYET	104C	NOUT	00C8	TIMYET	13B1
FIND	10C2	NTA	12FA	TRACK	1053
FINIS	10C1	NUMBER	12AE	UNPACK	1208
GETNUM	1332	OFFSET	1129	UNPKIT	13DB
GETPTR	1160	OSTEP	142E	VOLCNT	11E9
HTR	0073	OTHER	12F2	VOLIN	114B
HTRCK	136A	OUTSTP	1425	VOLOUT	1136
HTRCOL	103F	OVER	1224	WAIT	118C
HTRDLY	10F6	PACKIT	12ED	WATCH	121C

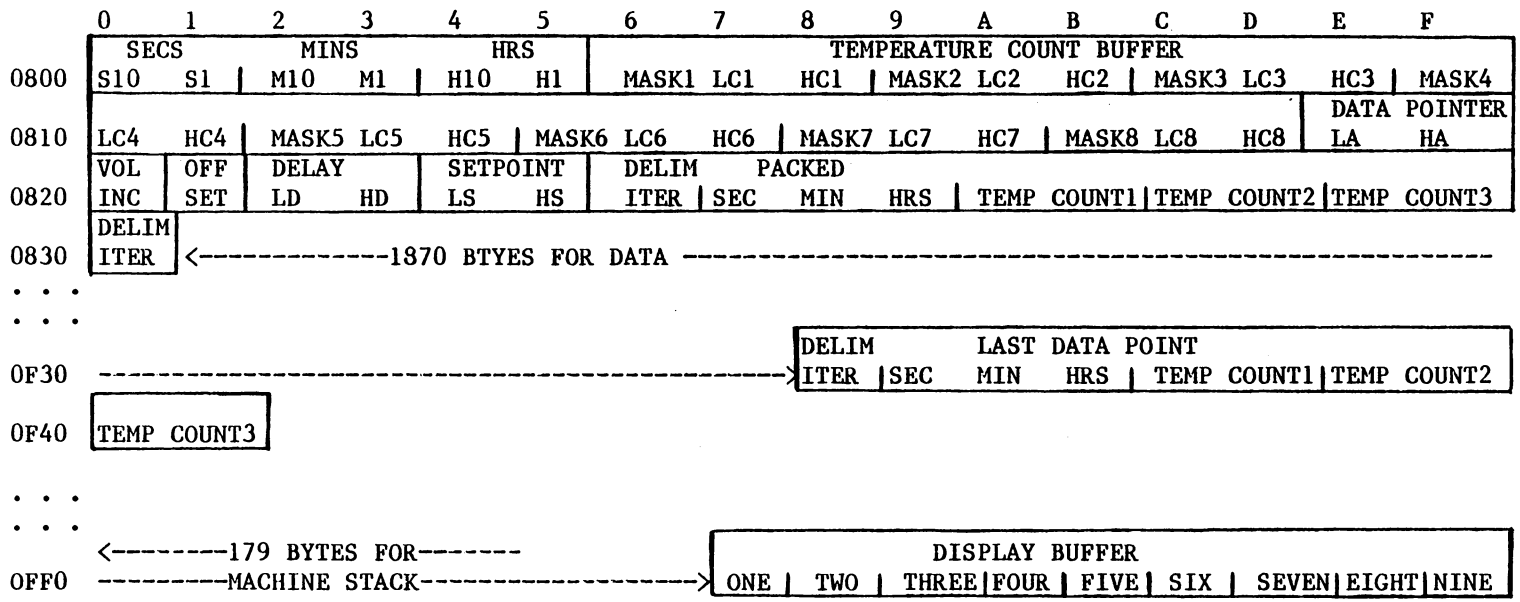

ALLOCATION OF WRITE AND READ MEMORY ON PAM

Appendix C. DIFFUSION/SOLUBILITY MEASUREMENTS

I. Manual apparatus results.

II. Automated apparatus results.

mon:day:yr
01: 19: 84

Solute/Solvent: N2/CCl4 Gas Pressure: 747.7 torr
Cell Temperature: 25.0 deg C

Time hr:mn:sc	Time (sec1/2)	Volume Height	Gage (mm)	Volume (cc)
00:01:33	9.6	48.8	49.6	0.07
00:02:44	12.8	49.6	50.4	0.15
00:04:13	15.9	50.4	51.2	0.22
00:07:28	21.2	51.2	52.6	0.35
00:09:38	24.0	52.6	53.2	0.41
00:12:41	27.6	53.2	54.2	0.50
00:14:27	29.4	54.2	54.7	0.54
00:17:40	32.6	54.7	55.5	0.62
00:21:00	35.5	55.5	56.2	0.68
00:29:39		56.2	58.6	0.90
00:35:57		58.6	59.8	1.01
00:54:45		59.8	62.4	1.25
01:06:49		62.4	64.1	1.41
01:22:26		64.1	66.0	1.58
01:43:52		66.0	68.3	1.80
02:23:01		68.3	71.7	2.11
03:00:42		71.7	74.2	2.34
03:28:28		74.2	76.5	2.55
04:07:59		76.5	80.0	2.87
04:38:53		80.0	82.7	3.12
05:25:49		82.7	87.2	3.54
06:05:06	Time	87.2	90.0	3.79
09:22:43	(sec)	90.0	93.2	4.09
16:00:26	57626	93.2	95.8	4.33
18:58:25	68305	95.8	96.6	4.40
22:34:16	81256	96.6	97.9	4.52
26:44:07	96247	97.9	99.8	4.70
37:20:34	134434	99.8	103.2	5.01
42:36:07	153367	103.2	105.2	5.19
50:45:43	182743	105.2	107.0	5.36
60:52:00	219120	107.0	110.5	5.68
66:53:45	240825	110.5	111.8	5.80
74:01:03	266463	111.8	114.7	6.07
76:23:27	275007	114.7	115.5	6.14
85:44:11	308651	115.5	118.4	6.41

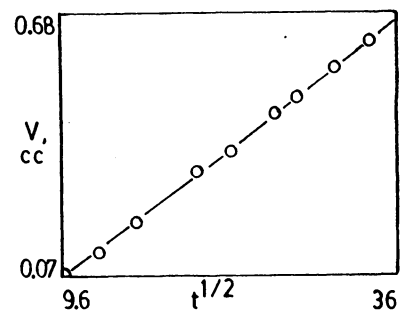

Open Tube Slope:
2.36e-2 cc/sec 1/2

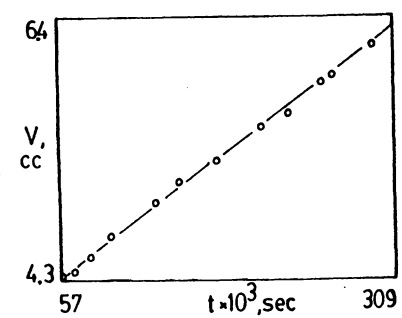

Capillary Disk Slope:
8.23e-6 cc/sec

mon:day:yr
01: 25: 84

Solute/Solvent: N2/CCl4 Gas Pressure: 760.8 torr
Cell Temperature: 25.0 deg C

Time hr:mn:sc	Time (secl/2)	Volume Height	Gage (mm)	Volume (cc)
00:02:17	11.7	44.9	46.2	0.12
00:03:29	14.4	46.2	46.9	0.18
00:05:14	17.7	46.9	47.5	0.24
00:06:37	19.9	47.5	48.2	0.30
00:08:06	22.0	48.2	48.9	0.37
00:10:13	24.7	48.9	49.5	0.42
00:12:24	27.3	49.5	50.0	0.47
00:14:11	29.2	50.0	50.3	0.50
00:15:25	30.4	50.3	50.8	0.54
00:18:37	33.4	50.8	51.5	0.61
00:22:37	36.8	51.5	52.3	0.68
00:26:42	40.0	52.3	52.8	0.73
00:31:46		52.8	53.5	0.79
00:37:20		53.5	54.5	0.88
00:43:15		54.5	55.2	0.95
00:51:15		55.2	56.1	1.03
00:58:16		56.1	56.9	1.10
01:06:52		56.9	57.8	1.18
01:20:23		57.8	59.2	1.32
01:39:13		59.2	60.8	1.46
02:02:26		60.8	62.7	1.64
02:24:11		62.7	64.0	1.76
02:41:14		64.0	65.2	1.87
03:13:26		65.2	67.2	2.05
03:41:12		67.2	68.7	2.19
04:13:28	Time	68.7	70.9	2.39
07:04:08	(sec)	70.9	76.4	2.90
12:45:28	45928	76.4	79.0	3.14
21:05:26	75926	79.0	80.9	3.32
35:07:06	126426	80.9	84.5	3.65
38:28:12	138492	84.5	85.9	3.78
41:31:36	149496	85.9	87.2	3.90
47:34:49	171289	87.2	88.5	4.02
58:09:21	209361	88.5	92.3	4.36
64:01:28	230488	92.3	93.8	4.50
70:46:36	254796	93.8	96.6	4.76
81:58:09	295089	96.6	100.6	5.13
86:10:33	310233	100.6	101.5	5.21
89:54:29	323669	101.5	102.6	5.31
106:10:22	382222	102.6	108.7	5.88
118:55:06	428106	108.7	112.3	6.21

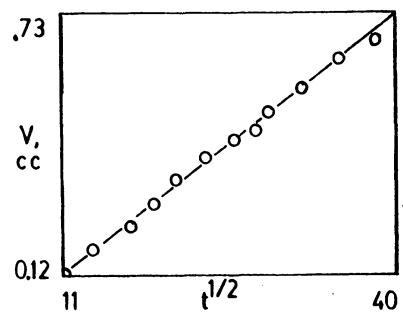

Open Tube Slope:
2.19e-2 cc/sec 1/2

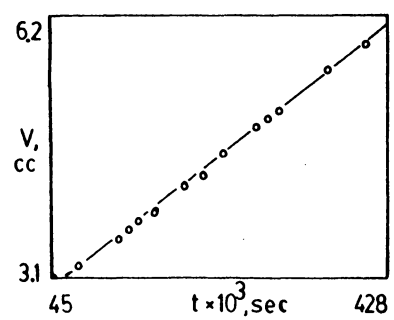

Capillary Disk Slope:
8.26e-6 cc/sec

mon:day:yr
03: 03: 84

Solute/Solvent: N2/CCl4 Gas Pressure: 772.5 torr
Cell Temperature: 25.0 deg C

Time hr:mn:sc	Time (secl/2)	Volume Gage Height (mm)		Volume (cc)
00:01:09	8.3	132.8	134.2	0.13
00:02:46	12.9	134.2	135.0	0.20
00:03:56	15.4	135.0	135.6	0.26
00:05:57	18.9	135.6	136.6	0.35
00:08:10	22.1	136.6	137.4	0.42
00:10:28	25.1	137.4	138.1	0.49
00:12:30	27.4	138.1	138.7	0.54
00:14:43	29.7	138.7	139.2	0.59
00:17:36	32.4	139.2	140.0	0.66
00:20:21	34.9	140.0	140.5	0.71
00:28:00	41.0	140.5	141.9	0.84
00:39:38		141.9	143.3	0.97
00:49:21		143.3	144.9	1.11
01:07:20		144.9	146.3	1.24
01:26:05		146.3	149.2	1.51
01:45:17		149.2	150.5	1.63
02:47:50		150.5	155.3	2.07
03:24:04		155.3	157.2	2.25
04:32:14		157.2	162.5	2.74
05:49:15		162.5	165.1	2.97
06:33:07	Time	165.1	166.1	3.07
07:21:41	(sec)	166.1	167.0	3.15
14:23:30	51810	167.0	169.5	3.38
17:08:24	61704	169.5	169.6	3.39
21:23:17	76997	169.6	171.4	3.56
25:06:05	90365	171.4	172.3	3.64
34:53:23	125603	172.3	175.8	3.96
37:12:36	133956	175.8	176.3	4.01
44:14:50	159290	176.3	177.7	4.14
47:51:24	172284	177.7	178.7	4.23
49:54:39	179679	178.7	179.2	4.27
58:59:19	212359	179.2	182.8	4.60
65:10:49	234649	182.8	184.4	4.75
72:16:46	260206	184.4	187.5	5.04
84:04:53	302693	187.5	191.8	5.43
87:48:37	316117	191.8	192.4	5.49
91:55:17	330917	191.1	193.2	5.68
97:01:38	349298	193.2	194.1	5.76

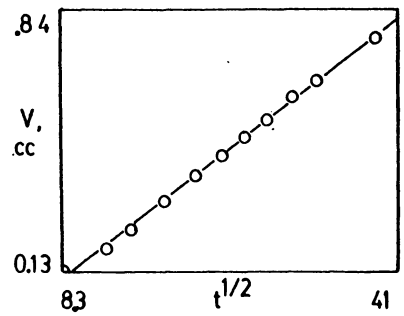

Open Tube Slope:
2.23e-2 cc/sec 1/2

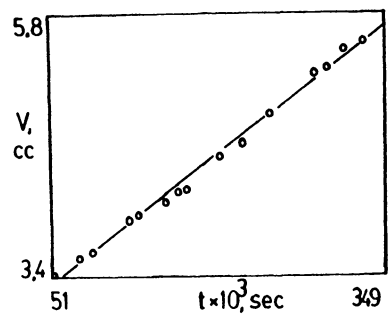

Capillary Disk Slope:
8.24e-6 cc/sec

mon:day:yr
03: 09: 84

Solute/Solvent: N2/CCl4 Gas Pressure: 761.8 torr
Cell Temperature: 25.0 deg C

Time hr:mn:sc	Time (secl/2)	Volume Height	Gage (mm)	Volume (cc)
00:01:09		77.3	78.2	0.08
00:02:20	11.8	78.2	78.7	0.13
00:03:47	15.1	78.7	79.5	0.20
00:05:24	18.0	79.5	80.2	0.27
00:07:00	20.5	80.2	80.9	0.33
00:09:30	23.9	80.9	81.6	0.40
00:11:53	26.7	81.6	82.2	0.45
00:13:27	28.4	82.2	82.7	0.50
00:15:36	30.6	82.7	83.0	0.52
00:18:15	33.1	83.0	83.6	0.58
00:20:58		83.6	84.3	0.64
00:25:13		84.3	85.0	0.71
00:30:29		85.0	85.7	0.77
00:37:48		85.7	86.7	0.86
00:48:11		86.7	88.2	1.00
01:00:10		88.2	89.9	1.16
01:22:40		89.9	92.3	1.38
01:46:58		92.3	94.2	1.55
02:11:16		94.2	96.5	1.77
02:48:28		96.5	98.7	1.97
03:26:38		98.7	101.5	2.23
04:07:07		101.5	104.1	2.47
04:44:58		104.1	105.3	2.58
05:41:11		105.3	106.0	2.64
06:26:12		106.0	106.6	2.70
06:53:49	Time	106.6	107.2	2.75
08:17:04	(sec)	107.2	107.8	2.80
15:16:30	54990	107.8	109.8	2.99
21:02:20	75740	109.8	111.3	3.13
25:33:46	92026	111.3	113.2	3.31
28:39:28	103168	113.2	114.2	3.40
37:13:09	133989	114.2	117.1	3.66
43:32:49	156769	117.1	118.8	3.82
48:41:29	175289	118.8	120.2	3.95
52:33:27	189207	120.2	121.5	4.07
58:33:53	210833	121.5	124.3	4.33
65:46:43	236803	124.3	125.8	4.47
73:26:03	264363	125.8	128.2	4.69

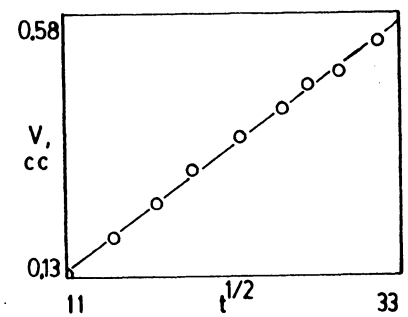

Open Tube Slope:
2.12e-2 cc/sec 1/2

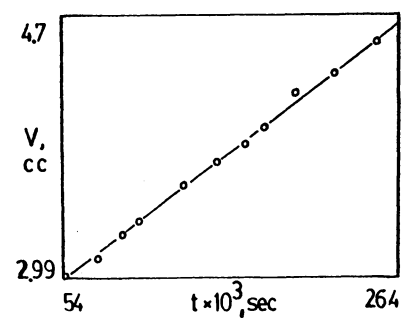

Capillary Disk Slope:
8.17e-6 cc/sec

mon:day:yr
03: 27: 84

Solute/Solvent: N2/CCl4 Gas Pressure: 1021.9 torr
Cell Temperature: 25.0 deg C

Time hr:mn:sc	Time (sec1/2)	Volume Gage Height (mm)		Volume (cc)
00:01:13	8.5	121.5	122.6	0.10
00:03:16	14.0	122.6	123.7	0.20
00:04:51	17.1	123.7	124.5	0.28
00:06:16	19.4	124.5	125.3	0.35
00:08:31	22.6	125.3	125.9	0.40
00:11:20	26.1	125.9	126.6	0.47
00:13:51	28.8	126.6	127.2	0.52
00:16:55	31.8	127.2	128.0	0.60
00:21:32	35.9	128.0	128.9	0.68
00:29:49	42.3	128.9	130.3	0.81
00:38:32		130.3	131.9	0.96
00:49:49		131.9	133.5	1.10
01:13:27		133.5	136.1	1.34
01:45:55		136.1	139.4	1.65
02:17:04		139.4	141.9	1.88
02:49:08		141.9	144.1	2.08
03:18:11		144.1	146.0	2.26
03:49:35		146.0	147.0	2.40
04:16:28		147.0	149.0	2.53
04:51:13	Time	149.0	150.6	2.68
05:08:22	(sec)	150.6	151.3	2.74
09:08:07	32887	151.3	152.7	2.87
10:03:51	36231	152.7	153.0	2.95
18:41:07	67267	153.0	156.1	3.23
23:43:11	85391	156.1	157.0	3.31
25:32:57	91977	157.0	157.5	3.36
31:28:52	113332	157.5	159.4	3.53
34:56:17	125777	159.4	160.1	3.59
44:20:20	159620	160.1	163.2	3.86
48:04:15	173055	163.2	164.4	3.98
53:28:19	192499	164.4	165.9	4.12
58:10:04	209404	165.9	166.8	4.20
68:41:34	247294	166.8	170.7	4.56
73:39:09	265149	170.7	172.4	4.72
79:16:12	285372	172.4	173.8	4.84
85:02:36	306156	173.8	175.4	4.99
93:50:51	337851	175.4	178.2	5.24
97:09:40	349780	178.2	179.5	5.37

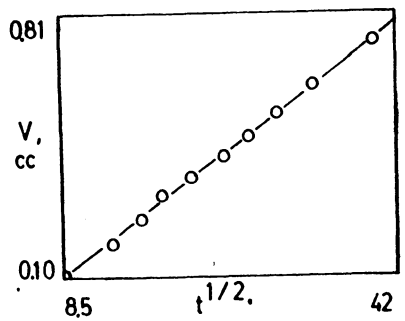

Open Tube Slope:
2.12e-2 cc/sec 1/2

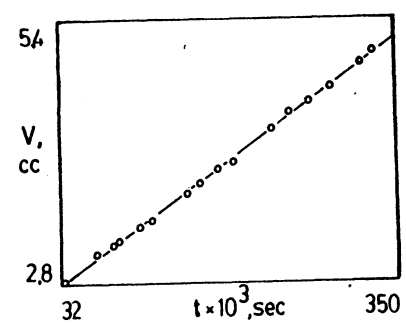

Capillary Disk Slope:
7.71e-6 cc/sec

mon:day:yr
03: 20: 84

Solute/Solvent: N2/CCl4 Gas Pressure: 1047.1 torr
Cell Temperature: 24.9 deg C

Time hr:mn:sc	Time (secl/2)	Volume Height	Gage (mm)	Volume (cc)
00:01:06	8.1	82.0	82.5	0.05
00:02:32	12.3	82.5	83.5	0.14
00:04:33	16.5	83.5	84.5	0.23
00:06:53	20.3	84.5	85.5	0.32
00:09:46	24.2	85.5	86.4	0.40
00:11:42	26.5	86.4	86.9	0.45
00:14:15	29.2	86.9	87.4	0.50
00:17:12	32.1	87.4	88.0	0.55
00:20:01	34.6	88.0	88.7	0.62
00:23:34	37.6	88.7	89.5	0.69
00:29:10	41.8	89.5	90.3	0.76
00:36:10		90.3	91.7	0.89
00:43:13		91.7	92.4	0.96
00:52:14		92.4	93.7	1.08
01:02:02		93.7	94.7	1.17
01:05:54		94.7	95.4	1.23
01:30:35		95.4	98.0	1.47
01:53:27		98.0	99.8	1.64
02:25:52		99.8	102.1	1.85
03:16:22		102.1	105.5	2.16
04:01:55		105.5	107.5	2.35
04:38:57		107.5	109.2	2.50
05:27:14		109.2	110.8	2.65
06:21:57	Time	110.8	112.4	2.80
07:28:35	(sec)	112.4	115.5	3.09
10:05:54	36354	115.5	117.2	3.24
20:27:40	73660	117.2	122.2	3.70
25:06:10	90370	122.2	122.8	3.76
27:32:31	99151	122.8	123.8	3.85
31:55:00	114900	123.8	125.5	4.01
35:00:25	126025	125.5	126.3	4.08
44:23:16	159796	126.3	130.2	4.44
50:54:47	183287	130.2	132.1	4.61
54:29:35	196175	132.1	133.1	4.71
61:29:12	221352	133.1	135.8	4.95
70:30:51	253851	135.8	139.5	5.30
73:18:08	263888	139.5	139.8	5.32
83:40:31	301231	139.8	143.3	5.64

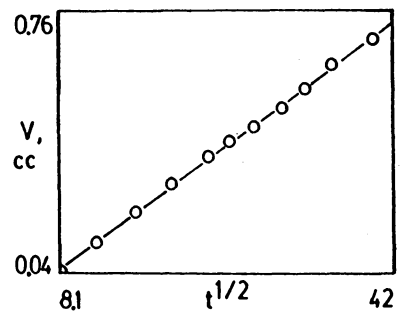

Open Tube Slope:
2.13e-2 cc/sec 1/2

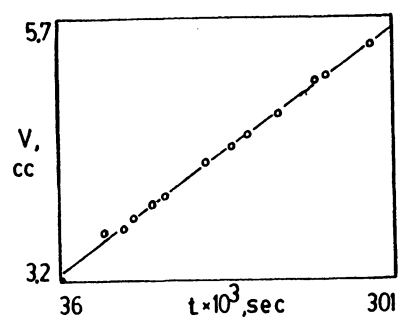

Capillary Disk Slope:
8.99e-6 cc/sec

mon:day:yr
04: 04: 84

Solute/Solvent: N2/CCl4 Gas Pressure: 961.4 torr
Cell Temperature: 25.0 deg C

Time hr:mn:sc	Time (sec1/2)	Volume Height	Gage (mm)	Volume (cc)
00:01:45	10.2	67.1	68.5	0.13
00:03:02	13.5	68.5	69.2	0.19
00:05:25	18.0	69.2	70.3	0.29
00.07:48	21.6	70.3	71.4	0.40
00:12:45	27.6	71.4	72.8	0.52
00:17:23	32.3	72.8	74.0	0.64
00:24:18	38.2	74.0	75.5	0.77
00:48:55	54.2	75.5	79.3	1.12
01:45:22		79.3	85.5	1.69
02:12:20		85.5	87.6	1.89
02:47:52		87.6	90.2	2.13
03:39:29		90.2	93.5	2.43
04:34:13		93.5	96.2	2.68
05:23:25		96.2	98.3	2.87
05:44:31		98.3	99.4	2.97
12:18:27	Time	99.4	110.9	4.03
20:16:22	(sec)	110.9	114.3	4.35
27:13:33	98013	114.3	116.4	4.54
35:53:32	128132	116.4	119.5	4.83
45:17:47	163067	119.5	122.2	5.07
48:52:22	175942	122.2	123.0	5.15
51:30:04	185404	123.0	123.9	5.23
62:41:18	225678	123.9	128.7	5.67
68:03:02	244982	128.7	128.9	5.69
75:44:41	272681	128.9	131.9	5.97

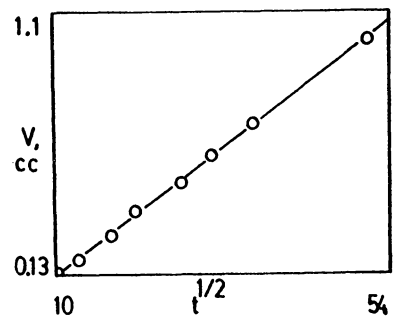

Open Tube Slope:
2.29e-2 cc/sec 1/2

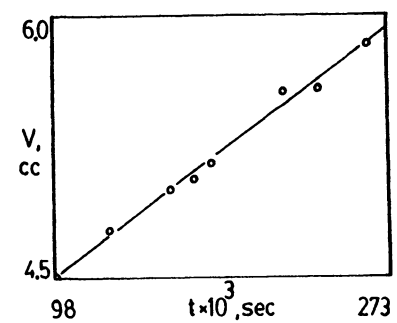

Capillary Disk Slope:
8.14e-6 cc/sec

mon:day:yr
04: 17: 84

Solute/Solvent: N2/CCl4 Gas Pressure: 1033.4 torr
Cell Temperature: 24.9 deg C

Time hr:mn:sc	Time (sec)	Volume Height	Gage (mm)	Volume (cc)
00:01:22	9.0	83.0	84.2	0.11
00:02:52	13.1	84.2	85.4	0.22
00:04:34	16.6	85.4	86.2	0.29
00:06:50	20.2	86.2	87.1	0.38
00:09:14	23.5	87.1	87.9	0.45
00:12:52	27.8	87.9	88.8	0.53
00:16:25	31.4	88.8	89.6	0.61
00:20:45	35.3	89.6	90.6	0.70
00:27:28	40.5	90.6	91.7	0.80
00:36:31	46.8	91.7	93.0	0.92
00:46:58		93.0	94.6	1.07
01:06:23		94.6	97.2	1.31
01:21:09		97.2	98.5	1.43
01:48:42		98.5	101.3	1.68
02:12:15		101.3	102.9	1.83
03:21:12		102.9	107.7	2.27
04:59:30		107.7	111.5	2.62
06:26:07		111.5	114.5	2.90
08:00:03		114.5	117.2	3.15
09:29:02	Time	117.2	119.0	3.32
11:37:00	(sec)	119.0	121.1	3.51
13:58:12	50292	121.1	123.6	3.74
24:16:29	87389	123.6	127.5	4.10
28:25:13	102313	127.5	128.3	4.17
33:18:33	119913	128.3	129.7	4.30
39:39:55	142795	129.7	131.9	4.50
49:02:18	176538	131.9	134.8	4.77
53:10:36	191436	134.8	135.3	4.82
57:57:55	208675	135.3	137.1	4.92
64:24:04	231844	137.1	139.2	5.18
80:31:50	289910	139.2	143.9	5.61
84:00:13	302413	143.9	144.5	5.66
89:36:22	322582	144.5	146.6	5.82
99:12:31	357151	146.2	151.5	6.31
109:26:27	393987	151.5	154.1	6.55
121:29:05	437345	154.1	158.1	6.92

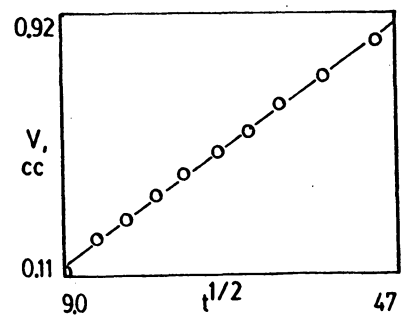

Open Tube Slope:
2.13e-2 cc/sec 1/2

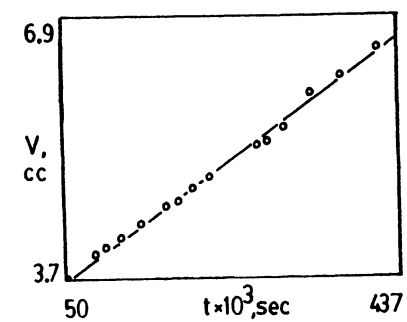

Capillary Disk Slope:
7.67e-6 cc/sec

mon:day:yr
04: 24: 84

Solute/Solvent: N2/CCl4 Gas Pressure: 517.7 torr
Cell Temperature: 25.0 deg C

Time hr:mn:sc	Time (secl/2)	Volume Height	Gage (mm)	Volume (cc)
00:01:09	8.3	28.9	29.6	0.06
00:02:50	13.0	29.6	30.5	0.15
00:05:04	17.4	30.5	31.4	0.23
00:07:29	21.2	31.4	32.2	0.31
00:10:49	25.5	32.3	33.5	0.42
00:12:12	27.1	33.5	34.1	0.48
00:15:07	30.1	34.1	35.1	0.57
00:18:51	33.6	35.1	36.0	0.65
00:27:05	40.3	36.0	37.8	0.82
00:36:00		37.8	39.3	0.96
00:55:10		39.3	41.9	1.20
01:26:38		41.9	44.1	1.40
02:11:42		44.1	49.1	1.86
02:43:56		49.1	51.5	2.08
03:12:22		51.5	53.1	2.23
03:55:41		53.1	55.5	2.45
04:29:40		55.5	56.9	2.58
04:53:39		56.9	57.6	2.64
05:29:20	Time	57.6	59.0	2.77
05:46:37	(sec)	59.0	59.8	2.84
14:37:22	52642	59.8	72.5	4.02
21:34:04	77644	72.5	73.8	4.14
34:16:20	123380	73.8	77.8	4.50
40:46:58	146818	77.8	78.0	4.52
50:00:00	180000	78.0	81.0	4.80
58:32:09	210729	81.0	82.8	4.96
64:27:57	232077	82.8	85.1	5.18
74:34:07	268447	85.1	90.0	5.63
83:19:06	299946	90.0	92.7	5.88
85:35:00	318900	92.7	94.3	6.02

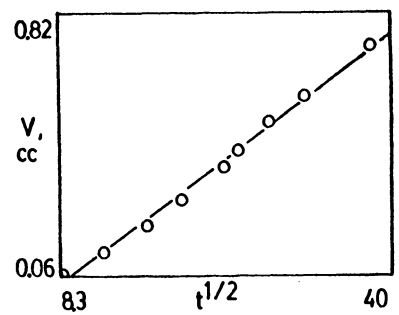

Open Tube Slope:
2.42e-2 cc/sec 1/2

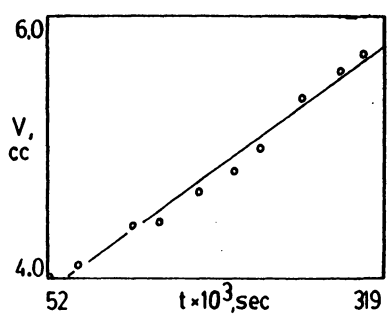

Capillary Disk Slope:
7.64e-6 cc/sec

mon:day:yr
05: 02: 84

Solute/Solvent: N2/CCl4 Gas Pressure: 370.0 torr
Cell Temperature: 25.0 deg C

Time hr:mn:sc	Time (secl/2)	Volume Gage Height (mm)	Volume (cc)
00:01:14		217.3 217.8	0.05
00:03:42		217.8 218.6	0.12
00:05:49	18.7	218.6 218.8	0.14
00:08:14	22.2	218.8 219.5	0.20
00:10:53	25.5	219.5 220.0	0.25
00:13:51	28.8	220.0 220.9	0.33
00.17.24	32.3	220.9 221.6	0.40
00:20:40	35.2	221.6 222.3	0.46
00:24:42	38.4	222.3 222.9	0.52
00:29:49	42.3	222.9 223.9	0.61
00:36:13		223.9 224.9	0.70
00:43:16		224.9 225.8	0.78
00:56:17		225.8 227.2	0.91
01:13:14		227.2 228.3	1.01
01:28:01		228.3 229.9	1.16
01:45:29		29.9 231.1	1.27
02:20:19		231.1 233.2	1.46
02:48:31		233.2 234.8	1.61
03:50:37		234.8 236.1	1.73
05:05:59		236.1 241.6	2.24
06:11:57	Time	241.6 244.1	2.47
07:48:03	(sec)	244.1 245.3	2.58
10:50:22	39022	245.3 245.9	2.63
14:13:31	51211	245.9 247.2	2.75
24:41:27	88887	247.2 249.4	2.96
28:17:20	101840	249.4 250.1	3.02
32:58:10	118690	250.1 250.8	3.09
38:42:57	137377	250.8 252.6	3.25
48:46:48	175608	252.6 254.9	3.46
52:47:10	190030	254.9 256.0	3.56
62:27:49	224869	256.0 258.4	3.79
71:34:28	257668	258.4 262.0	4.12

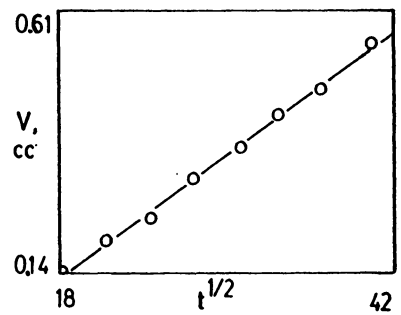

Open Tube Slope:
1.99e-2 cc/sec 1/2

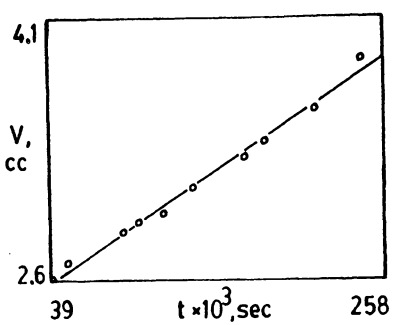

Capillary Disk Slope:
6.71e-6 cc/sec 1/2

mon:day:yr
05: 09: 84

Solute/Solvent: N2/CCl4 Gas Pressure: 441.0 torr
Cell Temperature: 25.0 deg C

Time hr:mn:sc	Time (sec1/2)	Volume Height	Gage (mm)	Volume (cc)
00:01:13		49.2	50.0	0.07
00:03:18	14.1	50.0	50.8	0.15
00:05:20	17.9	50.8	51.7	0.23
00:07:53	21.7	51.7	52.5	0.30
00:10:00	24.5	52.5	53.2	0.37
00:12:14	27.1	53.2	53.9	0.43
00:15:04	30.1	53.9	54.5	0.49
00:18:30	33.3	54.5	55.3	0.56
00:21:11	35.6	55.3	56.2	0.64
00:29:29	42.0	56.2	57.7	0.78
00:34:23	45.5	57.7	58.2	0.83
00:44:00		58.2	59.6	0.96
00:57:12		59.6	61.1	1.10
01:15:05		61.1	63.0	1.27
01:33:34		63.0	64.5	1.41
02:19:54	Time	64.5	67.4	1.68
05:23:12	(sec)	67.4	77.8	2.63
10:40:29	38429	77.9	85.0	3.30
16:05:32	57932	85.0	85.4	3.33
23:47:13	85633	85.4	88.7	3.64
34:11:20	123080	88.7	92.6	4.00
48:12:59	173579	92.6	94.9	4.21
61:29:31	221371	94.9	97.3	4.43
71:44:32	258272	97.3	98.9	4.58
73:29:18	264558	98.9	102.9	4.94
75:24:01	271441	102.9	103.5	5.00
83:02:07	298927	103.5	105.1	5.15
93:22:25	336145	105.1	107.5	5.37
100:53:52	363232	107.5	108.5	5.46
108:50:44	391840	108.5	110.7	5.66
117:38:38	423518	110.7	114.6	6.02
120:54:40	435280	114.6	116.8	6.22

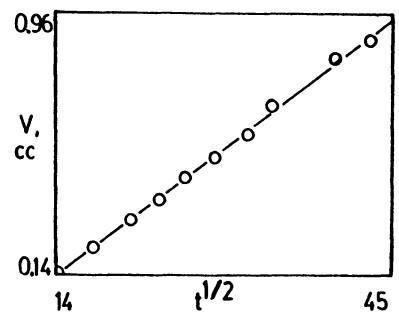

Open Tube Slope:
2.24e-2 cc/sec 1/2

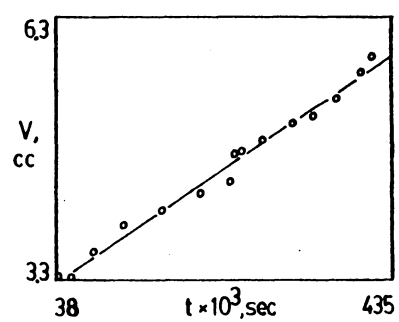

Capillary Disk Slope:
7.07e-6 cc/sec

mon:day:yr
09: 26: 84

Solute/Solvent: N2/CCl4 Gas Pressure: 687.7 torr
Cell Temperature: 26.1 deg C

Time hr:mn:sc	Time (sec1/2)	Volume Gage Height (mm)		Volume (cc)
00:01:33	9.6	334.8	335.6	0.07
00:02:16	11.7	335.6	336.2	0.13
00:03:54	15.3	336.2	337.0	0.20
00:05:51	18.7	337.0	337.7	0.27
00:08:30	22.6	337.7	338.2	0.31
00:13:50	28.8	338.2	339.4	0.42
00:17:17	32.2	339.4	340.1	0.49
00:21:10	35.6	340.1	340.7	0.54
00:25:03	38.8	340.7	341.5	0.62
00:29:02	41.7	341.5	342.4	0.70
00:35:24		342.4	343.9	0.84
00:42:04		343.9	344.8	0.92
00:49:47		344.8	345.8	1.01
01:24:37		345.8	349.4	1.34
01:34:17		349.4	350.3	1.43
01:56:45		350.3	352.5	1.63
02:12:12		352.5	353.2	1.69
02:51:14		353.2	356.0	1.95
03:37:05		356.0	358.4	2.17
03:52:34		358.4	358.8	2.21
04:31:59		358.8	361.1	2.42
05:25:20		361.1	363.8	2.67
12:01:48		363.8	373.5	3.56
16:24:03	Time	373.5	376.7	3.86
19:37:07	(sec)	376.7	377.9	3.97
22:48:51	82131	377.9	380.5	4.21
25:05:29	90329	380.5	381.9	4.34
28:54:40	104080	381.9	382.9	4.43
36:23:57	131037	382.9	385.7	4.69
40:57:31	147451	385.7	385.9	4.71
46:47:21	168441	385.9	388.6	4.95
60:59:01	219541	388.6	392.9	5.35
77:02:13	277333	392.9	396.4	5.67

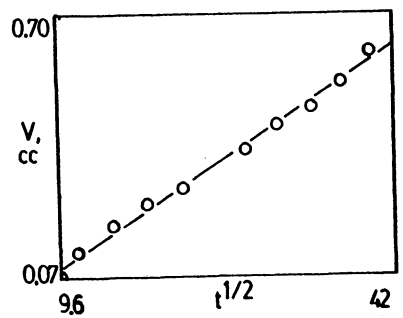

Open Tube Slope:
1.83e-2 cc/sec 1/2

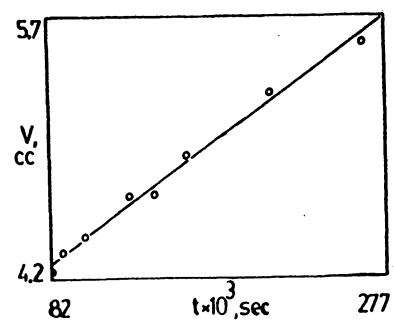

Capillary Disk Slope:
7.49e-6 cc/sec

mon:day:yr
10: 28: 84

Solute/Solvent: N2/CCl4 Gas Pressure: 727.6 torr
Cell Temperature: 25.9 deg C

Time hr:mn:sc	Time (secl/2)	Volume Gage Height (mm)		Volume (cc)
00:00:57		142.5	143.2	0.06
00:02:03	11.9	143.2	143.6	0.10
00:03:08	13.7	143.6	144.1	0.15
00:04:38	16.6	144.1	144.5	0.18
00:07:08	20.7	144.5	145.9	0.31
00:12:25	27.3	145.9	146.9	0.41
00:16:30	31.5	146.9	148.0	0.51
00:20:54	35.4	148.0	148.7	0.57
00:28:21	41.2	148.7	150.0	0.69
00:34:26	45.4	150.0	150.7	0.76
00:39:36	48.7	150.7	151.6	0.84
00:50:40	55.1	151.6	152.8	0.95
01:02:54		152.8	154.3	1.09
01:19:14		154.3	156.0	1.24
01:30:11		156.0	156.8	1.32
01:50:34		156.8	158.0	1.42
02:15:55		158.0	160.2	1.63
02:43:37		160.2	162.3	1.82
03:15:07		162.3	163.8	1.96
03:53:58		163.8	166.1	2.17
04:20:22		166.1	167.3	2.28
04:43:13		167.3	168.2	2.37
05:07:55		168.2	168.9	2.43
06:25:53		168.9	171.4	2.66
07:59:34	Time	171.4	173.8	2.88
09:29:21	(sec)	173.8	175.5	3.04
12:43:40	45820	175.5	178.6	3.32
14:59:02	53942	178.6	179.0	3.36
23:51:02	85862	179.0	182.9	3.72
28:56:23	104183	182.9	184.4	3.93
35:18:50	127130	184.4	185.5	4.03
39:20:24	141624	185.5	186.4	4.12
40:41:41	146501	186.4	187.3	4.20
47:53:53	172433	187.3	190.2	4.47
52:46:00	189960	190.2	190.7	4.51
57:35:01	207301	190.7	190.9	4.58
59:47:23	215243	190.9	192.4	4.72
65:29:49	235789	192.4	193.1	4.78
72:02:47	259367	193.1	197.1	5.15

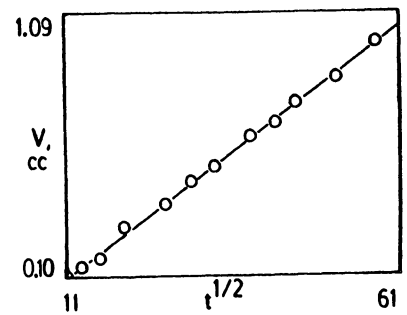

Open Tube Slope:
1.95e-2 cc/sec 1/2

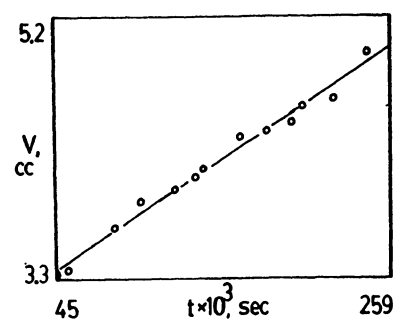

Capillary Disk Slope:
7.99e-6 cc/sec

mon:day:yr
06: 05: 84

Solute/Solvent: Ar/CCl4 Gas Pressure: 569.5 torr
Cell Temperature: 25.3 deg C

Time hr:mn:sc	Time (secl/2)	Volume Height	Gage (mm)	Volume (cc)
00:01:04	8.0	47.1	48.2	0.10
00:02:29	12.2	48.2	50.0	0.27
00:04:42	16.8	50.0	52.1	0.46
00:07:29	21.2	52.1	54.1	0.64
00:10:25	25.0	54.1	55.5	0.77
00:13:01	27.9	55.5	56.8	0.89
00:16:56	31.9	56.8	58.3	1.03
00:20:17	34.9	58.3	59.8	1.17
00:24:07	38.0	59.8	61.3	1.31
00:27:42	40.8	61.3	62.4	1.41
00:35:55	46.4	62.4	65.0	1.65
00:49:37		65.0	68.4	1.96
01:11:01		68.4	73.0	2.39
01:33:54		73.0	78.2	2.86
02:17:04		78.2	85.0	3.49
02:46:27		85.0	89.3	3.89
03:22:05		89.3	93.5	4.27
05:41:48		93.5	105.5	5.38
06:51:08		105.5	109.5	5.75
07:46:45	Time	109.5	112.7	6.04
08:40:20	(sec)	112.7	115.7	6.32
17:14:14	62054	115.7	128.7	7.51
19:47:32	71252	128.7	130.9	7.72
23:06:16	83176	130.9	133.2	7.93
29:59:46	107986	133.2	136.6	8.24
32:55:56	118556	136.6	137.6	8.34
41:50:05	150605	137.6	144.9	9.01
45:54:54	165294	144.9	145.5	9.06
50:57:56	183476	145.5	148.5	9.34
56:01:37	201697	148.5	150.7	9.54
66:18:16	238696	150.7	157.9	10.20
69:56:21	251781	157.9	161.1	10.50
75:31:40	271900	161.1	162.0	10.58

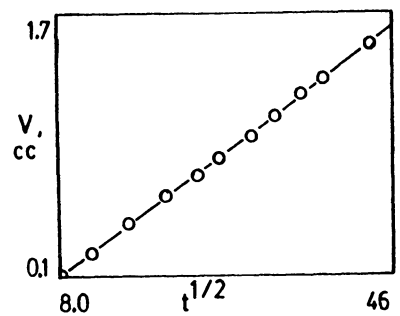

Open Tube Slope:
4.00e-2 cc/sec 1/2

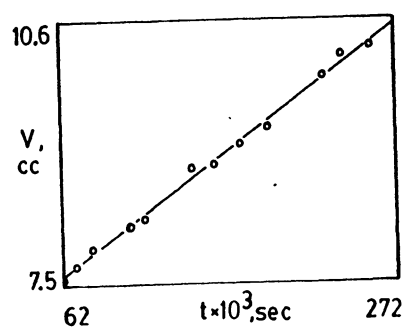

Capillary Disk Slope:
14.8e-6 cc/sec

mon:day:yr
06: 14: 84

Solute/Solvent: Ar/CCl4 Gas Pressure: 737.2 torr
Cell Temperature: 25.3 deg C

Time hr:mn:sc	Time (secl/2)	Volume Height	Gage (mm)	Volume (cc)
00:01:12	8.5	83.7	85.0	0.12
00:02:51	13.1	85.0	87.2	0.32
00:05:06	17.5	87.2	89.2	0.51
00:08:48	23.0	89.2	91.6	0.73
00:12:09	27.0	91.6	93.1	0.86
00:15:38	30.6	93.1	95.0	1.04
00:19:15	34.0	95.0	96.6	1.19
00:24:30	38.3	96.6	98.5	1.36
00:30:22	42.7	98.5	100.4	1.54
00:35:41		100.4	101.7	1.66
00:41:22		101.7	103.3	1.81
00:51:52		103.3	105.8	2.04
01:20:39		105.8	111.7	2.58
02:06:17		111.7	118.1	3.17
03:45:14		118.1	126.7	3.96
04:55:29		126.7	130.5	4.31
06:10:37		130.5	132.8	4.52
06:42:48	Time	132.8	134.0	4.63
09:13:20	(sec)	134.0	137.8	4.98
12:11:28	43888	137.8	140.0	5.19
21:25:30	77130	140.0	146.9	5.82
26:31:33	95493	146.9	149.1	6.02
30:18:28	109108	149.1	150.7	6.17
34:34:51	124491	150.7	152.6	6.34
36:37:54	131874	152.6	154.3	6.50
47:24:13	170653	154.3	160.8	7.10
53:39:32	193172	160.8	164.0	7.40
60:47:18	218838	164.0	168.2	7.78
70:15:08	252908	168.2	137.2	8.24

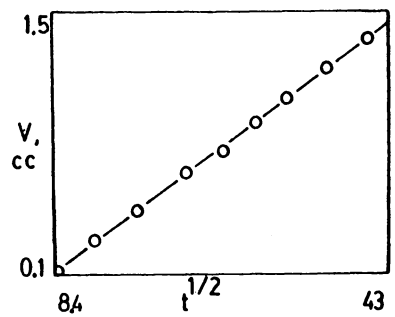

Open Tube Slope:
4.13e-2 cc/sec 1/2

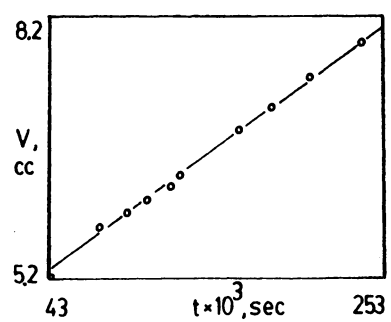

Capillary Disk Slope:
14.4e-6 cc/sec

mon:day:yr
06: 22: 84

Solute/Solvent: Ar/CCl4 Gas Pressure: 754.9 torr
Cell Temperature: 25.3 deg C

Time hr:mn:sc	Time (secl/2)	Volume Height	Gage (mm)	Volume (cc)
00:01:23		27.5	29.1	0.15
00:03:24	14.3	29.1	31.3	0.35
00:04:51	17.1	31.3	33.2	0.52
00:06:50	20.2	33.2	34.7	0.66
00:08:23	22.4	34.7	35.6	0.75
00:10:14	24.8	35.6	36.8	0.86
00:13:06	28.0	36.8	38.2	0.99
00:15:12	30.2	38.2	39.5	1.11
00:17:16	32.2	39.5	40.4	1.19
00:19:19	34.0	40.4	41.4	1.28
00:24:46	38.5	41.4	43.3	1.46
00:31:19	43.3	43.3	45.5	1.66
00:38:44		45.5	47.8	1.87
00:42:34		47.8	50.4	2.11
00:54:57		50.4	52.3	2.28
01:00:17		52.3	53.4	2.39
01:19:20		53.4	57.6	2.77
01:38:13		57.6	60.7	3.06
01:55:44		60.7	63.6	3.32
02:28:55		63.6	68.8	3.80
03:04:19		68.8	73.5	4.24
04:04:47		73.5	80.7	4.90
04:22:43		80.7	81.9	5.01
06:34:42		81.9	91.5	5.89
07:14:42		91.5	94.3	6.15
07:55:11		94.3	96.4	6.34
08:46:07		95.0	97.4	6.57
09:51:43	Time	97.4	99.3	6.74
19:07:05	(sec)	99.3	110.9	7.81
24:38:57	88737	110.9	116.5	8.32
27:43:06	99786	116.5	118.6	8.52
30:56:59	111419	118.6	120.7	8.17
35:23:58	127438	120.7	123.3	8.95
42:56:53	154613	123.3	127.8	9.37
45:47:05	164825	127.8	130.3	9.60
49:19:21	177561	130.3	132.1	9.76
52:18:20	188300	132.1	133.1	9.85
56:36:29	203789	133.1	135.5	10.07
66:56:19	140979	135.5	142.6	10.72
71:10:46	256246	142.6	145.1	10.95

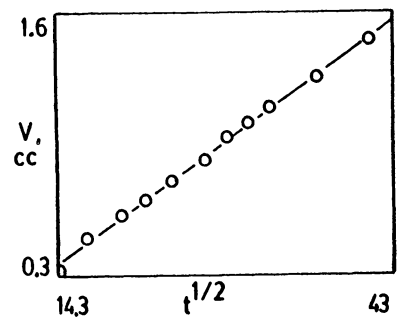

Open Tube Slope:
4.44e-2 cc/sec 1/2

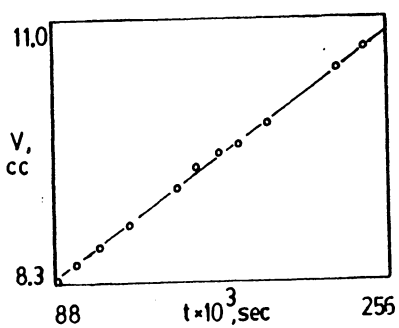

Capillary Disk Slope:
15.5e-6 cc/sec

mon:day:yr
06: 26: 84

Solute/Solvent: Ar/CCl4 Gas Pressure: 697.2 torr
Cell Temperature: 25.3 deg C

Time hr:mn:sc	Time (secl/2)	Volume Height	Gage (mm)	Volume (cc)
00:01:20	8.9	4.9	6.4	0.14
00:02:39	12.6	6.4	8.0	0.29
00:04:16	16.0	8.0	9.3	0.41
00:06:02	19.0	9.3	11.0	0.56
00:08:08	22.1	11.0	12.3	0.68
00:10:35	25.2	12.3	13.8	0.82
00:12:47	27.7	13.8	14.9	0.92
00:15:00	30.0	14.9	16.1	1.03
00:17:52	32.7	16.1	17.3	1.14
00:20:23	35.0	17.3	18.2	1.22
00:23:22	37.4	18.2	19.4	1.34
00:28:22	41.2	19.4	21.1	1.49
00:33:17		21.1	22.6	1.63
00:43:15		22.6	25.2	1.87
00:54:25		25.2	27.9	2.11
01:15:46		27.9	32.9	2.57
01:44:23		32.9	38.2	3.07
02:13:23		38.2	42.8	3.49
02:43:38		42.8	46.4	3.82
03 28:44		46.4	52.0	4.34
04:21:22		52.0	56.9	4.79
05:11:25		56.9	61.4	5.20
09:04:11		61.4	74.4	6.40
19:39:34		74.4	91.2	7.95
22:17:27	Time	91.2	94.1	8.21
24:21:20	(sec)	94.1	95.4	8.34
28:15:01	101701	95.4	96.4	8.43
31:44:03	114243	96.4	97.5	8.53
33:27:39	120459	97.5	99.5	8.71
35:29:55	127795	99.5	100.8	8.83
43:39:58	157198	100.8	106.0	9.31
44:41:54	160914	106.0	106.8	9.38
54:03:02	194582	106.8	111.9	9.85
57:34:31	207271	111.9	113.7	10.02

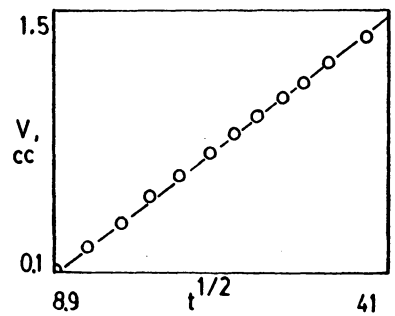

Open Tube Slope:
4.23e-2 cc/sec 1/2

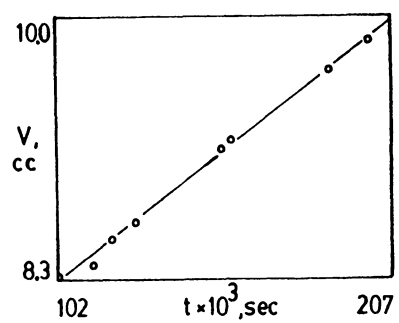

Capillary Disk Slope:
15.6e-6 cc/sec

mon:day:yr
06: 30: 84

Solute/Solvent: Ar/CCl4 Gas Pressure: 689.8 torr
Cell Temperature: 25.3 deg C

Time hr:mn:sc	Time (secl/2)	Volume Height	Gage (mm)	Volume (cc)
00:01:20	8.9	63.4	65.2	0.17
00:02:30	12.2	65.2	66.4	0.28
00:03:42	14.9	66.4	67.4	0.36
00:05:28	18.1	67.4	68.8	0.50
00:07:18	20.9	68.8	70.4	0.64
00:09:16	23.6	70.4	71.5	0.75
00:11:35	26.4	71.5	72.7	0.86
00:14:34	29.6	72.7	74.1	0.99
00:17:23	32.3	74.1	75.4	1.11
00:20:28	35.0	75.4	76.7	1.22
00:23:01	37.2	76.7	77.8	1.33
00:26:54	40.2	77.8	78.9	1.43
00:31:07	43.2	78.9	80.2	1.55
00:36:41		80.2	82.1	1.72
00:40:21		82.1	83.0	1.81
00:44:36		83.0	84.2	1.92
00:50:31		84.2	86.1	2.09
00:54:53		86.1	87.3	2.20
01:11:54		87.3	90.9	2.53
01:49:35		90.9	97.3	3.12
02:20:56		97.3	102.5	3.60
03:08:07		102.5	108.4	4.14
04:26:20		108.4	116.7	4.91
05:03:32		116.7	119.9	5.20
06:05:30		119.9	125.2	5.69
08:29:09	Time	125.2	132.3	6.34
12:41:07	(sec)	132.3	141.7	7.21
21:22:12	76932	141.7	151.7	8.31
24:49:26	89366	151.7	154.8	8.42
29:16:32	105392	154.8	157.4	8.66
33:19:25	119965	157.4	159.6	8.86
35:55:04	129304	159.6	161.4	9.03
44:39:10	160750	161.4	167.2	9.56
54:28:49	196129	167.2	173.1	10.10
59:08:06	212886	173.1	176.9	10.45
68:54:23	248063	176.9	182.1	10.93
72:26:34	260794	182.1	184.5	11.15
76:48:50	276530	184.5	185.7	11.26

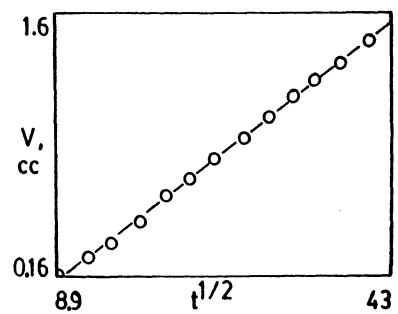

Open Tube Slope:
4.13e-2 cc/sec 1/2

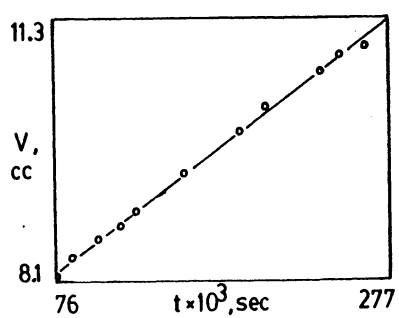

Capillary Disk Slope:
15.9e-6 cc/sec

mon:day:yr
09: 10: 85

Solute/Solvent: O2/CCl4 Gas Pressure: 588.8 torr
Cell Temperature: 26.6 deg C

Time hr:mn:sc	Time (sec1/2)	Volume Gage Height (mm)		Volume (cc)
00:01:30	9.4	261.1	263.3	0.20
00:02:46	12.9	263.3	264.5	0.31
00:04:25	16.3	264.5	265.9	0.44
00:06:30	19.7	265.9	267.6	0.60
00:08:19	22.3	267.6	268.6	0.70
00:10:38	25.2	268.6	269.8	0.80
00:12:38	27.5	269.8	270.9	0.90
00:15:08	30.1	270.9	271.8	0.99
00:18:19	33.2	271.8	272.8	1.08
00:21:43	36.1	272.8	274.1	1.20
00:26:07	39.6	274.1	275.5	1.33
00:31:01	43.1	275.5	277.1	1.47
00:36:36		277.1	278.6	1.61
00:40:34		278.6	279.7	1.71
00:48:17		279.7	281.2	1.85
01:04:19		281.2	284.5	2.15
02:09:59		284.5	294.4	3.07
04:19:20		303.2	309.8	4.48
05:31:04		309.8	318.0	5.24
06:02:28		318.0	321.7	5.58
08:36:04		321.7	333.1	6.63
14:42:36		333.1	346.5	7.86
16:31:18	Time	346.5	348.4	8.04
19:26:29	(sec)	348.4	350.8	8.26
21:24:18	77058	350.8	352.5	8.42
24:13:36	87216	352.5	355.6	8.70
29:06:15	104775	355.6	359.6	9.07
39:20:52	141652	358.4	365.5	9.72
46:09:07	166157	365.5	367.7	9.93
52:09:08	187748	367.7	369.7	10.11
54:50:38	197438	369.7	370.8	10.21
59:12:55	213175	370.8	373.7	10.48
64:17:31	231451	373.7	376.9	10.77
70:16:16	252976	376.9	379.8	11.04
74:43:20	269000	379.8	382.3	11.27

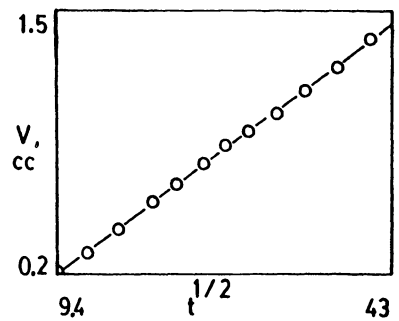

Open Tube Slope:
3.77e-2 cc/sec 1/2

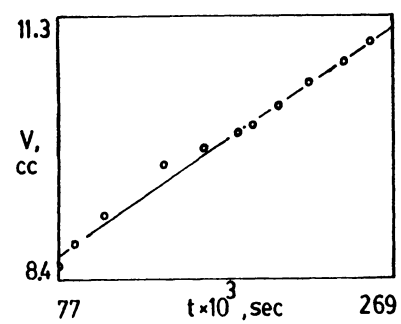

Capillary Disk Slope:
14.0e-6 cc/sec

mon:day:yr
11: 30: 84

Solute/Solvent: O2/CCl4 Gas Pressure: 706.7 torr
Cell Temperature: 25.2 deg C

Time hr:mn:sc	Time (secl/2)	Volume Gage Height (mm)		Volume (cc)
00:01:06	8.1	166.4	168.8	0.22
00:02:32	12.3	168.8	170.8	0.41
00:04:43	16.8	170.8	172.9	0.60
00:06:45	20.1	172.9	174.0	0.70
00:10:18	14.8	174.0	176.2	0.90
00:13:04	28.0	176.2	177.8	1.05
00:17:11	32.1	177.8	179.2	1.18
00:20:22	35.0	179.2	180.7	1.32
00:24:26	38.3	180.7	181.9	1.43
00:30:42	42.9	181.9	183.7	1.59
00:34:42	45.6	183.7	184.9	1.70
00:41:33	49.9	184.9	186.8	1.88
00:54:35		186.8	190.2	2.19
01:22:30		190.2	195.7	2.70
01:38:59		195.7	198.3	2.94
02:19:26		198.3	204.7	3.52
03:10:22		204.7	210.8	4.09
05:28:50		210.8	223.3	5.24
09:29:36		223.3	237.0	6.50
11:59:14	Time	237.0	242.1	6.97
21:43:29	(sec)	242.1	254.6	8.12
28:51:11	103871	254.6	257.6	8.40
34:30:24	124224	257.6	260.8	8.69
37:49:00	136140	260.8	263.2	8.91
46:11:48	166308	263.2	267.1	9.27
50:58:34	183514	267.1	268.5	9.40
54:36:56	196616	268.5	271.0	9.64
57:34:00	207240	271.0	273.5	9.86
62:15:08	224108	273.5	275.7	10.07
69:13:24	249204	275.7	279.8	10.44
75:27:00	271620	275.7	280.5	10.89

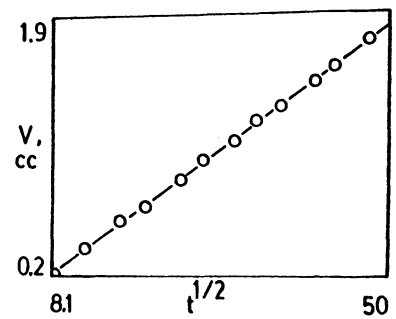

Open Tube Slope:
3.93e-2 cc/sec 1/2

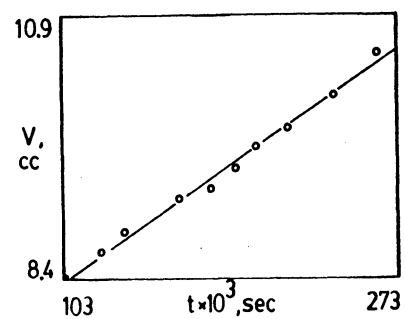

Capillary Disk Slope:
14.3e-6 cc/sec

mon:day:yr
12: 19: 84

Solute/Solvent: O2/CCl4 Gas Pressure: 756.4 torr
Cell Temperature: 25.8 deg C

Time hr:mn:sc	Time (secl/2)	Volume Gage Height (mm)	Volume (cc)
00:01:05	8.1	191.0 193.2	0.20
00:02:27	12.1	193.2 194.8	0.35
00:05:26	18.1	194.8 198.1	0.65
00:08:15	22.2	198.1 200.0	0.83
00:11:02	25.7	200.0 201.9	1.00
00:18:17	33.1	201.9 205.3	1.32
00:22:33	36.8	205.3 207.0	1.47
00:26:36	39.9	207.0 208.4	1.60
00:35:08	45.9	208.4 211.1	1.85
00:45:58		211.1 214.0	2.11
00:59:55		214.0 217.9	2.48
01:15:28		217.9 220.8	2.74
01:34:03		220.8 224.3	3.07
01:56:35		224.3 228.2	3.43
02:42:51		228.2 234.3	3.99
03:23:47		234.3 239.1	4.43
05:40:34		239.1 249.2	5.36
06:39:57		249.2 251.4	5.56
08:16:05		251.4 254.9	5.89
10:53:39	Time	254.9 257.9	6.16
12:09:30	(sec)	257.9 259.1	6.27
19:08:12	68892	259.1 264.5	6.77
22:56:14	82574	264.5 268.2	7.11
26:55:44	96944	268.2 272.2	7.48
43:06:41	155201	272.2 282.6	8.44
46:48:20	168500	282.6 286.5	8.80
50:59:05	183545	286.5 290.1	9.13
66:14:52	238492	290.1 298.5	9.90
73:02:54	262974	298.5 302.6	10.28

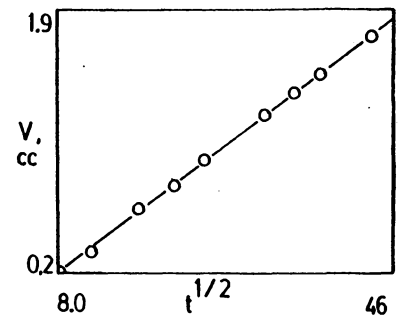

Open Tube Slope:
4.41e-2 cc/sec 1/2

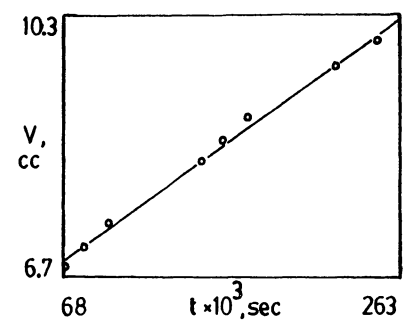

Capillary Disk Slope:
18.0e-6 cc/sec

mon:day:yr
01: 17: 84

Solute/Solvent: N2/C6H6 Gas Pressure: 796.3 torr
Cell Temperature: 25.3 deg C

Time hr:mn:sc	Time (secl/2)	Volume Gage Height (mm)		Volume (cc)
00:01:45	10.6	289.6	290.6	0.09
00:02:30	12.2	290.6	291.2	0.15
00:03:50	15.2	291.2	291.9	0.21
00:05:36	18.3	291.9	292.7	0.28
00:08:04	22.0	292.7	293.7	0.35
00:10:27	25.0	293.4	294.1	0.41
00:13:31	28.4	294.1	294.8	0.48
00:15:59	31.0	294.8	295.5	0.54
00:18:55	33.7	295.5	296.0	0.58
00:25:23	39.0	296.0	296.8	0.66
00:29:10	41.8	296.8	297.7	0.75
00:37:17		297.7	298.7	0.84
00:50:52		298.7	300.5	1.00
01:00:34		300.5	301.4	1.09
01:14:07		301.4	302.6	1.20
01:47:30		302.6	307.4	1.64
02:17:23		307.4	310.3	1.91
03:33:46		310.3	315.1	2.35
04:12:49		315.1	317.1	2.53
06:45:20	Time	317.1	322.6	3.04
09:35:41	(sec)	322.6	324.2	3.19
19:27:43	70063	324.2	329.1	3.64
25:29:08	91748	329.1	330.2	3.74
27:48:05	100085	330.2	331.3	3.84
31:46:11	114371	331.3	331.9	3.90
44:24:54	159894	331.9	336.7	4.34
50:12:33	180753	336.7	338.2	4.48
57:50:44	208244	338.2	339.9	4.63
67:13:27	242007	339.9	345.2	5.12
74:02:38	266558	345.2	346.2	5.21

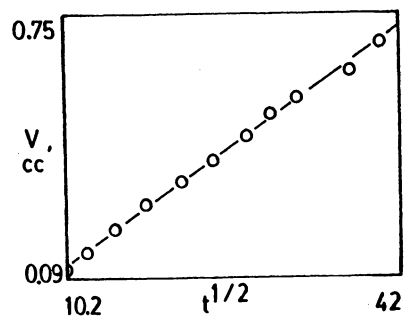

Open Tube Slope:
2.01e-2 cc/sec 1/2

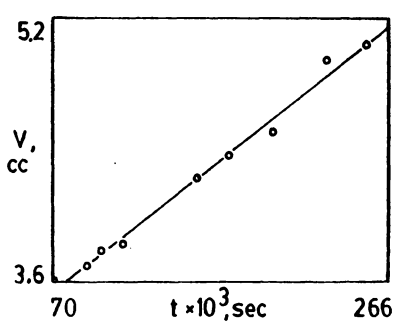

Capillary Disk Slope:
8.61e-6 cc/sec

mon:day:yr
05: 14: 84

Solute/Solvent: N2/C6H6 Gas Pressure: 642.5 torr
Cell Temperature: 25.2 deg C

Time hr:mn:sc	Time (secl/2)	Volume Gage Height (mm)	Volume (cc)
00:01:18		264.4 265.3	0.08
00:02:47	12.9	265.3 266.4	0.18
00:04:50	17.0	266.4 267.3	0.27
00:07:01	20.5	267.3 268.0	0.33
00:09:14	23.5	268.0 269.1	0.43
00:12:53	27.8	269.1 269.7	0.49
00:16:11	31.2	269.7 270.8	0.59
00:24:56	38.7	270.8 272.3	0.73
00:29:44	42.2	272.3 273.4	0.83
00:38:53		273.4 275.5	1.02
00:45:17		275.5 276.8	1.14
01:04:14		276.8 278.8	1.33
01:32:48		278.8 281.7	1.59
01:54:46		281.7 283.8	1.79
02:30:35		283.8 286.2	2.01
02:54:11		286.2 287.8	2.16
03:58:22		287.8 291.1	2.46
05:51:46		291.1 293.7	2.70
08:03:56	Time	293.7 293.9	2.72
16:32:10	(sec)	293.9 297.5	3.05
23:07:05	83225	297.5 299.4	3.22
29:22:10	105730	299.4 301.2	3.39
31:58:24	115104	301.2 302.8	3.54
40:32:35	145955	302.8 306.4	3.87
43:29:16	156556	306.4 307.2	3.94
50:17:12	181032	307.2 309.3	4.14
56:01:25	201685	309.3 311.4	4.33
64:21:34	231694	311.4 316.9	4.84
69:48:21	251301	316.9 318.4	4.97
73:27:20	264440	318.4 320.1	5.13

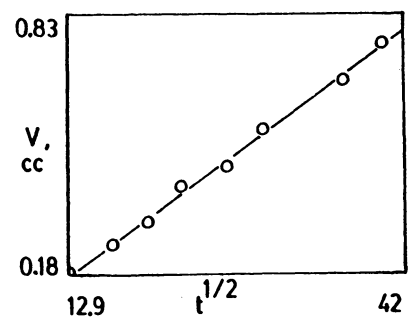

Open Tube Slope:
2.18e-2 cc/sec 1/2

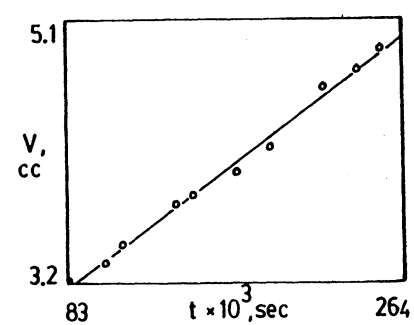

Capillary Disk Slope:
10.6e-6 cc/sec

mon:day:yr
05: 21: 84

Solute/Solvent: N2/C6H6 Gas Pressure: 781.4 torr
Cell Temperature: 25.2 deg C

Time hr:mn:sc	Time (sec1/2)	Volume Gage Height (mm)	Volume (cc)
00:01:36		247.9 249.3	0.13
00:02:59	13.3	249.3 250.2	0.21
00:05:30	18.2	250.2 251.1	0.29
00:07:37	21.4	251.1 252.1	0.39
00:10:54	25.6	252.1 253.2	0.49
00:14:16	29.2	253.2 254.0	0.56
00:19:52	34.5	254.0 255.1	0.66
00:23:22	37.4	255.1 255.8	0.73
00:28:30	41.4	255.8 256.6	0.80
00:33:47	45.0	256.6 257.2	0.86
00:37:56		257.2 257.8	0.91
00:45:39		257.8 258.8	1.00
00:55:00		258.8 260.0	1.11
01:05:47		260.0 261.3	1.23
01:15:25		261.3 262.2	1.32
02:06:46		262.2 266.2	1.69
03:06:28		266.2 269.8	2.01
03:33:23		269.8 270.9	2.12
06:27:00		270.9 277.5	2.73
08:24:31		277.5 278.2	2.79
10:48:14		278.2 279.5	2.91
16:40:37	Time	279.5 282.8	3.21
20:45:15	(sec)	282.8 285.0	3.41
23:43:45	85425	285.0 286.4	3.54
26:47:17	96437	286.4 286.8	3.58
30:25:33	109533	286.8 287.7	3.66
33:33:25	120805	287.7 288.6	3.74
40:45:48	146748	288.6 291.7	4.02
44:38:55	160735	291.7 293.1	4.15
52:06:26	187586	293.1 295.0	4.32
54:37:10	196630	295.0 296.5	4.45
59:38:37	214717	296.5 299.0	4.68
64:57:17	233837	299.0 301.6	4.91
68:57:28	248248	301.6 302.7	5.01
72:19:59	260399	302.7 304.6	5.18

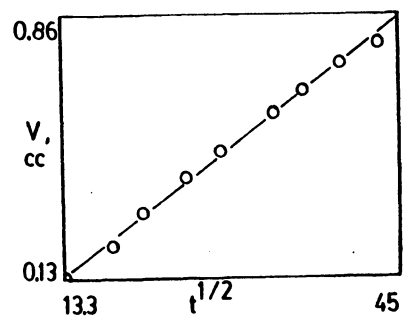

Open Tube Slope:
2.09e-2 cc/sec 1/2

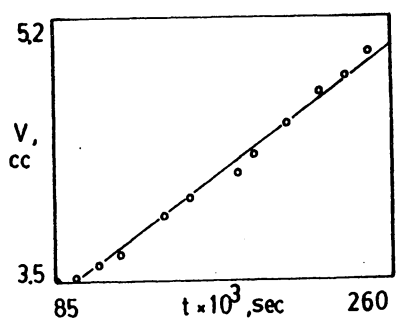

Capillary Disk Slope:
9.75e-6 cc/sec

mon:day:yr
06: 07: 84

Solute/Solvent: N2/C6H6 Gas Pressure: 661.7 torr
Cell Temperature: 25.2 deg C

Time hr:mn:sc	Time (sec1/2)	Volume Gage Height (mm)	Volume (cc)
00:01:46		215.3 216.8	0.14
00:02:49		216.8 217.8	0.23
00:04:39	16.7	217.8 219.0	0.34
00:08:17	22.3	219.0 220.3	0.46
00:12:08	27.0	220.3 221.4	0.56
00:17:04	32.0	221.4 222.5	0.66
00:21:01	35.5	222.5 223.4	0.75
00:25:57	39.4	223.4 223.9	0.79
00:30:36	42.8	223.9 224.8	0.87
00:36:36	46.9	224.8 225.7	0.96
00:42:07		225.7 226.3	1.01
00:52:11		226.3 227.6	1.13
01:06:41		227.6 228.9	1.25
01:50:05	Time	228.9 232.8	1.61
04:45:01	(sec)	232.8 241.9	2.45
07:29:17	26957	241.9 243.3	2.58
17:04:32	61472	243.3 247.9	3.00
21:03:18	75798	247.9 249.4	3.14
24:13:34	87214	249.4 249.7	3.17
28:10:25	101425	249.7 250.6	3.25
31:09:51	112191	250.6 252.2	3.40
35:47:56	128876	252.2 254.3	3.59
42:51:56	154316	254.3 257.2	3.86
48:34:44	174884	257.2 258.3	3.96
52:47:30	190050	258.3 259.4	4.06
60:32:44	217964	259.4 262.5	4.34
70:09:47	252587	262.5 265.3	4.60
76:28:58	275338	265.3 267.2	4.77
80:23:43	289423	267.2 268.4	4.88

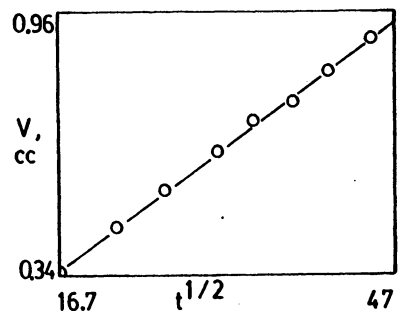

Open Tube Slope:
2.02e-2 cc/sec 1/2

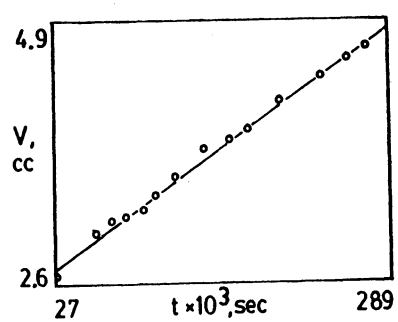

Capillary Disk Slope:
8.62e-6 cc/sec

mon:day:yr
06: 22: 84

Solute/Solvent: N2/C6H6 Gas Pressure: 662.7 torr
Cell Temperature: 25.2 deg C

Time hr:mn:sc	Time (secl/2)	Volume Gage Height (mm)	Volume (cc)
00:01:44	10.2	296.1 297.7	0.15
00:03:40	14.8	297.7 298.8	0.25
00:06:50	20.2	298.8 300.0	0.36
00:08:42	22.8	300.0 300.5	0.40
00:11:02	25.7	300.5 301.1	0.46
00:14:15	29.2	301.1 301.8	0.52
00:17:59	32.8	301.8 302.6	0.60
00:21:24	35.8	302.6 303.3	0.66
00:25:30	39.1	303.3 303.8	0.71
00:30:08	42.5	303.8 304.5	0.77
00:37:58		304.5 305.5	0.86
00:47:14		305.6 306.7	0.97
01:09:38		306.7 309.3	1.21
01:16:19		309.3 309.7	1.24
01:58:48		309.7 314.1	1.65
02:29:00		314.1 315.7	1.80
03:22:09		315.7 318.8	2.08
10:02:57	Time	318.8 323.6	2.52
18:27:45	(sec)	320.9 325.6	2.97
24:27:13	88033	325.6 326.5	3.05
27:47:30	100050	326.5 327.4	3.13
32:51:46	118306	327.4 329.2	3.29
42:36:18	153378	329.2 333.1	3.65
45:31:53	163913	333.1 333.9	3.72
50:38:58	182338	333.9 335.6	3.88
55:31:00	199860	335.6 338.0	4.10
59:49:34	215374	338.0 339.2	4.21
68:27:26	246446	339.2 341.3	4.40
74:12:33	267153	341.3 343.1	4.57

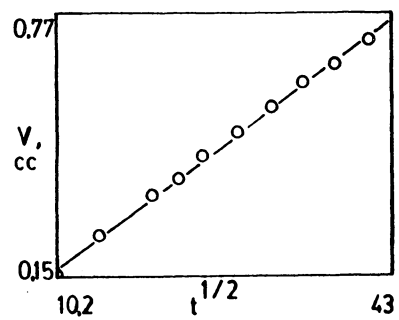

Open Tube Slope:
1.93e-2 cc/sec 1/2

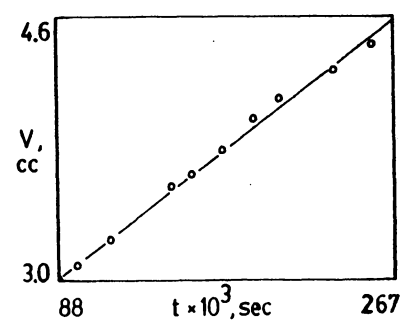

Capillary Disk Slope:
8.78e-6 cc/sec

mon:day:yr
08: 13: 85

Solute/Solvent: Ar/C6H6 Gas Pressure: 612.4 torr
Cell Temperature: 27.0 deg C

Time hr:mn:sc	Time (secl/2)	Volume Gage Height (mm)		Volume (cc)
00:01:30	9.5	277.2	279.4	0.20
00:02:24	12.0	279.4	280.4	0.29
00:03:18	14.1	280.4	281.7	0.41
00:04:32	16.5	281.7	282.5	0.48
00:05:28	18.0	282.5	283.6	0.59
00:06:45	20.1	283.6	284.6	0.68
00:08:13	22.2	284.6	285.7	0.78
00:10:02	24.5	285.7	286.7	0.87
00:13:39	28.6	286.7	288.2	1.01
00:15:49		288.2	289.5	1.13
00:18:32		289.5	290.9	1.26
00:22:17		290.9	293.0	1.46
00:25:21		293.0	294.8	1.62
00:31:08		294.8	298.6	1.97
00:34:38		298.6	299.6	2.06
00:51:43		299.6	306.9	2.74
01:24:46		306.9	317.3	3.69
02:06:17		317.3	325.2	4.42
02:40:11		325.2	329.6	4.83
04:01:52		329.6	335.5	5.37
05:29:56		335.5	338.9	5.68
07:33:27	Time	338.9	342.1	5.98
12:29:20	(sec)	342.1	351.8	6.87
14:47:28	53248	351.8	356.2	7.28
23:38:06	85086	356.2	370.6	8.60
25:34:01	92041	370.6	372.7	8.80
27:37:07	99427	372.7	374.3	8.94
32:50:11	118211	374.3	380.5	9.51
37:23:44	134624	380.5	387.8	10.18
39:04:30	140670	387.8	391.0	10.48
41:23:13	148993	391.0	394.4	10.79
42:27:48	152868	394.4	396.1	10.95
45:26:13	163573	396.1	401.1	11.41
46:05:00	165900	401.1	402.2	11.51

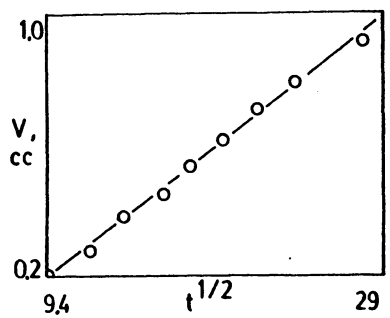

Open Tube Slope:
4.39e-2 cc/sec 1/2

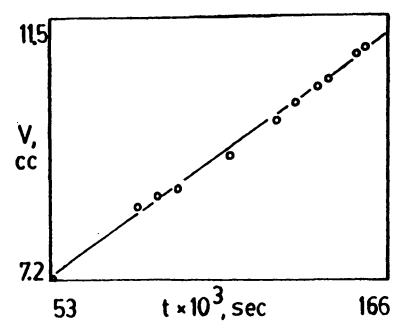

Capillary Disk Slope:
36.7e-6 cc/sec

mon:day: yr
08: 16: 85

Solute/Solvent: Ar/C6H6 Gas Pressure: 621.4 torr
Cell Temperature: 25.6 deg C

Time hr:mn:sc	Time (sec1/2)	Volume Gage Height (mm)		Volume (cc)
00:01:07	8.11	225.9	227.8	0.17
00:02:26	12.1	227.8	229.7	0.35
00:03:52	15.2	229.7	231.1	0.47
00:05:22	17.9	231.1	232.3	0.59
00:07:04	20.6	232.3	233.5	0.70
00:09:36	24.0	233.5	235.2	0.86
00:11:49	26.6	235.2	236.7	0.99
00:14:16	29.2	236.7	237.8	1.10
00:18:04		237.8	239.8	1.28
00:23:00		239.8	242.3	1.51
00:27:43		242.3	244.7	1.73
00:30:01		244.7	246.2	1.87
00:35:04		246.2	248.8	2.11
00:41:26		248.8	252.1	2.41
00:50:27		252.1	255.8	2.75
01:05:41		255.8	262.8	3.40
01:21:33		262.8	266.4	3.73
02:23:00	Time	266.4	278.4	4.84
03:25:34	(sec)	278.4	284.8	5.42
11:05:22	39922	284.8	297.8	6.62
13:21:41	48101	297.8	299.8	6.81
18:04:52	65092	299.8	303.3	7.13
20:40:01	74401	303.3	305.9	7.37
24:10:52	87052	305.9	309.2	7.67
26:07:36	94056	309.2	310.8	7.82
28:12:58	101578	310.8	312.7	7.99
29:54:55	107695	312.7	314.4	8.15
33:56:42	122202	314.4	319.2	8.59
37:28:37	134917	319.2	322.5	8.90
40:27:15	145635	322.5	325.1	9.14
42:16:37	152197	325.1	326.5	9.26
44:29:09	160149	326.5	328.0	9.40
46:45:48	168348	328.0	330.4	9.62
49:45:51	179151	330.4	334.1	9.97
52:01:08	187268	334.1	336.8	10.21
54:17:52	195472	336.8	339.4	10.45
59:29:40	214180	339.4	344.5	10.92
63:24:34	228274	344.5	346.4	11.09
65:45:46	236746	346.4	348.2	11.26
67:23:37	242617	348.2	349.5	11.38
69:41:27	250887	349.5	351.9	11.60
72:09:56	259796	351.9	355.8	11.96

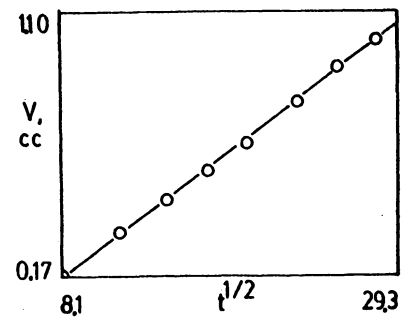

Open Tube Slope:
4.38e-2 cc/sec 1/2

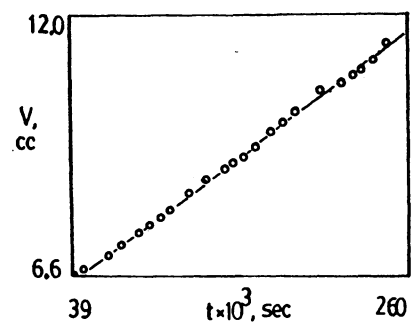

Capillary Disk Slope:
24.3e-6 cc/sec

mon:day:yr
08: 20: 85

Solute/Solvent: Ar/C6H6 Gas Pressure: 589.2 torr
Cell Temperature: 25.6 deg C

Time hr:mn:sc	Time (secl/2)	Volume Gage Height (mm)		Volume (cc)
00:01:18	8.8	251.8	253.9	0.19
00:02:21	11.9	253.9	255.5	0.34
00:03:32	14.6	255.5	256.7	0.45
00:05:08	17.5	256.7	258.1	0.58
00:07:02	20.5	258.1	259.5	0.71
00:09:38	24.0	259.5	260.9	0.84
00:11:21	26.1	260.9	261.9	0.93
00:14:02	29.0	261.9	263.0	1.03
00:17:21		263.0	264.2	1.14
00:20:20		264.2	265.2	1.23
00:25:37		265.2	266.7	1.37
00:30:26		266.7	267.6	1.46
00:45:26		267.6	269.8	1.66
01:00:02		269.8	271.3	1.80
01:29:25		271.3	272.8	1.93
02:03:33		272.8	273.4	1.99
02:52:29		273.4	276.2	2.25
04:48:06	Time	276.2	278.7	2.48
06:24:54	(sec)	278.7	280.2	2.62
11:46:27	42387	280.2	286.5	3.20
14:56:47	53807	286.5	288.8	3.41
17:04:14	61454	288.8	289.5	3.47
19:02:03	68523	289.5	290.5	3.56
21:44:49	78289	290.5	292.1	3.71
25:36:01	92161	292.1	296.4	4.10
28:34:29	102869	296.4	300.0	4.44
29:47:01	107221	300.0	301.2	4.55
30:20:39	109239	301.2	302.1	4.63
37:26:34	134794	302.1	309.2	5.29
40:37:04	146224	309.2	311.5	5.50
42:13:57	152037	311.5	312.8	5.61
45:11:46	162706	312.8	314.4	5.77
47:54:31	172471	314.4	317.2	6.02
52:24:07	188647	317.2	323.2	6.58
54:05:59	194759	323.2	325.0	6.74
61:00:30	219630	325.0	331.7	7.36
65:29:08	235748	331.7	334.5	7.62
68:02:19	244939	334.5	335.4	7.70
72:12:37	259957	335.4	338.2	7.96

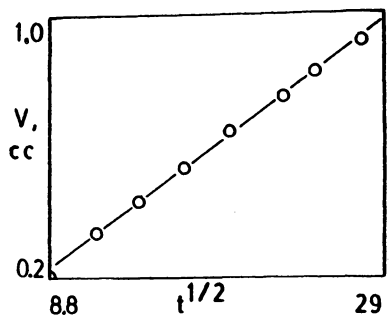

Open Tube Slope:
4.14e-2 cc/sec 1/2

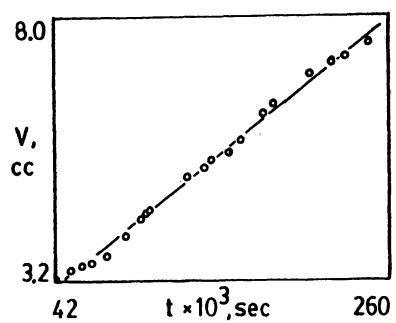

Capillary Disk Slope:
23.4e-6 cc/sec

mon:day:yr
08: 24: 85

Solute/Solvent: Ar/C6H6 Gas Pressure: 630.7 torr
Cell Temperature: 25.5 deg C

Time hr:mn:sc	Time (secl/2)	Volume Gage Height (mm)	Volume (cc)
00:01:05		265.7 267.9	0.20
00:02:43		267.9 269.4	0.34
00:04:48		269.4 270.8	0.47
00:07:41		270.8 271.9	0.57
00:10:08		271.9 272.6	0.63
00:15:54		272.6 273.7	0.74
00:23:06		273.7 274.4	0.80
00:31:54		274.4 275.5	0.90
00:41:14		275.5 275.8	0.93
01:21:10		275.8 278.5	1.18
02:02:02		278.5 279.4	1.26
03:10:00		279.4 281.2	1.43
04:18:25	Time	281.2 282.4	1.54
07:16:30	(sec)	282.4 286.2	1.89
09:07:38	32858	286.2 287.8	2.04
15:41:53	56513	287.8 295.2	2.72
17:11:21	61881	295.2 296.7	2.86
21:40:51	78411	296.7 301.0	3.25
24:17:05	87425	301.0 303.4	3.47
27:24:16	98656	303.4 305.6	3.67
29:23:22	105802	305.6 308.2	3.91
35:52:20	129140	308.2 315.1	4.55
41:12:31	148351	315.1 320.6	5.06
43:15:27	155727	320.6 322.0	5.18
45:35:02	164102	322.0 323.9	5.36
47:41:19	171679	323.9 325.5	5.51
49:41:09	178869	325.5 327.5	5.69
52:42:02	189722	327.5 331.6	6.07
54:58:37	197917	331.6 334.1	6.20
57:33:21	207201	334.1 336.4	6.51
58:46:37	211597	336.4 337.2	6.58
65:28:08	235688	337.2 343.4	7.15
69:07:17	248837	343.4 345.4	7.34
72:04:23	259463	345.4 347.3	7.52

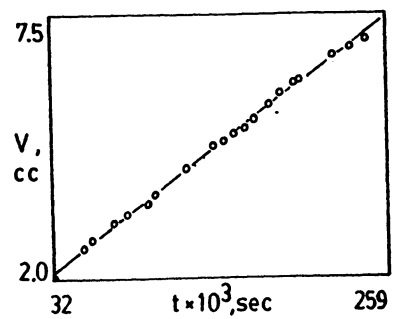

Capillary Disk Slope:
24.6e-6 cc/sec

mon:day:yr
09: 08: 85

Solute/Solvent: Ar/C6H6 Gas Pressure: 609.7 torr
Cell Temperature: 25.2 deg C

Time hr:mn:sc	Time (secl/2)	Volume Gage Height (mm)		Volume (cc)
00:01:27	9.3	236.1	238.9	0.26
00:02:59	13.4	238.9	240.7	0.42
00:05:08	17.5	240.7	242.6	0.60
00:07:42	21.5	242.6	244.6	0.78
00:10:13	24.8	244.6	246.4	0.95
00:14:17		246.4	250.0	1.28
00:18:44		250.0	253.7	1.62
00:21:30		253.7	255.9	1.82
00:26:56		255.9	259.5	2.15
00:30:49		259.5	261.8	2.37
00:35:19		261.8	264.3	2.60
00:40:25		264.3	266.8	2.82
00:45:14		266.8	269.2	3.05
00:50:21		269.2	271.2	3.23
00:59:12		271.2	274.6	3.54
01:28:36		274.6	282.5	4.27
02:00:03		282.5	288.2	4.80
02:25:32		288.2	290.8	5.04
03:49:13		290.8	297.8	5.68
04:58:32		297.8	301.0	5.98
06:32:13		301.0	304.9	6.34
08:16:14		304.9	308.3	6.65
09:01:55	Time	308.3	309.6	6.77
16:43:48	(sec)	309.6	320.5	7.77
18:47:13	67633	320.5	322.7	7.98
26:24:29	95069	322.7	330.9	8.73
28:20:36	102036	330.9	333.7	8.99
30:19:27	109167	333.7	336.4	9.24
32:24:35	116675	336.4	339.8	9.55
33:53:01	121981	339.8	341.4	9.70
40:30:58	145858	341.4	348.6	10.36
42:38:47	153527	348.6	350.6	10.54
46:18:22	166702	350.6	352.9	10.75
48:29:34	174574	352.9	354.9	10.94
50:02:41	180161	354.9	355.8	11.02
52:03:04	187384	355.8	357.9	11.22
54:32:24	196344	357.9	360.7	11.47
56:37:45	203865	360.7	364.3	11.80
57:41:25	207685	364.3	366.8	12.03
58:48:54	211734	366.8	369.4	12.27
65:21:48	235308	369.4	375.2	12.81
67:41:34	243694	375.2	376.8	12.95
71:57:49	259069	376.8	377.3	13.00

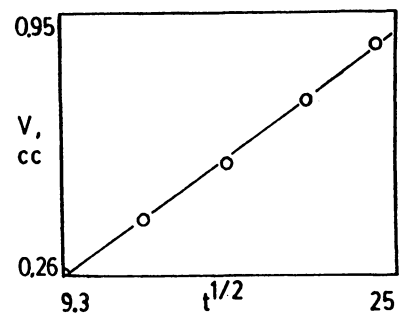

Open Tube Slope:
4.46e-2 cc/sec 1/2

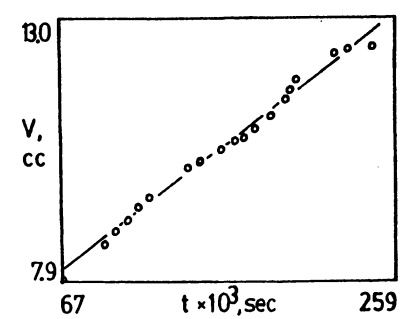

Capillary Disk Slope:
27.3e-6 cc/sec

mon:day:yr
07: 16: 85

Solute/Solvent: O2/C6H6 Gas Pressure: 563.8 torr
Cell Temperature: 25.2 deg C

Time hr:mn:sc	Time (secl/2)	Volume Gage Height (mm)	Volume (cc)
00:01:36	9.8	193.8 195.8	0.18
00:02:40	12.6	195.8 197.1	0.30
00:04:49	17.0	197.1 199.1	0.49
00:09:25	23.8	199.1 201.3	0.69
00:11:21	26.0	201.3 202.2	0.77
00:13:53	28.9	202.2 203.4	0.88
00:17:49	32.7	203.4 204.7	1.00
00:21:12	35.7	204.7 205.9	1.11
00:25:05	38.7	205.9 206.8	1.20
00:31:28	43.5	206.8 208.7	1.37
00:37:34		208.7 210.0	1.49
00:42:51		210.0 211.2	1.60
00:49:17		211.2 212.4	1.71
00:53:59		212.4 213.4	1.81
00:59:04		213.4 214.4	1,90
01:07:12		214.4 215.7	2.02
01:15:21		215.7 216.8	2.12
02:25:34		216.8 218.3	2.26
02:31:36		218.3 225.4	2.91
03:02:19		225.4 228.1	3.16
03:40:37		228.1 230.7	3.40
04:37:38		230.7 232.9	3.60
06:39:26		232.9 236.2	3.91
07:43:20		236.2 239.6	4.22
09:38:39		239.6 245.4	4.75
17:27:52	Time	245.4 251.9	5.35
22:24:32	(sec)	251.9 253.0	5.45
24:47:25	89245	253.0 253.5	5.50
29:29:19	106159	253.5 255.8	5.71
34:25:36	123936	255.8 259.4	6.04
42:36:58	153418	259.4 266.7	6.71
46:37:17	167837	266.7 267.7	6.81
50:14:42	180882	267.7 268.3	6.86
59:27:48	214068	268.3 273.5	7.34
66:50:09	240609	273.5 279.5	7.89
72:29:41	260981	279.5 279.9	7.93

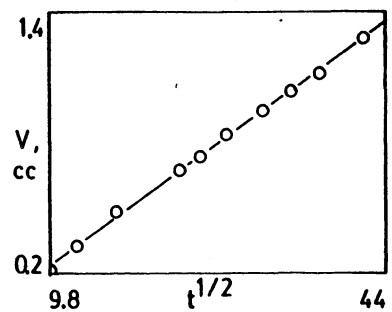

Open Tube Slope:
3.47e-2 cc/sec 1/2

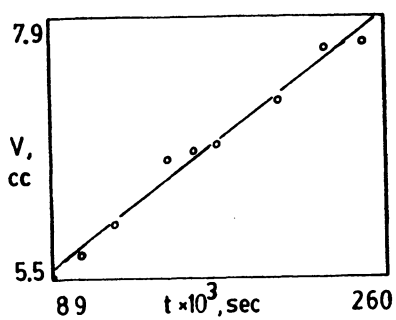

Capillary Disk Slope:
14.70e-6 cc/sec

mon:day:yr
07: 23: 85

Solute/Solvent: O2/C6H6 Gas Pressure: 611.6 torr
Cell Temperature: 25.2 deg C

Time hr:mn:sc	Time (secl/2)	Volume Gage Height (mm)		Volume (cc)
00:01:17		157.5	158.8	0.12
00:03:00		158.8	160.7	0.29
00:05:10	17.6	160.7	162.9	0.50
00:07:56	21.8	162.9	164.3	0.63
00:12:17	27.1	164.3	166.3	0.81
00:16:08	31.1	166.3	167.5	0.92
00:18:15	33.1	167.5	168.6	1.02
00:23:46	37.8	168.6	170.1	1.16
00:27:14	40.4	170.1	171.2	1.26
00:34:00	45.2	171.2	172.9	1.42
00:41:59	50.1	172.9	174.8	1.59
00:50:04	54.8	174.8	176.4	1.74
01:30:39		176.4	182.7	2.32
02:02:41		182.7	187.0	2.72
02:50:57		187.0	192.3	3.21
03:14:37		192.3	194.6	3.42
04:00:10		194.6	198.5	3.78
04:45:04	Time	198.5	201.7	4.07
05:28:54	(sec)	201.7	204.7	4.35
10:24:44	37484	204.7	225.6	6.27
18:49:12	67752	225.6	231.8	6.84
23:58:08	86288	231.8	233.7	7.02
30:10:39	108639	233.7	236.3	7.26
33:54:49	122089	236.3	239.1	7.52
43:01:37	154897	239.1	244.6	8.02
49:12:42	177162	244.6	248.4	8.37
52:24:55	188695	248.4	249.7	8.49
58:26:08	210368	249.7	253.7	8.86
61:36:42	221802	253.7	255.7	9.04
72:48:37	262117	255.7	261.9	9.62
76:22:37	274957	261.9	263.5	9.72

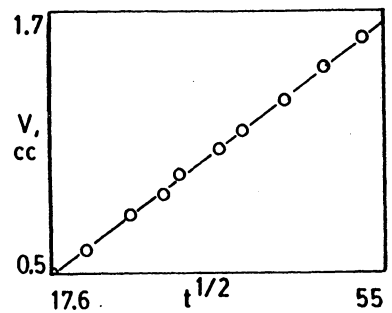

Open Tube Slope:
3.37e-2 cc/sec 1/2

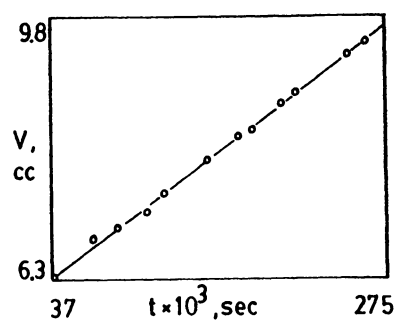

Capillary Disk Slope:
14.71e-6 cc/sec

mon:day:yr
07: 29: 85

Solute/Solvent: O2/C6H6 Gas Pressure: 601.7 torr
Cell Temperature: 25.0 deg C

Time hr:mn:sc	Time (sec1/2)	Volume Gage Height (mm)		Volume (cc)
00:01:01	7.8	224.5	225.6	0.10
00:03:23	14.2	225.6	228.4	0.36
00:05:21	17.9	228.4	229.6	0.47
00:07:41	21.5	229.6	231.2	0.62
00:10:02	24.5	231.2	232.2	0.71
00:14:03	29.0	232.2	234.1	0.88
00:18:07	33.0	234.1	235.6	1.02
00:20:31	35.1	235.6	236.7	1.12
00:23:54	37.9	236.7	237.9	1.23
00:29:56	42.4	237.9	239.4	1.37
00:33:38	44.9	239.4	240.2	1.44
00:38:56		240.2	241.5	1.57
00:49:15		241.5	243.9	1.79
01:04:11		243.9	246.6	2.04
01:19:37		246.6	248.8	2.24
02:00:04		248.8	254.6	2.77
03:36:25		254.6	263.2	3.56
04:05:39		263.2	265.0	3.73
04:53:32	Time	265.0	267.2	3.93
06:20:27	(sec)	267.2	270.3	4.22
12:59:52	46792	270.3	278.5	4.97
21:11:10	76270	278.5	285.2	5.59
26:35:11	95711	285.2	286.5	5.71
28:13:19	101599	286.5	286.7	5.73
30:43:16	110596	286.7	288.2	5.87
34:29:51	124191	288.2	291.7	6.19
38:26:04	138364	291.7	294.1	6.41
45:32:46	163966	294.1	298.6	6.82
50:42:18	182538	298.6	301.2	7.06
54:35:31	196531	301.2	301.7	7.11
58:09:36	209376	301.7	306.2	7.52
62:20:00	224400	306.2	309.1	7.79
69:20:42	249642	309.1	313.2	8.17
74:56:38	269798	313.2	315.7	8.40

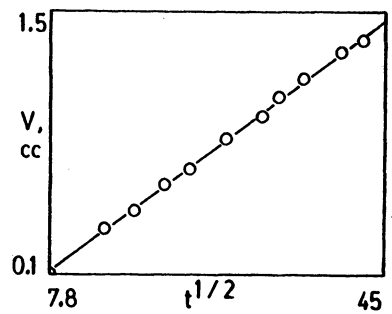

Open Tube Slope:
3.66e-2 cc/sec 1/2

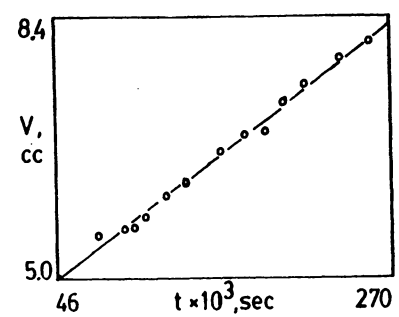

Capillary Disk Slope:
15.47e-6 cc/sec

mon:day:yr
08: 02: 85

Solute/Solvent: O2/C6H6 Gas Pressure: 606.5 torr
Cell Temperature: 25.2 deg C

Time hr:mn:sc	Time (secl/2)	Volume Gage Height (mm)		Volume (cc)
00:01:12	8.4	204.3	207.5	0.29
00:03:37	14.7	207.5	210.4	0.56
00:06:06	19.1	210.4	212.2	0.73
00:08:58	23.2	212.2	214.0	0.89
00:11:38	26.4	214.0	215.4	1.02
00:15:13	30.2	215.4	216.7	1.14
00:21:29	35.9	216.7	218.7	1.33
00:26:28	39.8	218.7	220.1	1.45
00:31:54	43.7	220.1	221.6	1.59
00:38:54		221.6	223.3	1.75
00:56:20		223.3	227.2	2.11
01:33:48		227.2	233.4	2.68
02:06:33		233.4	237.9	3.09
02:34:21	Time	237.9	241.3	3.41
03:04:35	(sec)	241.3	244.2	3.67
10:34:59	38099	244.2	266.1	5.69
16:46:48	60408	266.1	267.6	5.83
25:10:28	90628	267.6	273.6	6.38
35:44:41	128681	273.6	279.4	6.92
43:25:10	156310	279.4	283.3	7.28
47:45:36	171936	283.3	286.6	7.58
54:55:15	197715	286.6	292.8	8.15
61:22:44	220964	292.8	294.1	8.27
67:05:27	241527	294.1	296.9	8.53
70:13:57	252537	296.9	299.2	8.74
71:25:29	257129	299.2	300.0	8.81
84:40:18	304818	300.0	308.3	9.58

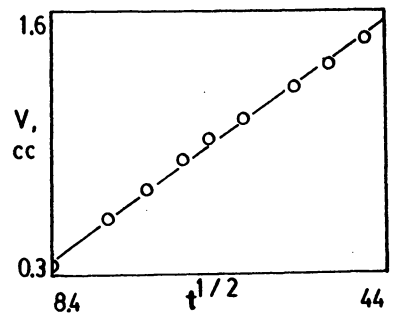

Open Tube Slope:
3.63e-2 cc/sec 1/2

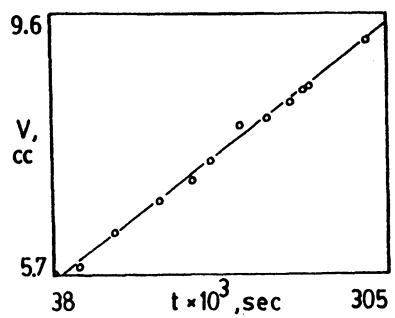

Capillary Disk Slope:
14.76e-6 cc/sec

mon:day:yr
01: 10: 85

Solute/Solvent: O2/H2O Gas Pressure: 624.1 torr
Cell Temperature: 25.6 deg C

Time hr:mn:sc	Time (sec1/2)	Volume Gage Height (mm)		Volume (cc)	
00:02:21		279.2	284.2	0.07	
00:05:33	18.2	284.2	284.9	0.08	
00:09:07	23.4	284.9	285.9	0.10	
00:14:33	29.5	285.9	287.8	0.13	
00:19:18	34.0	287.8	288.8	0.14	
00:25:09	38.8	288.8	290.2	0.16	
00:30:19	42.6	290.2	291.1	0.18	
00:36:23	46.7	291.1	292.0	0.19	
00:42:37		292.0	294.0	0.22	
00:49:49		294.0	294.9	0.23	
00:59:44		294.9	296.1	0.25	
01:09:20		296.1	298.4	0.28	
01:23:00		298.4	300.5	0.32	
01:44:09		300.5	303.9	0.36	
02:25:29		303.9	309.5	0.45	
03:12:48		309.5	314.6	0.52	
04:33:25	Time	314.6	320.4	0.61	
05:25:25	(sec)	320.4	322.6	0.64	
10:38:07	38287	322.6	340.6	0.91	Temperature
19:24:52	69892	340.6	358.6	1.18	Variation
21:51:50	78710	358.6	352.9	1.09	(deg C)
25:00:38	90038	352.9	352.3	1.08	-1.6
29:07:33	104833	352.3	348.7	1.03	-0.6
34:39:34	124774	348.7	354.3	1.11	-0.1
35:56:52	129412	354.3	355.5	1.13	-0.6
52:47:00	190020	355.5	362.2	1.23	-1.6
55:23:31	199411	362.2	368.8	1.33	-1.8
58:54:58	212098	368.8	365.4	1.28	-1.0
64:20:34	231634	365.4	359.6	1.19	+1.4
68:21:40	246100	359.6	360.1	1.20	+1.4
71:31:13	257833	360.1	358.0	1.17	+2.4
79:25:52	285952	358.0	361.9	1.22	+1.7
85:40:04	308404	361.9	359.9	1.19	+2.4

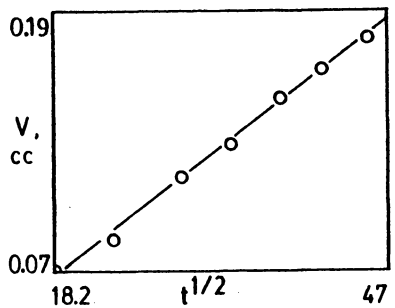

Open Tube Slope:
0.378e-2 cc/sec 1/2

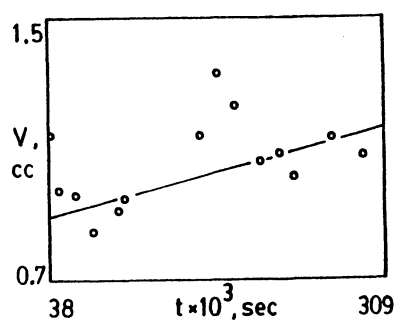

Capillary Disk Slope:
0.082e-6 cc/sec

mon:day: yr
02: 13: 85

Solute/Solvent: N2/CCl4 Gas Pressure: 666.3 torr
Cell Temperature: 0.0 deg C

Time hr:mn:sc	Time (sec1/2)	Oven QDT Count	Syringe QDT Count	Hood QDT Count	Volume (cc)
00:00:28		10348	3388	3154	0.06
00:00:36		10241	3389	3214	0.14
00:00:43	6.6	10241	3389	3214	0.18
00:01:23	9.1	10339	3389	3274	0.28
00:02:13	11.5	10323	3388	3293	0.31
00:05:19	17.9	10300	3389	3319	0.37
00:07:47	21.6	10277	3387	3326	0.43
00:09:08	23.4	10339	3389	3334	0.50
00:14:02	29.0	10330	3383	3342	0.56
00:14:10	29.2	10330	3383	3342	0.62
00:21:05	35.6	10368	3382	3349	0.68
00:21:12	35.7	10368	3382	3349	0.74
00:21:20	35.8	9996	3382	3343	0.81
00:33:33	44.9	10308	3388	3359	0.87
00:33:43	45.0	10308	3388	3359	0.93
00:41:38	50.0	10299	3388	3364	0.99
00:52:08	55.9	10347	3384	3362	1.05
00:52:15		10008	3382	3354	1.12
01:36:07		10351	3375	3353	1.18
01:36:15		10005	3374	3347	1.24
01:56:10		10282	3371	3350	1.30
02:24:22		10286	3372	3351	1.36
04:21:42		10299	3385	3362	1.43
05:38:25		10281	3385	3365	1.49
13:52:05	Time	10342	3452	3430	1.55
13:52:13	(sec)	10342	3452	3430	1.61
27:12:27	97947	10356	3376	3355	1.67
27:13:11	97991	10362	3378	3362	1.74
32:06:38	115598	10362	3397	3381	1.80
32:06:45	115605	10104	3399	3381	1.86
32:42:13	117733	10164	3397	3372	1.80
32:43:27	117807	10154	3398	3371	1.74
32:43:35	117815	10261	3399	3370	1.67
45:35:55	164155	10349	3379	3376	1.74
45:36:03	164163	10003	3377	3359	1.80
45:44:42	164682	10294	3381	3364	1.86
45:44:53	164693	10323	3381	3370	1.92
46:04:18	165858	10299	3385	3370	1.98
48:27:46	174466	10122	3380	3353	2.05
53:14:06	191646	10304	3379	3360	2.11
67:32:01	243121	10145	3353	3323	2.70
67:36:27	243387	10322	3365	3342	2.23
67:50:55	244255	10404	3367	3349	2.29
67:51:03	244263	9988	3367	3349	2.36

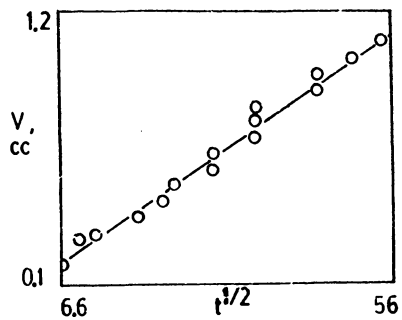

Open Tube Slope:
1.83e-2 cc/sec 1/2

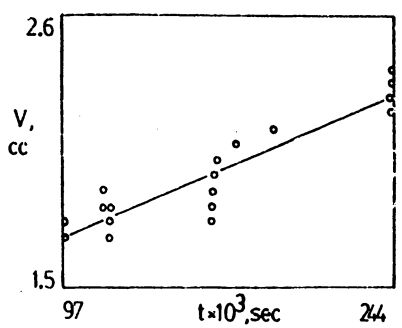

Capillary Disk Slope:
3.88e-6 cc/sec

mon:day:yr
02: 18: 85

Solute/Solvent: N2/CCl4 Gas Pressure: 673.5 torr Cell Temperature: 0.0 deg C

Time hr:mn:sc	Time (secl/2)	Oven QDT Count	Syringe QDT Count	Hood QDT Count	Volume (cc)
00:00:39		10258	3295	3226	0.06
00:00:48		10287	3294	3234	0.14
00:00:55		10287	3294	3234	0.19
00:01:03		10228	3294	3238	0.25
00:01:53		10270	3293	3246	0.31
00:02:24		10305	3293	3248	0.37
00:03:18		10263	3292	3251	0.43
00:03:54		10311	3293	3253	0.50
00:06:45		10156	3290	3251	0.56
00:09:06	23.4	10329	3291	3256	0.62
00:14:07	29.1	10298	3288	3254	0.68
00:15:48	30.8	10289	3288	3257	0.74
00:18:49	33.6	10299	3284	3259	0.81
00:27:58	41.0	10310	3281	3257	0.93
00:34:53	45.7	10310	3286	3257	0.99
00:36:23	46.7	10273	3285	3262	1.05
00:45:19	52.1	10253	3290	3270	1.12
00:49:38		10291	3294	3271	1.18
01:06:23		10297	3279	3263	1.24
01:30:37		10292	3275	3253	1.30
03:23:38		10323	3273	3254	1.36
11:21:11		10299	3268	3252	1.46
11:22:55	Time	10305	3269	3257	1.49
13:58:13	(sec)	10316	3274	3261	1.55
19:30:06	70206	10286	3257	3249	1.61
29:02:42	104562	10302	3259	3234	1.67
30:14:12	108852	10312	3259	3238	1.74
32:51:04	118264	10265	3268	3250	1.80
36:32:54	131574	10288	3282	3262	1.86
44:03:28	158608	10311	3264	3241	1.92
46:51:11	168671	10318	3266	3247	1.98
47:01:08	169268	10320	3266	3247	2.05
47:34:51	171291	10288	3261	3249	2.11
54:42:49	196969	10278	3258	3241	2.17
54:57:23	197843	10299	3267	3251	2.23
70:41:12	254472	10270	3212	3184	2.29

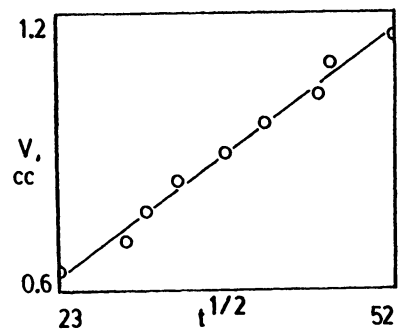

Open Tube Slope:
1.78e-2 cc/sec 1/2

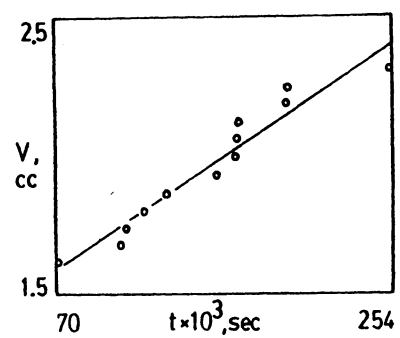

Capillary Disk Slope:
4.30e-6 cc/sec

mon:day:yr
02: 26: 85

Solute/Solvent: N2/CCl4 Gas Pressure: 650.3 torr Cell Temperature: 0.0 deg C

Time hr:mn:sc	Time (sec1/2)	Oven QDT Count	Syringe QDT Count	Hood QDT Count	Volume (cc)
00:00:07		10289	3346	3086	0.06
00:00:21		10289	3346	3086	0.12
00:00:29		10289	3346	3086	0.19
00:01:06		10462	3348	3240	0.25
00:02:06	11.2	10305	3370	3315	0.31
00:04:38	16.7	10323	3412	3356	0.37
00:06:34	19.8	10409	3421	3380	0.43
00:08:19	22.3	10380	3427	3394	0.50
00:09:25	23.8	10405	3431	3405	0.56
00:12:39	27.5	10395	3439	3426	0.62
00:15:40	30.6	10388	3452	3444	0.68
00:20:41	35.2	10368	3459	3469	0.74
00:26:56	40.2	10378	3470	3489	0.81
00:44:49		10367	3498	3525	0.87
01:14:06		10361	3520	3555	0.93
01:51:54		10335	3511	3569	0.99
03:41:49		10387	3518	3572	1.05
03:59:11		10381	3524	3578	1.12
07:54:44	Time	10396	3545	3593	1.18
11:27:26	(sec)	10423	3549	3549	1.24
13:28:12	48492	10400	3546	3602	1.30
27:30:35	99035	10290	3428	3386	1.36
27:53:40	100420	10271	3426	3391	1.43
27:59:25	100765	10308	3432	3432	1.49
29:52:57	107577	10318	3426	3396	1.55
32:36:53	117413	10340	3427	3386	1.61
32:37:01	117421	9992	3428	3387	1.67
47:15:17	170117	10303	3422	3366	1.74
47:15:25	170125	10303	3422	3366	1.80
51:14:35	184475	10308	3425	3367	1.86
51:14:44	184484	10308	3425	3367	1.92
55:07:24	198444	10271	3420	3369	1.98
59:05:05	212705	10263	3417	3370	2.05
59:05:23	212723	10289	3419	3369	2.11
61:55:48	266148	10296	3409	3351	2.17
61:56:00	266160	10125	3410	3353	2.23

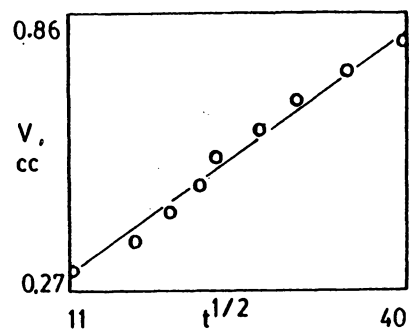

Open Tube Slope:
1.84e-2 cc/sec 1/2

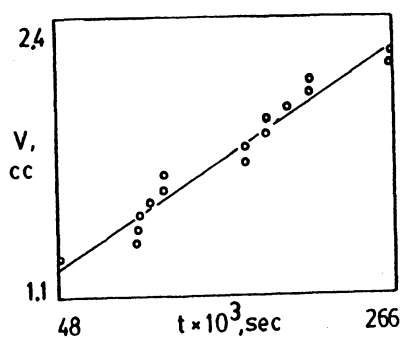

Capillary Disk Slope:
4.28e-6 cc/sec

mon:day:yr
01: 16: 85

Solute/Solvent: N2/CCl4 Gas Pressure: 665.0 torr Cell Temperature: 10.0 deg C

Time hr:mn:sc	Time (sec1/2)	Oven QDT Count	Syringe QDT Count	Hood QDT Count	Volume (cc)
00:00:32	5.6	7293	3450	3212	0.06
00:00:55	7.4	7373	3452	3218	0.12
00:01:19	8.9	7410	3456	3242	0.19
00:01:26	9.3	7410	3456	3242	0.24
00:03:53	15.3	7396	3456	3344	0.31
00:06:05	19.1	7390	3458	3349	0.37
00:08:22	22.4	7343	3454	3338	0.43
00:09:10	23.4	7377	3452	3350	0.50
00:11:38	26.4	7382	3456	3352	0.56
00:14:37	29.6	7375	3461	3350	0.62
00:18:36	33.4	7368	3458	3347	0.68
00:24:04		7369	3457	3339	0.74
00:44:53		7338	3454	3305	0.81
00:50:33		7456	3455	3310	0.87
01:06:04		7349	3453	3301	0.93
03:19:05		7383	3416	3276	0.99
03:24:38		7347	3410	3267	1.05
11:42:23		7349	3420	3284	1.12
11:46:55		7389	3429	3287	1.18
11:56:54	Time	7390	3432	3291	1.24
24:12:23	(sec)	7392	3381	3259	1.30
28:33:07	102787	7372	3415	3269	1.36
31:23:06	112986	7354	3426	3273	1.42
36:54:20	132860	7364	3443	3297	1.49
42:47:05	154025	7389	3405	3268	1.55
42:57:34	154654	7365	3407	3268	1.61
52:14:05	188045	7363	3414	3265	1.67
52:21:51	188511	7367	3419	3269	1.73
53:04:35	191075	7356	3406	3265	1.80
54:20:22	195622	7358	3423	3275	1.86
61:06:34	219994	7379	3418	3286	1.92
61:20:21	220821	7400	3424	3288	1.98
61:26:21	221181	7394	3427	3291	2.05
61:43:06	222186	7354	3429	3297	2.11
68:41:06	247266	7365	3419	3279	2.17
77:11:23	277883	7363	3402	3271	2.23
77:12:39	277959	7354	3410	3282	2.29
77:25:36	278736	7372	3428	3290	2.35
78:53:06	283986	7394	3412	3291	2.42

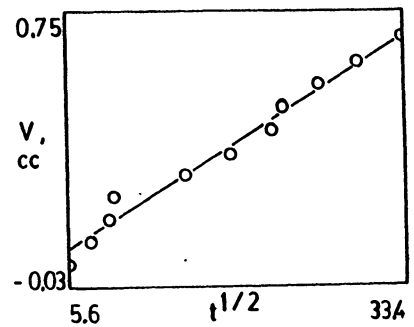

Open Tube Slope:
2.12e-2 cc/sec 1/2

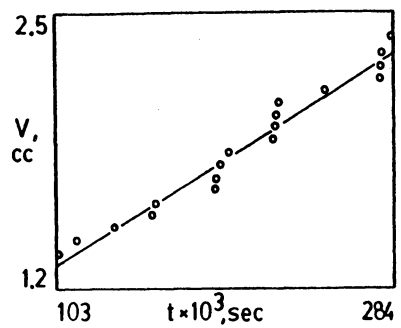

Capillary Disk Slope:
5.71e-6 cc/sec

mon:day:yr
01: 21: 85

Solute/Solvent: N2/CCl4 Gas Pressure: 676.0 torr Cell Temperature: 10.0 deg C

Time hr:mn:sc	Time (sec1/2)	Oven QDT Count	Syringe QDT Count	Hood QDT Count	Volume (cc)
00:01:04		7339	3608	3415	0.06
00:01:49		7357	3609	3419	0.12
00:02:37		7338	3610	3421	0.19
00:05:04	17.4	7315	3614	3408	0.25
00:06:05	19.1	7352	3615	3423	0.31
00:07:26	21.1	7330	3614	3423	0.37
00:12:04	26.9	7316	3615	3414	0.43
00:13:37	28.6	7377	3613	3425	0.50
00:17:08	32.1	7333	3600	3424	0.56
00:22:26	36.7	7359	3594	3411	0.62
00:25:34	39.2	7382	3592	3421	0.68
00:28:52	41.6	7349	3596	3412	0.74
00:30:11	42.6	7376	3604	3424	0.81
00:39:53	48.9	7333	3613	3420	0.86
00:52:21	56.0	7323	3617	3424	0.93
01:51 08		7348	3583	3434	0.99
03 04:26		7374	3580	3400	1.12
06:18:23		7374	3576	3401	1.18
06:28:09		7362	3577	3404	1.24
08:33:49		7371	3576	3407	1.30
15:18:53		7344	3548	3397	1.36
25:07:23	Time	7343	3459	3308	1.43
25:12:52	(sec)	7384	3463	3322	1.49
26:30:22	95422	7403	3444	3312	1.55
35:23:33	120213	7355	3469	3324	1.61
38:28:53	138533	7337	3474	3330	1.67
38:37:53	139073	7325	3479	3333	1.74
42:37:53	153473	7350	3487	3348	1.80
42:43:39	153819	7331	3488	3350	1.86
42:50:24	154224	7364	3490	3355	1.92
55:45:35	200735	7366	3411	3274	1.98
57:01:52	205312	7320	3423	3274	2.05
57:02:09	205329	7357	3423	3281	2.11

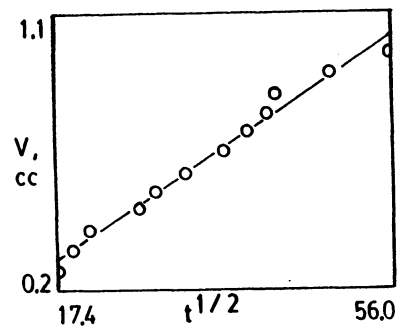

Open Tube Slope:
2.00e-2 cc/sec 1/2

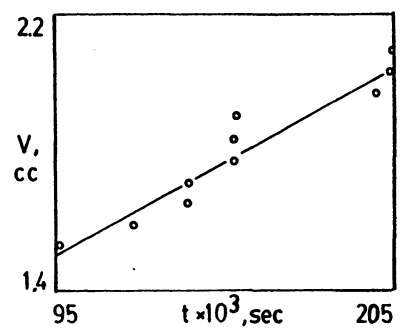

Capillary Disk Slope:
4.95e-6 cc/sec

mon:day:yr
01: 26: 85

Solute/Solvent: N2/CCl4 Gas Pressure: 642.0 torr Cell Temperature: 10.0 deg C

Time hr:mn:sc	Time (sec1/2)	Oven QDT Count	Syringe QDT Count	Hood QDT Count	Volume (cc)
00:00:37		7363	3461	3291	0.06
00:00:45		7243	3459	3282	0.12
00:00:52		7243	3459	3282	0.19
00:01:04	8.0	7343	3460	3297	0.25
00:01:57	10.8	7359	3457	3285	0.31
00:02:36	12.5	7349	3455	3298	0.37
00:03:38	14.8	7354	3452	3299	0.43
00:05:22	17.9	7381	3456	3302	0.50
00:07:48	21.6	7383	3459	3307	0.56
00:07:56	21.8	7383	3459	3307	0.62
00:10:53	25.5	7379	3457	3305	0.68
00:15:33	30.5	7349	3459	3309	0.74
00:18:05	32.9	7367	3460	3312	0.81
00:22:48	37.0	7373	3460	3314	0.87
00:22:58		7373	3460	3314	0.93
00:37:38		7307	3455	3298	0.99
00:37:55		7369	3457	3311	1.05
00:56:37		7337	3453	3290	1.12
01:16:20		7320	3451	3502	1.18
01:21:07		7365	3456	3310	1.24
01:27:20		7352	3460	3318	1.30
05:34:22		7397	3435	3298	1.36
05:40:22	Time	7394	3440	3304	1.43
05:55:37	(sec)	7384	3445	3316	1.49
21:16:04	76564	7331	3464	3314	1.55
21:17:07	76627	7369	3466	3327	1.61
30:16:48	109008	7364	3505	3363	1.67
30:16:56	109016	7364	3505	3363	1.74
35:38:28	128308	7317	3423	3282	1.80
35:43:22	128602	7341	3424	3281	1.86
35:57:37	129457	7331	3428	3284	1.92
37:40:49	135649	7338	3404	3259	1.98
37:40:57	135657	7338	3404	3259	2.05
50:29:49	181789	7340	3404	3259	2.11

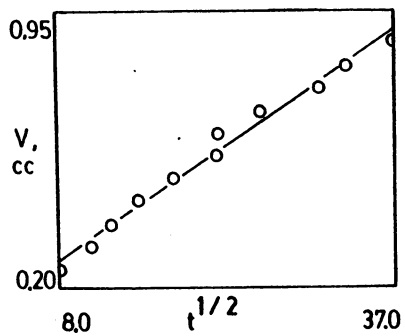

Open Tube Slope:
2.19e-2 cc/sec 1/2

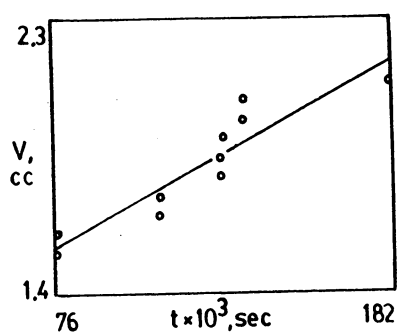

Capillary Disk Slope:
5.64e-6 cc/sec

mon:day:yr
02: 06: 85

Solute/Solvent: N2/CCl4 Gas Pressure: 625.9 torr Cell Temperature: 10.0 deg C

Time hr:mn:sc	Time (secl/2)	Oven QDT Count	Syringe QDT Count	Hood QDT Count	Volume (cc)
00:04:22	16.1	7322	3387	3194	0.06
00:05:52	18.8	7330	3388	3198	0.12
00:07:13	20.8	7325	3388	3202	0.19
00:09:37	24.0	7362	3384	3205	0.25
00:12:04	26.9	7344	3383	3206	0.31
00:14:32	29.5	7336	3379	3208	0.37
00:17:17	32.2	7371	3378	3211	0.43
00:17:27	32.4	7371	3378	3211	0.50
00:21:09	35.6	7344	3373	3210	0.56
00:25:05	38.8	7352	3376	3214	0.62
00:29:19	41.9	7335	3378	3218	0.68
00:34:04	45.2	7346	3379	3222	0.74
00:39:22	48.6	7343	3380	3224	0.81
00:47:41	53.5	7325	3378	3223	0.87
01:07:33		7334	3381	3225	0.93
01:18:20		7370	3381	3223	0.99
02:15:34		7356	3363	3210	1.05
10:59:24		7322	3402	3239	1.12
11:09:03		7334	3415	3258	1.18
11:24:37	Time	7371	3403	3255	1.24
19:18:19	(sec)	7362	3405	3252	1.30
25:26:05	91565	7337	3437	3287	1.36
27:13:17	97997	7335	3400	3248	1.43
29:02:36	104556	7359	3399	3252	1.49
35:17:22	127042	7316	3466	3288	1.55
35:18:10	127090	7346	3475	3306	1.61
35:26:06	127566	7350	3470	3320	1.67
45:47:04	164824	7335	3418	3265	1.74
47:43:54	171834	7336	3401	3237	1.80
48:41:48	175308	7359	3409	3258	1.86
50:27:24	181644	7340	3434	3268	1.92
53:40:54	193254	7339	3412	3251	1.98
59:40:33	214833	7343	3438	3285	2.05
59:48:21	215301	7360	3441	3291	2.11
68:23:04	246184	7367	3412	3267	2.17
71:29:09	257349	7323	3416	3255	2.23
71:29:55	257395	7371	3417	3272	2.29

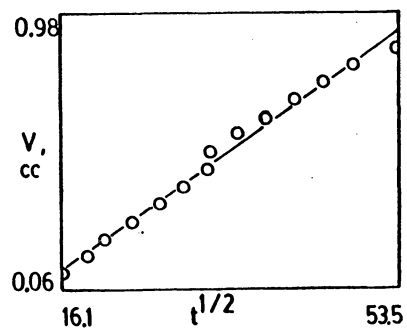

Open Tube Slope:
2.26e-2 cc/sec 1/2

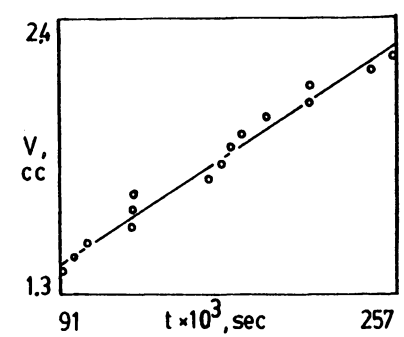

Capillary Disk Slope:
5.23e-6 cc/sec

mon:day:yr
09: 11: 85

Solute/Solvent: N2/CCl4 Gas Pressure: 725.4 torr Cell Temperature: 25.4 deg C

Time hr:mn:sc	Time (secl/2)	Oven QDT Count	Syringe QDT Count	Hood QDT Count	Volume (cc)
00:00:07		4945	3358	3068	0.06
00:00:15		4949	3358	3068	0.12
00:00:23		4949	3358	3068	0.19
00:00:31		4938	3356	3066	0.25
00:00:40	6.3	4938	3356	3066	0.31
00:01:18	8.8	4947	3338	3066	0.38
00:02:06	11.2	4935	3334	3065	0.44
00:03:03	13.5	4951	3336	3065	0.50
00:04:12	15.9	4963	3338	3065	0.56
00:05:32	18.2	4954	3338	3064	0.63
00.07:02	20.5	4496	3341	3065	0.69
00:08:41	22.8	4974	3342	3065	0.75
00:10:22	24.9	4977	3343	3065	0.81
00:12:03	26.9	4971	3344	3066	0.88
00:14:08	29.1	4983	3343	3065	0.94
00:16:33	31.5	4981	3344	3064	1.00
00:18:51	33.6	4980	3344	3064	1.06
00:21:18	35.7	4967	3344	3063	1.13
00:24:49	38.6	4964	3345	3061	1.19
00:28:03	41.0	4973	3345	3061	1.25
00:30:54		4966	3346	3062	1.32
00:35:07		4969	3345	3059	1.38
00:39:37		4970	3346	3059	1.44
00:44:08		4958	3348	3058	1.50
00:49:06		4953	3345	3057	1.57
00:53:34		4951	3344	3057	1.63
01:00:21		4948	3344	3055	1.69
01:06:22		4951	3347	3055	1.75
01:12:24		4958	3345	3054	1.81
01:20:52		4948	3346	3053	1.88
01:28:33		4959	3343	3053	1.94
01:35:24		4956	3343	3053	2.00
01:43:24		4970	3346	3054	2.07
01:48:36		4966	3346	3056	2.13
01:52:49		4983	3347	3060	2.19
01:57:51		4955	3347	3060	2.25
02:04:34		4979	3347	3063	2.32
02:10:33		4963	3348	3063	2.38
02:19:48		4973	3344	3062	2.44
02:27:08		4959	3346	3063	2.50
02:39:07		4962	3347	3060	2.57
02:53:33		4962	3344	3056	2.63
03:03:49		4959	3347	3056	2.69

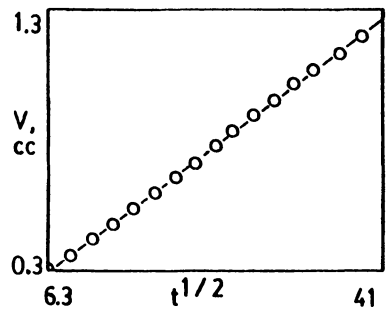

Open Tube Slope:
2.76e-2 cc/sec 1/2

Time hr:mn:sc		Oven QDT Count	Syringe QDT Count	Hood QDT Count	Volume (cc)
03:16:52		4956	3347	3054	2.75
03:26:21		4972	3349	3056	2.82
03:32:06		4981	3346	3060	2.88
03:38:07		4968	3347	3062	2.94
03:48:33		4965	3346	3063	3.01
04:03:35		4959	3344	3060	3.07
04:19:19		4966	3346	3061	3.13
04:42:23		4960	3345	3055	3.19
05:08:19		4971	3348	3055	3.26
05:17:04		4982	3343	3060	3.32
05:32:21		4963	3348	3062	3.38
05:57:09		4957	3349	3059	3.44
06:52:04		4974	3347	3056	3.51
07:03:53	Time	4979	3347	3061	3.57
08:34:52	(sec)	4956	3348	3054	3.63
08:46:20	31760	4979	3349	3062	3.69
10:36:07	38167	4965	3345	3060	3.76
14:07:35	50855	4978	3347	3061	3.82
15:44:35	56675	4969	3348	3060	3.88
19:11:35	69055	4982	3351	3062	3.94
21:01:34	75694	4964	3351	3061	4.01
22:40:54	81654	4969	3350	3061	4.07
26:24:07	95047	4974	3349	3062	4.13
27:56:50	100610	4979	3349	3059	4.19
27:59:20	100760	4979	3350	3060	4.26
29:42:19	106939	4968	3351	3059	4.32
31:33:22	113602	4978	3352	3060	4.38
33:24:50	120290	4978	3352	3061	4.44
35:19:36	127176	4966	3349	3062	4.51
39:16:35	141395	4974	3352	3064	4.57
40:57:50	147470	4976	3354	3064	4.63
46:26:36	167196	4961	3351	3060	4.70
48:11:38	173498	4972	3353	3053	4.76
53:00:04	190804	4974	3363	3060	4.82
53:09:04	191344	4977	3362	3064	4.88
54:42:52	196972	4973	3367	3064	4.94
55:10:23	198623	4972	3367	3070	5.01
58:30:35	210635	4979	3370	3069	5.07

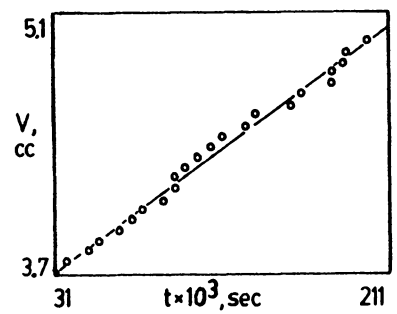

Capillary Disk Slope:
7.62e-6 cc/sec

The vita has been removed from the scanned document